Revisiting aryl *N*-methylcarbamate acetylcholinesterase inhibitors as potential insecticides to combat the malaria-transmitting mosquito, *Anopheles gambiae*

Joshua Alan Hartsel

Dissertation submitted to the faculty of the Virginia Polytechnic Institute and State University in partial fulfillment of the requirements for the degree of

DOCTOR OF PHILOSOPHY
IN
CHEMISTRY

Paul R. Carlier, Chairman
Paul A. Deck
Felicia A. Etzkorn
Richard D. Gandour
James M. Tanko

April 21, 2011
Blacksburg, VA

Keywords: aryl carbamate, acetylcholinesterase, species-selective inhibitors, malaria, insecticide-treated nets, *Anopheles gambiae*, propoxur, terbam, *tert*-alkylphenol

Revisiting aryl *N*-methylcarbamate acetylcholinesterase inhibitors as potential insecticides to combat the malaria-transmitting mosquito, *Anopheles gambiae*

Joshua Alan Hartsel

ABSTRACT

My graduate work focused on the syntheses and pharmacology of species-selective aryl methylcarbamate acetylcholinesterase inhibitors to combat the malaria-transmitting mosquito, *Anopheles gambiae*. We identified six novel carbamates that demonstrated levels of target selectivity exceeding our project milestone of 100-fold. Among the C2-substituted phenylcarbamates examined (class II), 2'-(2-ethylbutoxy)phenyl *N*-methylcarbamate (**9bd***) was extraordinarily selective (570-fold $\pm$ 72). The high level of selectivity observed for many of the class II carbamates was attributed to a helical displacement within the active site of *An. gambiae* acetylcholinesterase, able to accommodate carbamates with larger C2-substituted secondary β-branching side chains. Conversely, this type of side chain forms unfavorable interactions within the active site of human acetylcholinesterase. The C3-substituted carbamates (class I), such as terbam (**9c**), were less selective than many of the class II carbamates; however, class I carbamates related to terbam (**9c**) were highly toxic to *An. gambiae*. In particular, the contact toxicity measured for **9c** (LC_{50} = 0.037 mg/mL) was equal to the commonly used agricultural insecticide, propoxur (**9a**, LC_{50} = 0.037 mg/mL). In total, seventy aryl carbamates were screened for their inhibition potency and contact toxicity towards *An. gambiae*.

The common final step in all of these syntheses was the carbamoylation of a phenol, which normally proceeded in a 70 to 90% yield. Thirty seven novel carbamates

are reported out of the seventy two prepared. Although sixteen of the phenols were commercially available, the others were prepared with known and adapted synthetic methodologies. The emerging structure-activity relationships led us to focus on the synthesis of 3-*tert*-alkylphenols (Class I) and 2-alkoxy or 2-alkylthio-substituted phenols (Class II). Three methods particularly stand out: First, we applied the methods of Tanaka to prepare 3-*tert*-alkylphenols wherein a methyl group was replaced by a trifluoromethyl group. Second, we adapted the methods of Tanaka to prepare 3-*tert*-alkylphenols that lack fluorine substitution. This method is competitive with the little known method of Reetz to convert aryl ketones to the corresponding 1,1-dimethylalkyl group and allows one to access electron rich *tert*-alkyl-substituted aromatics that are not accessible by the Friedel-Crafts alkylation (Friedel-Crafts restricted). Third, we found a convenient and high-yielding method for selective *S*-alkylation of 2-mercaptophenol. In addition to the synthesis of carbamates, the preparation of one hundred three intermediates, phenols, and electron rich *tert*-alkyl arenes are reported.

Acknowledgements

Graduate school has been a challenging test of work ethic, scientific ability, and continued passion for learning. As it comes to a close I have to look back and be thankful for so many family members, friends, and helpful colleagues who have supported me along the way. I would like to especially thank my mother, Katie Blankenship, and stepfather, Hurley Blankenship, who continue to offer their loyal and loving support. The valuable lessons they have taught to me early in life have contributed to my achievements today.

It has been both an honor and a blessing to work under the guidance of Prof. Paul Carlier. He has been an inspirational role-model to me and offered countless hours of patient guidance that have made my graduate experience both enjoyable and abundant in medicinal and organic chemistry knowledge. In addition to the understanding of fundamental chemistry, perhaps the most valuable lessons learned from Prof. Carlier have been the ability to put my thoughts onto paper. The quintessential ability to convey ones thoughts in writing have been priceless, and will stay with me throughout the course of my life. Words can't express my wholehearted gratitude for your encouragement and support.

I would like to thank all of my committee members: Paul Deck, Felicia Etzkorn, Richard Gandour, and Jim Tanko; for their suggestions that have helped improve my writing and presentation skills. Special thanks are owed to the members of Jeffrey Bloomquist's laboratory for their collaborative effort in evaluating the inhibition potency and contact toxicity of so many carbamates. I would specifically like to thank Bloomquist group members Troy Anderson and James Mutunga for their data contribution and

commitment to our research. My sincere gratitude is also owed to Dr. Wong for her one-on-one guidance to properly evaluate AChE-ligand interactions. Dr. Wong generated many of the graphics in the text. I am grateful to the many other Carlier group members including Ming Ma, Christopher Monceaux, Neeraj Patwardhan, Larry Williams, Nipa Deora, and Jason Harmon who have helped improve my lab technique and mastery of modern organic chemical transformations. I would also like to thank Charles Carfagna, as finalizing the text from UC Irvine would not have been possible without his help at Virginia Tech.

Table of Contents

List of Figures

List of Schemes

List of Tables

List of Equations

List of Abbreviations

Acetylcholinesterase (AChE)
Acetylcholine (ACh)
Acetylthiocholine (ACTh)
Alzheimer's disease (AD)
Anopheles gambiae (*An. Gambiae*)
Catalytic active site (CAS)
Center for Disease Control (CDC)
Diethylaminosulfur trifluoride (DAST)
Dichlorodiphenyltrichloroethane (DDT)
Drosophila melanogaster (*D. Melanogaster*)
N,*N*-diethyl-3-toluamide (DEET)
(5,5'-dithiobis)-2-nitrobenzoic acid (DTNB)
Flavin-dependent monooxygenases (FMO)
Food and Drug Administration (FDA)
Indoor-residual spraying (IRS)
Insecticide-treated nets (ITNs)
Knockdown resistance (kdr)
Morpholinosulfur trifluoride (MOST)
Musca domestica (*M. Domestica*)
Organophosphates (OPs)
Organophosphate induced delayed neuropathy (OPIDN)
Peripheral anionic site (PAS)
Piperonyl butoxide (PBO)
Rupert-Prakash reagent (CF_3SiMe_3)
Synergistic ratio (SR)
Thin layer chromatography (TLC)
5-thio-2-nitrobenzoic acid (TNB)
Torpedo californica (*T. californica*)
World Health Organization (WHO)

Chapter 1: Malaria and acetylcholinesterase as a mosquitocidal target

1.1 An introduction to malaria

In the year 1902 Ronald Ross was awarded the Nobel Prize for demonstrating that mosquitoes transmitted malaria.[1] He named *Anopheles gambiae* (*An. gambiae*) "the world's most dangerous animal to humans"[1] and naively assumed that this discovery would rapidly lead to a cure for the disease. To date, the World Health Organization (WHO) estimates that 250 million cases of malaria occur worldwide each year, causing approximately 1 million deaths.[2] Therefore, it is hard to ignore the devastating effects of malaria in endemic regions of Sub-Saharan Africa where more than 90% of malaria related deaths occur.[3] The disturbing statistics show that 20% of childhood deaths in Africa are due to malaria, and the average child there will suffer between 1.6 to 5.4 episodes of malaria every year. To put the numbers in perspective, malaria takes the life of one African child every 30 seconds.[2]

Although most malaria deaths occur in Sub-Saharan Africa, the WHO has stated that nearly half the world's population (3.3 billion people) is at risk of infection.[2] The United States has remained free of malaria for decades, but its reemergence poses a real threat to future generations.[4] As a case in point, the Center for Disease Control (CDC) reported 2 cases of malaria in Loudon County Virginia in 1998 and 2002. The *Plasmodium vivax* parasite was transmitted to residents from the native North American *Anopheles quadrimaculatus s.l.* moquito.[5] International travel, environmental changes, and the emergence of drug and insecticide resistance have collectively contributed to the spread of malaria to areas otherwise devoid of the disease.[4, 6]

Anopheline mosquitoes play a key role in the transmission of malaria,[4, 5] but do not themselves cause malaria. Instead they act as a vector for the *Plasmodia* parasites that cause malaria.[3, 7] Approximately 95% of all malaria related deaths are specifically caused by the parasite, *Plasmodium falciparum*.[7] Other species of the *Plasmodium* genus, including *P. vivax, P. ovale, and P. malariae*, are responsible for additional human malaria-related deaths.[4] In addition to transmitting malaria, mosquitoes are a particularly effective vectors, transmitting a host of diseases including dengue fever, the West Nile virus, yellow fever, Rift Valley fever, and encephalitis.[1, 8]

The *Plasmodia* parasites are transmitted to humans exclusively through the salivary glands of infected female *Anopheles* mosquitoes, because only female *Anopeheles* blood-feed.[9] In addition to enabling parasite transmission, the blood meal provides the females with proteins essential to proper egg development.[4] Following the mosquito's infectious blood meal, the human circulatory system transports the injected sporozites to the liver, where they undergo metamorphosis to asexually reproducing merozoites (Figure 1.1).[9] Malaria symptoms such as a fever and chills are associated with the lysing of red blood cells that result from merozoite reproduction. Infection commonly takes 6 to 14 days to manifest into the visible symptoms associated with the disease.[9] After the merozoite stage of the *Plasmodium* life

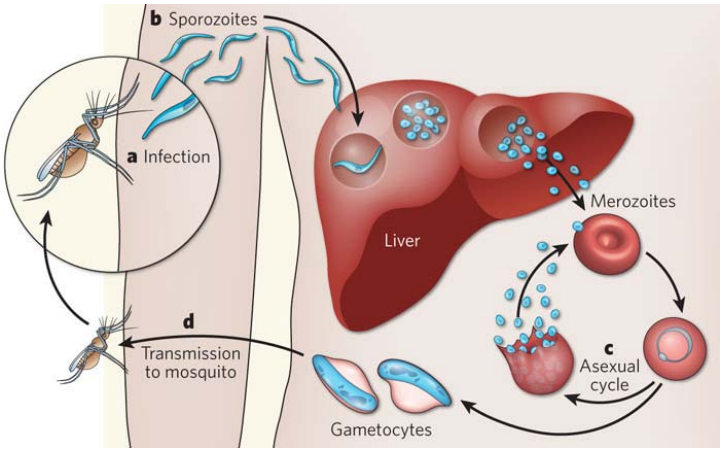

Figure 1.1. The transmission and life-cycle of *Plasmodia* parasites responsible for malaria. With copyright permission from the Nature Publishing Group.[9]

cycle, gametocytes enter the blood stream.[9] The human can then infect disease-free female *Anopheles* mosquitoes during a subsequent blood meal. Male *Anopheles* mosquitoes exclusively feed on plant nectars and therefore are not vectors of malaria.[10]

The western world was also once stricken with malaria, but the disease was eradicated by the middle of the 20th century by improving sanitation, draining standing water, and spraying dichlorodiphenyltrichloroethane (**1**, DDT; Figure 1.2).[11] The eradication of malaria from the most developed countries along with the environmental concerns associated with spraying DDT (**1**) ultimately led to a loss of interest in malaria control in African communities.[3] A lack of sufficient funding for malaria research persisted until The Bill and Melinda Gates Foundation initiated the Grand Challenges in Global Health in 2003.[12] This 200-million dollar medical research initiative has spawned a plethora of innovative ideas aimed at mitigating the drastic effects of malaria. A brief overview of these methods will be discussed in turn.

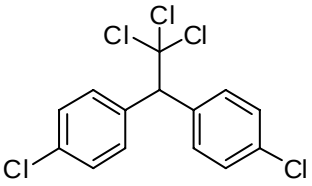

Figure 1.2. (**1**, DDT) dichlorodiphenyltrichloroethane

The multifaceted strategies currently underway to reduce the human-impact of malaria include i) developing effective drugs to treat malaria,[13, 14] ii) reducing human-mosquito contact with attractants/repellants,[15, 16] iii) genetically modifying strains of mosquitoes that are less effective at transmitting infectious diseases to humans,[17] iv) infecting mosquitoes with microorganisms that reduce their competence as vectors,[18] or v) developing safe-alternative insecticides that more effectively terminate the vector species, *An. gambiae*.[19] The first and last strategies are at risk due to evolving resistance mechanisms in the *Plasmodia* parasites to traditional drugs such as chloroquine (**2**),[20, 21]

and in the *Anopheline* vector to traditional pyrethroid insecticides.[22] Historically vector control has been the cheapest and most successful approach.[9]

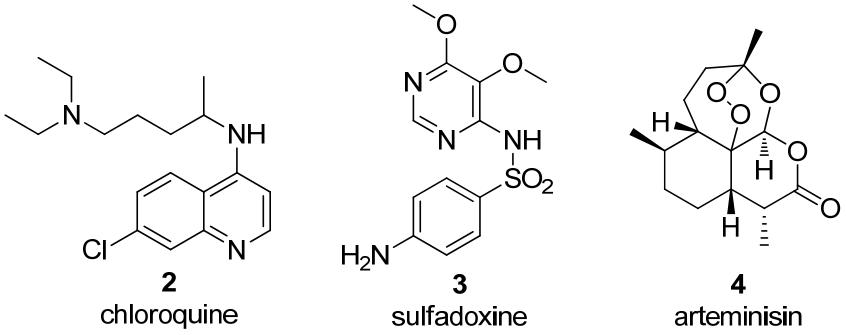

Figure 1.3. Chloroquine, sulfadoxine , and arteminisin anti-malarial drugs.

Treatment for malaria usually consists of a combination of chloroquine (**2**), sulfadoxine (**3**), and arteminisin (**4**) based drugs that disrupt the replication of the *Plasmodium* parasites (Figure 1.3).[13] Unfortunately, widespread resistance to chloroquine (**2**) has spread to nearly all regions of Africa since first reported in 1979.[14] Moreover, *Plasmodium falciparum* is growing increasingly resistant to sulfadoxine (**3**), the successor of chloroquine (**2**). Apart from blood schizontocidal drugs (e.g., **2** and **3**, schizont - merozoite-infected liver cell), arteminisin therapies have to this point shown little cross resistance and provide a rapid resolution of clinical symptoms.[13] Arteminisin based combination therapies (with sulfadoxine, **3**) enhance the efficacy and shorten the duration of treatment relative to arteminisin (**4**) treatment alone.[13]

To compliment effective drug treatments, preventative measures play a key role in reducing malaria mortality in malaria-endemic regions. Implementing successful preventative control programs requires an understanding of the ecological relationship shared between mosquitoes and humans. For example, how are mosquitoes attracted to humans and what can be done to prevent blood-feeding responsible for malaria transmission? *An. gambiae* primarily locate humans through olfaction, but little is known

about the molecular basis for this process.[15] Fifty *An. gambiae* olfactory receptors have been identified that are acutely stimulated by attractants in human sweat such as ammonia and an array of carboxylic acids such as lactic acid.[16]

Chemical compounds modulating the olfactory response can attract mosquitoes into traps, but can also interfere with their navigation or repel them. *N*,*N*-Diethyl-3-toluamide (**5**, DEET; Figure 1.4) is the most widely used mosquito repellent[23] found in household products such as OFF!™. Despite the effectiveness of DEET (**5**), its precise mode of action remains a topic still debated in the literature.[23-25] It has long been accepted that DEET blocked the electrophysiological response of insects to attractive odors such as lactic acid.[26] However, recent studies suggest that DEET has repellency properties in the absence of lactic acid.[25] More recent evidence suggests that DEET attenuates the electrophysiological response to 1-octen-3-ol.[24, 25] Although the mode of action of DEET is not fully understood, repellants can effectively mitigate malaria transmission by preventing the mosquitoes from locating humans.

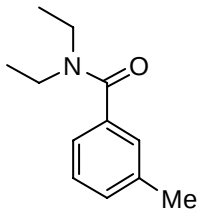

Figure 1.4. (**5**, DEET) *N*,*N*-diethyl-3-toluamide.

Zwiebel and coworkers have undertaken the task of identifying *An. gambiae* odorant receptors responding to specific classes of odorants These investigations have culminated in the identification of a female *An. gambiae* specific odorant receptor known as *Ag*Or1 that is uniquely responsive to human sweat component 4-methylphenol.[27] Future endeavors by Zweibel aim to construct attractants that can simultaneously target multiple human-specific odorant receptors in an effort to prevent the likelihood of single point mutations conferring resistance at one particular receptor site.[8]

The introduction of genetically manipulated mosquitoes into wild populations is another potential strategy to mitigate the transmission of infectious disease. Researchers at UC Irvine are engineering flightless female *Aedes aegypti* (yellow fever and dengue fever mosquito) that would be incapable of traveling and potentially infecting humans with dengue fever.[17] These genetically modified mosquitoes (*Aedes aegypti*) have been engineered so that they do not contain a muscle necessary for flight. If this technology were realized, its application to *An. gambiae* could be envisioned. Genetic modification still has its drawbacks since laboratory strains must survive in, invade, and outcompete wild populations of mosquitoes.[9]

Alternatively, O'Neill and coworkers have shown that the life-span of *Wolbachia* (bacteria)-infected *Aedes aegypti* mosquitoes are reduced by approximately 50%.[18] Furthermore, *Wolbachia* is passed by the female to its eggs[18] preventing the need for reintroduction of the *Wolbachia* over time. Since pathogens generally require relatively long periods relative to their life-span to mature, only elderly mosquitoes are infectious. In addition to reducing the life-span of *Aedes aegypti*, the mosquitoes infected with genetically-modified *Wolbachia* are dramatically less conducive to carrying the dengue virus. As the field of insect immunology advances, it may be possible to generate *Wolbachia*-infected *An. gambiae*, and assess the effect of infection on *An. gambiae* lifetime and *Plasmodium s.p.* replication.

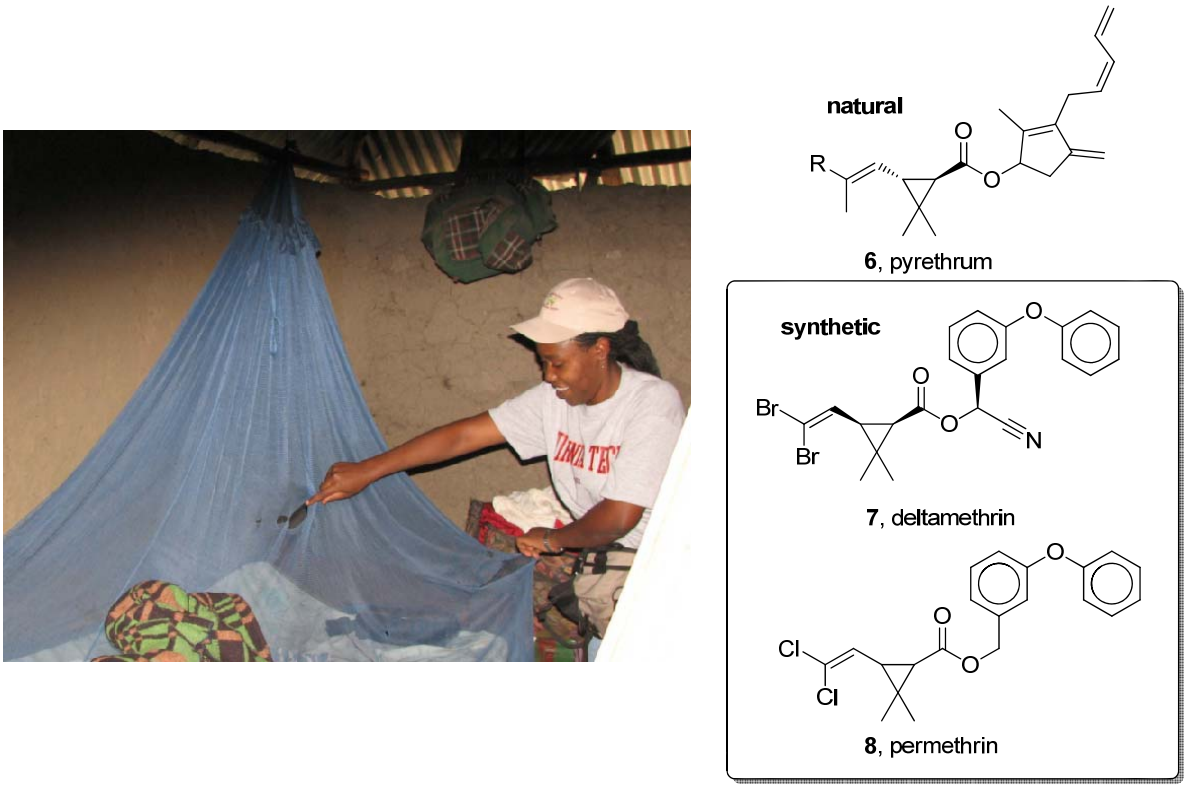

Figure 1.5. ITNs are used as a first line of defense against the transmission of malaria. ITNs are generally impregnated with pyrethroid insecticides deltamethrin and permethrin. Photo credit: Deborah Carlier.

Insecticides can directly mitigate the spread of malaria by terminating the vector species, *An. gambiae*. Current vector-based control strategies include techniques such indoor-residual spraying (IRS) where insecticides are directly sprayed onto the inner and outer walls of the dwelling and/or insecticide-treated nets (ITNs) impregnated with pyrethroid insecticides such as deltamethrin (**7**) and permethrin (**8**, Figure 1.5). Naturally occurring pyrethrum insecticides (**6**) were first discovered in pyrethrum flowers such as *Chrysanthemum cinerarifolium*. The pyrethrum extract isolated from the *Chrysanthemum* flowers was found to contain six closely related insecticidal esters collectively known as pyrethrins.[28] Due to the limited stability of the naturally occurring pyrethrum insecticides (**6**), investigators found that slight structural modifications to the pyrethrum

pharmacophore enhanced the stability without adversely affecting the toxicity.[28] Therefore, ITNs are impregnated with synthetic pyrethroids and currently provide a first line of defense to millions threatened with malaria infection.[29]

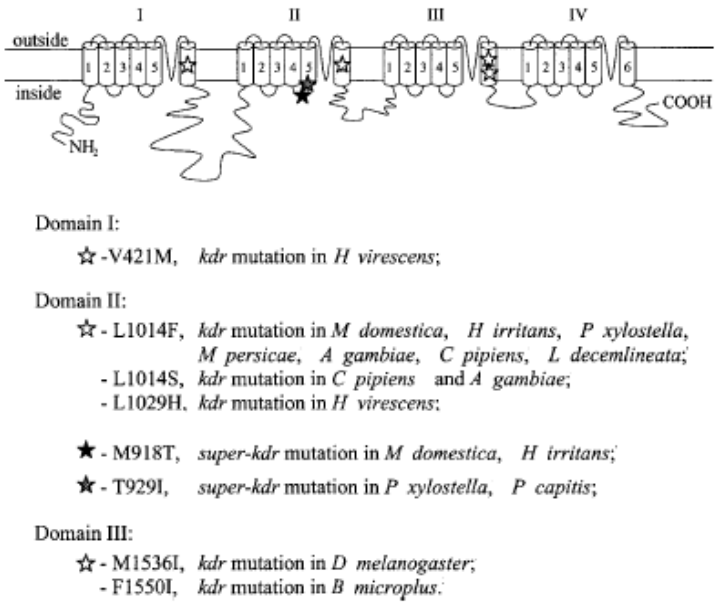

Figure 1.6. Pyrethroids preferentially bind to the open conformation of sodium channels unique to insects relative to mammals. The binding interaction paralyzes and terminates the insect. There are several point mutations confirmed in a variety of species of insects that confer kdr. With copyright permission from John Wiley and Sons.[30]

Pyrethroid insecticides modulate the gated kinetics of neuronal sodium channels located specifically within insects.[30] Figure 1.6 is a simplified cartoon of the membrane bound protein that pyrethroids target. The protein is segmented into several independent sodium channels that are organized into aggregated domains (domains I-IV).[30] The studies suggest that deltamethrin (**6**) preferentially binds to the open conformation of insect-specific para sodium channel and not the human α-subunit equivalent.[30] This binding interaction results in the paralysis and death of the insect.

Due to the safe mammalian toxicity profile of many voltage-gated sodium ion channel modulators, they are the only class of insecticides currently implemented by the WHO for application on ITNs.[31] Unfortunately, due to the widespread use of pyrethroids

and DDT (**1**), *An. gambiae* mosquitoes are becoming increasingly "knockdown resistant" to voltage gated sodium ion channel modulators.[22] Site directed mutagenesis has confirmed that point mutations L1014F and/or L1014S lead to knock down resistance in *An. gambiae*.[32, 33] Furthermore, as Figure 1.6 shows, both of these point mutations were found in the S6 transmembrane segment of domain II in the sequence.[30] To further exacerbate the problem, researchers have found an additional M918T point mutation conferring >100-fold desensitization to deltamethrin that has been termed super-kdr.[30, 32] Therefore, it is essential to develop other classes of insecticides that are both safe and effective against resistant strains of *An. gambiae*.

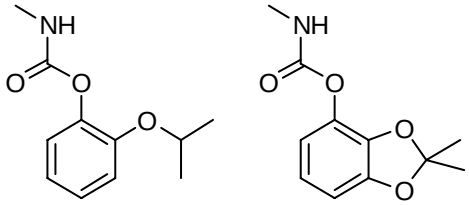

9a propoxur **9b** bendiocarb

Figure 1.7. Phenylcarbamates propoxur and bendiocarb are approved for IRS but not for ITNs.

To date, AChE is the only other biological target that has been successfully exploited for insecticide design. In addition, no resistance for AChE inhibitors has been linked to pyrethroid induced kdr. Carbamate AChE inhibitors have been successfully applied for decades as a means to control agricultural pests,[34] but up until now no appreciable target-selectivity has been demonstrated for *An. gambiae* AChE relative to human AChE. The lingering concerns over human toxicity have likely dissuaded the WHO from approving any carbamate for ITNs. In contrast, the WHO has approved two phenylcarbamates for IRS (**9a**, propoxur and **9b**, bendiocarb Figure 1.7). However, very few investigations have focused their attention on the insecticidal activity of carbamates towards mosquitoes.[35-37] To the best of our knowledge, there have been no published structure-activity relationships of carbamate toxicity to mosquitoes since the 1960s.[35-37] In fact, because these publications

appeared only in the Bulletin of the World Health Organization, they were not abstracted by Chemical Abstracts Service. We were therefore unaware of their existence until quite late in my Ph.D. research. From the beginning of my research however, we were able to take many valuable lessons from literature published by Metcalf et al. on the inhibition of *Musca domestica* (*M. domestica,* housefly) AChE with phenylcarbamate insecticides.[38-44] Throughout the text phenyl *N*-methylcarbamates will be numbered **9** and the letter will describe the functional groups pendant to the ring. A discussion of the structure-activity relationships of various carbamates will commence in Chapter 2.

1.2.1 Acetylcholinesterase: *Role in animal physiology*

AChE is a remarkable enzyme found across a diverse range of organisms including mammals, insects, plants, algae, and fungi and is vital to the proper cholinergic neurotransmission in the central nervous system.[45] Chemical warfare agents, pesticides, natural toxins (fasciculin)[46] and even therapeutic agents such as Alzheimer's disease (AD) treatments ascribe their activity to inhibition of AChE.[47] Therefore, AChE inhibitors find wide application and can have either therapeutic or toxic effects depending on the degree of inhibition.

1.2.2 The cholinergic hypothesis

Selective reversible and pseudoirreversible AChE inhibitors have found use as therapeutic drugs. Improved learning, memory, and behavior have been linked to the mild inhibition of AChE in AD patients.[48-50] The "cholinergic hypothesis" states that it is possible to improve cognition by inhibiting AChE and increasing the concentration of ACh within the synaptic cleft.[51] Although early stages of AD can be alleviated by the proper regulation of AChE,[52, 53] the progression of AD leads to irreversible brain

degeneration associated with the loss of cholinergic neurons.[54] Thus in mid- and late-stage AD, AChE inhibitors do not provide any therapeutic benefit. As the disease progresses symptoms such as memory loss and impaired judgment lead to the loss of speech and finally end in death.[54]

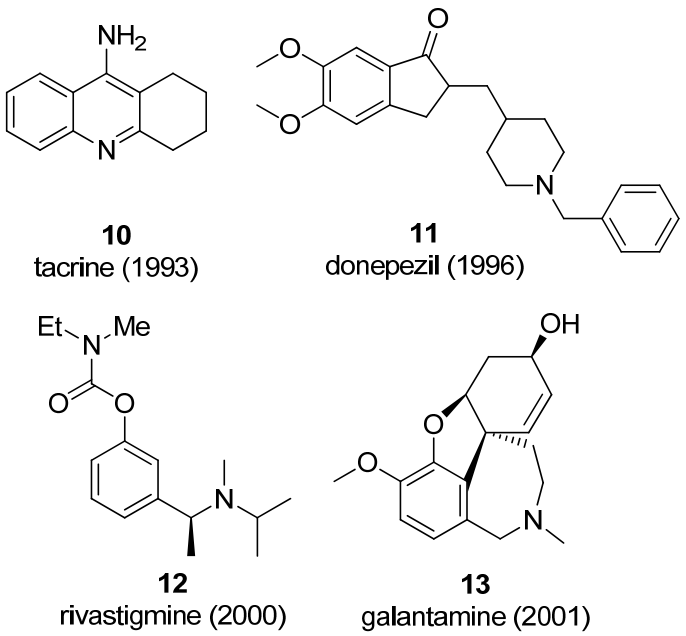

Figure 1.8. FDA approved AD drugs tacrine, donepezil, rivastigmine, and galantamine are known to alleviate the early symptoms of AD through the enhancement of central cholinergic function.[54, 56]

Efforts to treat memory loss associated with AD led to the development of many reversible and pseudo-irreversible AChE inhibitors, four of which have been approved by the FDA (Figure 1.8). Consequently, the majority of modern chemical literature on AChE inhibitors is related to AD, rather than to insecticides. In 1993 the first reversible AChE inhibitor, tacrine (**10**), was approved by the FDA.[55, 56] Since then many other drugs including donepezil (**11**, 1996), rivastigmine (**12**, 2000), and galantamine (**13**, 2001) have been added to the FDA approval list.[54, 56] However, rivastigmine (**12**) is the only carbamate approved by the FDA for AD treatment.

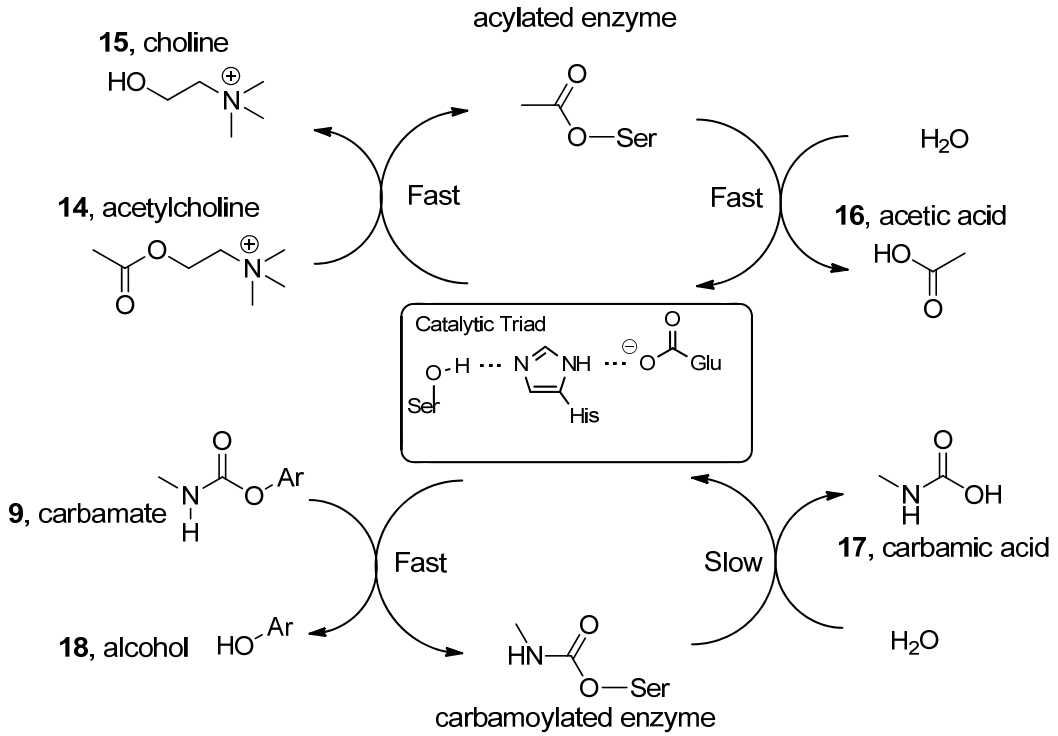

Figure 1.9. Substrate processing and mechanism of inhibition occurs at the active site serine. Both the substrate and carbamate undergo fast acylation of the active serine. The key distinction between the two pathways is the slow hydrolysis of the carbamoylated active site.

Cholinergic neurotransmission is a rapid process, occurring within a few milliseconds from the release of ACh (**14**) from the presynaptic neuron until hydrolysis. After the depolarization of the cholinergic terminal, ACh (**14**) is released where it migrates across the synaptic cleft and binds to the muscarinic and nicotinic receptors located on the postsynaptic neuron.[57] AChE is responsible for terminating neurotransmission by hydrolyzing the substrate, ACh (**14**). The enzymatic cycle for substrate processing is shown in the upper catalytic cycle in Figure 1.8. Acylation of the active site serine and hydrolysis of the acylated enzyme are both a rapid process generating the metabolites choline (**15**) and acetic acid (**16**).[58] One of the remarkable features of AChE is the rate at which it can perform hydrolysis of the substrate. This process is so rapid that the concentration of substrate around the enzyme is depleted relative to the bulk solution, suggesting that the enzyme is able to hydrolyze the substrate

at rates near the diffusion limit.[46] Depending on the species, these rates range from 200 (human) to 16,000 (*Torpedo californica*) sec^{-1}.[45, 59] The Carlier group has determined that *An. gambiae* falls within this range at 667 sec^{-1} (unpublished results).

Reversible inhibitors like tacrine (**10**) impede substrate turnover by non-covalently binding with key residues within the enzyme.[51] However, carbamate inhibitors covalently modify the active site serine, directly preventing the hydrolysis of the substrate (**14**, ACh). Covalent modification of the active site serine occurs in a similar fast step for both the substrate (**14**) and carbamate inhibitor (**9**). In contrast to substrate turnover, the half-life for the hydrolysis of the *N*-methylcarbamoylated active site was determined to be 30 minutes.[60] The slow hydrolysis of the carbamoylated active site relative to the acetylated active site can be attributed to the decreased electrophilicity of carbamates compared to esters such as ACh (**14**). The inhibition of AChE leads to the buildup of ACh (**14**) within the synaptic cleft, over-stimulation of the receptor sites, and eventually cholinergic toxicity.[61] Symptoms of toxicity include irritability, tremors, convulsions, paralysis, and death.[40] Therefore, it is not surprising that phenyl *N*-methylcarbamate AChE inhibitors (**9**) have successfully been employed as potent insecticides.

The efficiency of AChE can be partly attributed to the nucleophilicity of the catalytic serine within the catalytic triad. However, the catalytic serine is activated for nucleophilic attack by hydrogen bonding interactions with key residues such as histidine and glutamate

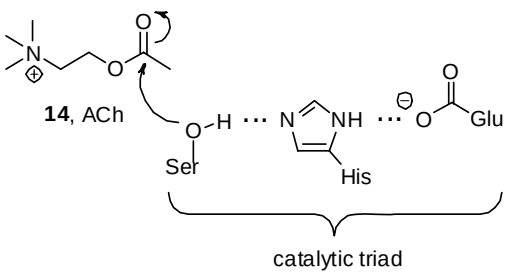

Figure 1.10. Catalytic triad residues histidine and glutamate activate the serine for nucleophilic attack.

within the catalytic triad (Figure 1.10).[62, 63] The coordinated roles of these key residues within the catalytic triad (S200···H440···E327, *Torpedo californica* numbering) were confirmed when studies involving site directed mutagenesis (H440G) drastically reduced the enzymatic activity relative to the native enzyme.[64]

Scheme 1.1. Kinetic model for the inhibition of AChE by pseudo-irreversible carbamate inhibitors.

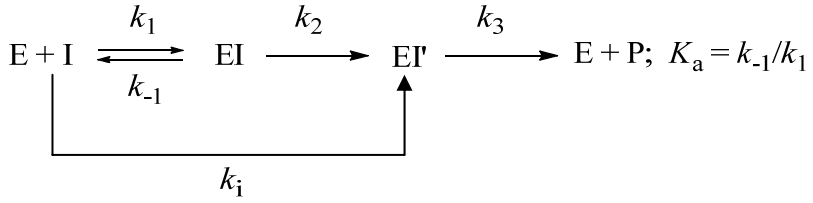

The inhibition of AChE by pseudo-irreversible carbamate inhibitors likely proceeds via a multi-step reaction mechanism, which we have simplified to two steps in Scheme 1.1. The enzyme-inhibitor complex (EI) is formed in a fast equilibrium step (denoted K_a or binding affinity, mM^{-1}). At a glance the inhibition mechanism shown in Scheme 1.1 resembles Michaelis-Menten kinetics for enzyme processing of substrate. As written, the association constant K_a is the inverse of the dissociation constant K_d, which is similar to K_m as they both pertain to substrate dissociation from the enzyme. The carbamoylation rate constant (k_2), plays a similar mathematical role to k_{cat}, which in Michaelis-Menten kinetics is the unimolecular rate constant (turnover number) for conversion of the (ES) complex to (E) and (P). The apparent bimolecular rate constant k_i (min^{-1} mM^{-1}) equals k_2 divided by K_d has units of min^{-1} mM^{-1}, just like k_{cat} divided by K_m, the so-called "catalytic efficiency" of the enzyme for turnover of the substrate. Therefore, the measured k_i values represent the "inhibition efficiency" of the carbamates. The overall apparent bimolecular rate constant (k_i, mM^{-1} min^{-1}) is itself a product of the rate of carbamoylation (k_2, min^{-1}) and the binding affinity (K_a, mM^{-1}).

1.2.3 Organophosphate AChE inhibitors

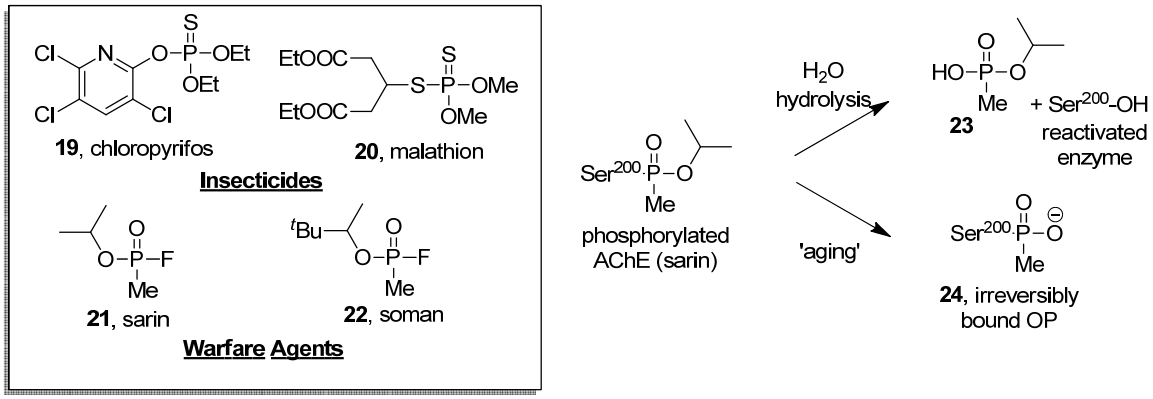

Figure 1.11. Chloropyrifos and malathion are common OP insecticides. Alternatively, soman, and sarin were developed as chemical warfare agents. After phosphorylation of the active site, OPs can undergo two divergent pathways: i) hydrolysis to reactivate the enzyme or ii) "aging". The latter process renders the OP irreversibly bound to the enzyme. [58, 66]

Organophosphates (OPs) have long been used as agricultural insecticides and as chemical warfare agents due to their potent inhibition of AChE.[66] OP insecticides such as chloropyrifos (**19**) and malthion (**20**) are widely used to control agricultural pests. For example, the EPA estimates that 10 million pounds of chloropyrifos (**19**) are applied to US crops annually.[67] The irreversible and indiscriminate binding of OP inhibitors has excluded their use from ITNs and IRS due their high mammalian toxicity. The high inhibition potency of OPs is due to several factors, including the ground state tetrahedral structure that closely resembles the transition state of the substrate ACh (**14**). As Linus Pauling suggested decades ago, enzymes enhance the reaction rate by lowering the transition state energy.[68] The exceptionally slow hydrolysis rates of the OP-bound AChE make these inhibitors extraordinarily toxic when compared with carbamates. In fact, the hydrolysis of the phosphorylated active site can take days and the *O*-dealkylation of the OP-bound AChE can permanently deactivate the enzyme in a process known as "aging" (Figure 1.11).[58] If this process takes place the enzyme is permanently bound, forever terminating the enzyme's ability to hydrolyze ACh.

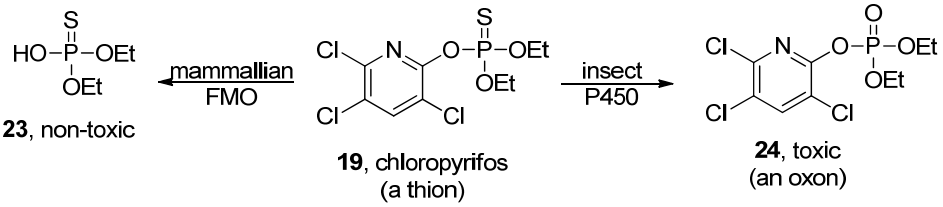

Figure 1.12. Chloropyrifos acts as a proinsecticide targeting insect P450 bioactivation. Mammalian FMO provides an alternate route for detoxification.[69, 70]

OP-based insecticides generally contain a phosphorus-sulfur double bond (a thion) that confers low mammalian toxicity (Figure 1.12).[69, 70] Such compounds are poor AChE inhibitors due to reduced electrophilicity; instead, they function as "proinsecticides". Bioactivation of the phosphorous-sulfur double bond (thion) by cytochrome P-450 monooxygenases to the phosphorus-oxygen double bond species (oxon) plays a prominent role in the toxicity to insects (Figure 1.12).[70] However, in mammals, flavin-dependent monooxygenases (FMO) apparently play a central role in metabolism of thion-containing OPs, effectively detoxifying them.[70]

In addition to mammalian AChE activity, OPs have been linked to human neurodegenerative disorders. In particular, low level exposure to OPs has been linked to a serious progressive neurodegenerative condition called organophosphate induced delayed neuropathy (OPIDN). Although this process is not fully understood, studies suggest that OPs play a key role in the inhibition of neurotoxic esterase.[71] This troubling off-target behavior discouraged us from further exploring OPs as selective mosquitocides.

1.3.1 The structure of AChE

Prior to the development of protein purification techniques, sequencing, and site-directed mutagenesis, investigators could only speculate on the binding domains responsible for the catalytic efficiency of AChE. The primary structure remained elusive until the protein was sequenced and the catalytic triad (S200···H440···E327) was

confirmed by Schumacher et. al. (1986).[72] By 1991, Sussman and Silman et al. had obtained the first X-ray crystal structure of *Tc*AChE (PDB ID 1ACE), revealing a wealth of structural information.[73] Many subsequent publications employ the *Tc*AChE nomenclature to identify key residues in other species. The abundant quantities of AChE obtainable from the organs of Pacific electric ray (*Torpedo californica*) along with the catalytic efficiency of *Tc*AChE make this species convenient for model use. Throughout the text, the nomenclature for *Tc*AChE will be used to identify key residues unless otherwise stated.

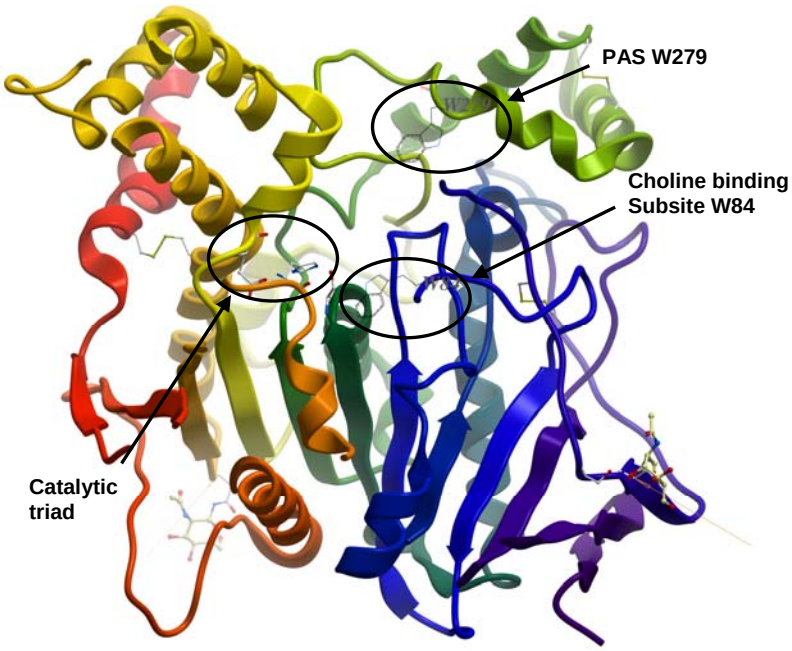

Figure 1.13. The ribbon representation of *Tc*AChE (PDB ID 1EA5) shows key sub-sites within the enzyme. The catalytic triad is depicted in the top left region where the backbone of the residues is colored in grey while the oxygen and nitrogen atoms are colored in red and blue respectively. In addition to the catalytic triad, the choline binding site (W84) and peripherheral anionic site residue W279 are shown dark grey. (Ribbon representation generated by Dr. Dawn Wong).

The ribbon representation of *Tc*AChE (PDB ID 1EA5)[63] shown in Figure 1.13 is oriented for the reader to look down through the active site gorge. The mouth of the gorge is located 20 Å from the catalytic triad (Figure 1.13, carbon backbone colored in

grey) within the catalytic active site (CAS).[49, 62] The choline binding site, or W84, is also located within the CAS proximally to the catalytic triad. Although not shown, aromatic residues Y121 and F330 are found leading into the CAS and form a tight bottleneck-like passageway approximately 5 Å in diameter.[62, 63] It is widely accepted that breathing motions within the enzyme must accommodate the entrance of the substrate which has quaternary ammonium head 6.4 Å in diameter.[62, 63, 74]

Prior to obtaining a crystal structure it was believed that the positively charged ACh head was drawn into the CAS by an electronic steering mechanism via a cluster of negatively charged residues.[75] AChE's isoelectronic point (pI = 4.5) was well below the physiological pH, suggesting the surface of the enzyme had negatively charged character.[59] However, the crystal structure pointed out that the gorge and CAS were mostly composed of aromatic residues that were conserved throughout the animal kingdom (crystal structure data from human, fruit fly, mouse, and electric eel).[49, 76, 75] Other sub-sites within the CAS that are not visible in Figure 1.13 are the acyl pocket and the oxyanion hole. Each of these sub-sites (catalytic triad, choline binding site, acyl pocket, and the oxyanion hole) will be discussed in succession.

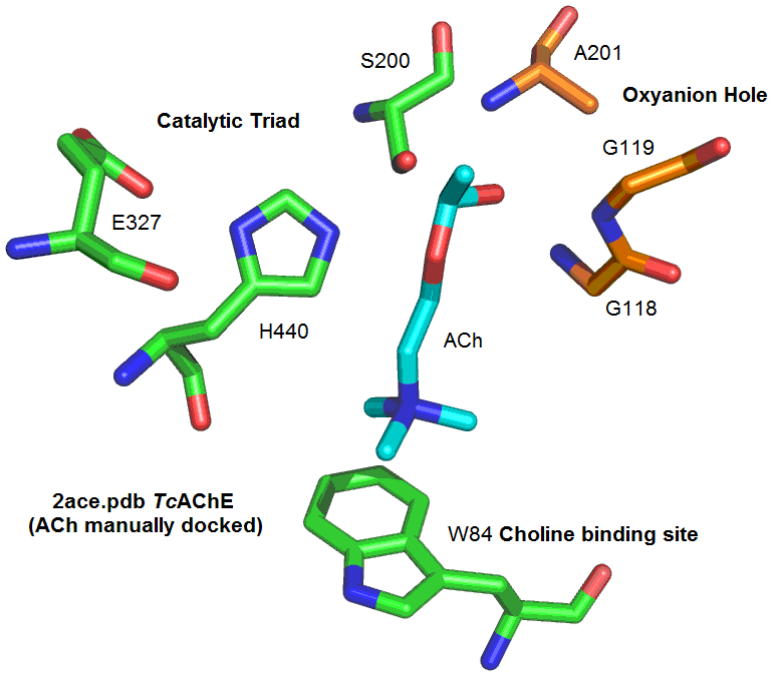

Figure 1.14. The substrate ACh is manually docked within the CAS of *Tc*AChE (PDB ID 2ACE). The major sub-sties shown within the CAS include the catalytic triad, choline binding site, and the oxyanion hole. (Graphic generated by Dr. Dawn Wong).

As previously mentioned, the residues composing the gorge and CAS are largely aromatic residues. One key aromatic residue, W84 (choline binding site), is believed to be associated with the positively charged quaternary ammonium head located on ACh (**14**) in a cation-pi interaction.[49, 63, 77] By manually docking ACh (**14**, Figure 1.14) within the active site, Dr. Dawn Wong has provided evidence that suggests that the quaternary ammonium head on ACh (**14**) is situated just above the choline binding site (W84). In addition, the catalytic triad and oxyanion hole are also interacting with the manually docked substrate within the CAS.

The oxyanion hole sub-site is composed of highly conserved G118, G119, and A201 residues (bronze, Figure 1.14). These key residues stabilize the negative charge buildup on the carbonyl oxygen in the transition state upon nucleophilic attack by S200.[63, 45, 60] Site-directed mutagenesis has confirmed that two of these three residues

provide sufficient stabilization to maintain the catalytic efficiency of the enzyme.[45] Additionally, the acyl pocket is composed of aromatic residues W233, F288, F290, and F331 that are believed to have hydrophobic interactions with the methyl group on ACh (**14**).[46, 63]

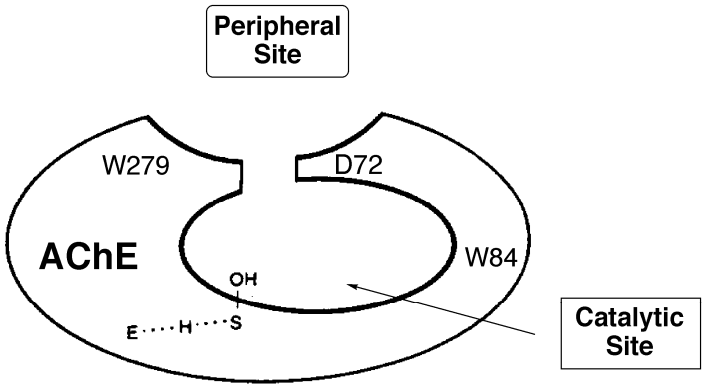

Figure 1.15. This highly simplified cartoon highlights the catalytic binding site in addition to the peripheral sub-site that is capable of binding ligands through pi-pi stacking interactions. Adapted from Rosenberry.[78]

The highly simplified cartoon shown in Figure 1.15 illustrates the relationship between the CAS and a peripheral anionic site (PAS) located at the mouth of the gorge.[78] PAS residues W279, Y70, and D72 can bind ligands through pi-pi or cation-pi stacking interactions.[49] Experimental evidence suggests that PAS ligands can also impede substrate turnover.[63, 78] Although not well understood, two opposing theories attempt to explain PAS inhibition by either i) blocking water molecules from entering the active site gorge or, ii) blocking the traffic of substrate or exit of the choline product.[63] The role of these PAS residues were confirmed via site-directed mutagenesis in binding studies on PAS-selective ligands such as propidium.[63, 78]

1.3.2 High resolution X-ray crystal structures of carbamate-bound AChE

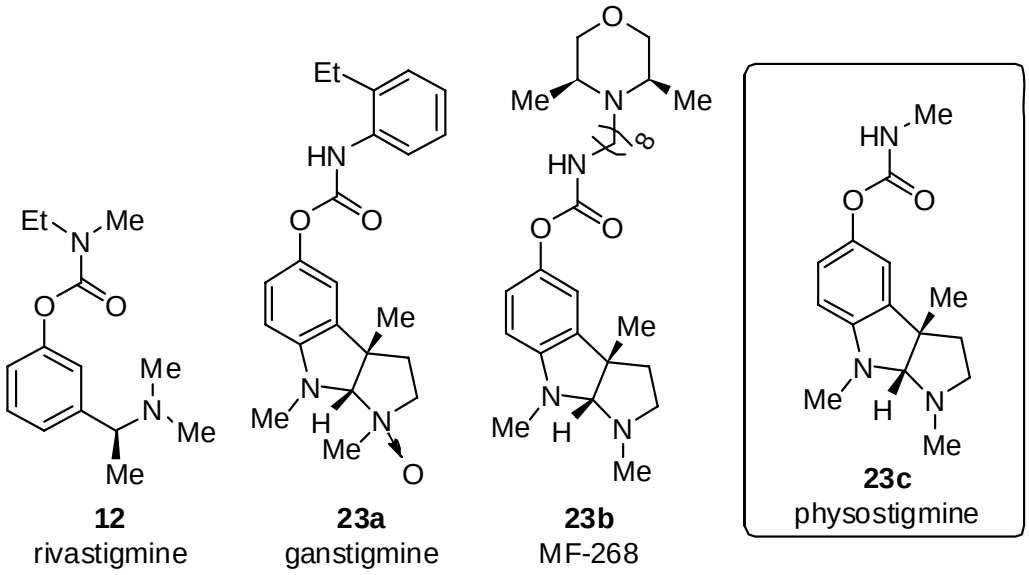

Figure 1.16. To date only three high resolution crystal structures of carbamate-bound AChE have been published. The latter two carbamates, ganstigmine,and MF-268 were designed from naturally occurring phenyl N-methylcarbamate, physostigmine.

Since the publication of the first crystal structure of *Tc*AChE, several high resolution X-ray structures have become available. As of March 2011, a search of the Protein Data Bank[79] revealed that 144 X-ray crystal structures of AChE had been resolved with greater than 3.2 Å resolution. To date, only three carbamate AChE co-crystal structures have been published (PDB ID 1GQR,[80] 2BAG,[48] and 1OCE[81]). However, the co-crystal structures of **12**, **23a**, or **23b** (Figure 1.16) with AChE were aimed at drug design for AD and not insecticide development.

The rivastigmine-bound crystal structure helped identify key binding interactions between AChE and carbamate inhibitors (Figure 1.17).[45] Although the co-crystal structure of **12** and *Tc*AChE (1OCE) was the first to confirm the covalent bond between the carbamate and active site serine,[81] each of the carbamate bound crystal structures verifies this mechanism of inactivation. The latter two carbamates (**23a** and **23b**) were

designed based on naturally occurring physostigmine (**23c**). Physostigmine (**23c**) was isolated from the calabar bean (*Physostigma venenosum* bean) and was perhaps the first toxic carbamate discovered by indigenous tribal communities.[77, 82]

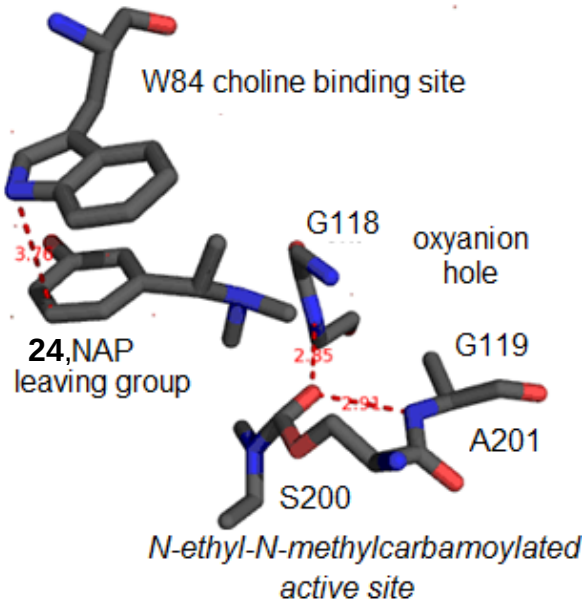

Figure 1.17. The co-crystal structure of rivastigmine and *Tc*AChE confirmed the covalent bond between the carbamate and the active site serine. In addition, the phenol leaving group (NAP) was retained within the active site gorge by interactions with the choline binding site (W84).

One intriguing feature of the rivastigmine bound crystal structure (2.2 Å resolution) is the retention of the phenol leaving group, (-)-*S*-3-[1-(dimethylamino)-ethyl]phenol (**24**, NAP) within the CAS (Figure 1.17).[80] NAP (**24**) is itself a competitive reversible inhibitor of *Tc*AChE with a binding affinity of 0.5 μM.[80] The X-ray structure revealed that this affinity was due in large part to an interaction with the choline binding site W84.[80] In addition to the retention of the NAP (**24**) leaving group within the CAS, several key residues within the oxyanion hole (A201 and G119) were found hydrogen bonding with the carbonyl oxygen of the *N*-ethyl-*N*-methylcarbamoylated active site. Although not shown, additional hydrophobic interactions were also observed between the carbamate methyl group and aromatic residues F288 and F290 were found in the acyl pocket. Based on CA measurements, the overall the crystal structure of rivastigmine (**12**) bound conjugate was relatively similar (0.26 rmsd) to the native conformation. Small variations from the native confirmation were found at the bottom of the active site gorge within the CAS.

In contrast to rivastigmine (**12**), the co-crystal structure of ganstigmine (**23a**)[48] and MF268 (**23b**)[81] did not show the retention of the phenolic leaving group within the active site of the *Tc*AChE conjugate. The expulsion of the leaving group in these two structures has raised questions as to whether there is potentially a "back door" exit located within the CAS.[83] However, the "back door" exit theory remains controversial. The co-crystal structure of ganstigmine (**23a**) and *Tc*AChE reaffirmed the covalent bond between the carbamate and the active site serine. Other key hydrogen bonding and hydrophobic interactions between the oxyanion hole and acyl pocket were also observed within the CAS.[48] The MF268 co-crystal structure (**23b**, PDB ID 1OCE, Figure 1.18)[81] is also representative of these interactions, but also is slightly more informative with regards to its eight carbon methylene tether spanning from the S200 to the PAS W279 (D). The X-ray crystal structure revealed that there was a cation-pi stacking interaction between PAS residue W279 (D) and the protonated morpholino group located at the on the carbamate nitrogen.[81]

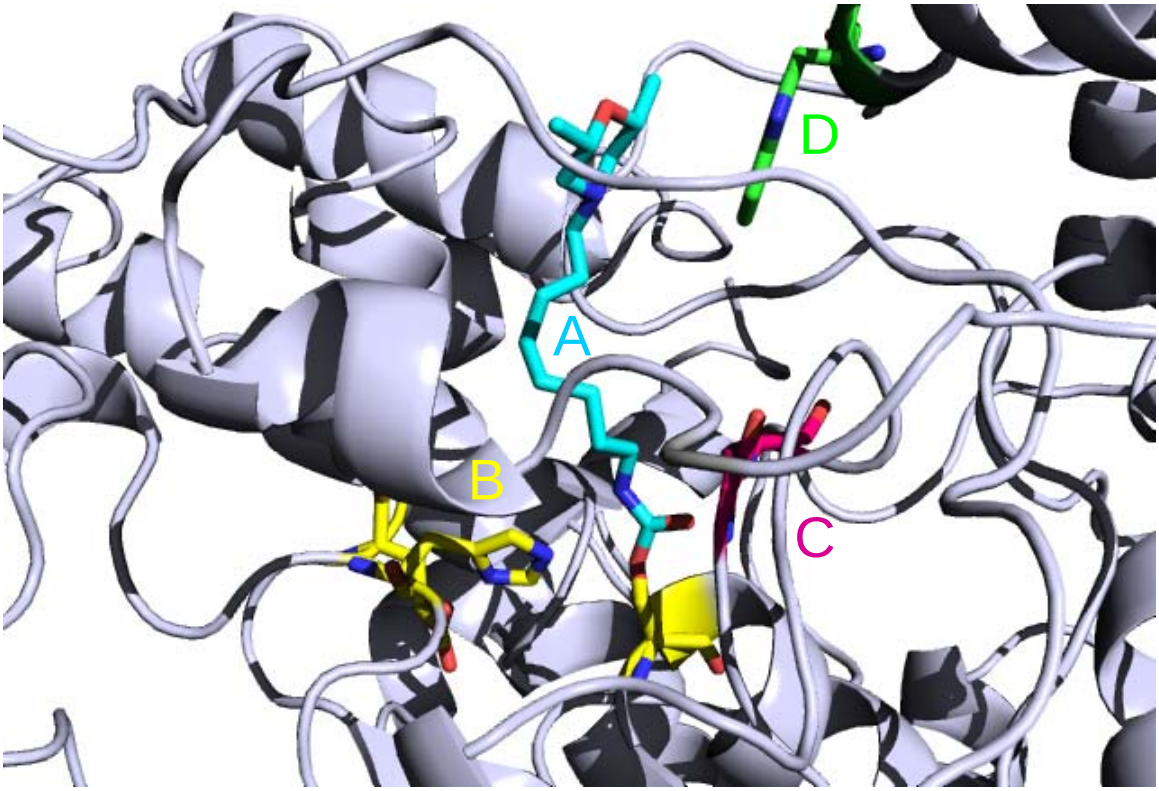

Figure 1.18. The co-crystal structure of MF268 and *Tc*AChE (PDB ID 1OCE) reveals several key binding features within the enzyme. The turquoise colored portion (A) represents the carbamoylated active site where the nitrogen-substituent is extending out into the gorge and forming key cation-pi stacking interactions with W279 (D). Furthermore, the oxyanion hole residues (C) were within proximal distance with the carbamate carbonyl oxygen. The catalytic triad is colored in yellow (B).

1.3.3 The structure of *An. gambiae* AChE

Despite this wealth of structural information available for mammalian AChE, only one species of insect AChE (*D. melanogaster*, fruit fly) has been crystallized (PDB ID 1QO9, 1QON, 1DX4).[84] To date, there are no X-ray structures of *Ag*AChE to aid in the design of *Ag*AChE–selective inhibitors. It is natural to assume that insects, specifically *An. gambiae* and *D. melanogaster*, would share more similarity than *An. gambiae* and human. If this were the case, then the resolved crystal structure for *D. melanogaster* AChE would be useful for predicting the structure of *An. gambiae* AChE. However, this supposition turned out to be incorrect. Surprisingly, *D. melanogaster* AChE shares only 41% sequence identity (56% similarity) with *An. gambiae* AChE,

perhaps due to the fact that the major ACh-hydrolyzing enzymes of these two species are encoded by different genes. *An. gambiae* is one of several insect species known to carry two AChE genes (*ace*-1 and *ace*-2), but a range of compelling evidence suggests that *Ag*AChE is encoded by the non-homologous *ace*-1 gene.[85] The nearly 250 million years of evolution separating *An. gambiae* from *D. melanogaster* could account for the distinctions between the two insects' genes encoding for AChE.[86]

Although the sequence identity of *An. gambiae* compared to human AChE is marginally higher (49%, with 65% similarity) than that with *D. melanogaster* AChE, the overall low sequence identity suggests that it may be possible to develop AChE inhibitors with high target selectivity for *An. gambiae* relative to human AChE. To date, house flies (*M. domestica*) have been the prominent species of insects investigated for carbamate activity.[40] Due to the non-homologous genes encoding for *D. melanogaster* and *M. domestica* relative to *An. gambiae*, the relevance of this data is questionable as a guide in the development of insecticides targeting *Ag*AChE.

Radíc and Taylor have recently published an excellent large-scale alignment of 125 AChE sequences;[45] similar multiple sequence alignments have also recently been published by Pezzementi et al.[87] and Pang.[88] Figure 1.19 presents portions of the alignment of *Torpedo californica* AChE (*Tc*AChE), *h*AChE, *Ag*AChE, and *Dm*AChE. Six key regions of the enzyme are selected for comparison: the catalytic triad, the oxyanion hole, the choline-binding site, the acyl pocket, the peripheral site, and the "flexible peripheral site loop." This latter region has previously been referred to as the "acyl pocket loop",[45, 89] and in *Tc*AChE as the "W279-S291 loop", where its flexibility has been noted.[51, 90-92] For ease of reference, Figure 1.19 also provides the appropriate

human, *An. gambiae*, and *D. melanogaster* residue numberings to accompany the conventional *Tc*AChE numberings.

	catalytic triad			oxyanion hole		choline-binding site	
	200	327	440	116	201	84	330
Tc	TIFGE**S**AGGAS	**E**	**H**	YG**GG**F	**A**	W	FF
	203	334	447	119	204	86	337
human	TLFGE**S**AGAAS	**E**	**H**	YG**GG**F	**A**	W	YF
	199	325	439	116	200	84	328
Ag ace-1	TLFGE**S**AGAVS	**E**	**H**	FG**GG**F	**A**	W	YF
	238	367	480	148	239	83	370
Dm ace-2	TLFGE**S**AGSSS	**E**	**H**	YG**GG**F	**A**	W	YF

	acyl pocket			peripheral site					flexible peripheral site loop	
	233	288	290	70	72	121	279	334	279	291
Tc	W	F	F	Y	D	Y	W	YG	WNVLPFDSIFRFS	
	236	295	297	72	74	124	286	341	286	298
human	W	F	F	Y	D	Y	W	YG	WHVLPQESVFRFS	
	232	286	288	70	72	121	280	332	280	289
Ag ace-1	W	C	F	I	D	Y	W	YY	WGTL---GICEFP	
	271	328	330	69	71	153	321	374	321	331
Dm ace-2	W	L	F	E	Y	M	W	YD	WNSY--SGILSFP	

Figure 1.19 Alignment of *Torpedo californica*, human, *Anopheles gambiae* (*ace*-1), and *Drosophila melanogaster* (*ace*-2) AChE. SwissProt codes: ACES TORCA (*Tc*); ACES HUMAN (human); ACES ANOGA (*Ag ace*-1); ACES DROME (Dm ace-2). Residues marked in bold are essential for catalysis. By convention, numbering is based on that of the catalytic subunit/mature form of *Tc*AChE, as defined by X-ray structures of the protein (e.g., PDB ID 2ace).[19]

Identity between human and *An. gambiae ace*-1 is extremely high throughout the catalytic triad region, the oxyanion hole, and the choline-binding site. However, interesting and potentially useful differences are seen in the acyl pocket, the peripheral site, and the flexible peripheral site loop. Finally, the significant difference in residue numberings between *D. melanogaster* and the other species following *T. Californica* residue 104 (not shown in Figure 1.19) is a consequence of the so-called "hydrophilic insertion" of 31 amino acids, which appears characteristic of the *ace*-2 gene, at least in diptera (di=two, ptera=wings).[85]

1.4 *An. gambiae* resistance to carbamate insecticides

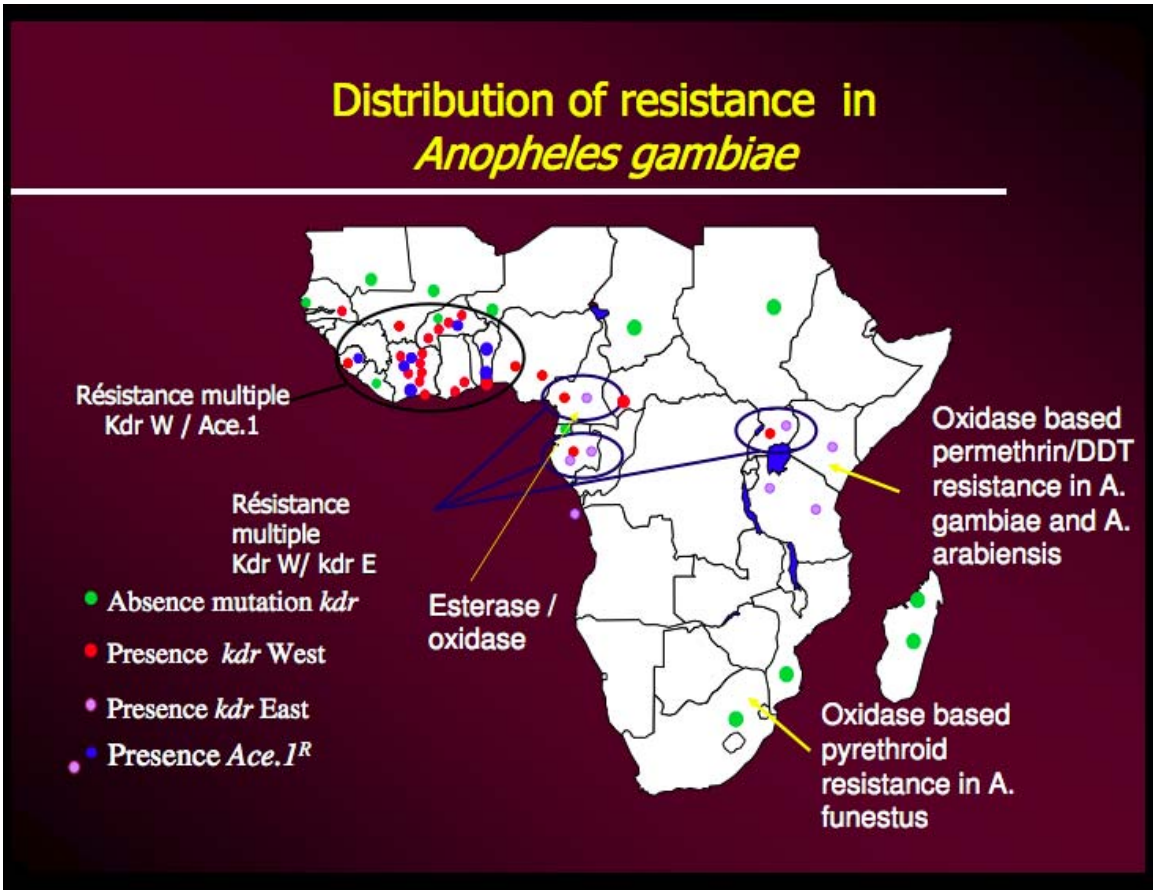

Figure 1.20. Distribution of insecticide resistance found throughout Africa for *An. gambiae.* With permission from Mark Rowland (London School of Hygiene and Tropical Medicine).

Insects are truly a remarkable group of organisms able to seemingly counter every attempt to limit their population. In addition to pyrethroid-induced kdr,[30] Weill and coworkers have reported a G119S point mutation in *Culex pipiens* and *Ag*AChE associated with resistance to organophosphate and carbamate AChE inhibitors.[93, 94] The G119S mutation is localized within the oxyanion hole and is believed to emerge as prolonged exposure to OP and carbamate AChE inhibitors selects for this resistance mutation.[94] This resistance mechanism is not observed in insects expressing the non-

homologous ace-2 gene and has only been observed in insects expressing the ace-1 gene.[94]

Pyrethroid resistance is becoming increasingly widespread throughout sub-Saharan Africa (Section 1.1). Conversely, carbamate and OP resistance is isolated within small geographical regions using an over-abundance of agricultural insecticides (blue dots in Figure 1.20). This resistance mechanism is sparsely distributed throughout western Africa where the majority of malaria outbreaks are occurring. Unfortunately, insecticide resistance is also spreading to eastern regions. Also mentioned previously, pyrethroids and carbamates target orthogonal biological processes, voltage-gated sodium ion channel modulation and AChE inhibition respectively. By employing a rotation of carbamate-treated and pyrethroid-treated ITNs, we hope to minimize resistance associated with either mechanism.

1.5 Conclusion

ITNs impregnated with pyrethroids currently provide the first line of defense against malaria transmission that disproportionately afflicts the poorest nations in sub-Saharan Africa and Southeast Asia. The improper overuse of pyrethroid insecticides have caused resistance mechanisms to emerge and necessitated the deployment of safe alternatives that could potentially include target-selective *Ag*AChE inhibitors. To date no appreciable selectivity for *Ag*AChE has been demonstrated, and perhaps this is why no carbamates have been approved by the WHO for ITN deployment.

Our project milestones include the identification of phenyl *N*-methylcarbamate inhibitors with greater than 100-fold target selectivity for *An. gambiae* relative to human AChE. Ideally, these selective candidates will maintain comparable contact toxicity to

propoxur (**9a**), a commercially available benchmark. These levels of target-selectivity may ease the lingering concerns of human toxicity and provide a platform for the development of carbamates with a safe mammalian toxicity profile applicable to ITNs. The lead insecticides could also be applied by IRS spraying methods as well. As described in Chapter 2, several of our compounds have surpassed the selectivities observed for propoxur (**9a**) and bendiocarb (**9b**), the only two carbamates approved for IRS. Furthermore, Chapter 2 will focus on structural elements of the phenylcarbamates that confer optimum mosquitocidal properties such as inhibition potency, target-selectivity, and contact toxicity towards *An. gambiae*.

1.6 References

1. Scott, M. Developmental genomics of the most dangerous animal. *Proc. Natl. Acad. Sci. U. S. A.* **2007,** *104*, 11865-11866.

2. 10 facts on malaria. http://www.who.int/features/factfiles/malaria/en/index.html (2010).

3. Greenwood, B.; Mutabingwa, T. Malaria in 2002. *Nature* **2002,** *415*, 670-672.

4. Zucker, J. Changing patterns of autochthonous malaria transmission in the United States: A review of recent outbreaks. *Emerging Infect. Dis.* **1996,** *2*, 37-43.

5. Robert, L.; Santos-Chiminera, P.; Andre, R.; Schultz, G.; Lawyer, P.; Nigro, J.; Masuoka, P.; Wirtz, R.; Neely, J.; Gaines, D.; Cannon, C.; Pettit, D.; Garvey, C.; Goodfriend, D.; Roberts, D. *Plasmodium*-infected *Anopheles* mosquitoes collected in Virginia and Maryland following local transmission of *Plasmodium vivax* malaria in Loudoun County, Virginia. *J. Am. Mosq. Control Assoc.* **2005,** *21*, 187-193.

6. Zhou, G.; Minakawa, N.; Githeko, A.; Yan, G. Association between climate variability and malaria epidemics in the East African highlands. *Proc. Natl. Acad. Sci. U. S. A.* **2004,** *101*, 2375-2380.

7. Hoffman, S.; Subramanian, G.; Collins, F.; Venter, J. *Plasmodium*, human and *Anopheles* genomics and malaria. *Nature* **2002,** *415*, 702-709.

8. Schmidt, C. Outsmarting olfaction: the next generation of mosquito repellents. *Environ. Health Persp.* **2005,** *113*, 468-471.

9. Mihalakis, Y.; Renaud, F. Malaria: Evolution in vector control. *Nature* **2009,** *462*, 298-300.

10. Manda, H.; Gouagna, L.; Nyandat, E.; Kabiru, E.; Jackson, R.; Foster, W.; Githure, J.; Beier, J.; Hassanali, A. Discriminative feeding behaviour of Anopheles gambiae s.s. on endemic plants in western Kenya. *Med. Vet. Entomol.* **2007,** *21*, 103-111.

11. Eradication of malaria in the United States (1947-1951). http://www.cdc.gov/malaria/history/eradication_us.htm (2010).

12. Varmus, H.; Klausner, R.; Zerhouni, E.; Acharya, T.; Daar, A.; Singer, P. Grand challenges in global health. *Science* **2003,** *302*, 398-399.

13. Antimalarial drug combination therapy: Report of WHO technical consultation. In *WHO/CDS/RBM/2001.35*, Organization, W. H., Ed. Geneva, 2001.

14. Antimalarial drug policies: data requirements, treatment of uncomplicated malaria and the management of malaria in pregnancy. In Organization, W. H., Ed. WHO/MAL/94.1070: Geneva, 2000.

15. Carey, A.; Wang, G.; Su, C.; Zwiebel, L.; Carlson, J. Odourant reception in the malaria mosquito *Anopheles gambiae*. *Nature* **2010,** *464*, 66-71.

16. Liu, C.; Pitts, R.; Bohbot, J.; Jones, P.; Wang, G.; Zwiebel, L. Distinct olfactory signaling mechanisms in the malaria vector mosquito *Anopheles gambiae*. *PLOS One* **2010,** *8*, 1-17.

17. Fu, G.; Lees, R.; Nimmo, D.; Aw, D.; Jin, L.; Gray, P.; Berendonk, T.; White-Cooper, H.; Scaife, S.; Phuc, H.; Marinotti, O.; Jasinskiene, N. Female-specfic flightless phenotype for mosquito control. *Proc. Natl. Acad. Sci. U. S. A.* **2010,** *107*.

18. McMeniman, C.; Lane, R.; Cass, B.; Fong, A.; Sidhu, M.; Wang, Y.; O'Neill, S. Stable introduction of a Life-Shortening *Wolbachia* Infection into the Mosquito *Aedes aegypti*. *Science* **2009,** *323*, 141-144.

19. Carlier, P.; Anderson, T.; Wong, D.; Hsu, D.; Hartsel, J.; Ma, M.; Wong, E.; Choundhury, R.; Lam, P.; Totrov, M.; Bloomquist, J. Towards a species-selective acetylcholinesterase inhibitor to control the mosquito vector of malaria, *Anopheles gambiae*. *Chem. Biol. Interact.* **2008,** *175*, 368-375.

20. Fryauff, D.; Tuti, S.; Mardi, A.; Masbar, S.; patipelohi, R.; Leksana, B.; Kain, K.; Bangs, M.; Richie, T.; Baird, J. Chloroquine-resistant *Plasmodium vivax* in transmigration settlements of West Kalimantan, Indonesia. *Am. J. Trop. Med. Hyg.* **1998,** *59*, 513-518.

21. Mutabingwa, T.; Nzila, A.; Mberu, E.; Nduati, E.; Winstanley, P.; Hills, E.; Watkins, W. Chlorproguanil-dapsone for treatment of drug-resistant *falciparum* malaria in Tanzania. *Lancet* **2001,** *358*, 1218-1223.

22. N'Fuessan, R.; Corbel, V.; Bonnet, J.; Yates, A.; Asidi, A.; Boko, P.; Odjo, A.; Akogbeto, M.; Rowland, M. Evaluation of indoxacarb, an oxadiazine insecticide for the

control of pyrethroid-resistant *Anopheles gambiae* (*Diptera:Culicidae*). *J. Med. Entomol.* **2007,** *44*, 270-276.

23. Ditzen, M.; Pellegrino, M.; Vosshall, L. Insect odorant receptors are molecular targets of the insect repellent. *Science* **2008,** *319*, 1838-1842.

24. Pickett, J.; Birkett, M.; Logan, J. DEET repels ORNery mosquitoes. *Proc. Natl. Acad. Sci. U.S.A.* **2008,** *105*, 13195-13196.

25. Syed, Z.; Leal, W. Mosquitoes smell and avoid the insect repellent DEET. *Proc. Natl. Acad. Sci. U.S.A.* **2008,** *105*, 13598-13603.

26. Davis, E. Insect repellents: Concepts of their mode of action relative to potential sensory mechansims in mosquitoes (Diptera: Culicidae). *J. Med. Entomol.* **1985,** *22*, 237-243.

27. Hallem, E.; Fox, N.; Zwiebel, L.; Carlson, J. Olfaction: mosquito receptor for human-sweat odorant. *Nature* **2004,** *427*, 212-213.

28. Casida, J. Pyrethrum flowers and pyrethroid insecticides. *Environ. Health Persp.* **1980,** *34*, 189-202.

29. Sexton, J. Impregnated bed nets for malaria control: Biological success and social responsibility. *Am. J. Trop. Med. Hyg.* **1994,** *50*, 72-81.

30. Vais, H.; Williamson, M.; Devonshire, A.; Usherwood, P. The molecular interactions of pyrethroid insecticides with insects and mammalian sodium channels. *Pes Manag. Sci.* **2001,** *57*, 877-888.

31. Insecticide-treated bed nets. http://www.cdc.gov/malaria/malaria_worldwide/reduction/itn.html (2010).

32. Martinez-Torres, D.; Chandre, F.; Williamson, M.; Darriet, F.; Berge, J.; Devonshire, A.; Guillet, P.; Pasteur, N.; Pauron, D. Molecular characterization of pyrethroid knockdown resistance (kdr) in major malaria vector *Anopheles gambiae s.s.* *Insect Mol. Biol.* **1998,** *7*, 179-184.

33. Ranson, H.; Jensen, B.; Vulule, J.; Wang, X.; Hemingway, J.; Collins, F. Identification of a point mutation in the voltage-gated sodium channel gene of Kenyan *Anopheles gambiae* associated with resistance to DDT and pyrethroids. *Insect Mol. Biol.* **2000,** *9*, 491-497.

34. O'Brien, R. *Insecticides, action, and metabolism*. Academic Press: New York, 1967; p 332.

35. Hadaway, A.; Barlow, F. The relative toxicity to adult mosquitos of derivatives of phenyl N-methylcarbamate. *B. World Health Organ.* **1965,** *33*, 129-140.

36. Hadaway, A.; Barlow, F. The toxicity to adult mosquitos and the residual properties of some *N*-acyl N-methylcarbamates. *B. World Health Organ.* **1966,** *35*, 454-458.

37. Hadaway, A.; Barlow, F. Relationships between some physical properties of insecticides and their intrinsic and contact toxicities to adult mosquitos (*Anopheles stephensi*). *B. World Health Organ.* **1966,** *56*, 569-579.

38. Kolbezen, M. J.; Metcalf, R. L.; Fukuto, T. R. Insecticidal activity of carbamate cholinesterase inhibitors. *Agric. Food Chem.* **1954,** *2*, 864-870.

39. Metcalf, R.; Fukuto, T.; Winton, M. Insecticidal carbamates: Comparison of the activities of *N*-methyl and *N,N*-dimethylcarbamates of various phenols. *J. Econ. Entomol.* **1962,** *55*, 345-347.

40. Metcalf, R. L. Structure-activity relationships for insecticidal carbamates. *B. World Health Organ.* **1971,** *44*, 43-78.

41. Metcalf, R. L.; Fukuto, T. R. Effects of chemical structure on intoxication and detoxication of phenyl N-methylcarbamates in insects. *J. Agr. Food Chem.* **1965,** *13*, 220-231.

42. Metcalf, R. L.; Fukuto, T. R. Some effects of molecular structure upon anticholinesterase and insecticidal activity of substituted phenyl N-methylcarbamates. *J. Agr. Food Chem.* **1967,** *15*, 1022-1029.

43. Metcalf, R. L.; Fukuto, T. R.; Frederickson, M. Insecticide activity and structure: Para-substituted meta-xylenyl diethyl phosphates and *N*-methylcarbamates as anticholinesterases and insecticides. *J. Agr. Food Chem.* **1964,** *12*, 231-236.

44. Metcalf, R. L.; Fukuto, T. R.; Frederickson, M.; Peak, L. Insecticidal activity of alkylthiophenyl N-methylcarbamates. *J. Agr. Food Chem.* **1965,** *13*, 473-477.

45. Radic, Z.; Taylor, P. Structure and Function of Cholinesterases. In *Toxicology of Organophosphate & Carbamate Compounds*, Gupta, R., Ed. Elsevier Academic Press: Burlington, MA, 2006; pp 161-186.

46. Silman, I.; Sussman, J. Acetylcholinesterase: 'classical' and 'non-classical' functions and pharmacology. *Curr. Opin. Pharmacol.* **2005,** *5*, 293-302.

47. Gupta, R. C. Introduction. In *Toxicology of Organophosphate and Carbamate Compounds*, Gupta, R. C., Ed. Elevier Academic Press: Burlington, MA, 2006; pp 3-4.

48. Bartolucci, C.; Siotto, M.; Ghidini, E.; Amari, G.; Bolzoni, P. T.; Racchi, M.; Villetti, G.; Delcanale, M.; Lamba, D. Structural determinants of *Torpedo californica*

acetylcholinesterase inhibition by the novel and orally active carbamate based anti-alzheimer drug ganstigmine (CHF-2819). *J. Med. Chem.* **2006,** *49*, 5051-5058.

49. Wong, D. M.; Greenblatt, H. M.; Dvir, H.; Carlier, P. R.; Han, Y.-F.; Pang, Y.-P.; Silman, I.; Sussman, J. L. Acetylcholinesterase complexed with bivalent ligands related to huperzine A: Experimental evidence for species-dependent protein-ligand complementarity. *J. Am. Chem. Soc.* **2003,** *125*, 363-373.

50. Marco, J. L.; Rios, C. d. l.; Garcia, A. G.; Vellarroya, M.; Carreiras, M. C.; Martins, C.; Eleuterio, A.; Morreale, A.; Orozco, M.; Luque, F. J. Synthesis, biological evaluation and molecular modelling of diversely functionalized heterocyclic derivatives as inhibitors of acetylcholinesterase/butyrlcholinesterase and modulators of Ca^{2+} channels and nicotinic receptors. *Bioorganic & Medicinal Chemistry* **2004,** *12*, 2199-2218.

51. Rydberg, E. H.; Brumshtein, B.; Greenblatt, H. M.; Wong, D. M.; Shaya, D.; Williams, L. D.; Carlier, P. R.; Pang, Y.-P.; Silman, I.; Sussman, J. L. Complexes of alkylene-linked tacrine dimers with *Torpedo californica* acetylcholinesterase: Binding of bis(5)-tacrine produces a dramatic rearrangement in the active-site gorge. *J. Med. Chem.* **2006,** *49*, 5491-5500.

52. Bolognesi, M. L.; Andrisano, V.; Bartolini, M.; Cavalli, A.; Minarini, A.; Recanatini, M.; Tumiatti, M. R.; Melchiorre, C. Heterocyclic inhibitors of AChE acylation and peripheral sites. *Farmaco* **2005,** *60*, 465-473.

53. Bolognesi, M. L.; Andrisano, V.; Bartolini, M.; Banzi, R.; Melchiorre, C. Propidium-based polyamine ligands as potent inhibitors of acetylcholinesterase and acetylcholinesterase-induced Amyloid-β aggregation. *J. Med. Chem.* **2005,** *48*, 24-27.

54. Munoz-Ruiz, P.; Rubio, L.; Garcia-Palomero, E.; Dorronsoro, I.; Monte-Millan, M. d.; Valenzuela, R.; Usan, P.; Austria, C. d.; Bartolini, M.; Andrisano, V.; Bidon-Chanal, A.; Orozco, M.; Luque, F. J.; Medina, M.; Martinez, A. Design, synthesis, and biological evaluation of dual binding site acetylcholinesterase inhibitors: New disease-modifying agents for alzheimer's disease. *J. Med. Chem.* **2005,** *48*, 7223-7233.

55. Rosini, M.; Andrisano, V.; Bartolini, M.; Bolognesi, M. L.; Hrelia, P.; Minarini, A.; Tarozzi, A.; Melchiorre, C. Rational approach to discover multipotent anti-alzheimer drugs. *J. Med. Chem.* **2005,** *48*, 360-363.

56. Woltjer, R. L.; Milatovic, D. Therapeutic Uses of Cholinesterase Inhibitors and Neurodegenerative Diseases. In *Toxicology of Organophosphates & Carbamate Compounds*, Gupta, R. C., Ed. Elsevier Academic Press: Burlington, 2006; pp 25-33.

57. Hosokawa, M.; Satoh, T. Structure, function, and regulation of carboxylesterases. In *Toxicology of Organophosphate and Carbamate Compounds*, Gupta, R. C., Ed. Ed. Elsevier Academic Press: Burlington, MA, 2006; pp 219-232.

58. Timchalk, C. Physiologically based pharmacokinetic modeling of organophosphorus and carbamate pesticides In *Toxicology of Organophosphate & Carbamate Compounds*, Gupta, R. C., Ed. Elsevier Academic Press: Burlington, MA, 2006; pp 103-125.

59. Nolte, H.-J.; Rosenburry, T. L.; Neumann, E. Effective charge on acetylcholinesterase active sites determined from the ionic strength dependance of association rate constants with cationic ligands. *Biochemistry* **1980,** *19*, 3705-3711.

60. Sultatos, L. G. Interactions of Organophosphorous and Carbamate Compounds with Cholinesterases. In *Toxicology of Organophosphate & Carbamate Compounds*, Gupta, R. C., Ed. Elsevier Academic Press: Burlington, MA, 2006; pp 209-218.

61. Garcia, S. J.; Aschner, M.; Syversen, T. Interspecies Variation in Toxicity of Cholinesterase Inhibitors. In *Toxicology of Organophosphate & Carbamate Compounds*, Gupta, R. C., Ed. Elsevier Academic Press: Brlington, MA, 2006; pp 145-158.

62. Niu, C.; Xu, Y.; Xu, Y.; Luo, X.; Duan, W.; Silman, I.; Sussman, J. L.; Zhu, W.; Chen, K.; Shen, J.; Jiang, H. Dynamic mechanism of E2020 binding to acetylcholinesterase: A steered molecular dynamics simulation. *J. Phys. Chem.* **2005,** *109*, 23730-23738.

63. Colletier, J.-P.; Fournier, D.; Greenblatt, H. M.; Stojan, J.; Sussman, J. L.; Zaccai, G.; Silman, I.; Weik, M. Structural insights into substrate traffic and inhibition in acetylcholinesterase. *The EMBO Journal* **2006,** *25*, 2746–2756.

64. Gibney, G.; Camp, S.; Dionne, M.; K, M.-Q.; Taylor, P. Mutagenesis of essential functional residues in acetylcholinesterase. *Proc. Nat. Acad. Sci. U.S.A.* **1990,** *87*, 7546-7550.

65. Copeland, R. *Evaluation of enzyme inhibitors in drug discovery: A guide for medicinal chemists and pharmacologists*. John Wiley & Sons, Inc.: Hoboken, New Jersey, 2005; p 271.

66. Satoh, T. Global Epidemiology of Organophosphate and Carbamate Poisonings. In *Toxicology of Organophosphate & Carbamate Compounds*, Gupta, R. C., Ed. Elsevier Academic Press: Burlington, MA, 2006; pp 89-100.

67. Chloropyrifos Facts. In Agency, E. P., Ed. 2002; pp 738-F-01-006.

68. Pauling, L. Molecular architecture and of biological reactions. *Chem. Eng. News* **1946,** *24*, 1375-1377.

69. Henderson, M.; Krueger, S.; Siddens, L.; Stevens, J.; Williams, D. *S*-Oxygenation of the thioether organophosphate insecticides phorate and disulfoton by human lung flavin-containing monooxygenase 2. *Biochem. Pharmacol.* **2004,** *68*, 959-967.

70. Sehlmeyer, S.; Wang, L.; Langel, D.; Heckel, D.; Mohangheghi, H.; Petschenka, G.; Ober, D. Flavin-dependent monooxygenases as a detoxification mechanism in insects: New insights from the Arctiids (Lepidoptera). *PLOS One* **2010,** *5*, e10435.

71. Lotti, M.; Johnson, M. Neurotoxicity of organophosphorus pesticides: Predictions can be based on in vitro studies with hen and human enzymes. *Arch. Toxicol.* **1978,** *41*, 215-221.

72. Schumacher, M.; Camp, S.; Maulet, Y.; Newton, M.; MacPhee-Quigley, K.; Taylor, S. S.; Friedman, T.; Taylor, P. Primary structure of *Torpedo californica* acetylcholinesterase deduced from its cDNA sequence. *Nature* **1986**, 407-409.

73. Sussman, J. L.; Harel, M.; Frolow, F.; Oefner, C.; Goldman, A.; Toker, L.; Silman, I. Atomic structure of acetylcholinesterase from *Torpedo californica*: a prototypic acetylcholine-binding protein. *Science* **1991,** *253*, 872-879.

74. Lushington, G.; Guo, J.; Hurley, M. Acetylcholinesterase: Molecular modeling with the Whole Toolkit. *Curr. Top. Med. Chem.* **2006,** *6*, 57-73.

75. Luo, W.; Yu, Q.-s.; Zhan, M.; Parrish, D.; Deschamps, J. R.; Kulkarni, S. S.; Holloway, H. W.; Alley, G. M.; Lahiri, D. K.; Brossi, A.; Greig, N. H. Novel Anticholinesterases Based on the Molecular Skeletons of Furobenzofuran and Methanobenzodioxepin. *J. Med. Chem.* **2005,** *48*, 986-994.

76. Zeev-Ben-Mordehai, T. S., I.; Sussman, J. L. Acetylcholinesterase in Motion: Visualizing Conformational Changes in Crystal Structures by a Morphing Procedure. *Biopolymers* **2003,** *68*, 395-406.

77. Luo, W.; Yu, Q.-s.; Kulkarni, S. S.; Parrish, D. A.; Holloway, H. W.; Tweedie, D.; Shafferman, A.; Lahiri, D. K.; Brossi, A.; Greig, N. H. Inhibition of human acetyl- and butyrylcholinesterase by novel carbamates of (-)- and (+)- tetrahydrofurofuran and methanobenzodioxepine. *J. Med. Chem.* **2006,** *49*, 2174-2185.

78. Szegletes, T.; Mallender, W.; Rosenberry, T. Nonequilibrium analysis alters the mechanistics interpreatation of inhibition of acetylcholinesterase by peripheral site ligands. *Biochemistry* **1998,** *37*, 4206-4216.

79. Berman, H. M.; Westbrook, J.; Feng, Z.; Gilliland, G.; Bhat, T. N.; Weissig, H.; Shindyalov, I. N.; Bourne, P. E. The Protein Data Bank. *Nucl. Acids Res.* **2000,** *28*, 235-242.

80. Bar-On, P.; Millard, C. B.; Harel, M.; Dvir, H.; Enz, A.; Sussman, J. L.; Silman, I. Kinetic and structural studies on the interaction of cholinesterases with anti-alzheimer drug rivastigmine. *Biochemistry* **2002,** *41*, 3555-3564.

81. Bartolucci, C.; Perola, E.; Cellai, L.; Brufani, M.; Lamba, D. "Back door" opening implied by the crystal structure of a carbamoylated acetylcholinesterase. *Biochemistry.* **1999,** *18*, 5714-5719.

82. Kuhr, R. J.; Dorough, H. W. *Carbamate Insecticides: Chemistry, Biochemistry, and Toxixology*. CRC Press: Cleveland, OH, 1976; p 1-101.

83. Gilson, M.; Straatsma, T.; McCammon, J.; Ripoll, D.; Faerman, C.; Axelsen, P.; Silman, I.; Sussman, J. Open "back door" in a molecular dynamics simulation of acetylcholinesrase. *Science* **1994,** *263*, 1276-1278.

84. Harel, M.; Kryger, G.; Rosenberry, T. L.; Mallender, W. D.; Lewis, T.; Fletcher, R. J.; Guss, J. M.; Silman, I.; Sussman, J. L. Three-dimensional structures of *Drosophila melanogaster* acetylcholinesterase and of its complexes with two potent inhibitors. *Protein Sci.* **2000,** *9*, 1063-1072.

85. Weill, M.; Fort, P.; Bertomieu, A.; Dubois, M.; Pasteur, N.; Raymond, M. A novel acetylcholinesterase gene in mosquitoes codes for the insecticide target and is non-homologous to the ace gene in Drosophila. *Proc. R. Soc. Lond. B* **2002,** *269*, 2007-2016.

86. Gaunt, M.; Miles, M. An insect molecular clock dates the origin of the insects and accords with palaeontological and biogeographic landmarks. *Mol. Biol. Evol.* **2002,** *19*, 748-761.

87. Pezzementi, L.; Rowland, M.; Wolfe, M.; Tsigelny, I. Inactivation of an invertebrate acetylcholinesterase by sulfhydryl reagents: the roles of two cysteines in the catalytic gorge of the enzyme. *Invert. Neurosci.* **2006,** *6*, 47-55.

88. Pang, Y. New acetylcholinesterase target site for malaria mosquito control. *PLOS One* **2006,** *1*, 1-8.

89. Millard, C. B.; Kryger, G.; Ordentlich, A.; Greenblatt, H. M.; Harel, M.; Raves, M. L.; Segall, Y.; Barak, D.; Shafferman, A.; Silman, I.; Sussman, J. L. Crystal structures of aged phosphonylated acetylcholinesterase: Nerve agent reaction products at the atomic level. *Biochemistry.* **1999,** *38*, 7032-7039.

90. Greenblatt, H.; Guillou, C.; Guenard, D.; Argaman, A.; Botti, S.; Badet, B.; Thal, C.; Silman, I.; Sussman, J. The complex of a bivalent derivative of galanthamine with Torpedo acetylcholinesterase displays drastic deformation of the active-site gorge: implications for structure-based drug design. *J. Am. Chem. Soc.* **2004,** *126*, 15405-15411.

91. Haviv, H.; Wong, D. M.; Greenblatt, H. M.; Carlier, P. R.; Pang, Y.-P.; Silman, I.; Sussman, J. L. Crystal packing mediates enantioselective ligand recognition at the peripheral site of acetylcholinesterase. *J. Am. Chem. Soc.* **2005,** *127*, 11029-11036.

92. Morel, N.; Bon, S.; Greenblatt, H.; Belle, D. V.; Wodak, S.; Sussman, J.; Massoulie, J.; Silman, I. Effect of mutations within the peripheral anionic site on the stability of acetylcholinesterase. *Mol. Pharmacol.* **1999,** *55*, 982–992.

93. Weill, M.; Lurfalla, G.; Mogensen, K.; Chandre, F.; Berthomieu, A.; Berticat, C.; Pasteur, N.; Philips, A.; Fort, P.; Raymond, M. Insecticide resistance in mosquito vectors. *Nature* **2003,** *423*, 136-137.

94. Weill, M.; Malcolm, C.; Chandre, F.; Mogensen, K.; Berthomieu, A.; Marquine, M.; Raymond, M. The unique mutation in *ace*-1 giving high insecticide resistance is easily detectable in mosquito vectors. *Insect Mol. Biol.* **2004,** *13*, 1-7.

Chapter 2. The pharmacology and toxicology of carbamate insecticides

As discussed in Chapter 1, AChE is a proven biological target to control the populations of insect species. This chapter will focus on the evaluation of carbamate AChE inhibitors as insecticides. In section 2.1 the methods used to evaluate carbamate inhibition potency and contact toxicity will be reviewed. Section 2.2.1 will review the literature on carbamates for inhibition of *M. domestica* (housefly) AChE and toxicity to this species. In section 2.2.2, a structure-activity-guided approach will be used to evaluate the inhibition potency and contact toxicity of the carbamates toward *An. gambiae*. The synthesis of the carbamates will be described in Chapter 3.

2.1 Biological assays

2.1.1 Enzyme inhibition assays

Enzymatic inhibition potencies of insecticidal phenylcarbamate AChE inhibitors have conventionally been determined by measuring their IC_{50} values against common housefly (*Musca domestica*) AChE.[1-9] Generally, residual AChE activity is measured over a range of inhibitor concentrations after a fixed preincubation period using the colorimetric Ellman Assay. This assay was pioneered in the 1960s and is used throughout the AChE field to measure residual enzymatic activity.[10] Due to its widespread use we have adopted this method to measure the inhibition potencies of our carbamate inhibitors.

Scheme 2.1. The Ellman Assay allows for the calorimetric determination of AChE activity.

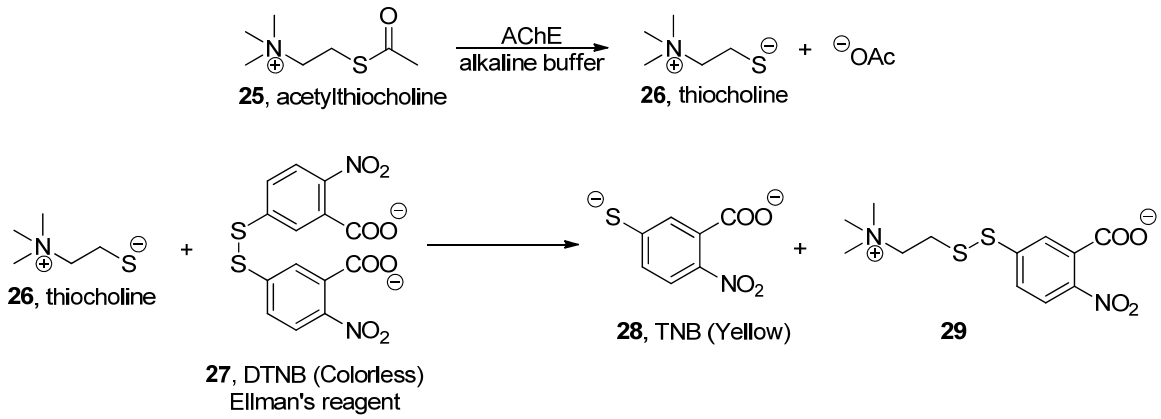

Scheme 2.1 illustrates how AChE processes the pseudosubstrate, acetylthiocholine (**25**, ATCh), generating thiocholine (**26**) and acetate. Thiocholine (**26**) rapidly reacts with (5,5'-dithiobis)-2-nitrobenzoic acid (**27**, DTNB) generating yellow 5-thio-2-nitrobenzoic acid (**28**, TNB) that can be detected by UV-vis spectroscopy (λ = 405 nm). The rate of formation of TNB (**28**) was compared to the hydrolysis of **25** without inhibitor present and both were corrected for background. The reduction in residual AChE activity as a result of phenylcarbamate inhibition gives a direct way to measure the inhibitory potency. One common way to report the inhibition potency of carbamate AChE inhibitors is at the inhibitor concentration necessary to elicit 50% residual activity (IC_{50}). In Chapter 2, all of the IC_{50} values were determined by the Bloomquist group. Professor Jeffrey R. Bloomquist is our major collaborator on the malaria project; he was formerly a member of the Entomology Department of Virginia Tech and is now at the University of Florida.

Since previous investigators had used the IC_{50} value as a measurement of inhibition potency of carbamates towards *M. domestica*,[1-9] the inhibition of *An. gambiae* AChE was initially reported with this parameter. The procedure used to obtain the IC_{50}

value will now be briefly described. Inhibition of AChE (*Ag ace*-1 and *h*AChE) was determined at pH 7.8 at 25 ^{o}C using the Ellman assay.[10] The enzyme was incubated with inhibitors for 10 min prior to addition of DTNB (**27**) and ATCh (**25**); concentrations of DTNB and ATCh were 0.3 and 0.4 mM, respectively at the start of the inhibition studies. Five to seven inhibitor concentrations (run in triplicate) were used to construct dose–response curves (Prism 4, GraphPad Software, San Diego, CA). Recombinant *An. gambiae* AChE (*Ag ace*-1) was provided by Professor Eric Wong (Animal and Poultry Sciences, Virginia Tech) in the form of a centrifuged cell lysate and diluted 10 : 1 with buffer (0.1M sodium phosphate, pH 7.8, containing 0.3% Triton X-100) prior to use. Recombinant human AChE (lyophilized powder, Sigma C1682) was quoted to have a specific activity of 2,790 U/mg.

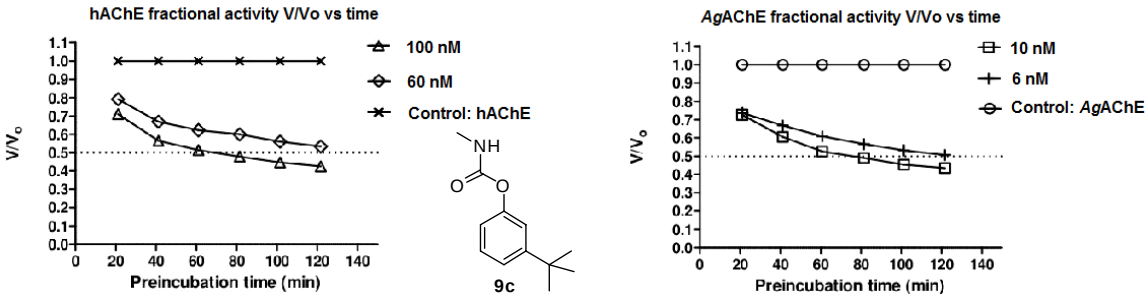

Figure 2.1. Residual velocity of human and *An. gambiae* AChE versus time at various concentrations of lead Class I phenyl *N*-methylcarbamate (**9c**, terbam). Experiments performed by Dr. Dawn Wong of the Carlier Group. The phenyl *N*-methylcarbamates shown within Chapter 2 are numbered **9**.

The progressive inactivation characteristic of carbamate inhibition was clearly demonstrated in Figure 2.1, which shows the effect of preincubation time (t) on residual velocity (v/v_0). At steady state equilibrium (t > 120 min) we can estimate the IC_{50} values of 6 and 60 nM for **9c** against *Ag* and hAChE respectively. The ratio of IC_{50} values ($hIC_{50}/AgIC_{50}$) observed at steady state equilibrium indicated that **9c** was approximately 10-fold selective for *An. gambiae* relative to *h*AChE. Most of the IC_{50} values determined

by the Bloomquist group employed a ten minute preincubation period, and these values provide a convenient and fairly accurate estimate of inhibition potency and target selectivity. Note that if IC_{50} values are measured before attainment of steady state, significantly higher values will be observed.

As demonstrated in Figure 2.1 for the inhibition of *Ag*AChE by phenylcarbamate **9c**, steady state equilibrium was not achieved until approximately 120 minutes. If conducted according to industry standard, IC_{50} values are to be collected at steady state equilibrium. [11, 12] Some measured IC_{50} values were highly variable, leading to some weak structure-activity relationships, as discussed below. The suspect examples were believed to be due in part to the imprecise control of the 10 minute preincubation time. In addition, variable concentrations of dimethylsulfoxide used in the inhibition assays (dilution method A) could also account for some of the variability observed in the measured IC_{50} values.

Despite the widespread use of the IC_{50} reversible inhibition potency criterion in the literature to measure the activity of carbamate inhibitors,[1-9] several factors drew our attention to possible inadequacies of this approach. First, the inhibition of our carbamate inhibitors was measured at the same preincubation reported in the literature (10 min).[1-9] Second, a simple inspection of Scheme 1.1 (Chapter 1) demonstrates that carbamate inhibition of AChE is a multistep process and not simply a reversible association. The most sound experimental approach would seem to involve determination of K_a and k_2 separately, and this approach has been reported in the literature.[11, 12] By deconvoluting binding affinity (K_a, mM^{-1}) from carbamoylation (k_2, min^{-1}) much could be learned regarding the effect of structural variation on these separate events. However, we were

hesitant to take this approach given the time-intensive nature of these experiments and the large number of inhibitors we needed to evaluate.

Finally, during the 10th International Conference on Cholinesterase Biology in Sibenik, Croatia (September 2009), several conferees recommended to that we consider measuring apparent second order rate constants k_i (mM^{-1}, min^{-1}). This parameter explicitly measures the loss of enzymatic activity with time, consistent with the progressive inactivation expected from a pseudo-irreversible carbamate inhibitor. Although measurement of k_i does not allow binding (K_a) and carbamoylation (k_2) to be deconvoluted, its focus on time-dependent inhibition was more justified mechanistically than was IC_{50}, and it has been applied in the literature.

2.1.2 Live mosquito toxicity assay

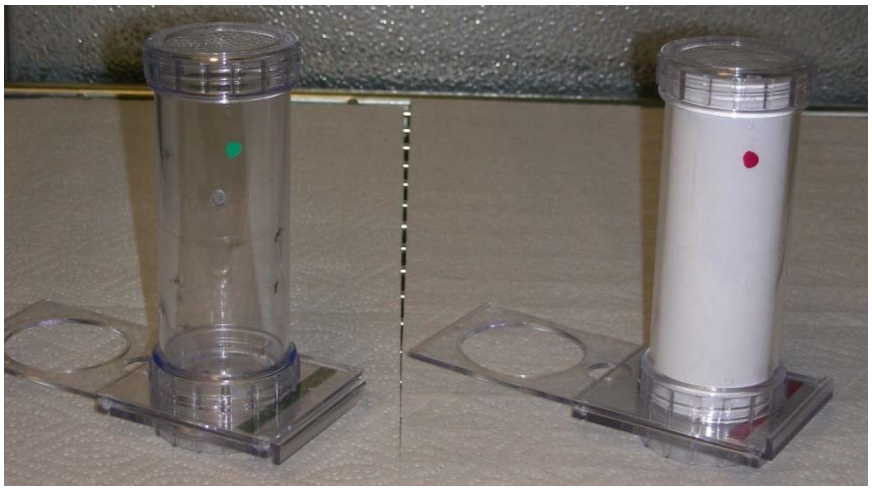

Figure 2.2. The tubes used to conduct the WHO toxicity studies consisted of the holding tube on the left (contains the mosquitoes before and after exposure to the filter paper) and the exposure tube on the right (filter paper treated with phenylcarbarbamate insecticide).

Perhaps the most important factor in determining the efficacy of insecticides is the toxicity to the target insect species. Contact toxicity to *An. gambiae* was assessed using the WHO filter paper protocol on wild type (G3-strain, susceptible) *An. gambiae* mosquitoes.[13] The apparatus in Figure 2.2 was used to determine carbamate toxicity by

exposing twenty five non-blood fed mosquitoes to a pretreated carbamate filter paper for one hour (right tube). After the one hour exposure, the mosquitoes were then transferred to a holding tube free of carbamate insecticides (left tube) where mortality could be calculated at one and twenty-four hour periods. These data were used to extrapolate and report the lethal concentration to induce a percent mortality.

The combination of inhibition potency, mosquito toxicity, and target selectivity data helped guide our research in the direction necessary to discover potentially new and improved insecticides targeting the malaria mosquito, *An. gambiae*. In addition to simply terminating the target species, it was also essential to engineer the mosquitocides to possess minimal mammalian toxicity since they are intended for ITNs. However, before entering a discussion of *An. gambiae* insecticides, I would like to focus on published carbamate insecticide data predominately collected on the inhibition of common housefly (*M. domestica*) AChE.[1-9] In addition, the cited publications also give a frame of reference for the effects of the phenylcarbamate substituent on contact toxicity.[1-9] Before discussing the literature data, I would like to note that error estimates for IC_{50} and LD_{50} were not reported in the literature. Furthermore, the toxicity was expressed in terms of an LD_{50}: the amount of insecticide applied topically to live *M. domestica* that causes 50% mortality. The LC_{50} value will be used to report contact toxicity towards *An. gambiae*.

2.2 Structure activity relationships of carbamates

2.2.1 Enzyme inhibition potency and contact toxicity of phenylcarbamates against *M. domestica* in the literature

Table 2.1. The effects of altering region A on the inhibition potency towards *M. domestica* AChE and toxicity to *M. domestica*.[1, 4]

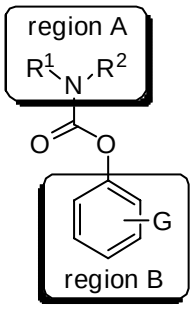

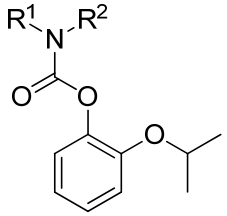

9a (R^1=Me, R^2=H)
30a (R^1=Me, R^2=Me)
31a (R^1=Et, R^2=H)

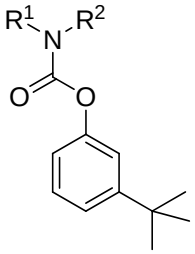

9c (R^1=Me, R^2=H)
30c (R^1=Me, R^2=Me)
31c (R^1=Et, R^2=H)

carbamate	*IC_{50} (nM)[a]*	*LD_{50} (μg/g)*	*IC_{50} (nM)[a]*	*LD_{50}*
9	690	26	400	50
30	13,000	375	1,800	>500
31	ND	ND	20,000	>500

[a] IC_{50} values were determined by Professor Metcalf at 36.5 °C after a 10 minute preincubation period between inhibitor and enzyme.

Previous investigators optimized the carbamate pharamacophore by altering region A (the *N*-substituents) or region B (the *O*-substituent) as shown in the upper left hand corner of Table 2.1. When the *tert*-butylphenyl substituent (region B) was held constant the *N*-methylcarbamate (**9c**, IC_{50} = 400 nM)[4] was a significantly more potent inhibitor of *M. domestica* AChE relative to the *N*,*N*-dimethyl (**30c**, IC_{50} = 1,800 nM)[4] and *N*-ethyl carbamates (**31c**, IC_{50} = 20,000 nM)[1]. Although the *N*-ethylcarbamate analog of propoxur, or **31a**, was not screened for its inhibition potency, the *N*-methylcarbamate **9a** (IC_{50} = 690 nM) was a more potent inhibitor compared with the *N*,*N*-dimethylcarbarbamate **30a** (IC_{50} = 13,000 nM). In addition to the potent AChE inhibition, *N*-methylcarbamates **9a** (LD_{50} = 26 μg/g) and **9c** (LD_{50} = 50 μg/g) were significantly

more toxic than the *N*,*N*-dimethylcarbamates **30a** (LD_{50} = 375 μg/g), **30c** (LD_{50} > 500 μg/g), and *N*-ethylcarbamate **31c** (LD_{50} > 500 μg/g). Among all carbamate insecticides used in agriculture, *N*-methylcarbamates are almost exclusively used due to their potent contact toxicity towards a range of insect species.[1, 4-6]

Metcalf demonstrated that phenyl *N*-methylcarbamates undergo aqueous hydrolysis as much as $10^4 - 10^5$ more rapidly than phenyl *N*,*N*-dimethylcarbamates at pH 7.9.[7] The consequence of the decreased hydrolytic stability of the phenyl-*N*-alkylcarbamates relative to phenyl-*N*,*N*-dialkylcarbamates is also observed in the hydrolysis of the carbamoylated active site S200. For instance, after carbamoylation of human AChE with rivastigmine (**12**), a phenyl-*N*-ethyl *N*-methylcarbamate, only 10% reactivation was observed after 48 hours.[14] Although the *N*,*N*-dialkylcarbamates remain covalently bound to the active site serine for longer periods of time, the *N*-alkylcarbamates are much more potent AChE inhibitors, and confer higher contact toxicity.[1, 4, 6, 15]

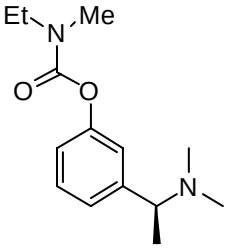

12, rivastigmine

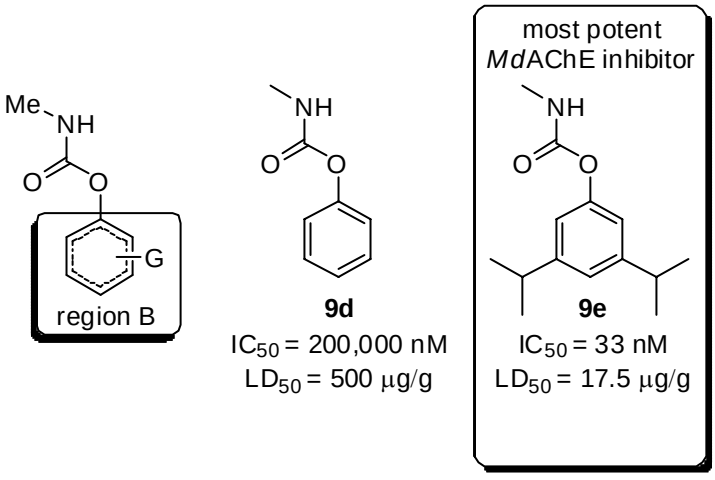

Figure 2.3. Optimization of region B of the carbamate pharmacophore.[6] Incubation period for IC_{50} determination: 10 minutes at 36.5 °C.

Metcalf and Fukuto laid the groundwork for substituent effects around region B of the phenyl *N*-methylcarbamates (Figure 2.3).[1-3, 5-9, 11, 12] Their work paved the way for many of the phenyl *N*-methylcarbamate insecticides in use today. Due to the potent inhibition of *M. domestica* AChE by phenyl *N*-methylcarbamates, region B was optimized with the *N*-methyl (region A) substituent held constant. The inhibition potency of the unsubstituted phenyl *N*-methylcarbamate (**9d**, IC_{50} = 200,000 nM, Figure 2.3) will be used as a reference to compare the effects of substituents on the ring. For comparison purposes the most potent *M. domestica* AChE inhibitor was found to be carbamate **9e** bearing 3,5-diisopropyl functionality (IC_{50} = 33 nM). In addition to a higher inhibition potency observed for **9e**, the contact toxicity observed for **9e** (LD_{50} = 17.5 μg/g) was also significantly greater than for unsubstituted phenyl *N*-methylcarbamate (**9d**, LD_{50} = 500 μg/g).[6]

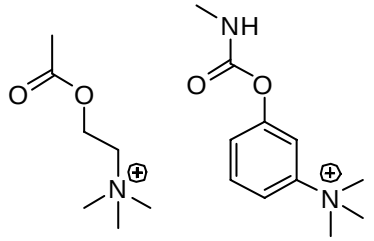

14
acetylcholine

9f, miotine
IC_{50} = 18 nM
LD_{50} = > 500 μg/g

Figure 2.4. Miotine was one of the first carbamates tested for AChE inhibition potency. Incubation period for the IC_{50} determination: 10 minutes at 36.5 °C.[16]

Carbamate **9f** was one of the first phenyl carbamates tested for its AChE inhibition potency.[16] Miotine (**9f**) is an interesting phenyl *N*-methylcarbamate due to the quaternary nitrogen substituent in the C3-position. The permanent positive charge on **9f** resembles the natural substrate, ACh (**14**, Figure 2.4) potentially accounting for miotine's potent inhibition of *M. domestica* AChE (IC_{50} = 18 nM).[6] Recall from Chapter 1 (Figure 1.14) that the manually docked substrate (**14**) within the CAS indicated that the positively charged choline amino group was involved in cation-pi stacking interactions with the choline binding site.[17, 18] The inhibition data suggested that

key binding interactions with the choline binding site (W84) could be contributing to the inhibition potency observed for carbamate **9f**.

Although miotine (**9f**) was a potent inhibitor of *M. domestica* AChE, the LD_{50} value was determined to be greater than 500 μg/g.[6] The high enzyme inhibition potency and extremely low contact toxicity observed for carbamate **9f** were completely divergent. This dichotomy is of key importance to our project as intrinsic AChE inhibitory power may not be the only factor contributing to contact toxicity.[1] Other factors associated with contact toxicity include the i) transfer efficiency of the carbamate from the delivery substrate to the mosquito, ii) penetration efficiency of the carbamate through the cuticle, iii) stability to metabolic degradation *in vivo*, and iv) ability of the insecticide to enter the CNS. [1, 7, 19] It is fundamentally important that phenylcarbamate insecticides not contain charged species such quaternary or protonated nitrogens. Insecticides not compliant with this rule are inherently less toxic due their inability to cross the hydrophobic barriers of the insect cuticle (non-living epidermis on the outer foot of insects) and lipophilic sheath surrounding the nervous system.

We will now discuss some of the important parameters governing the relationship between potent insecticides and functionality around region B of the phenyl *N*-methylcarbamates. Due to the large degree of variety of substituents examined, the Carlier group has regioselectively subdivided the phenyl *N*-methylcarbamates into class I and class II subclasses (Table 2.2). Class I carbamates feature a C3-alkyl substituent whereas class II carbamates have a C2-substituent (where X was equal to a sulfur, oxygen, or carbon).

Table 2.2. Enzyme inhibition potency of alkyl-substituted phenyl *N*-methylcarbamates towards *M. domestica* AChE.[1, 5, 6]

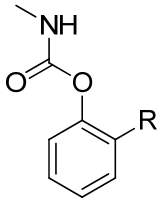

class II

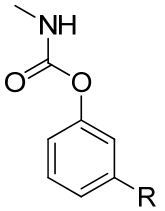

class I

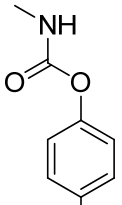

R	*carbamate*	*IC_{50} (nM)*	*carbamate*	*IC_{50} (nM)*	*carbamate*	*IC_{50} (nM)*
Me	**9g**	140,000	**9l**	8,000	**9p**	100,000
Et	**9h**	13,000	**9m**	4,800	**9q**	38,000
i-Pr	**9i**	6,000	**9n**	340	**9r**	70,000
sec-Bu	**9j**	1,100	**9o**	160	**9s**	1,800
tert-Bu	**9k**	6,000	**9c**	400	**9t**	150,000

Preincubation period for IC_{50} determination: 10 minutes at 36.5 ^{o}C.

Class I C3-alkyl carbamates in column II of Table 2.2 (**9l**, **m**, **n**, **o**, and **c**) were potent inhibitors of *M. domestica* AChE relative to the C2-(**9g**, **h**, **i**, **j**, and **k**) and the C4-(**9p**, **q**, **r**, **s**, and **t**) regioisomers.[1, 5, 6] In addition to ideally positioned C3-alkyl substituents, an increase in the molecular volume occupied by the C3-position also corresponded to an increase in the inhibition potency as follows: **9l**, Me (IC_{50} = 8,000 nM) < **9m**, Et (IC_{50} = 4,800 nM) < **9c**, *t*-Bu (IC_{50} = 400 nM) ~ **9n**, *i*-Pr (IC_{50} = 340 nM) < **9o**, *s*-Bu (IC_{50} = 160 nM).[1, 5, 6] The 3-isopropyl (**9n**) and 3-*tert*-butyl (**9c**) phenyl *N*-methylcarbamates were equipotent inhibitors suggesting that going from a secondary C3-center to a tertiary C3-center did not considerably enhance the activity of class I carbamates against *M. domestica* AChE. Among the 2^{o}-alkyl substituted class I phenyl *N*-methylcarbamates examined, **9o** (bearing a *sec*-Bu group) was slightly more potent than **9n** (bearing an isoPr group). Racemic **9o** exhibited the highest activity (IC_{50} = 160 nM) towards housefly AChE of the class I phenyl *N*-methylcarbamates examined.[1, 5, 6]

A similar relationship between increasing the size of the C3-substituent and inhibition potency could not be drawn with respect to toxicity (Table 2.2).[1, 5, 6] In fact, carbamate **9l** (R = CH_3, LD_{50} = 50 μg/g) was equally toxic compared with the *tert*-butyl analog **9c** (LD_{50} = 50 μg/g). Despite the fact that **9l** is a 20-fold weaker inhibitor of *M. domestica* AChE compared with **9c** (Table 2.2) it was still equally toxic (Table 2.3). These data emphasize an important point - enzyme potency is not the only factor determining contact toxicity.[1, 5, 6] Although there was a large degree of variation observed in the inhibition potency of class I carbamates, the contact toxicity observed for the phenyl *N*-methylcarbamates **9l-o**, and **9c** vary only by a factor of three.

Table 2.3. Contact toxicity of class I carbamates against *M. domestica*.[1, 5, 6]

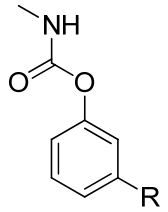

carbamate	*R*	*LD_{50} (μg/g)*
9l	CH_3	50
9m	C_2H_5	140
9n	iso-C_3H_7	90
9o	*sec*-C_4H_9	100
9c	*tert*-C_4H_9	50

Table 2.4. Structure-activity relationship of alkoxy and alkylthio-substituted phenyl *N*-methylcarbamates against *M. domestica*.[3, 9]

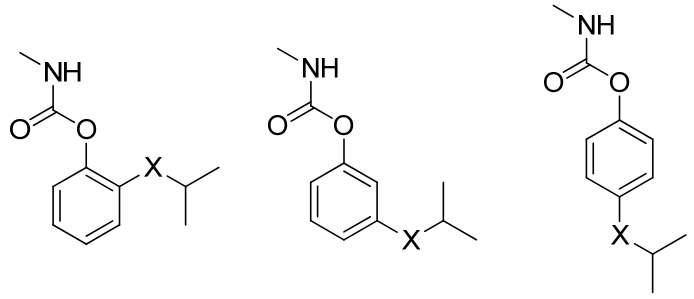

carbamate	*regioisomer*	*X*	*IC_{50} (nM)*	*LD_{50} (μg/g)*
9a	C2-	O	690	26
9t	C3-		9,200	180
9u	C4-		88,000	>500
9v	C2-	S	140	23
9w	C3-		1,800	47
9x	C4-		9,000	700

Preincubation period for the IC_{50} determination: 10 minutes at 36.5 ^{o}C.

Metcalf extended his investigations of phenyl *N*-methylcarbamates to pendant heteroalkyl side chains as shown in Table 2.4.[2, 3, 6, 9] Propoxur (**9a**) is perhaps the most widely known phenyl *N*-methylcarbamate attributed to Metcalf and can be identified by the C2-isopropoxy group. Propoxur is a potent inhibitor of *M. domestica* AChE (**9a**, IC_{50} = 690 nM) and is also highly toxic (LD_{50} = 26 μg/g).[2, 3, 6, 9] A comparison of the C2-(**9a**, IC_{50} = 690 nM) and C3-(**9t**, IC_{50} = 9,200 nM) regioisomers with the C4-regioisomer (**9u**, IC_{50} = 88,000 nM) shows that the isopropoxy group is best positioned at C2.[2, 3, 6, 9] Correspondingly, the LD_{50} values followed the same trend where the C2-regioisomer **9a** (LD_{50} = 26 μg/g) was more toxic than the C3- (**9t**, LC_{50} = 180 μg/g) and C4-regisomer (**9u**, LD_{50} = > 500 μg/g).[2, 3, 6, 9] Metcalf also extended his investigations to alkylthio-substituted phenylcarbamates homologs **9v-x** where the same trend was observed for inhibition potency and contact toxicity: C2-regioisomer (**9v**, IC_{50} = 140 nM, LD_{50} = 23

μg/g) > C3-regioisomer (**9w**, IC_{50} = 1,800 nM, LD_{50} = 47 μg/g) > C4-regioisomer (**9x**, IC_{50} = 9,000 nM, LD_{50} = 700 μg/g). In the examples highlighted in Table 2.4 there is a good correlation between IC_{50} and LD_{50}. Moreover, these results indicate that heteroalkyl substitution is optimal at position C2.

Table 2.5. The effects of branching patterns on inhibition potency and toxicity of class II carbamates against *M. domestica*.[2, 3, 6, 9]

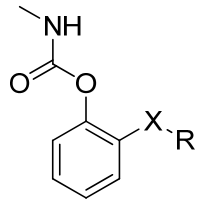

carbamate	*XR*[a]	*IC_{50} (nM)*	*LD_{50} (μg/g)*	*carbamate*	*XR*[a]	*IC_{50} (nM)*	*LD_{50} (μg/g)*
9y		37,000	93	**9ac**		900	49
9z	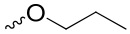	8,700	105	**9ad**	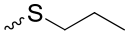	180	20
9a	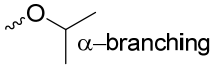	690	26	**9v**	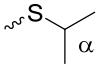	140	23
9aa	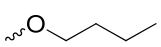	12,000	175	**9ae**	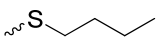	160	34
(±)-**9ab**	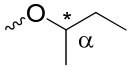	3,100	50	(+)-**9af**	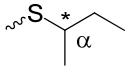	120	38
				(-)-**9af**		80	37
				9ag	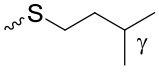	740	270

[a] The greek symbol indicates the location of the branch point. [b] Preincubation period for IC_{50} determination: 10 minutes at 36.5 °C.

The available inhibition potency data and toxicity data for *M. domestica* was assembled in Table 2.5 to highlight the effects of heteroalkyl substitution on the class II alkoxy and alkylthiophenyl *N*-methylcarbamates.[2, 6-9] The effects of substitution will be broken into chain length and types of branching patterns such as straight chain (**9y**, **z**, **aa**, **ac**, **ad** , and **ae**), α-branched (**9a**, **ab**, **v**, and **af**), or γ-branching (**9ag**) subtypes. The effect

of the side chain length and branching patterns on inhibition potency of the 2-alkoxyphenyl *N*-methylcarbamates were as follows: CH_3O (**9y**) < *N*-C_4H_9O (**9aa**) < *N*-C_3H_7O (**9z**) < *sec*-C_4H_9O (**9ab**) < < iso-C_3H_7O (**9a**).[3, 6, 9] Propoxur (**9a**) was the most potent inhibitor and as might be expected, the most toxic of the class II carbamates bearing alkoxy substituents. Unfortunately, there were no examples describing the inhibition of AChE by class II β- and γ-branching 2-alkoxyphenyl *N*-methylcarbamates to compare with *An. gambiae*.

The 2-alkylthiophenyl *N*-methylcarbamates (X = S) were consistently more potent *M. domestica* AChE inhibitors compared to the 2-alkoxyphenyl *N*-methylcarbamates.[2, 6, 9] In fact, the C2-alkylthio homologs listed in Table 2.5 (**9ac**, **ad**, **v**, **ae**, and **ae**) were between 10 to 200-fold more potent than the alkoxy homologs (**9y**, **z**, **a**, **aa**, and **ab** respectively).[2, 6, 9] The resolved *sec*-butylthio enantiomers (+)-**9af** (IC_{50} = 120 nM) and (-)-**9af** (IC_{50} = 80 nM) were the most potent *M domestica* AChE inhibitors of the class II *N*-methylcarbamates. The data collected on AChE inhibition also suggested that there was a strong correlation between secondary-α-branching and high inhibition potency (i.e., **9v**, IC_{50} = 140, (+)-**9af**, IC_{50} = 120 nM, and (-)-**9af**, IC_{50} = 80 nM).[2, 6, 9] In contrast to the secondary-α-branching class II carbamates, the γ-branching carbamate **9ag** (IC_{50} = 740 nM) was one of the least powerful alkylthio-substituted AChE inhibitors examined in Table 2.5.[9]

The 2-alkylthiophenyl *N*-methylcarbamates were also slightly more toxic towards *M. domestica* compared with the 2-alkoxyphenyl *N*-methylcarbamates (Table 2.5). It is interesting to note that the sulfur homolog (**9v**, IC_{50} = 140 nM) of propoxur (**9a**, IC_{50} = 690 nM), was approximately 5-fold more potent towards *M. domestica* AChE.[7] Despite

the enhanced inhibition potency observed for the sulfur homolog **9v** (LD_{50} = 23 μg/g), it was equally toxic to *M. domestica* compared with propoxur (**9a**, LD_{50} = 26 μg/g).[2, 3, 6, 9] Interestingly, the most toxic class II carbamate shown was 2-*n*-propylthiophenyl *N*-methylcarbamate (**9ad**, LD_{50} = 20 μg/g).[9]

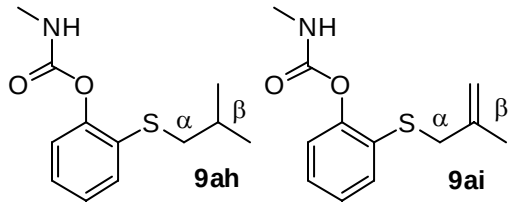

Figure 2.5. β-branching class II phenyl-*N*-methylcarbamates reported in the literature.[20]

Although Metcalf provides no examples of β-branching class II phenyl *N*-methylcarbamates (Figure 2.4), there are two examples of β-branching alkylthiophenyl *N*-methylcarbamates (**9ah-ai**) in a 1963 German patent regarding termites resistant to carbamates (Figure 2.5).[20] Unfortunately, there was no inhibition data reported to compare the β-branching with other 2-alkylthiophenyl *N*-methylcarbamates.

2.2.2 Enzyme inhibition potency and contact toxicity of phenylcarbamates against *An. gambiae*

Prior to our work, examination of carbamate inhibition potency against *An. gambiae* AChE had not been performed. Therefore, it is not surprising that no appreciable target selectivity for *An. gambiae* AChE has ever been demonstrated. As mentioned above in section 2.1, we examined the inhibition potency of these carbamates against both *An. gambiae* and human AChE. The target selectivity reported is calculated as follows: human IC_{50} / *An. gambiae* IC_{50}. When inactivation rate constants were determined the target selectivity is defined as *An. gambiae* k_i / human k_i (Equation 2-1). All k_i values were determined by Dr. Dawn Wong of the Carlier group and the error was propagated according to the equation for quotients (Equation 2-2) or sums (Equation 2-3).[21] Whereas error estimates are explicitly determined for k_i, we estimate $\pm$ 20% error in

the reported IC_{50} and LC_{50} values. In contrast to the low IC_{50} values indicating potent inhibition, high k_i values correspond to more potent AChE inhibitors.

$$\text{Selectivity} = k_i\,(Ag) / k_i\,(\text{human}), \quad (2\text{-}1)$$

$$\text{Propagation of error from quotients} \quad \frac{\Delta f}{fx} = \sqrt{\left(\frac{\Delta x}{fx}\right)^2 + \left(\frac{\Delta y}{fy}\right)^2} \quad (2\text{-}2)$$

$$\text{Propagation of error from a sum)} \quad \Delta f = \sqrt{\Delta x^2 + \Delta y^2} \quad (2\text{-}3)$$

Table 2.6. Insecticidal properties of commercially available carbamates against *An. gambiae*.

	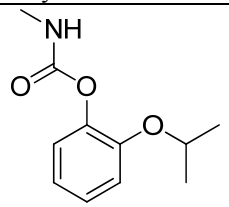 **9a**	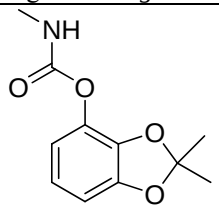 **9b**
An. gambiae hmg IC_{50} (nM)[a]	101 (16-fold)	65 (4-fold)
An. gambiae hmg k_i ($mM^{-1}min^{-1}$)	310 ± 14	870 ± 3.7
Human recomb. k_i ($mM^{-1}min^{-1}$)	17 ± 0.56	110 ± 0.56
Selectivity (*Ag* k_i / h k_i)	(18-fold ± 1.0)	(8-fold ± 0.6)
LC_{50} (mg/mL)[c]	0.037	0.041

[a] human IC_{50} value can be calculated by multiplying the selectivity (in paranthesis) by the *An. gambiae* IC_{50} value (SEM ± 20%). [b] Error in selectivity was calculated according to the propagation of error for quotients with the following equation: *Ag* k_i / h k_i. [c] concentration (mg/mL) of an ethanol solution (2 mL), soaked into a 180 cm^2 filter paper causing % mortality (SEM ± 20%) of *An. gambiae* at 24 h under standard WHO contact toxicity conditions.

Due to the powerful effects of many of the class I and class II phenylcarbamates towards *M. domestica* AChE,[1-9] we began our investigation on known carbamates to examine their effects against *An. gambiae* AChE. Propoxur (**9a**) and bendiocarb (**9b**) are two widely used agricultural insecticides and have been approved by the WHO for IRS. However, no carbamates have been approved for use on ITNs (section 1.1). After testing for the inhibition potency of propoxur (**9a**, IC_{50} = 101 nM, 16-fold) and bendiocarb (**9b**,

IC_{50} = 65 nM, 4-fold), we observed that carbamates **9a** and **9b** were marginally selective for *An. gambiae* relative to human AChE (Table 2.6). Examination of the inhibition potency based on the apparent second order inactivation rate constant (k_i) confirmed that that commercial carbamates **9a** (18-fold) and **9b** (8-fold) were only mildly selective for *An. gambiae* AChE.

A thorough investigation of the structure-activity relationships will be presented in the following sections and compared to that conducted by Metcalf on *M. domestica*. We have expanded upon the known phenylcarbamates and prepared several novel compounds indicated by the * symbol. In agreement with the previous discussion of the carbamates we will begin with optimization of region A, and then discuss the optimization of region B located on the pharmacophore.

Table 2.7. Inhibition potency, target selectivity, and contact toxicity to *An. gambiae* as a result of altering region A of the phenylcarbamate pharmacophore.[22]

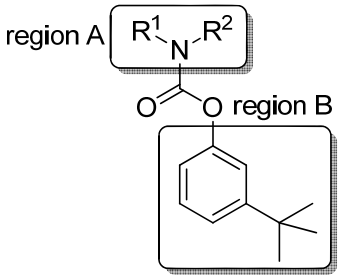

carbamate[a]	R^1	R^2	*IC_{50}, nM*[b] *(selectivity)*	*percent mortality*[c] *(mg/mL)*
9c	Me	H	3.1 (86-fold)	50% @ 0.037
30c	Me	Me	5,900 (0.7-fold)	13% @ 1
31c[d]	Et	H	4,000 (0.6-fold)	100% @ 1
32c*[d]	*N*-hexyl	H	> 100,000 < 0.007-fold)	13% @ 1
33c*	isopropyl	H	540,000 (0.3-fold)	Non-toxic @ 1

[a] Novel carbamates are indicated by the * symbol. [b] IC_{50} (SEM $\pm$ 20%) value measured at room temperature with inhibitor dilution method A. human IC_{50} value can be calculated by multiplying the selectivity by the *An. gambiae* IC_{50} value. [c] Concentration (mg/mL) of an ethanol solution (2 mL), soaked into a 180 cm^2 filter paper causing % mortality (SEM $\pm$ 20%) of *An. gambiae* at 24 h under standard WHO contact toxicity conditions. [d] prepared by Jenna Templeton (undergraduate under the guidance of the author in the Carlier research group).

Although there are differences between *M. domestica* and *An. gambiae* AChE (section 1.3.2), *N*-methyl substitution at region A of the carbamate was essential to the insecticidal activity towards both insect species. When region B was held constant (3-*tert*-butylphenol, Table 2.7), the inhibition potency decreased dramatically when region A of the phenylcarbamate was altered from the *N*-methyl analog (**9c**, IC_{50} = 3.1 nM). For example, the inhibition potency of the *N,N*-dimethyl (**30c**, IC_{50} = 5,900 nM) and *N*-ethyl (**31c**, IC_{50} = 4,000 nM) analogs of **9c** were drastically reduced. Furthermore, the *N,N*-dimethyl (**30c**, 0.7-fold) and *N*-ethyl (**31c**, 0.6-fold) analogs were selective for human relative to *An. gambiae* AChE. Extending the *N*-alkyl substituent from *N*-methyl (**9c**) to the *N*-hexyl (**32c**) homolog resulted in a significant loss in the inhibition potency (IC_{50} > 100,000 nM) towards *An. gambiae* AChE. Moreover, carbamate **32c** was drastically more selective for human AChE (<0.007-fold) relative to other variants of **9c**. The poor inhibition of carbamate **33c** (IC_{50} = 540,000 nM) suggests that like other carbamates occupying larger volumes around region A of the carbamate (eg. **30c-33c**), the bulky *N*-isopropyl substituent was too large to undergo rapid carbamoylation of the active site serine. Not only were carbamates **30c-33c** less potent than **9c** as enzyme inhibitors, they were also significantly less toxic than **9c** (LC_{50}>1 mg/mL and LC_{50} = 0.037 mg/mL respectively). Therefore, the rest of the text will be dedicated to *N*-methylcarbamates where structural modifications were performed on region B of the carbamate.

2.2.2.1 Class I phenyl *N*-methylcarbamates and *An. gambiae*

Table 2.8. The inhibition potency and contact toxicity towards *An. gambiae* of C2-, C3-, and C4-regioisomers of *tert*-butyl *N*-methylcarbamate.

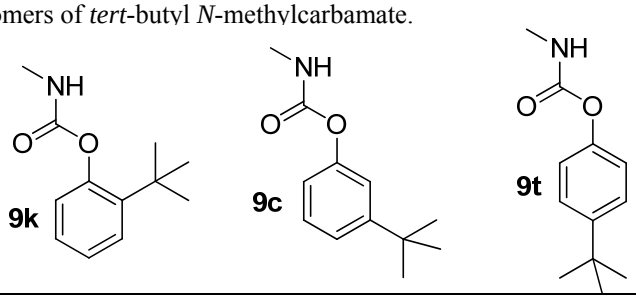

carbamate	*regioisomer*	*IC_{50} (nM)*[a]	*percent mortality (mg/mL)*[b]
9k	C2-	79,000	100% @ 5
9c	C3-	3.1	50% @ 0.037
9t	C4-	72,000	ND

[a] IC_{50} (SEM ± 20%) value collected from homogenate *Ag*AChE. [b] Selectivity defined as *h*AChE IC_{50}/*Ag*AChE IC_{50}. [c] concentration (mg/mL) of an ethanol solution (2 mL), soaked into a 180 cm^2 filter paper (dried 24 h before use) to cause the indicated % mortality (SEM ± 20%) of *An. gambiae* at 24 h under standard WHO contact toxicity conditions (1 hr exposure to treated filter paper followed by transfer to holding tube for 23 hr).

The C2- (**9s**), C3- (**9c**), and C4- (**9t**) regioisomers of *tert*-butylphenyl *N*-methylcarbamate were screened to confirm that the class I C3-regioisomer (**9c**) was also optimal for the inhibition of *An. gambiae* AChE (Table 2.8). Table 2.1 shows that potent inhibition of *M. domestica* AChE resulted from C3-alkyl substituents.[1] A comparison of the C2-(**9k**, IC_{50} = 79,000 nM) and C4-(**9t**, IC_{50} = 71,780 nM) regioisomers indicate that **9k** and **9t** are poor inhibitors of *An. gambiae* AChE relative to the C3-regioisomer (**9c**, IC_{50} = 3.1 nM). Furthermore, the target selectivity for **9k** and **9t** could not be determined, as no measurable inhibition of human AChE was observed at 100,000 nM inhibitor concentration and little inhibition was observed for *An. gambiae* AChE (IC_{50} = 79,000 and 72,000 nM respectively). The contact toxicity was not determined for carbamate **9t**; however, the low inhibition potency suggests that **9t** would also confer low contact toxicity. In addition, the C2-substituted analog **9k** (100% mortality at 5 mg/mL) is likely

less toxic than **9c** (LC_{50} = 0.037 mg/mL) based on the high concentrations necessary to induce 100% mortality.

Table 2.9. Structure-activity relationship of class I phenyl *N*-methylcarbamates against *An. gambiae*.

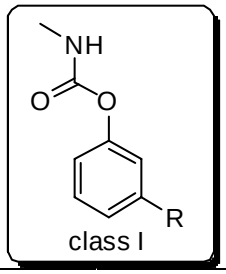

carbamate	*R*	*IC_{50} (hmg, nM)*[a]	*selectivity*[b]	*percent mortality (mg/mL)*[c]
9d	H	39,000	3-fold	ND
9al	Cl	26,000	3-fold	100% @ 1
9am	Br	24,000	4-fold	100% @ 1
9an	I	5,200	13-fold	100% @ 1
9l	Me	4,800	4-fold	100% @ 0.25
9m	Et	630	4-fold	100% @ 1
9ao	Pr	1,500	1-fold	Non-toxic @ 1
9n[d]	Bu	85	16-fold	100% @ 0.5
9o	i-Pr	27	6-fold	100% @ 5
(±)-**9p**	*sec*-Bu	9	2-fold	ND
9c	*tert*-Bu	3.1	86-fold	50% @ 0.037
9ap	*c*-C_6H_{11}	810	15-fold	Non-toxic @ 1
9aq	Ph	18,000	2-fold	ND

[a] IC_{50} (SEM ± 20%) value collected from homogenate *Ag*AChE. [b] Selectivity defined as *h*AChE IC_{50}/*Ag*AChE IC_{50}. [c] Concentration (mg/mL) of an ethanol solution (2 mL), soaked into a 180 cm^2 filter paper (dried 24 h before use) to cause the indicated % mortality (SEM ± 20%) of *An. gambiae* at 24 h under standard WHO contact toxicity conditions. [d] Prepared by Dr. Ming Ma in the Carlier research group.

The IC_{50} values, contact toxicity, and target selectivity for class I phenyl *N*-methylcarbamates have been assembled in Table 2.9 to illustrate substituent effects at the

C3-position. To provide a reference point for the substituent effects at position C3 we will begin our discussion of *Ag*AChE inhibition potency with the unsubstituted phenyl *N*-methylcarbamate (**9d**, IC_{50} = 39,000 nM). Examination of the C3-halophenyl *N*-methylcarbamates revealed that bulky and less-electronegative halogens resulted in higher inhibition potency and selectivity compared to the smaller, more electron withdrawing halogens. As a case and point, 3-iodophenyl *N*-methylcarbamate (**9an**, IC_{50} = 5,200 nM) conferred higher inhibition potency than the 3-bromo (**9am**, IC_{50} = 24,000 nM) and 3-chloro (**9al**, IC_{50} = 26,000 nM) homologs. The results summarized in Table 2.9 indicated that the 3-chloro-(**9al**, 3-fold selective) and 3-bromo-substituted (**9am**, 4-fold) phenyl *N*-methylcarbamates were also less selective for *An. gambiae* AChE compared with the 3-iodo-substituted homolog **9an** (13-fold). All 3-halophenyl *N*-methylcarbamates caused 100% *An. gambiae* mortality at 1 mg/mL under WHO contact toxicity conditions.

Although electronic factors appear to play a role in the inhibition potency of carbamates, class I phenyl *N*-methylcarbamates bearing more lipophilic C3-alkyl substituents were more potent inhibitors of *An. gambiae* AChE relative to the 3-halo analogs (**9al-an**). For example, the smallest class I carbamate 3-methylphenyl *N*-methylcarbamate **9l** (IC_{50} = 4,800 nM, Table 2.9) was a more potent inhibitor of *An. gambiae* AChE than the 3-halo-phenyl *N*-methylcarbamates (**9al-an**). Branched C3-alkyl substituents such as 3-isopropyl (**9o**, IC_{50} = 27 nM), 3-*sec*-butyl (**9p**, IC_{50} = 9 nM), and 3-*tert*-butyl (**9c**, IC_{50} = 3.1 nM) phenyl *N*-methylcarbamates were the most potent inhibitors of *An. gambiae* AChE. This trend suggested that van der Waals interactions could potentially play a large role in the potent inhibition observed for the class I phenyl *N*-

methylcarbamates. However, the larger 3-cyclohexyl group (**9ap**, IC_{50} = 810 nM) conferred lower inhibitory potency relative to other secondary carbamates such as isopropyl-substituted carbamate **9o** (IC_{50} = 27 nM). Aromatic C3-substituents (**9aq**, IC_{50} = 18,350 nM) also had a negative effect on the enzyme inhibition potency relative to the 3-cyclohexyl analog **9ap** (IC_{50} = 810 nM).

Table 2.10. Comparison of insecticidal properties of terbam (**9c**) with butacarb (**9ar**) against *M. domestica* and *An. gambiae*.

	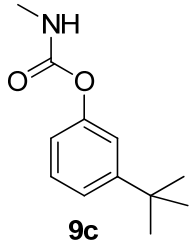 **9c**	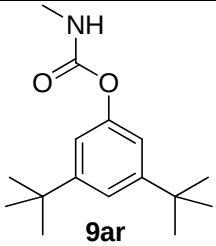 **9ar**
M. domestica hmg IC_{50} (nM)	400	78
LD_{50} (μg/g)	50	39
An. gambiae hmg IC_{50} (nM)	3.1[a] (86-fold)[b]	318[a] (1-fold)[b]
LC_{50} (G3, mg/mL)	0.037	ND

[a] Inhibition potency determined with serial dilution method A. [b] Human IC_{50} value can be calculated by multiplying the selectivity (in paranthesis) by the *An. gambiae* IC_{50} value (SEM $\pm$ 20%).

The most potent inhibitor of *M. domestica* AChE was 3,5-diisopropylphenyl-*N*-methylcarbamate (**9e**, IC_{50} = 33 nM, Figure 2.3).[6] It is not surprising that we also wanted to probe the effects of 3,5-dialkylsubstitution on the inhibition potency and contact toxicity towards *An. gambiae*. Terbam (**9c**) was one of the most promising class I phenyl *N*-methylcarbamate to come out of our studies; therefore, 3,5-*tert*-butylphenyl *N*-methylcarbamate (**9ar**) was a practical target of our investigations. Below, Table 2.10 compares of the insecticidal properties of the 3,5-disubstituted butacarb (**9ar**) with 3-substituted terbam (**9c**).

In contrast to *M. domestica*, the inhibition potency of **9ar** (IC_{50} = 318 nM) against *An. gambiae* AChE (Table 2.10) was drastically reduced from that of **9c** (IC_{50} = 3.1 nM) by a factor of 100. In addition to a resultant decrease in inhibition potency for *An. gambiae*, the 3,5-di-*tert*-butyl groups also resulted in a decrease in target selectivity observed for **9ar** (1-fold) compared with **9c** (86-fold). As previously discussed in section 1.5, *An. gambiae* AChE is encoded by a non-homologous ace-1 gene relative to *M. domestica* (encoded by the ace-2 gene). These differences could account for the divergence observed between the two species and help illustrate the importance of collecting species specific inhibition data to design species specific insecticides. Old insecticide data collected on housefly (*M. domestica*) may be helpful, but it does not indicate equipotent carbamates to combat the spread of malaria.

As a result of the high levels of target selectivity, potent enzyme inhibition, and high contact toxicity observed for carbamate **9c**, we wanted to build a library of analogs that could potentially lead to superior mosquitocides. However, we were surprised that slight modifications to C3-substituent resulted in a significant decrease in the target selectivity based on our IC_{50} determinations. Initially, we expected that a moderate enhancement in the size of the C3-alkyl substituent (**9as-au**) relative to **9c** would have a moderate effect on the target selectivity. However, as Table 2.11 demonstrated below, carbamates **9as**, **at**, and **au*** were only mildly selective for *An. gambiae* AChE. This observation was unexpected and led Dr. Dawn Wong to work out the problems associated with serial dilution method A, which will be discussed in the following paragraph. After developing and optimizing a protocol which we will refer to as serial dilution method C, Dr. Dawn Wong and Professor Jeff Bloomquist coined the phrase “the dimethylsulfoxide

effect" to account for the artificially high selectivity obtained for **9c** (86-fold) with dilution Method A. In contrast to earlier determinations (dilution method A), with serial dilution method C, phenyl *N*-methylcarbamates **9c**, **9as**, **at**, and **au*** were between 8- to 12-fold selective based on IC_{50} values and 5- to 13-fold selective based on the apparent second order inactivation rate constants (k_i). From this point onward we decided to rely on k_i values to assess inhibition potency. However, we have a considerable number of compounds for which k_i values are not available. In these cases we will report IC_{50} values. As will be seen below, in many cases, trends observed with k_i values are reproduced with IC_{50} values.

Table 2.11. The effects of the C3-substituent on the inhibition potency and contact toxicity against *An. gambiae*.

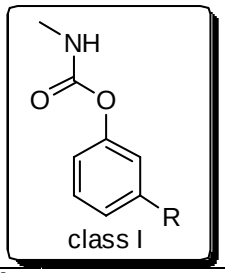

carbamate[a]	***R***	***hmg IC_{50}***[b] ***(nM), dilution method A***	***hmg IC_{50}***[c] ***(nM), dilution method C***	***hmg k_i ($mM^{-1}min^{-1}$)***[d]	***LC_{50} (mg/mL)***[e]
9c	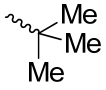	3.1 (86-fold)	16 (12-fold)	1,700 ± 25 (13-fold)	0.037
9as	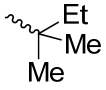	35 (1.4-fold)	3 (12-fold)	5,600 ± 160 (12-fold)	0.068
9at	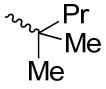	11 (1.1-fold)	7 (8-fold)	6,900 ± 110 (5-fold)	0.240
9au*	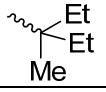	47 (1-fold)[d]	ND	6,100 ± 170 (11-fold)	72% @ 0.25

[a] Novel carbamates are indicated by the * symbol. [b] Serial dilution method A (SEM ± 20%). [c] Serial dilution method C with precisely controlled preincubation periods (SEM ± 10%). [d] Apparent second order inactivation rate constant determined for homogenate *Ag*AChE. [e] Concentration (mg/mL) of an ethanol solution (2 mL), soaked into a 180 cm^2 filter paper (dried 24 h before use) to cause the indicated % mortality (SEM ± 20%) of *An. gambiae* at 24 h under standard WHO contact toxicity conditions.

Attempts by the Bloomquist lab to reproduce the 3.1 nM IC_{50} value and 86-fold target selectivity initially obtained for carbamate **9c** became problematic, and we began to question the consistency of the preincubation periods used to collect the IC_{50} values. Additionally, Dr. Dawn Wong discovered that dilution of the carbamate inhibitors was not being performed according to industry-standard recommendations and will be referred to as serial dilution method A. Serial dilution method A used a 0.1 M dimethylsulfoxide stock solution of inhibitor that was consecutively diluted in 0.1 M sodium phosphate buffer (pH 7.8). The consecutive dilutions into sodium phosphate buffer resulted in an increasingly dilute solution with respect to dimethylsulfoxide. Ideally the dimethylsulfoxide concentration should remain constant, which ultimately led the Carlier group to employ the industry standard dilution protocol. For historical reasons, we call this dilution protocol "dilution method C". With this modified protocol, the 0.1 M dimethylsulfoxide stock solution was consecutively diluted with dimethylsulfoxide. After preparing a range of the desired inhibitor concentrations, they were then diluted with the 0.1 M sodium phosphate buffer to give a range of inhibitor concentrations at constant dimethylsulfoxide (0.1 %). Dilution method C and determination of the apparent second order inactivation rate constants helped confirm that terbam or **9c** (12-13-fold) was much less selective than previously believed based on the determined 86-fold selectivity previously reported (Table 2.11).

The determination of k_i values allowed us to more precisely measure the inhibition potency and selectivity of the carbamates. Higher k_i values correlate with more potent AChE inhibition, in contrast with the IC_{50} values. From these values we were able to learn that an increase in the length of the side chain from *tert*-butyl (**9c**, k_i = 1,700

$mM^{-1}min^{-1}$) to 1,1-dimethylpropyl (**9as**, k_i = 5,600 $mM^{-1}min^{-1}$) caused approximately a 4-fold increase in the rate of inhibition against homogenate *An. gambiae* AChE. Extending the side chain to 1,1-dimethylbutyl (**9at**) further enhanced the rate constant value to 6,900 $mM^{-1}min^{-1}$. Thus C3-substituents larger than *tert*-butyl improved the inhibition potency. Carbamate **9at** (k_i = 6,100 $mM^{-1}min^{-1}$) contained the largest C3 group and was also the most potent inhibitor of *An. gambiae* AChE. Although **9at** was a more powerful inhibitor relative to **9c**, larger C3-substituents had little effect on the target selectivity. For example, carbamate **9au*** (11-fold) and **9as** (12-fold) were determined to have similar selectivity compared to terbam (**9c**, 13-fold).

By increasing the size of the C3 side chain, enzyme inhibition was improved at the expense of *An. gambiae* contact toxicity. Carbamates **9as**, **at**, and **au*** were all more potent *An. gambiae* AChE inhibitors compared with **9c**, but also became less toxic as the C3-substituent grew in volume (**9as**, LC_{50} = 0.068, **9at**, LC_{50} = 0.240, and **9au***, LC_{50} = 72% mortality at 0.25 mg/mL). These contradictory observations were ascribed to metabolic detoxification pathways that can potentially mitigate the effects of carbamate insecticides. Known insecticide detoxification pathways include the oxidation by cytochrome P450s,[23] hydrolysis by carboxylesterases,[24] and degradation by glutathione *S*-transferases.[25] A combination of these destructive pathways could play a role in the decreased contact toxicity of the longer chain analogs (i.e., **9as-au***).

2.2.2.2 Class I fluorine containing phenylcarbamate insecticides

Terbam™ (**9c**) was a commercial carbamate explored in the 1970s as a potential agricultural insecticide.[1, 5, 6] Based on its selectivity calculated from rate constant data (13-fold), terbam was approximately as selective as propoxur (**9a**, 16-fold) towards *An.*

gambiae relative to human AChE. This data suggested that its application on ITNs would have equally harmful effects to mammals as the intended mosquito targets. However, toxicity data collected on the mouse suggested that enzyme selectivity might not be the only parameter conferring high species selectivity.[1, 26] Propoxur (**9a**) and terbam (**9c**) were equally toxic towards *An. gambiae* in the WHO contact toxicity protocol (LC_{50} = 0.037 mg/mL); however, terbam's (**9c**) low toxicity towards the mouse (LD_{50} = 470 mg/kg) relative to that observed for propoxur (**9a**, LD_{50} = 24 mg/kg) distinguish terbam (**9c**) as a superior candidate for ITN application.[1, 26]

Scheme 2.2. Oxidative metabolism pathways observed for terbam (**9c**).[27, 28]

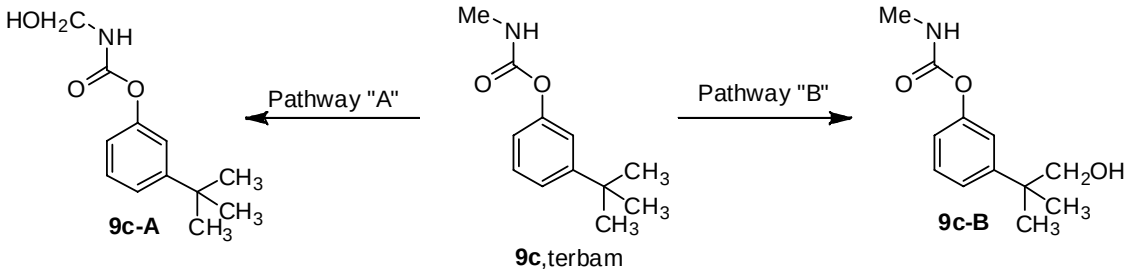

Oxidative metabolism by cytochrome P450-dependent monooxygenases provides a known mechanism for detoxification in insecticides.[23] Scheme 2.2 highlights two known insect oxidative pathways employed to detoxify terbam (**9c**).[27, 28] Pathway "A" leads to oxidation at the *N*-methyl position affording hydroxylated carbamate **9c-A**.[27, 28] Also susceptible are the methyl protons located on the *tert*-butyl center (**9c-B**, pathway "B"). The extended application of insecticides has been directly correlated to the up-regulation of P450 mediated detoxification in resistant *An. gambiae*.[31] Cytochrome P450 mediated oxidation of the *tert*-butyl moiety is a persistent problem within the pharmaceutical industry[29] providing a direct route to detoxify **9c**. Over 100 P450 monooxygenases have been located within the *An. gambiae* genome and are potentially

capable of performing this biological function.[30] Although carbamates **9as**, **at**, and **au*** (Table 2.11) are longer chain analogs of terbam (**9c**), they can presumably undergo a similar oxidation via pathway A or pathway B (Figure 2.10). Oxidative metabolism by cytochrome P450 monooxygenases could provide one explanation for the low toxicity-high enzymatic activity phenomenon. Additionally, inhibition of this destructive metabolic process could provide an opportunity to enhance the contact toxicity of the class I phenyl *N*-methylcarbamate mosquitocides.

Table 2.12. The effects of the PBO synergist on oxidative degradation pathways

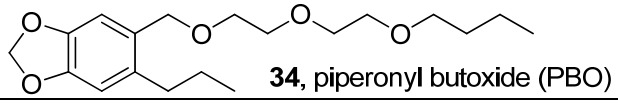

34, piperonyl butoxide (PBO)

	24 h Exposure, LD_{50}, ng/insect (95% CL)		
compound	***LD_{50} alone***	***LD_{50} + PBO***	***(SR)[a]***
propoxur (**9a**)	1.9 (1.5-2.4)	1.3 (1.0-1.6)	1.5
terbam (**9c**)	2.1 (1.6-2.7)	0.96 (0.70-1.2)	2.2

[a] SR = synergist ratio, LD_{50} of phenylcarbamate alone/LD_{50} with synergist. The work shown in Table 2.12 was conducted James Mutunga and Jeffrey Bloomquist.

By co-applying synergists such as pipernoyl butoxide (**34**, PBO), investigators have developed a way to mitigate the effects of P450s and occasionally improve the toxicity of insecticides.[31] To understand the extent of metabolism, James Mutunga (graduate student in the Bloomquist lab) tested propoxur (**9a**) and terbam (**9c**) with and without PBO (**34**, Table 2.12). The synergistic ratio (SR) was defined as the LD_{50} (w/out synergist) / LD_{50} (w/synergist). The higher the number, the greater extent the PBO prevented oxidative metabolism and the more toxic the insecticide. The results indicated that PBO modestly prevented oxidative metabolism for terbam (**9c,** SR = 2.2). The synergistic ratio was slightly lower for propoxur (**9a**, SR = 1.5) suggesting that PBO can

only mildly enhance the toxicity of **9a** and **9c** towards *An. gambiae*. Although these results did not strongly implicate P450-mediated detoxification, we nevertheless attempted chemical modification to reduce oxidation.

Fluorine-containing pharmacophores have been growing in popularity due to their enhanced stability to oxidative metabolism[32] and have successfully been implemented into non-carbamate insecticides currently in use for crop protection.[32] In 2007, Tanaka and coworkers were able to demonstrate that trifluoromethyl containing Neurokinin-1 and TRPV1 antagonists were capable of mitigating the effects of oxidative metabolism relative to the analogs void of fluorine.[29] Additional studies similarly suggest that the replacement of one methyl group of a *tert*-butyl group with a trifluoromethyl group reduces the susceptibility of the other methyl groups towards oxidation.[32, 33] This effect could likewise improve the contact toxicity of terbam (**9c**) by introducing the trifluoromethyl group to carbamates **9c** and **9as**. Since terbam (**9c**) was known to be metabolized via pathway "B" (Scheme 2.2), we had hoped the trifluoromethyl group would inhibit this detoxification pathway. From an economic and pharmacological perspective it was also advantageous to design phenylcarbamates that were inherently stable to oxidation (fluorine-containing phenyl *N*-methylcarbamates). This strategy could provide oxidative stability without the need of a synergist co-applicant.

Table 2.13. Insecticidal activity of the trifluoromethyl bioisosteres of terbam (**9c**).

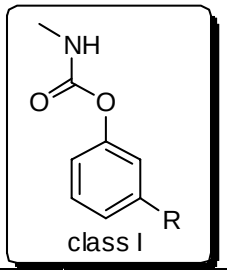

carbamate[a]	*R*	*AgIC$_{50}$ (nM) method A* [b]	*AgIC$_{50}$ (nM) method C* [c]	*hmg k_i ($mM^{-1}min^{-1}$)*[d]	*LC$_{50}$ (mg/mL)*[e]
9c	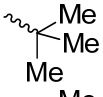	3.1 (86-fold)	16 (12-fold)	1,700 ± 25 (13-fold)	0.037
9av*	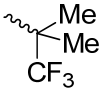	350 (7-fold)	280 (ND)	1,900 ± 28 (14-fold)	0.061
9as	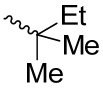	35 (1.4-fold)	3 (12-fold)	5,600 ± 160 (12-fold)	0.068
9aw*	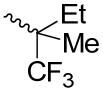	42[d] (2.4-fold)	11 (10-fold)	3,600 ± 62 (10-fold)	0.120

[a] Novel carbamates are indicated by the * symbol. [b] Serial dilution method A (SEM ± 20%). [c] Serial dilution method C (SEM ± 10%). [d] Apparent second order inactivation rate constant determined for homogenate *Ag*AChE. [e] Concentration (mg/mL) of an ethanol solution (2 mL), soaked into a 180 cm^2 filter paper (dried 24 h before use) to cause the indicated % mortality (SEM ± 20%) of *An. gambiae* at 24 h under standard WHO contact toxicity conditions.

Efforts to improve upon the contact toxicity by targeting the oxidative stability of trifluoromethyl bioisosteres (Table 2.13; **9av*** and **9aw***) were unsuccessful. The contact toxicity slightly decreased as a result of the trifluoromethyl groups in carbamates **9av*** and **9aw***. Compared with terbam (**9c**, LC_{50} = 0.037 mg/mL) the contact toxicity observed for the trifluoromethyl homolog (**9av***; LC_{50} = 0.061 mg/mL) was mildly lower. Furthermore, the same slight decrease in contact toxicity was observed for **9aw*** (LC_{50} = 0.120 mg/mL) compared with the trifluoromethyl homolog, carbamate **9as** (LC_{50} = 0.068 mg/mL). Although trifluoromethyl containing homologs **9av*** (k_i = 1,900 $mM^{-1}min^{-1}$) and **9aw*** (k_i = 3,600 $mM^{-1}min^{-1}$) were less toxic to *An. gambiae*, the inhibition potency was relatively unchanged compared with non-fluorine homologs **9c** (k_i = 1,700

$mM^{-1}min^{-1}$) and **9as** (k_i = 5,600 $mM^{-1}min^{-1}$) respectively. In addition, the target selectivity for *An.* gambiae remained relatively unchanged for the fluorine homologs (**9av***, 14-fold; **9aw***, 10-fold) compared to terbam (**9c**, 13-fold). No additional fluorinated class I carbamates were prepared since no enhancement in contact toxicity was observed for the trifluoromethyl containing bioisosteres **9av*** and **9aw***.

2.2.2.3 Class II phenylcarbamate mosquitocides (saturated side chain)

The observation by Metcalf and Fukuto that 2-alkoxy and 2-alkylthiophenyl *N*-methylcarbamates (Table 2.4) were potent *M. domestica* AChE inhibitors, and highly toxic, spawned our interest in these compounds, which we term class II phenyl *N*-methylcarbamates (Table 2.14). The work conducted by Metcalf was also extended by the Carlier group to include carbamate insecticides that have not been previously disclosed (**9ay*-bf***). The inhibition potency (IC_{50}) was also determined using both the homogenate and recombinant enzyme sources to construct an activity profile of straight, branched, cyclic, and aromatic side chains pendant to the C2-position of the phenyl *N*-methylcarbamates. As we will show in the following sections class II phenyl *N*-methylcarbamates could be modified to highly selective and potent *An. gambiae* AChE inhibitors.

Table 2.14. The inhibition potency and contact toxicity of the class II carbamates against *An. gambiae*.

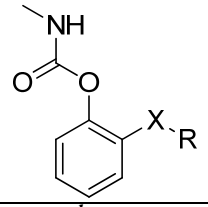

carbamate[a]	*XR*	*IC_{50}*[b] *(hmg, nM)*	*IC_{50}*[c] *(ace-1, nM)*	*percent mortality*[d] *(mg/mL)*
9ac		8,600 (1-fold)	--	--
9ax		240 (> 41-fold)	--	--
9ad	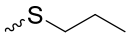	140 (16-fold)	--	--
9ae	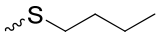	43 (20-fold)	83	100% @ 0.4
9v	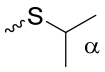	33 (29-fold)	141	100% @ 0.25
9a	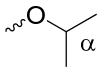	100 (16-fold)	120 (15-fold)	50% @ 0.037
9af	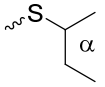	22 (25-fold)	--	100% @ 0.25
9ay*	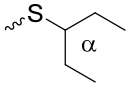	3 (23-fold)	--	100% @ 1
9ah	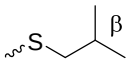	110 (74-fold)	91 (89-fold)	100% @ 1
9az*	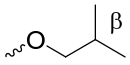	2,100 (32-fold)	650 (100-fold)	100% @ 0.25
9ba*	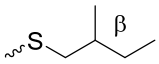	30 (118-fold)	27 (131-fold)	70% @ 1
9bb*	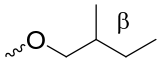	300 (230-fold)	--	100% @ 0.45
9bc*	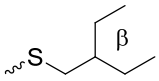	3 (1,200-fold)	3 (1,200-fold)	27 % @ 1
9bd*	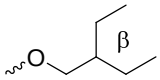	69 (1,400-fold)	10 (9,900-fold)	27% @ 1
9be*	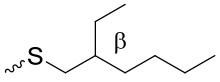	41,000 (0.09-fold)	--	--
9bf*	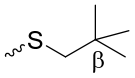	730 (1-fold)	290 (49-fold)	33% @ 1

9ag	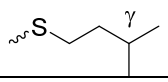	220 (19-fold)	--	0% @ 1

[a] Novel carbamates are indicated by the * symbol. [b] Enzyme inhibition assays determined with serial dilution method A on homogenate *An. gambiae* AChE (SEM ± 20%). [c] Enzyme inhibition assays determined with serial dilution method A on recombinant ace-1 *An. gambiae* AChE (SEM ± 20%). [d] Concentration (mg/mL) of an ethanol solution (2 mL), soaked into a 180 cm^2 filter paper (dried 24 h before use) to causes indicated % mortality (SEM ± 20%) of *An. gambiae* at 24 h under standard WHO contact toxicity conditions.

The IC_{50} values determined for the carbamates listed in Table 2.14 indicated that increasing the length of the C2- side chain from one to four carbons (i.e., **9ac, 9ax, 9ad,** and **9ae**) resulted in greater inhibition potency of *An. gambiae* AChE: n-Bu (**9ae**, IC_{50} = 43 nM) > n-Pr (**9ad**, IC_{50} = 140 nM) > Et (**9ax**, IC_{50} = 240 nM) > Me (**9ac**, IC_{50} = 8,600 nM). The dependence of inhibition potency on the length of the alkyl side chain was also observed with *M. domestica* (Table 2.5). A comparison of the branching patterns associated with butyl-substituted class II carbamates **9ae** (IC_{50} = 43 nM), **9af** (IC_{50} = 22 nM), and **9ah** (IC_{50} = 110 nM) indicated they were potent inhibitors of *An. gambiae* AChE. The β-branching isobutyl analog **9ah** (74-fold) was more selective compared with the *sec*-butyl α-branching **9af** (25-fold) and straight chain butyl **9ae** (20-fold) analogs. High levels of target selectivity were observed for other novel β-branching analogs such as **9az*** (32-fold), **9ba*** (118-fold), **9bb*** (230-fold), **9bc*** (1,200-fold), and **9bd*** (1,400-fold). Extending the side chain to that of 2'-(2-ethylhexyl)-phenyl *N*-methylcarbamate (**9be***, IC_{50} = 41,000 nM, 0.09-fold) resulted in a drastic loss in *An. gambiae* AChE potency and target selectivity, and larger analogs were not examined.

We also envisioned the effects of carbamates with tertiary centers at the β-branch such as carbamate **9bf** (IC_{50} = 730 nM, 1-fold). However, **9bf** was a weak *An. gambiae* AChE inhibitor compared with other class II carbamates shown in Table 2.14. Additionally, **9bf** elicited no target selectivity for *An. gambiae* over human AChE (1-fold

selective). Alternatively, branching at the γ-position rendered the phenylcarbamate **9ag** a poor inhibitor (IC_{50} = 220 nM) with low target selectivity (19-fold) compared with the β-branching analogs.

The high *An. gambiae* to human selectivities observed for β-branching carbamates **9ah** (89-fold), **9az*** (100-fold), **9ba*** (131-fold), **9bc*** (1,200-fold), and **9bd*** (9,900-fold) (recombinant AChE) were quite attractive to us. As discussed in section 2.3.1, terbam (**9c**) was also wrongly believed to be 86-fold selective based on the IC_{50} values determined with serial dilution method A. Consequently, we felt that reexamination of the inhibition potency of the class II phenyl *N*-methylcarbamates was necessary. This included measuring the apparent second order inactivation rate constant with serial dilution method C. The author participated in the determination of the rate constants in Figure 2.6, Table 2.15, and Table 2.17.

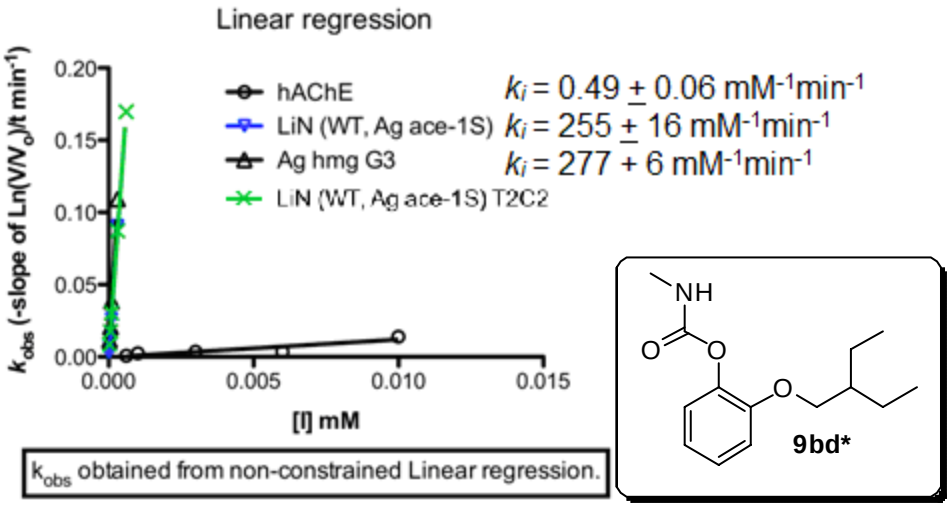

Figure 2.6. The inhibition of human and *An. gambiae* AChE by class II carbamate **9bd***.

The striking levels of target selectivity exhibited by carbamate **9bd*** for *An. gambiae* compared with human AChE is best illustrated in plots shown in Figure 2.6. The four lines correspond to three different enzyme sources: one human and three wild type

An. gambiae (recombinant and homogenate forms). The most noticeable feature of the Figure is the very high slope observed for the three overlapping mosquito lines, and the low slope for the human line. These slopes are reported to the right of the plots and reflect the apparent bimolecular inactivation rate constants (k_i). These lines were constructed in following way: observed inactivation pseudo-first order rate constants (k_{obs}, min^{-1}) were determined by plotting the logarithm of residual velocity ($\ln (v/v_0)$) versus the preincubation time a specified inhibitor concentration ($\ln(v/v_0) = -k_{obs*}t$). A plot of the observed pseudo-first order rate constants k_{obs} versus inhibitor concentration [I] was constructed to demonstrate the expected relationship of the pseudo-first order inactivation rate constants k_{obs} and the apparent bimolecular inactivation rate constant k_i ($k_{obs} = k_{i*}[I]$). As can be seen from Figure 2.6, good linearities and very small Y-intercepts are observed, indicating that the kinetics of inhibition meet our expectation at all three enzymes. Selectivity calculations were performed by dividing the *An. gambiae* k_i value (homogenate, $k_i = 277 \pm 6$ $mM^{-1}min^{-1}$ or recombinant, $k_i = 255 \pm 16$ $mM^{-1}min^{-1}$) by the human k_i value (recombinant, $k_i = 0.49 \pm 0.06$ $mM^{-1}min^{-1}$). The results indicated that while carbamate **9bd*** was no longer 1,400-fold selective based on IC_{50} values, it was still 565-fold (homogenate) and 520-fold (recombinant) selective for *An. gambiae* AChE. Carbamate **9bd*** was the most selective carbamate found throughout the course of my research.

Table 2.15. Target selectivity and inhibition potency of the β-branched class II carbamates determined by the apparent second order inactivation rate constant.

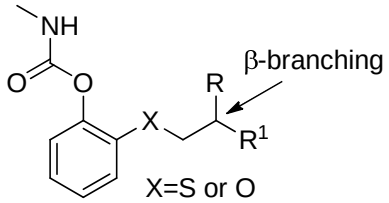

		X = S			*X = O*		
R	***R[1]***	***carbamate[a]***	***Ag k_i, $mM^{-1}min^{-1}$ (selectivity)[b]***	***h k_i, mM^{-1} min^{-1}***	***carbamate[a]***	***Ag k_i, $mM^{-1}min^{-1}$ (selectivity)[b]***	***h k_i, mM^{-1} min^{-1}***
Me	**Me**	**9ah**	ND	ND	**9az***	59 ± 1.0 (90-fold ± 4)	0.65 ± 0.025
Me	**Et**	**9ba***	1,000 ± 22 (60-fold ± 2)	17 ± 0.41	**9bb***	140 ± 4.0 (240-fold ± 11)	0.58 ± 0.024
Et	**Et**	**9bc***	1,800 ± 67 (120-fold ± 5)	15 ± 0.37	**9bd***	280 ± 6 (570-fold ± 72)	0.49 ± 0.062

[a] Novel carbamates are indicated by the * symbol. [b] Error in selectivity was calculated according to the propagation of error for products and quotients with Equation 2-2: *An. gambiae* k_i / human k_i.

The data collected in Table 2.15 indicated that several β-branching class II carbamates were over 100-fold selective based on the inactivation rate constants obtained for carbamates **9az*-bd*.** A trend was observed between the length of the β-branch and inhibition potency. For example, 2'-(2-methylpropoxy)-phenyl *N*-methylcarbamate (**9az***, k_i = 59 $mM^{-1}min^{-1}$, 90-fold) was slightly less potent and less selective than the 2-methylbutyoxyphenyl-*N*-methylcarbamte (**9bb***, k_i = 140 $mM^{-1}min^{-1}$, 240-fold). Furthermore, **9bb*** was a less selective, less potent inhibitor of *An. gambiae* AChE compared with 2-ethylbutoxyphenyl *N*-methylcarbamate (**9bd**, k_i = 280 $mM^{-1}min^{-1}$, 565-fold) which has a slightly longer side chain. A similar trend was observed for the analogous alkylthio-substituted carbamates **9ba*** and **9bc*** (Table 2.15). Although the oxygen homologs **9bb*** (236-fold) and **9bd*** (565-fold) were more selective inhibitors compared with the sulfur homologs **9ba*** (60-fold) and **9bc*** (120-fold) respectively, the inactivation rate constants (k_i) illustrated in Table 2.15 indicated that the sulfur homologs

9ba* (k_i = 1,000 $mM^{-1}min^{-1}$) and **9bc*** (k_i = 1,800 $mM^{-1}min^{-1}$) were significantly more potent *An. gambiae* AChE inhibitors. The carbamate can adopt a different conformation depending on the atom pendant to the aromatic ring. We have examined C-X-C groups where X was oxygen, sulfur, or a methylene unit. Changes to the C2-substituent could impact binding due to changes in the C-X-C bond angles and torsions to the aromatic ring.

Our modeling collaborators at Molsoft have searched for a structural explanation for the high selectivities observed for select Class II carbamates. Unfortunately, no single human to *An. gambiae* mutation can explain these selectivities. Rather, *in silico* models suggest that within the gorge a conserved helix is displaced in *An. gambiae* relative to human AChE (Figure 2.7). This displacement is due to the presence of additional bulky tyrosines (Y327 and Y333, instead of human S336 and G342; note that these residue side chains are not shown in Figure 2.7) at both ends of the helix that do not directly participate in ligand interactions. Our collaborators have proposed that that this displacement widens the gorge and allows the larger carbamates to occupy this volume in *An. gambiae* AChE. In contrast, these compounds cannot fit well within the gorge of human AChE, leading to poor inhibition potency of these compounds to human AChE.

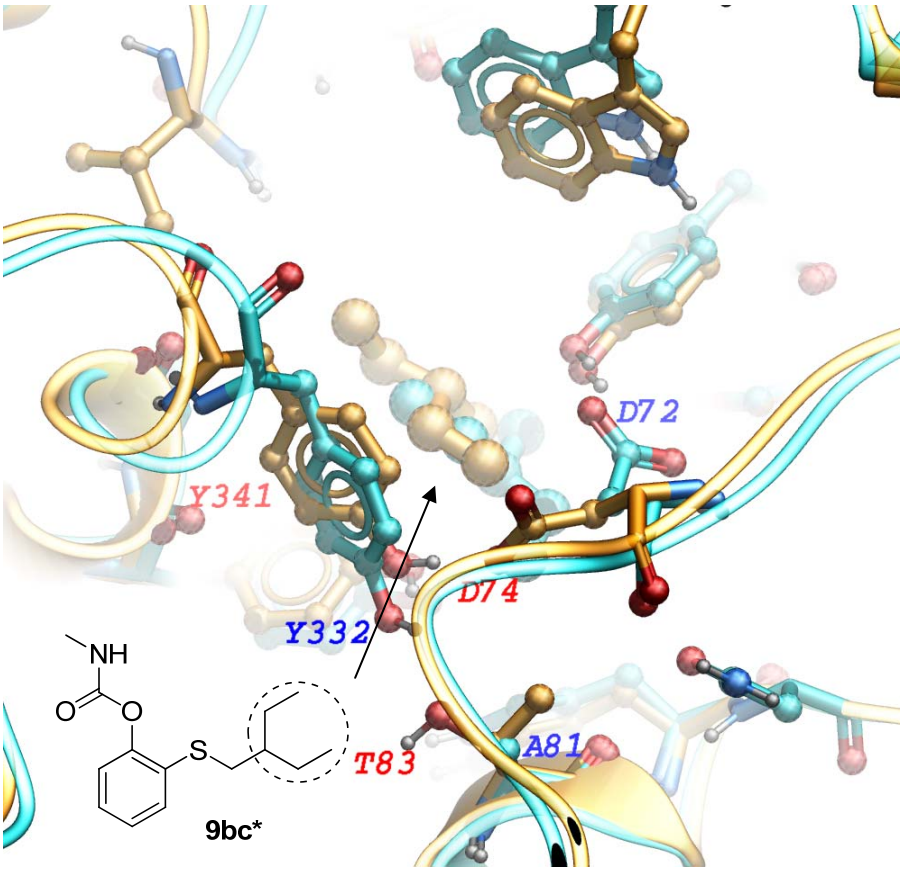

Figure 2.7. Molecular modeling of manually docked carbamate **9bc*** within the active site of *An. gambiae* and human AChE indicates that the selectivity of Class II carbamates is derived from a helical displacement. The *An. gambiae* AChE is colored cyano and the human AChE is colored gold. This graphic was contributed by our collaborators at Molsoft (Polo Lam and Max Totrov)

The helical displacement in *An. gambiae* relative to human AChE shifts the protein backbone and ultimately effects carbamate binding. In the center of Figure 2.7, represented by cyano-colored ball and sticks (*An. gambiae* bound **9bc***) or gold-colored ball and sticks (human bound **9bc***), is manually docked carbamate **9bc***. As indicated in the lower left hand portion of Figure 2.7, the side chain on carbamate **9bc*** is protruding into the gorge where the helical displacement is located. A pair of conserved tyrosines (*An. gambiae*, Y332; human, Y341) located on the helix play a role in the selective binding of the Class II carbamates. The measured α-C distances between Y332 (*An. gambiae*) and Y341 (human) was determined to be 1.0 Å, which is a significant

displacement in *An. gambiae* relative to human AChE (Figure 2.7). These key residues (Y332 and Y341) are located at the mouth of the gorge. In Figure 2.7 the D72 (*An. gambiae*), located at the peripheral site, is flipped 180 degrees in human AChE (D74). Although this is a provisional explanation, the modeling suggests that the displacement of the helix within the gorge shifts key residues that favor enzyme-ligand interactions between Class II carbamates and *An. gambiae* AChE.

Table 2.16. The inhibition potency observed for the β-branched conformationally constrained alkylthio-substituted carbamates.

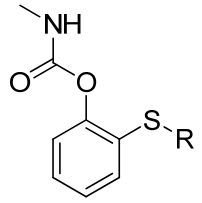

carbamate[a]	*SR*	*IC_{50} (nM)*[b]
9bc*	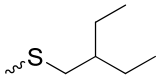	3
9bg*	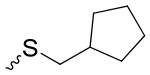	1,100
9bh*	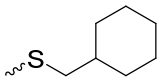	18,000

[a] Novel carbamates are indicated by the * symbol. [b] Homogenate *An. gambiae* AChE used in inhibition assays employing dilution method A (SEM ± 20%). The contact toxicity for **9bg*** and **9bh*** was not determined.

A comparison of the IC_{50} data collected for **9bc*** and the conformationally constrained analogs **9bg*** and **9bh*** indicated that cyclization of the 2-ethylbutyl side chain had devastating effects on the inhibitory potency towards *An. gambiae* AChE (Table 2.16). Although the inactivation rate constants for sulfur homologs **9bg*** and **9bh*** were not determined, the IC_{50} values indicated that **9bg*** (IC_{50} = 1,100 nM) and **9bh*** (IC_{50} = 18,000 nM) were very poor inhibitors relative to the open chain analog **9bc*** (IC_{50} = 3 nM). The contact toxicity was not determined for carbamates **9bg*** and **9bh***.

Table 2.17. Inhibition potency and target selectivity of the β-branched conformationally constrained alkoxy-substituted carbamates.

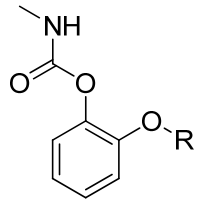

carbamate[a]	*OR*	*Ag k_i, ($mM^{-1}min^{-1}$)*[b]	*human k_i, ($mM^{-1}min^{-1}$)*	*(selectivity)*[c]
9bd*	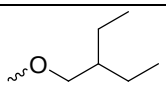	280 ± 11	0.49 ± 0.062	570-fold ± 75
9bi*	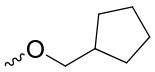	11 ± 0.15	0.27 ± 0.027	41-fold ± 4
9bj*	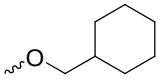	0.51 ± 0.03	0.21 ± 0.041	2-fold ± 0.4

[a] Novel carbamates are indicated by the * symbol. [b] Homogenate *An. gambiae* AChE was used in the inhibition assays with serial dilution method C. [c] Selectivity defined as *Ag* k_i / h k_i. Error in selectivity was calculated according to the propagation of error for products and quotients with Equation 2-2: *An. gambiae* k_i / human k_i. The contact toxicity for carbamates **9bi*** and **9bj*** was not determined.

As a result of higher levels of target selectivity of oxygen homolog **9bd*** relative to the sulfur homolog **9bc*** (Table 2.15), the inactivation rate constants were determined for conformationally constrained alkoxy-substituted homologs **9bi*** (k_i = 11 $mM^{-1}min^{-1}$, 41-fold) and **9bj*** (k_i = 0.51 $mM^{-1}min^{-1}$, 2-fold). Compared with the open chain conformer **9bd*** (k_i = 280 $mM^{-1}min^{-1}$, 570-fold), the conformationally constrained carbamates **9bi*** and **9bj*** were poor AChE inhibitors and much less selective for *An. gambiae* relative to human AChE (Table 2.17). Furthermore, the loss of inhibition potency and target selectivity was greater for the larger cyclohexylmethyl carbamate **9bj*** relative to the smaller cyclopentylmethyl carbamate **9bi***. The contact toxicities of the conformationally constrained analogs **9bi*** and **9bj*** were not determined.

Recall from Table 2.11 and Table 2.13 that a mild decrease in *An. gambiae* toxicity resulted from an increase in the chain length of the C3-substituent. The contact

toxicity data collected on class II carbamates suggested that the same was true for the highly selective β-branching carbamates listed in Table 2.15. For example, the C2-isobutoxy-substituted carbamate **9az*** (LC_{50} = 0.25 mg/mL) elicited high levels of contact toxicity. Conversely, the 2'-(2-ethylbutoxy) analog **9bd*** caused only 27% mortality at 1 mg/mL indicating that **9bd*** was much less toxic than the shorter chain analog **9az***. It is possible that the extended side chains make phenyl *N*-methylcarbamates more susceptible to oxidative metabolism and potentially better substrates for carboxylesterases[24] or glutathione *S*-transferases[25] which are subject to future investigations.

Scheme 2.3. Potential destructive oxidation causing the decreased inhibition potency and contact toxicity of the sulfur containing class II carbamates.

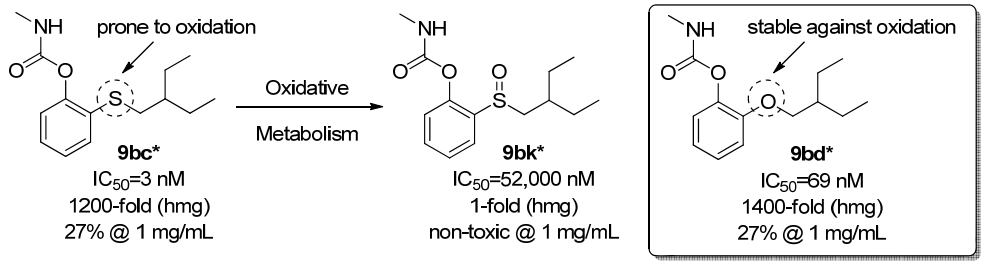

The class II carbamate with the highest level of contact toxicity was determined to be propoxur (**9a**, LC_{50} = 0.037 mg/mL). Compared to propoxur (**9a**), carbamate **9v** (LC_{50} = 0.25 mg/mL), or the alkylthio-substituted equivalent is not as toxic to *An. gambiae* (Table 2.15). The decreased toxicity of the sulfur relative to oxygen homologs was observed in many cases when the proximal side chain was held constant (eg. **9ba*-bd***). The persistently low toxicity of the alkylthio relative to alkoxy class II carbamates is possibly due to the oxidation of the sulfide to the sulfoxide *in vivo* (Scheme 2.3, **9bc*** to **9bk***). We synthetically prepared the sulfoxide (**9bk***) and found that it was significantly

less active at the enzyme level (IC_{50} = 52,000 nM) with no measurable contact toxicity at 1 mg/mL. The higher levels of contact toxicity observed for the class II alkoxyphenyl *N*-methylcarbamates relative to the alkylthio homologs could be a result of the oxidative stability of the arylether substituent within **9bd*** compared to the sulfide linkage observed in **9bc***.

Table 2.18. The C2-carbon analogue (**9bl***) of highly selective carbamates **9bc*** and **9bd*** and its effects on inhibition potency and contact toxicity.

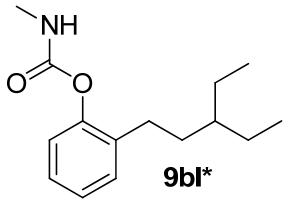

9bl*

carbamate[a]	*Ag k_i, $mM^{-1}min^{-1}$* [b]	*h k_i, $mM^{-1}min^{-1}$*	*(selectivity)*[c]	*percent mortality (mg/mL)*[d]
9bl*	75 ± 3.0	0.75 ± 0.03	100-fold ± 6	0% @ 1

[a] Novel carbamates are indicated by the * symbol. [b] Serial dilution method C was employed in the inhibition assays with homogenate AgAChE. [c] Selectivity defined as *Ag* k_i / h k_i. Error in selectivity was calculated according to the propagation of error for products and quotients with Equation 2-2: *An. gambiae* k_i / human k_i. [d] Concentration (mg/mL) of an ethanol solution (2 mL), soaked into a 180 cm^2 filter paper (dried 24 h before use) to cause the indicated % mortality (SEM ± 20%) of *An. gambiae* at 24 h under standard WHO contact toxicity conditions.

The 2'-(2-ethylpentyl)-substituent observed in carbamate **9bl*** mimicked the highly selective C2-oxygen (**9bd***) and C2-sulfur (**9bc***) analogs shown in Table 2.15. However, **9bl*** (k_i = 75 $mM^{-1}min^{-1}$) was measurably less potent compared with carbamates **9bc*** (k_i = 1,800 $mM^{-1}min^{-1}$) and **9bd*** (k_i = 280 $mM^{-1}min^{-1}$). In addition, carbamate **9bl*** (100-fold) was marginally less selective than the sulfur containing analog (**9bc***, 120-fold), but greater than 5-fold less selective than the oxygen analog (**9bd***, 565-fold). The hydrogen bonding ability of the C2-oxygen (**9bd***) could play a role in its selectivity since the sulfur (**9bc***) and carbon (**9bl***) analogs cannot act as hydrogen

bonding acceptors. Like many of the highly selective β-branching class II phenyl *N*-methylcarbamates (Table 2.18), **9bl*** was also non-toxic to *An. gambiae* at 1 mg/mL.

Table 2.19. Mosquitocidal properties of the α, β-branched phenyl *N*-methylcarbamates.

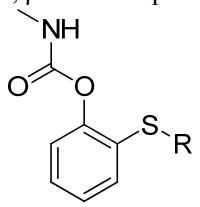

carbamate[a]	*R*	*IC_{50} (hmg, nM)*[b]	*percent mortality (mg/mL)*[c]
(±)-9bm*	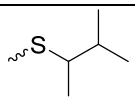	10 (243-fold)	100% @ 1
(mixed diastereomers)-9bn*	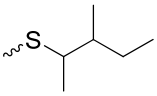	11 (113-fold)	6% @ 1
(±)-9bo*	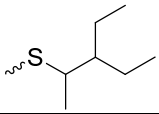	1,257 (79-fold)	7% @ 1

[a] Novel carbamate are indicated by the * symbol. [b] IC_{50} value collected from homogenate *Ag*AChE with serial dilution method A (SEM ± 20%). Parentheses represent the selectivity which is defined as *h*AChE IC_{50}/*Ag*AChE IC_{50}. [c] Concentration (mg/mL) of an ethanol solution (2 mL), soaked into a 180 cm^2 filter paper (dried 24 h before use) to cause the indicated % mortality of *An. gambiae* at 24 h under standard WHO contact toxicity conditions (SEM ± 20%).

Propoxur (**9a**) is understandably one of the most widely used carbamate insecticides due to its potent contact toxicity to a variety of insect species.[2, 3, 6, 9] The potent toxicity profile of propoxur (**9a**), a class II carbamate, is likely a function of the C2-isopropoxy group. In contrast to the α-branching secondary center observed in propoxur (**9a**), the β-branched class II phenylcarbamates **9bc*** (120-fold) and **9bd*** (565-fold) conferred higher levels of selectivity at the expense of contact toxicity (**9bc*** and **9bd*** caused 27% mortality of wild type *An. gambiae* at 1 mg/mL, Table 2.15). We envisioned that the α- and β-branches pendant at the C2-position (**9bm***, **9bn***, and **9bo***, Table 2.19) could potentially capitalize on the merits of both α-(high levels of contact toxicity) and β-branching (high levels of target selectivity). An examination of Table 2.19

indicated that **(±)-9bm*** (IC_{50} = 10 nM) and **9bn*** (mixed diastereomers, IC_{50} = 11 nM) are highly selective (243- and 113-fold respectively) and potent inhibitors of *An. gambiae* AChE. In contrast to **9bm*** and **9bn***, the larger C2-substituent observed in carbamate **9bo*** (IC_{50} = 1,257, 79-fold) had a negative effect on both inhibition potency and target selectivity. Although mild contact toxicity was observed for carbamates **9bm*** (100% mortality at 1 mg/mL), **9bn*** (6% mortality at 1 mg/mL) and **9bo*** (7% mortality at 1 mg/mL) were only mildly toxic to *An. gambiae*. Currently the IC_{50} values are the only available measurement of inhibition potency for carbamates **9bl*-bn***. Due to the potent inhibition of **9bm* - 9bo***, the oxygen analogs deserve future examination.

2.2.2.4 Class II phenylcarbamate mosquitocides (allyl side chain)

In addition to the saturated alkylthio- and alkoxy-substituted carbamates previously described in Table 2.15, we also evaluated the inhibition potency, target selectivity, and contact toxicity of the class II carbamates bearing C2-allythio and allyloxy side chains (**9bp**, **9ai**, **9bq*-bw,** Table 2.20). Although many of the β-branching carbamates were only mildly toxic (eg. **9az*-9bd***), the β-branching methyallyl-substituted carbamate **9ai** caused 100% *An. gambiae* mortality at 0.25 mg/mL. In addition, the β-branched 2-methallylthio-substituted carbamate **9ai** (Table 2.20) showed promise due to its high level of selectivity for *An. gambiae* AChE (77-fold) while still retaining a reasonable level of toxicicity. The saturated analog **9ah** (IC_{50} = 110 nM, 74-fold selective, Table 2.14) provides a comparison with the unsaturated homolog **9ai** (IC_{50} = 124 nM, 77-fold selective), which was determined to have an equivalent IC_{50} value and target selectivity for *An. gambiae* AChE. In contrast to carbamate **9ah** (100% mortality at 1 mg/mL), the carbamate bearing the unsaturated side chain (**9ai**) caused 100% mortality

at 0.25 mg/mL. Carbamate **9ai** provided further support that side chains branching in the β-position conferred the highest degree of target selectivity for *An.gambiae* AChE.

Table 2.20. Effects of an unsaturated side chain on the insecticidal activity of class II carbamates.

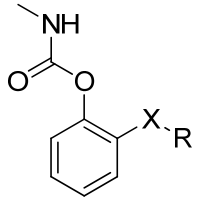

carbamate[a]	*XR*	*IC_{50} (hmg, nM)*[b]	*IC_{50} (ace-1, nM)*[c]	*percent mortality (mg/mL)*[d]
9bp	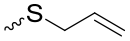	160 (10-fold)	40 (44-fold)	100% @ 0.5
9ai	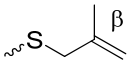	120 (77-fold)	170 (58-fold)	100% @ 0.25
9bq*	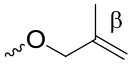	1,500 (46-fold)	ND	ND
9br	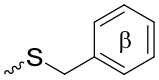	6,900 (2-fold)	3,800 (4-fold)	0% @ 1
9bs	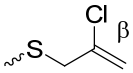	110 (27-fold)	260 (12-fold)	93%@1
9bt*	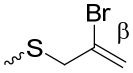	250 (7-fold)	170 (10-fold)	0% @ 1
9bu	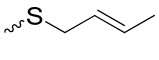	60 (9-fold)	70 (7-fold)	93% @ 0.5
9bv*	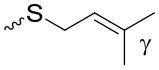	1,200 (2-fold)	400 (7-fold)	100% @ 5
9bw*	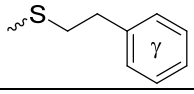	6,900 (2-fold)	ND	0% @ 1

[a] Novel carbamates are indicated by the * symbol. [b] Enzyme inhibition assays determined with serial dilution method A on homogenate *An. gambiae* AChE (SEM ± 20%). [c] Enzyme inhibition assays determined with serial dilution method A on recombinant ace-1 *An. gambiae* AChE (SEM ± 20%). [d] Concentration (mg/mL) of an ethanol solution (2 mL), soaked into a 180 cm^2 filter paper (dried 24 h before use) to causes indicated % mortality (SEM ± 20%) of *An. gambiae* at 24 h under standard WHO contact toxicity conditions.

The β-methyl group on the side chain of **9ai** played a key role in the high target selectivity measured for *An. gambiae* AChE relative to allylthiophenyl *N*-methylcarbamate **9bp** (10-fold, β-methyl group not present). Although the β-methyl group observed in carbamate **9ai** (IC_{50} = 120 nM) conferred high levels of target

selectivity, it did not appear to have much of an effect on the inhibition potency relative to unsubstituted carbamate **9bp** (homogenate *An. gambiae* IC_{50} = 160 nM). Unlike branching in the β-position, methyl branching in the γ-position had a negative effect on the inhibition potency of **9bv*** (IC_{50} = 1,200 nM) and **9bw*** (IC_{50} = 6,900 nM) relative to the straight chain allylic **9bp** (IC_{50} = 160 nM) and β-branching (**9ai**, IC_{50} = 120 nM) carbamates.

Similar to aromatic substitution at the C3-position (**9ap**, Table 2.6), an aromatic group pendant to the C2-position also have a negative effect on inhibition potency. Carbamates bearing a homobenzylic (**9bw***, IC_{50} = 6,900 nM) or benzylic (**9br,** IC_{50} = 6,900 nM) side chain were the poorest inhibitors of *An. gambiae* AChE in Table 2.20. Despite the lengthening of the C2-substituent by one carbon, the inhibition potency of the **9bw*** (IC_{50} = 6,900 nM) was nearly identical to the **9br** (IC_{50} = 6,900 nM). It is possible that the larger volume occupied by carbamates **9br** and **9bw** relative to **9ai** could account for the loss in inhibition potency. The carbamates bearing a vinylic chlorine (**9bs**) and vinylic bromine (**9bt***) were prepared based on the structure of **9ai**, to see if chlorine and bromine could substitute sterically for the methyl group. We observed that the inhibition potency determined against *An. gambiae* AChE for **9bs** (IC_{50} = 110 nM) and **9bt*** (IC_{50} = 250 nM) was relatively unchanged relative to **9ai** (IC_{50} = 120 nM). However, inhibition potency of human AChE was decreased as can be seen by selectivities of 27-fold and 7-fold for **9bs** and **9bt** respectively. This suggested that electronic factors governing the inhibition of human AChE by vinylic halide substituted carbamates **9bs** and **9bt*** could play larger role compared to *An. gambiae* AChE.

2.2.2.5 Insecticidal activity of combined class I-II phenyl *N*-methylcarbamates

We identified several C3-substituted phenyl *N*-methylcarbamates (Class I carbamates) with only modest target selectivity for inhibition of *An. gambiae* AChE relative to human AChE. However, terbam (**9c**) has emerged as our lead class I carbamate due to its high levels of toxicity observed for *An. gambiae* and to the reported lower oral mouse toxicity compared to propoxur (**9a**).[1, 26] In contrast to the high levels of contact toxicity observed for the class I carbamates, the class II carbamates were extraordinarily selective for *An. gambiae* AChE while simultaneously exhibiting lower contact toxicity (eg. **9bc*** and **9bd***). We hoped to capitalize on the contact toxicity of the class I carbamates all the while incorporating a C2-alkylthio side chain selectophore characteristic of the highly selective class II carbamates (Table 2.15).

Table 2.21. The inhibition potency and contact toxicity of the comibined class I and class II phenylcarbamates against *An. gambiae*.

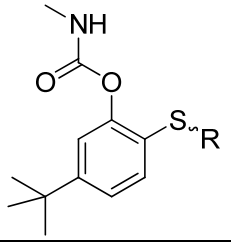

carbamate[a]	*R*	*IC_{50} (hmg, nM)*[b]	*percent mortality (mg/mL)*[b]
9bx*	Me	970 (0.66-fold)	0% @ 1
9by*	iso-Pr	75,000 (0.03-fold)	16% @ 1
9bz*	iso-Bu	38,000 (0.12-fold)	4% @ 1

[a] Novel carbamates are indicated by the * symbol. [b] Enzyme inhibition assays determined with serial dilution method A on homogenate *An. gambiae* AChE (SEM ± 20%). [c] Concentration (mg/mL) of an ethanol solution (2 mL), soaked into a 180 cm^2 filter paper (dried 24 h before use) to cause the indicated % mortality (SEM ± 20%) of *An. gambiae* at 24 h under standard WHO contact toxicity conditions.

The intended enhancement in insecticidal activity was not realized, as the 2-alkylthio-5-*tert*-butylphenyl *N*-methylcarbamates **9bx*** (0.66-fold), **9by*** (0.03-fold), and **9bz*** (0.12-fold) were strikingly more selective for human relative to *An. gambiae* AChE (Table 2.21). In addition, the inhibition potency observed for **9bx*-bz*** (IC_{50} = 970 – 75,000 nM) were determined to be low compared with terbam (**9c**, IC_{50} = 3.1 nM). Moreover, **9bx*-bz*** (LC_{50} > 1 mg/mL) were each significantly less toxic to *An. gambiae* relative to **9c** (LC_{50} = 0.037 mg/mL). The data indicated that 2,5-disubstitution on the combined class I-II carbamates disrupted favorable interactions within the active site of *An. gambiae* AChE, and yielded inferior carbamates compared to the class I or class II carbamates alone.

2.3 G119S point mutation conferring resistance carbamate and organophosphate insecticides

As previously mentioned in section 1.1 *An. gambiae* mosquitoes are growing increasingly resistant to pyrethroid insecticides largely due to their widespread use in pyrethroid treated bed-nets. However, carbamate resistance has also been observed in mosquitoes exposed to high levels of agricultural carbamate and organophosphate insecticides. Investigators have pinpointed the resistance mechanism to be a G119S mutation within the catalytic active site of AChE. The native G119 is a member of the oxyanion hole believed to stabilize the transition state for S200 attack on the ACh carbonyl. As we will show, this point mutation can have severe effects on the catalytic efficiency of AChE.

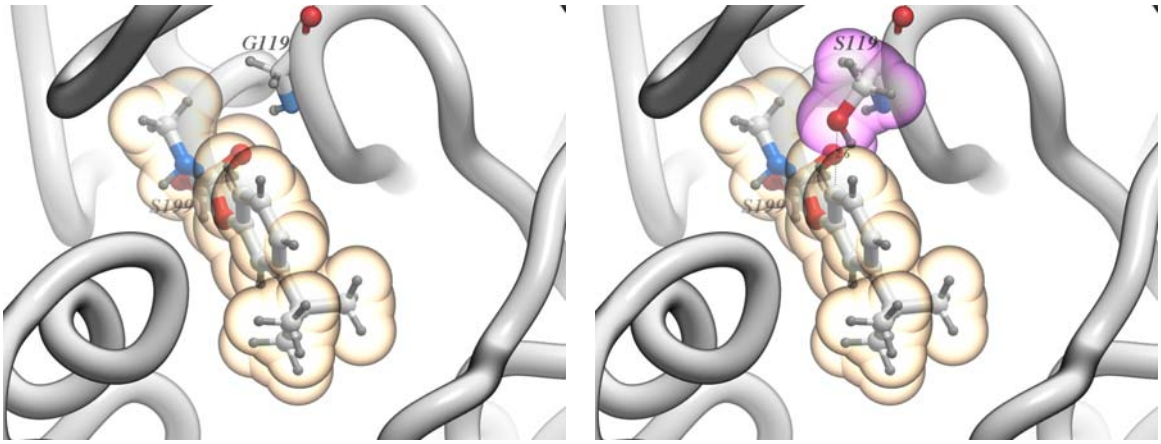

Figure 2.8. 3D homology models show that the G119S point mutation renders the enzyme less susceptible to phenylcarbamate inhibitors. The phenyl ring is clashing with the sterically hindered serine group. Photo credit: Max Totrov and Polo Lam.

Homology modeling of this mutation performed by our collaborators Max Totrov and Polo Lam (Molsoft) suggests that the G119S substitution sterically crowds the oxyanion hole, partially disrupting its function (Figure 2.8). The G119S point mutation is within close proximity to the catalytic S200 and additionally hinders nuleophilic attack of substrate, carbamate, and OP electrophiles. In *Culex pipiens* (common North American mosquito) an overall "fitness reduction" was observed as a result of the G119S mutation.[34] Our models of lead class I carbamate terbam (**9c**) indicated that the phenyl ring on the carbamate clashed with the larger mutated S119 relative to the native G119 within the active site oxyanion hole.

Table 2.22. The effects of the G119S resistance mutation on inhibition potency and contact toxicity of terbam, **9c**.

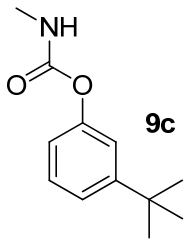

source of AChE	k_i $(mM^{-1}min^{-1})^a$	*percent mortality (mg/mL)*[b]
human	130 ± 3	ND
An. gambiae recomb. WT	1,100 ± 41	--
An. gambiae homog. WT	1,700 ± 25	50% @ 0.037[a]
An. gambiae recomb. G119S	0.47 ± 0.05	--
An. gambiae homog. Akron	0.50 ± 0.05	0% @ 5 mg/mL (>135-fold insensitivity)[c]

[a] Homogenate *An. gambiae* AChE was used in the inhibition assays with serial dilution method C. [b] Concentration (mg/mL) of an ethanol solution (2 mL), soaked into a 180 cm^2 filter paper (dried 24 h before use) to causes indicated % mortality (SEM ± 20%) of *An. gambiae* at 24 h under standard WHO contact toxicity conditions. [c] Insensitivity is defined as G119S LC_{50} / G119 wild type LC_{50}.

Terbam (**9c**) is a good example to demonstrate the devastating effects the G119S point mutation has on the inhibition potency and contact toxicity of carbamates towards *An. gambiae* AChE. The inactivation rate (k_i) for **9c** against the G3 wild type homogenate *An. gambiae* AChE was determined to be 1,700 $mM^{-1}min^{-1}$. In contrast, the inactivation rate constant (k_i) measured in the presence of Akron G119S mutant was determined to be 3,400-fold less potent (k_i = 0.50 $mM^{-1}min^{-1}$) relative to wild type homogenate *An. gambiae* AChE. Along with inhibition potency toward the G119S mutant, **9c** was > 135-fold less contact toxic to the resistant Akron G119S strain of *An. gambiae* (0% mortality at 5 mg/mL) relative to the G3 wild type strain of *An. gambiae* (LC_{50} = 0.037 mg/mL). To date we have not tested a phenylcarbamate that has comparable toxicities to the G3 wild type and AKRON G119S strains. Other workers in the Carlier group have however found other carbamates that can potentially inhibit G119S AChE, and that show good toxicity to AKRON *An. gambiae*.

2.4 Conclusion

Carbamates have been used for decades as insecticides; however, the screening of their efficacy against insects expressing AChE encoded by the *ace*-1 gene (i.e., *An. gambiae*) has remained absent in the literature. After screening seventy phenylcarbamates for inhibition potency towards *An. gambiae* AChE our research has culminated in the discovery of six novel carbamates (**9bb*-bd***, **9bl***, **9bm***, and **9bn***) that demonstrated levels of target selectivity that exceeded our project milestones of 100-fold for *An. gambiae* relative to human AChE. Although carbamates with $\geq$ 100-fold target selectivity were only mildly toxic to *An. gambiae*, they provide pivotal insight into structural requirements for selective binding to *An. gambiae* relative to human AChE.

Among the Class II phenylcarbamates examined thus far, compound **9bd*** has been shown be extraordinarily selective (570-fold $\pm$ 72) for *An. gambiae* relative to human AChE. Furthermore, it is one of the many new chemical entities protected under Virginia Tech intellectual property. The structure-activity relationships indicated that secondary branching at the β-position conferred the highest levels of selectivity for *An. gambiae* AChE (Figure 2.9). We have attributed these high levels of selectivity to a helical displacement in the gorge of *An. gambiae* AChE compared to human AChE (section 2.2.2.3). We believe that this displacement accommodates large β-branched class II carbamates.

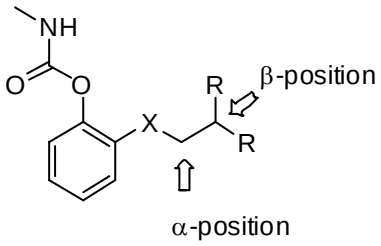

Figure 2.9. Properties of the class II carbamates conferring optimal mosquitocidal activity

In addition to the highly selective class II carbamates, we also revisited a previously reported class I carbamate, terbam (**9c**, LC_{50} = 0.037 mg/mL). We have shown

that terbam (**9c**) is equally toxic to *An. gambiae* as the commonly employed agricultural insecticide, propoxur (**9a**, LC_{50} = 0.037 mg/mL). Although terbam is a known insecticide, its use as potential carbamate for ITN application has yet to be implemented. The target selectivity conferred by terbam (**9c**, 12-fold) was only marginally lower compared with propoxur (**9a**, 16-fold, section 2.2.2.2). However, mammalian toxicity studies indicate terbam (**9c**) is 20-fold less toxic to the mammalian mouse control relative to propoxur (**9a**). This shows that terbam (**9c**) could potentially be one of the first carbamates examined for ITN application. To date, terbam (**9c**) remains the most toxic class I carbamate examined.

In our search for more powerful class I carbamates, we also explored the effects fluorine-containing type B class I carbamates on both inhibition potency and contact toxicity. Unfortunately, the fluorine-containing bioisosteres of terbam (**9av*** and **9aw***) were slightly less toxic. The potent toxicity observed for terbam (**9c**) also turned our attention to larger C3-substituted carbamates **9as**, **9at**, and **9au***. Although an increase in the inhibition potency of nearly 5-fold was observed for carbamates **9as**, **9at**, and **9au***, a slight decrease in contact toxicity was also observed compared to **9c**.

2.5 References

1. Kolbezen, M. J.; Metcalf, R. L.; Fukuto, T. R. Insecticidal Activity of Carbamate Cholinesterase Inhibitors. *J. Agr. Food Chem.* **1954,** 2, 864-870.

2. Mahfouz, A. M. M.; Metcalf, R. L. Influence of the Sulfur Atom on the Anticholinesterase and Insecticidal Properties of Thioether N-Methylcarbamates. *J. Agr. Food Chem.* **1969,** 17, 917-922.

3. Metcalf, R.; Fukuto, T.; Winton, M. Alkoxyphenyl-*N*-methylcarbamates as insecticides. *J. Econ. Ent.* **1960,** 53, 828-832.

4. Metcalf, R.; Fukuto, T.; Winton, M. Insecticidal carbamates: Comparison of the activities of *N*-methyl and *N,N*-dimethylcarbamates of various phenols. *J. Econ. Entomol.* **1962,** 55, 345-347.

5. Metcalf, R.; Fukuto, T.; Winton, M. Insecticidal carbamates: Position isomerism in relation to activity of substituted phenyl-*N*-methylcarbamates. *J. Econ. Ent.* **1962,** 55, 889-894.

6. Metcalf, R. L. Structure-activity relationships for insecticidal carbamates. *B. World Health Organ.* **1971,** 44, 43-78.

7. Metcalf, R. L.; Fukuto, T. R. Effects of Chemical Structure on Intoxication and Detoxication of Phenyl N-Methylcarbamates in Insects. *J. Agr. Food Chem.* **1965,** 13, 220-231.

8. Metcalf, R. L.; Fukuto, T. R. Some Effects of Molecular Structure upon Anticholinesterase and Insecticidal Activity of Substituted Phenyl N-Methylcarbamates. *J. Agr. Food Chem.* **1967,** 15, 1022-1029.

9. Metcalf, R. L.; Fukuto, T. R.; Frederickson, M.; Peak, L. Insecticidal Activity of Alkylthiophenyl N-Methylcarbamates. *J. Agr. Food Chem.* **1965,** 13, 473-477.

10. Ellman, G.; Courtney, K.; Valentino, J.; Featherstone, R. A new and rapid calorometric determination of acetylcholinesterase activity. *Biochem. Pharmacol.* **1961,** 7, 88-95.

11. Yu, C.-C.; Kearns, C. W.; Metcalf, R. L. Acetylcholinesterase Inhibition by Substituted Phenyl N-Alkylcarbamates. *J. Agr. Food Chem.* **1972,** 20, 537-540.

12. Yu, C.-c.; Metcalf, R. L.; Booth, G. M. Inhibition of Acetylcholinesterase from Mammals and Insects by Carbofuran and Its Related Compounds and Their Toxicities toward These Animals. *J. Agr. Food Chem.* **1972,** 20, 923-926.

13. Guidelines for testing mosquito adulticides for indoor residual spraying and treatment of mosquito nest. In World Health Organization: Geneva, 2006.

14. Bar-On, P.; Millard, C. B.; Harel, M.; Dvir, H.; Enz, A.; Sussman, J. L.; Silman, I. Kinetic and Structural Studies on the Interaction of Cholinesterases with Anti-Alzheimer Drug Rivastigmine. *Biochemistry* **2002,** 41, 3555-3564.

15. Kilsheimer, J. R.; Kaufman, H. A.; Foster, H. M.; Driscoll, P. R.; Glick, L. A.; Napier, R. P. Benzo [b] thienyl Carbamate Insecticides. *J. Agr. Food Chem.* **1969,** 17, 91-93.

16. Stevens, J.; Beutel, R. Physostigmine subsitutes. *J. Am. Chem. Soc.* **1941,** 63, 308-311.

17. Gupta, R. C. Introduction. In *Toxicology of Organophosphate and Carbamate Compounds*, Gupta, R. C., Ed. Elsevier Academic Press: Burlington, MA, 2006; pp 3-4.

18. Kuhr, R. J.; Dorough, H. W. *Carbamate Insecticides: Chemistry, Biochemistry, and Toxixology*. CRC Press: Cleveland, OH, 1976; p 1-101.

19. Fukuto, T. R. Approaches to the Design of Organic Insecticides. *J. Pest. Sci.* **1988,** 13, 137-150.

20. Heiss, R.; Schegk, E.; Schroder, G.; Wedemeyer, K. Termite resistant carbamates. DE1148107, 1963.

21. Andraos, J. On the propogation of statistical errors for a function of several variables. *J. Chem. Educ.* **1996,** 73, 150-154.

22. Carlier, P.; Bloomquist, J.; Paulson, S.; Wong, E. Species-selective insecticidal carbamates for mosquito control. 12/209,301, 2008.

23. Hemingway, J.; Hawkes, N.; McCarrol, L.; Ranson, H. The molecular basis of insecticide resistance in mosquitoes. *Insect Biochem. Mol. Biol.* **2004,** 34, 653-665.

24. Hemingway, J.; Karunaratne, S. Mosquito carboxyesterases: a review of the molecular biology and biochemistry of a major insecticide resistance mechanism. *Med. Vet. Entomol.* **1998,** 12, 1-12.

25. Enayati, A.; Ranson, H.; Hemingway, J. Insect glutathione transferases and insecticide resistance. *Insect Mol. Biol.* **2005,** 14, 3-8.

26. Kohn, G. K.; Ospenson, J. N.; Moore, J. E. Some Structural Relationships of a Group of Simple Alkyl Phenyl N-Methylcarbamates to Anticholinesterase Activity. *J. Agr. Food Chem.* **1965,** 13, 232-235.

27. Aizawa, H. Phenyl(Aryl) Carbamates. In *Metabolic Maps of Pesticides*, Academic Press: New York, 1982; pp 105-122.

28. Douch, P.; Smith, J. Metabolism of m-*tert*-butylphenyl-*N*-methylcarbamate in insects and mice. *Biochem. J.* **1971,** 125, 385-393.

29. Tanaka, H.; Shishido, Y. Synthesis of aromatic compounds containing a 1,1-dialkyl-2-trifluoromethylgroup, a bioisostere of the tert-alkyl moiety. *Bioorg. Med. Chem. Lett.* **2007,** 17, 6079-6085.

30. Ranson, H.; Claudianos, C.; Ortelli, F.; Abrall, C.; Hemingway, J. Evolution of supergene families associated with insecticide resistance. *Science* **2002**, 298.

31. Paul, A.; Harrington, L.; Scott, J. Evaluation of novel insecticides for control of dengue vector *Aedes aegypti* (Diptera: Culicidae). *J. Med. Entomol.* **2006,** 43, 55-60.

32. Jeshke, P. The unique role of fluorine in the design of active ingredients for modern crop protection. *ChemBioChem* **2004,** 5, 570-589.

33. Dolbier, W. Fluorine chemistry at the millennium. *J. Fluorine Chem.* **2005,** 126, 157-163.

34. Raymond, M.; Berticat, C.; Weill, M.; Pasteur, N.; Chevillon, C. Insecticide resistance in the mosquito *Culex pipiens*: what have we learned about adaptation? *Genetica* **2001,** 112, 287-296.

Chapter 3: Synthesis and characterization of phenylcarbamate *An. gambiae*-selective AChE inhibitors

3.1 General synthesis and characterization of phenylcarbamates

Chapter 2 described the structural properties of carbamate inhibitors that conferred optimal insecticidal activity against *An. gambiae*. Accordingly, efforts to synthesize and characterize the phenylcarbamate inhibitors will be discussed in Chapters 3 and 5. Since the carbamoylation of phenols was the final step in all our carbamate syntheses I will first describe the method used. Second, I will describe the synthesis of several classes of phenols that were not commercially available.

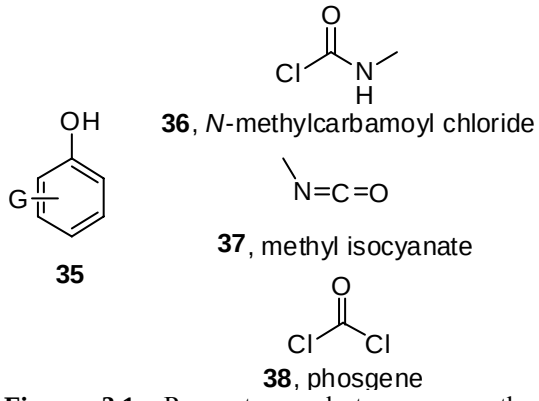

35

36, *N*-methylcarbamoyl chloride

37, methyl isocyanate

38, phosgene

Figure 3.1. Reagents used to prepare the phenylcarbamates.

Many of the commercial agricultural-carbamate insecticides were prepared from phenols (**35**) and methylisocyanate (**37**).[1] However, to avoid the use of this deadly-low boiling point reagent we chose to replace methylisocyanate (**37**, b.p. = 39 ^{o}C) with a solid, *N*-methylcarbamoyl chloride (**36**, m.p.= 45 ^{o}C; Figure 3.1). Nearly 25 years ago, 40 tons of methylisocyanate (**37**) escaped from an insecticide-producing Union Carbide plant in central India (Bhopal), causing the deaths of thousands of people. Alternative methods used to prepare *N*-methylcarbamates include the sequential addition of phosgene (**38**) and amines to phenols (**35**).[2] However, *N*-methylcarbamoyl chloride (**36**) is a much safer alternative to methylisocyanate (**37**) or phosgene (**38**).

Table 3.1 Synthesis of phenyl *N*-methylcarbamates from commercially available phenols.

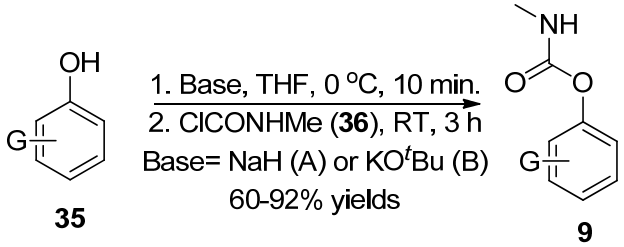

35 **9**

product	*group*	*isolated yield (method)*[a]
9d	H	91% (*A*)
9i	2-*i*-Pr	80% (*A*)
9k	2-*t*-Bu	67% (*A*)
9al	3-Cl	91% (*A*)
9am	3-Br	81% (*A*)
9n	3-*i*-Pr	85% (*A*)
9ca	3,5-diMe	85% (*A*)
9t	4-*t*-Bu	89% (*A*)
9c	3-*t*-Bu	86% (*A*), 72% (*B*)
9an	3-I	70% (*B*)
9l	3-Me	84% (*B*)
9m	3-Et	62% (*B*)
9aq	3-Ph	69% (*B*)
9cb	3-CF_3	81% (*B*)
9cc	3-F, 5-CF_3	59% (*B*)
9ar	3,5-di-*t*-Bu	82% (*B*)

[a] Isolated yields for the phenyl *N*-methylcarbamates after silica gel chromatography. Method A: The phenol (**35**) was deprotonated with NaH. Method B: The phenol (**35**) was deprotonated with KO^{t}Bu.

Table 3.1 describes the synthesis of phenyl *N*-methylcarbamates (**9d**, **i**, **k**, **al**, **am**, **n**, **ca**, **t**, **c**, **an**, **l**, **m**, **aq**, **cb**, **cc**, and **ar**) prepared from commercially available phenols (**35d**, **i**, **k**, **al**, **am**, **n**, **ca**, **t**, **c**, **an**, **l**, **m**, **aq**, **cb**, **cc**, and **ar**). The yields obtained ranged from 59 - 91%. Deprotonation of the phenol was conducted by use of 1.5 equivalents of either sodium hydride (*Method A*) or potassium *tert*-butoxide (*Method B*) in tetrahydrofuran. The phenolate anion generated was then treated with 2 equiv of *N*-

methylcarbamoyl chloride (**36**). After 3 h at room temperature the reactions were typically judged complete by TLC analysis. The resulting tetrahydrofuran reaction mixture was evaporated and the residue was purified by column chromatography. The phenol starting materials (**35**) were much less polar than the corresponding carbamates (**9**) providing for a facile separation on silica gel. Interestingly, despite our efforts to drive the reaction to completion by heating and extending the reaction times, residual starting material was always observed by TLC. The carbamates shown in Table 3.1 were white solids upon purification.

When potassium *tert*-butoxide (*Method B*) was used as the base, the byproduct *tert*-butyl *N*-methylcarbamate impurity (**39**) was also generated in the reaction (Figure 3.2). The impurity (**39**) was conveniently separated from the desired class I phenyl *N*-methylcarbamates (**9**) bearing C3-alkyl groups; however, in the instance of class II carbamates **9ba*** and **9bc***, the *tert*-butyl *N*-methylcarbamate impurity (**39**) coeluted. The problem of contamination by **39** was easily resolved by preparing **9ba*** and **9bc*** with sodium hydride as a base (method A). The presence of **39** was confirmed with ^{1}H NMR, HPLC, and HRMS and was particularly easy to identify in the ^{1}H NMR spectrum from the intense singlet at 1.44 ppm resulting from the protons on the methyl groups on the *tert*-butyl center

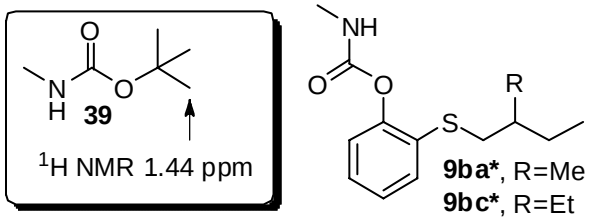

Figure 3.2. The use of potassium tert-butoxide can lead to tert-butyl N-methylcarbamate (**39**) impurity that co-elutes with carbamates **9ba*** and **9bc*** on silica gel. Novel compounds are indicated by the * symbol.

Table 3.2. Isolated yields for the phenyl-*N*,*N*-dimethylcarbamates.

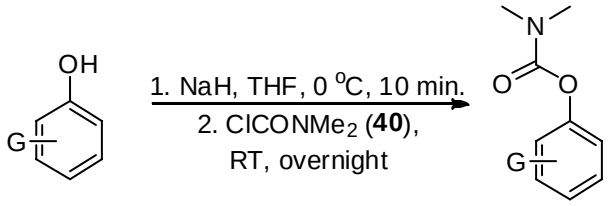

35 **30** (89-99%)

product	*group*	*isolated yield*[a]
30d	H	99%
30n	3-*i*-Pr	91%
30c	3-*t*-Bu	89%
30t	4-*t*-Bu	91%

[a] When *N*,*N*-dimethylcarbamoyl chloride was used as an electrophile the reaction time was extended to 24 h.

In addition to phenyl *N*-methylcarbamates, the more sterically encumbered phenyl *N*,*N*-dimethylcarbamates (**30c**, **d**, **n**, and **t**, Table 3.2) were also examined as potential insecticides. The phenyl *N*,*N*-dimethylcarbamates (**30**) were prepared by carbamoylation with *N*,*N*-dimethylcarbamoyl chloride (**40**, method C), instead of *N*-methylcarbamoyl chloride (**36**). In addition, method C employs an overnight reaction time compared with the three hour reaction time used to prepare the phenyl-*N*-methylcarbamates (**9**). High yields ranging from 89-99% were obtained on the phenyl *N*,*N*-dimethylcarbamates (**30c**, **d**, **n**, and **t**, Table 3.2).

Characterization of the phenylcarbamates and their intermediates were carried out using modern ^{1}H and ^{13}C NMR spectroscopy along with HRMS. When fluorine was present in a molecule, a ^{19}F NMR spectrum was also collected. One interesting aspect of the ^{1}H NMR spectra for the phenyl *N*-methylcarbamates was the presence of two resonances corresponding to the *N*-methyl and *N*-H protons. To illustrate this point we show the ^{1}H NMR spectrum of phenyl *N*-methylcarbamate **9d** in Figure 2.3. The

presence of major (~91%) and minor (~9%) resonances corresponding to the *N*-H protons at 5.1 and 4.8 ppm respectively (peaks A and B, Figure 3.3) and major and minor doublets at 2.9 and 3.0 ppm for the *N*-methyl group (peaks C and D) respectively is observed. Initially the minor resonances (peaks B & C) were ignored or presumed to arise from an impurity. However, after further consideration we have concluded that peaks B and C are a result of a higher energy rotamer (**9d-2**, Figure 3.3) that is observable on the NMR timescale.

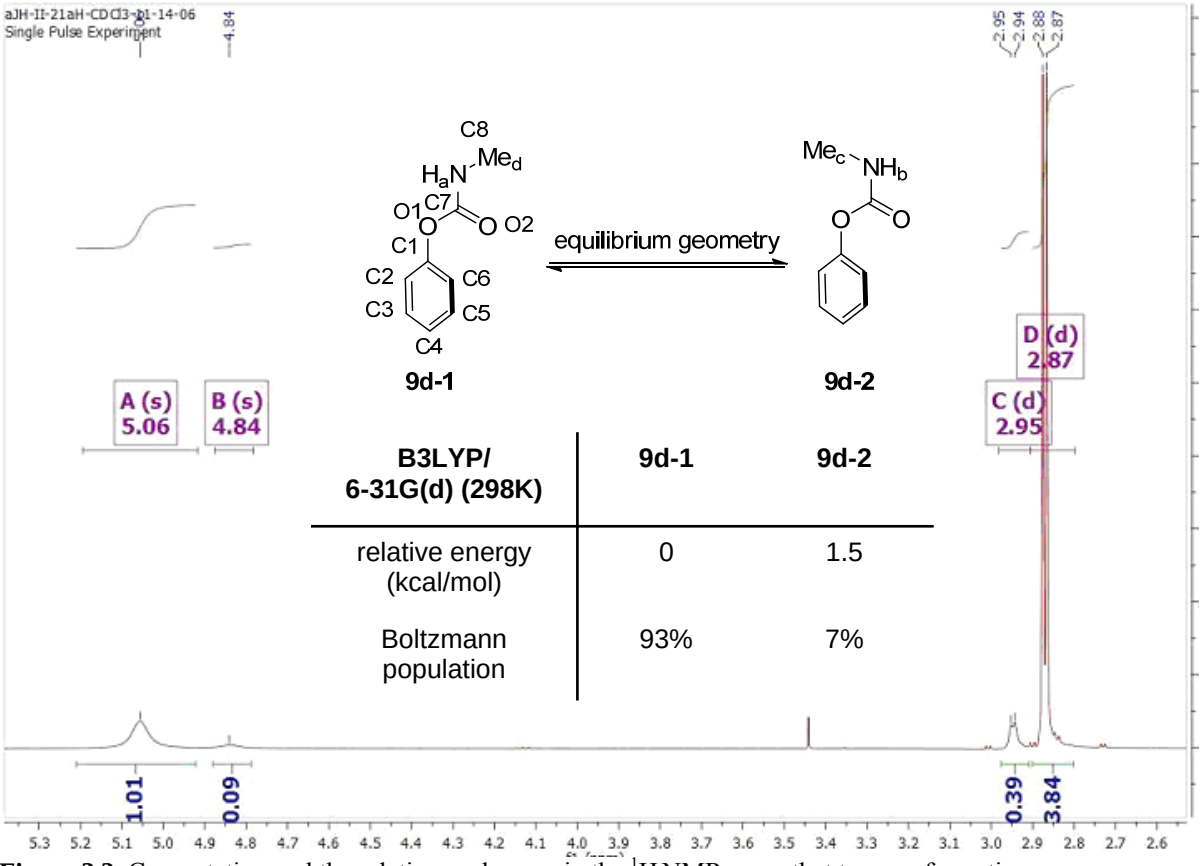

B3LYP/ 6-31G(d) (298K)	9d-1	9d-2
relative energy (kcal/mol)	0	1.5
Boltzmann population	93%	7%

Figure 3.3. Computation and the relative peak areas in the ^{1}H NMR agree that two conformations are populated by phenyl *N*-methylcarbamate (**9d**).

To provide support for this hypothesis, terbam (**9c**) was repeatedly recrystallized until refined to a high degree of purity. After obtaining a consistent melting point of

143.9 - 144.6 °C (lit. m.p. = 144.5 °C) the high purity of **9c** was verified with normal phase HPLC (> 95% pure). However, the persistent minor peaks were still present and could not be the result of a 7% impurity that was consistent with ^{1}H NMR. Therefore, computational chemistry was used to assess the energies of the lowest energy conformations of phenyl *N*-methylcarbamate **9d**; this molecule was chosen due its simplicity. Density functional (B3LYP 6-31G(d)) calculations were performed on 4 different starting geometries where the C1O1C7O2 and C8N1C7O2 dihedral angles were both set at 0 ° and 180 °. Conformation **9d-1** was found to be the lowest energy conformer, and conformation **9d-2** was 1.5 kcal/mol higher in energy compared to **9d-1**. The alternative two starting geometries reverted to the lower energy conformers **9d-1** or **9d-2**. At 298 K the Boltzmann population of conformer **9d-2** would be 7% which is very similar to the relative peak areas calculated from the ^{1}H NMR spectrum (9% based peaks A and B) of **9d**.

Conformations **9d-1** and **9d-2** in Figure 3.3 benefit from two types of resonance interactions of the O1 lone pairs. The first interaction is a π-type interaction of the p-type lone pair on O1 with the C7-O2 π* orbital (Figure 3.4, top). The second interaction involves overlap of the sp^2-type lone pair on O1 with the C7-O2 σ* orbital (illustrated for **9d-1** in Figure 3.4, bottom). Note that this orbital overlap is extensive for both the **9d-1** and **9d-2** conformations, which have a 0° C1O1C7O2 dihedral angle. In

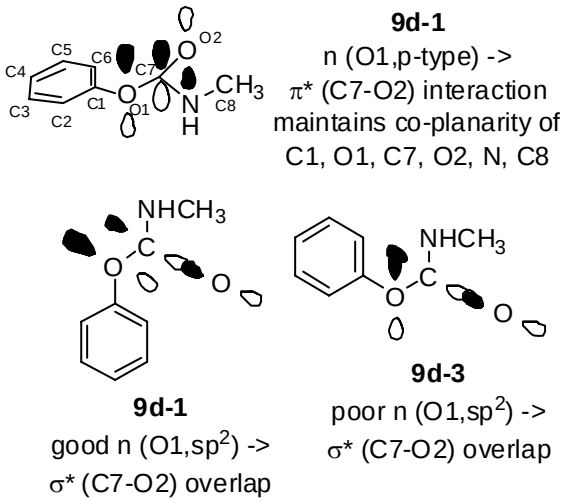

Figure 3.4. Secondary orbital interactions and their effects on the conformational energies of carbamates

contrast, conformation **9d-3** is expected to be much higher in energy than **9d-1** and **9d-2** because of poor n(O1, sp^2) -> σ* (C7-O2) overlap, resulting from the 180° C1O1C7O2 dihedral angle. A similar secondary electronic may be responsible for stabilizing **9d-1** relative to **9d-2**: perhaps overlap of the N1-H σ bond with the σ* (C7-O2) in **9d-1** is more extensive than overlap of the corresponding N1-C8 σ bond with the σ* (C7-O2) in **9d-2** (not shown in Figure 3.4). It is also interesting to note that the two low energy conformers **9d-1** and **9d-2** are oriented so that the aromatic ring is out of the plane with the carbamate carbonyl. For example, the dihedral angle (C6C1O1C7) observed for **9d-1** and **9d-2** was 45 degrees indicating non-coplanarity. This observation would suggest that the non-bonding electrons on O1 are only slightly involved in resonance with the aromatic ring, and are instead participating in n (O1) to π* (C7O2) orbital overlap.

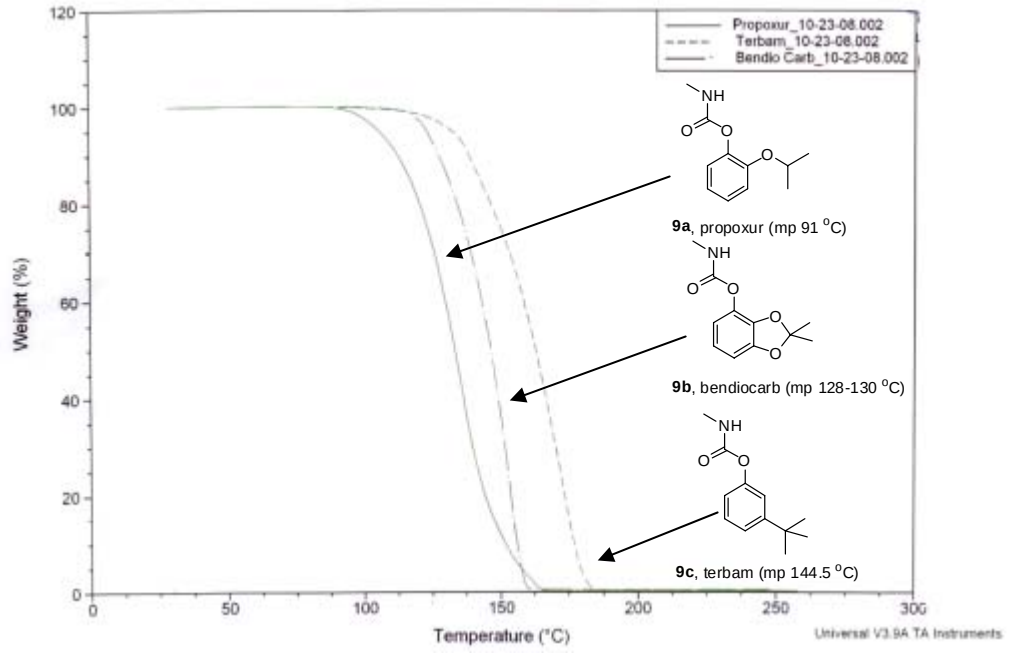

Figure 3.5. TGA analysis of three contact-toxic phenyl *N*-methylcarbamate insecticides (**9a**, **b**, & **c**).

In addition to being highly selective to mosquitoes, it is also desirable for carbamate insecticides used for ITNs to be thermally and hydrolytically stable. It is

widely accepted that carbamates can undergo thermal degradation to yield methylisocyanate (**37**) and the analogous phenol (**35**, Figure 3.5).[3] With the help of Dr. Sean Ramirez working under Professor Tim Long (Virginia Tech), we attempted to assess the thermal stability of three contact toxic agricultural insecticides i) propoxur (**9a**), ii) bendiocarb (**9b**), and iii) terbam (**9c**) by thermogravimetric analysis as depicted in Figure 3.5. Although the loss of methylisocyanate (**37**) and retention of the phenol (**35**) was anticipated (Scheme 3.1), 0% of the original mass for **9a**, **9b**, and **9c** was retained at 160 ^{o}C. Terbam (**9c**) had the highest melting point (144.5 ^{o}C) and showed a sigmoidal like decrease until 0% mass was retained at approximately 190 ^{o}C. The TGA analysis of **9a**, **9b**, and **9c** suggested that *N*-methylcarbamates vaporize at the onset of their melting points prior to any decomposition into the phenol (**35**) and methylisocyanate (**37**). This suggests that evaporation of the liquids under a stream of nitrogen is what we are observing.

Scheme 3.1 The decomposition mechanisms for phenyl *N*-methylcarbamates and phenyl *N*,*N*-dimethylcarbamates.[4]

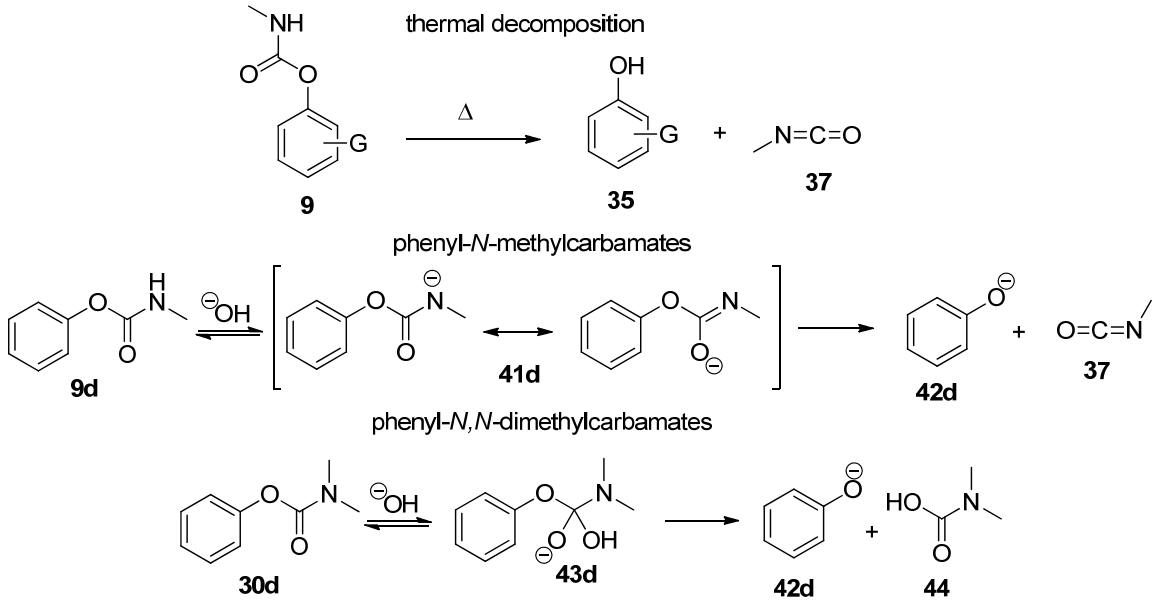

Carbamates generally have fairly long shelf lives due to their relatively low reactivity under atmospheric conditions at room temperature, high melting points, and low vapor pressure.[5] A variety of organic solvents can be used to dissolve the majority of carbamates, but phenylcarbamates are only sparingly soluble in water. Carbamates undergo slow decomposition in the presence of aqueous media and this process is accelerated at elevated temperatures and/or basic conditions.[5] Depending on the carbamate structure, the mechanism of alkaline decomposition can vary. Studies carried out on *N*-alkyl carbamate (**9d**) show that a proton is abstracted from the nitrogen to yield the resonance stabilized intermediate (**41d**).[4] This carbamate anion can then eject methylisocyanate (**37**) to yield the corresponding phenolate. Alternatively, the phenyl-*N*,*N*-alkylcarbamates represented by phenyl *N*,*N*-dimethylcarbamate **30d**, are attacked directly by the hydroxide nucleophile to form the tetrahedral intermediate (**43d**, Scheme 3.1).[4] The collapse of the tetrahedral intermediate (**43d**) results in *N*,*N*-dimethylcarbamic acid (**44**), which itself decomposes in protic media to carbon dioxide and dimethylamine.

3.2 Synthesis of Class I phenols and carbamates

3.2.1 Synthesis of Type A Class I fluorine containing phenols and carbamates

In Chapter 2 we discussed how many of our class I C3-substituted phenyl *N*-methylcarbamates bearing tertiary alkyl groups were promising lead insecticides. In addition to the class I phenyl *N*-methylcarbamates prepared from commercially available phenols (Table 3.1), we intended to incorporate fluorine into known class I pharmacophores to prevent the known oxidation

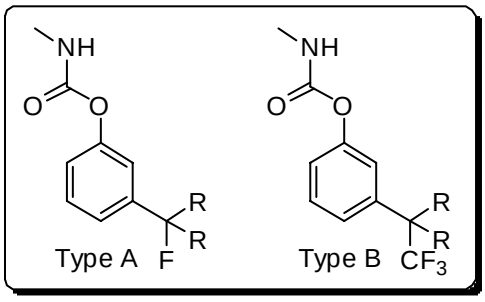

Figure 3.6. Type A and Type B fluorine containing class I phenyl N-methylcarbamates

pathways of analogs of terbam (**9c**, Scheme 2.2).[6] Terbam (**9c**) was one of the most promising class I carbamates to come out of our studies due to its potent contact toxicity. In section 2.2.2.1 we discussed how Tanaka and coworkers were able to improve on the oxidative stability towards human liver microsomes[7] by incorporating fluorine into known neurokinin-1 and TRPV1 ligands. Therefore, we believed that carbamate **9c** was a good candidate to incorporate fluorine into the C3-position (Figure 3.6). Two subtypes of fluorine containing class I phenyl *N*-methylcarbamates were investigated i) type A carbamates where the fluorine was incorporated in the benzylic position or ii) type B phenyl *N*-methylcarbamates that contained an α-trifluoromethyl group.

Scheme 3.2. Fluorination of benzylic alcohols and the cleavage of the *O*-benzyl protecting group. The novel compounds are indicated by the * symbol.

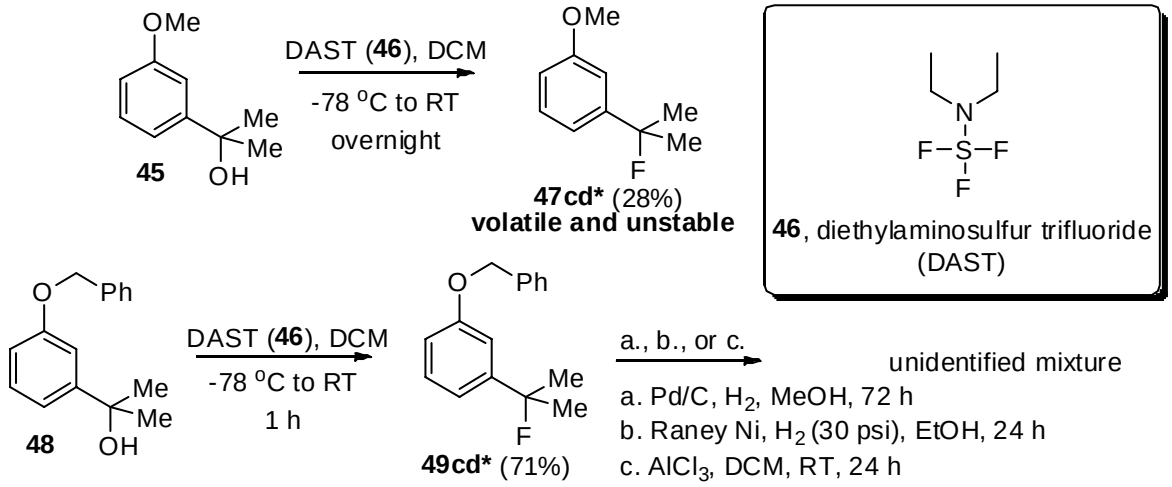

Fluorinating agents such as diethylaminosulfur trifluoride (**46**, DAST),[8] morpholinosulfur trifluoride (**21**, MOST),[9] and trifluoromethyltrimethylsilane (Rupert-Prakash reagent)[10] were employed to install fluorine into the class I carbamates. It was hoped that the tertiary benzylic fluoride **47cd*** could be used as a starting material to construct the analogous Type A fluorine containing phenyl *N*-methylcarbamate. The proposed synthetic pathway began with the fluorination of the tertiary benzylic alcohol **45** with DAST (**46**) in dichloromethane. Although product formation (**47cd***) was

observed by TLC, the elimination product was also observed in the ^{1}H NMR spectrum. After purifying the product (**47cd***) away from the elimination product a meager 28% yield was obtained. Upon standing the isolated colorless oil (**47cd***) underwent degradation into a white-gelatinous substance. In addition to instability issues observed for compound **47cd***, a substantial loss of mass was observed upon placing the isolated product under high vacuum. To obtain a ^{1}H and ^{13}C NMR spectrum, evaporation of the solvent was performed on the rotary evaporator at a temperature no greater than 35 ^{o}C.

To further decrease the volatility observed for compound **47cd***, a benzylic protecting group was installed as seen in compound **48** (Scheme 3.2). In addition to incorporating the *O*-benzylic group, the length of the reaction was also decreased to 1 hour at -78 ^{o}C to prevent formation of the elimination product. With these modifications to the reaction conditions, the *O*-benzyl protected ether (**49cd***) was isolated in a 71% yield compared with the anisole (**47cd***, 28% yield). Separation of compound **49cd*** from the competing alkene was not necessary since only trace quantity of alkene was generated in the reaction.

Attempts to cleave the *O*-benzyl ether group with Pd/C catalyzed hydrogenolysis (**49cd***) yielded a complex product mixture difficult to separate with chromatographic techniques (Scheme 3.2). Alternate routes to cleave the aryl ether were taken including a) Raney Ni catalyzed hydrogenolysis and the b) aluminum trichloride cleavage. Unfortunately, reaction attempts a, b, and c resulted in a complex mixture of products. The palladium catalyzed hydrogenolysis should have cleanly led to the phenol due to the relatively mild reaction conditions. The fact that pronounced decomposition occurred via

palladium catalyzed hydrogenolysis led us to believe that the electron rich phenol was less stable than the *O*-benzyl protected starting material (**49cd***, Scheme 3.2).

Scheme 3.3. The direct synthesis of the phenol **35cd** bearing a tertiary C3-benzylic fluoride. The novel compounds are indicated by the * symbol.

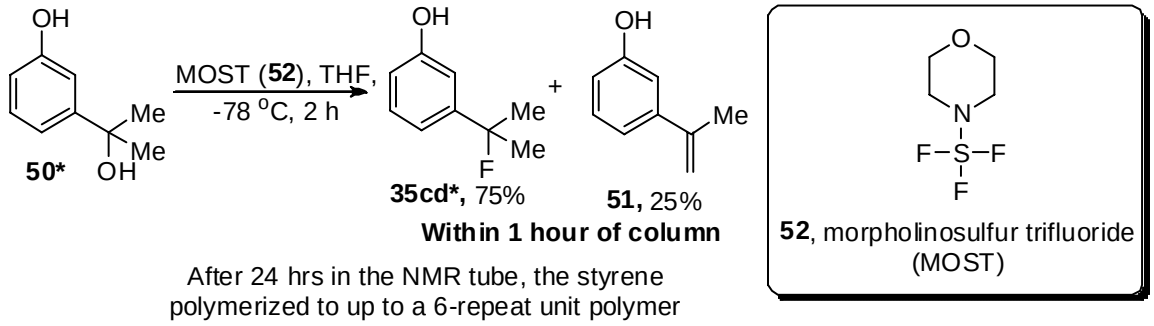

We tested the stability of the unprotected phenol (**35cd***) bearing the tertiary benzylic fluoride by directly preparing it from MOST (**52**, Scheme 3.3) and the benzylic alcohol **50***. MOST (**52**) is known to be a milder fluorinating agent relative to DAST (**46**);[8, 9] therefore, it was a particularly useful reagent due to the anticipated instability of the electron rich benzylic fluoride (**35cd***). The reaction was carried out with a slightly modified protocol compared to that depicted in Scheme 3.2, in which dichloromethane was replaced with tetrahydrofuran. The reaction was quenched with water, extracted, and purified on silica gel chromatography using dichloromethane and hexane as eluents due to their low boiling points and high vapor pressure. Analysis of the ^{1}H NMR spectrum of the isolated product (Note: one hour after purification on silica gel chromatography) revealed that two major products were present (**35cd*** and **51**). Based on the relative peak areas in the ^{1}H NMR spectrum, compound **35cd*** (75%) was found to be the major constituent. The remaining minor constituent (**51**, 25% of product mixture) was the elimination product. Upon standing overnight at room temperature the original colorless oil product decomposed into a white-gelatinous material similar to the decomposition of

the methoxy protected product (**47cd***) illustrated in Scheme 3.2. In contrast to the ^{1}H NMR spectrum, TLC analysis revealed that the NMR sample was still one spot where coincidentally the two products had the same R_f value.

We suspected that that polymerization had occurred, either of the styrene, or of the carbocation resulting from C-F cleavage. The presence of a six repeat unit oligomer (**53**) in the decomposed NMR sample was confirmed by employing HRMS (Figure 3.6). The instability of the tertiary benzylic fluoride-containing phenol **35cd*** suggested that the analogous Type A fluorine containing phenyl *N*-methylcarbamates would also be unstable and decompose into non-toxic compounds that would be ineffective as mosquitocides. Additional Type A carbamates were not examined as a result.

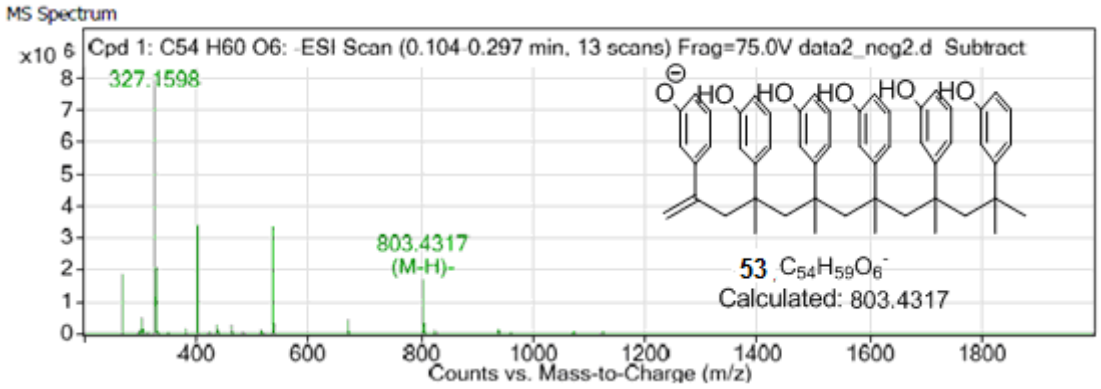

Figure 3.7. HRMS of NMR sample (**35cd**) was shown to contain **53** after standing at RT overnight.

The instability of **35cd*** was not anticipated since the carbon-fluorine bond is the strongest of the carbon bonds (eg., CH_3F, BDE = 115 kcal/mol).[11, 12] Upon encountering the unexpected instability of the benzylic fluoride intermediates, we set out on a literature search for others who had encountered the same phenomenon. Interestingly, in the 1980's a Virginia Tech chemistry professor, Milos Hudlicky,[13] also described the instability of benzylic fluorides. Eunsun Lee later (2009) reported on the instability of allylic fluorides and was able to show how allylic carbon-fluorine bonds were uniquely weak and could

readily undergo autocatalytic decomposition in the presence of trace amounts of acid or even being stored in borosilicate glass.[14] These results help explain the decomposition of the electron rich tertiary benzylic fluorides observed in Scheme 3.2 and 3.3. As a result we began to focus our attention on preparing type B trifluoromethyl-containing phenyl *N*-methylcarbamates (Figure 3.6).

3.2.2 Synthesis of type B Class I fluorine containing phenols and carbamates

3.2.2.1 Literature methods used to install trifluoromethyl nucleophiles and tertiary carbon centers

Recall from section 3.2.1 that type B Class I carbamates contain trifluoromethyl groups at the C3-position of the aromatic ring (Figure 3.6). In this section, we will examine some known techniques used to introduce the trifluoromethyl nucleophile to aryl ketones, and then use this technique to prepare C3-substitued benzylic alcohols.[10] Second, we will explore how Tanaka and coworkers[7] successfully developed a method to prepare tertiary trifluoromethyl-containing centers from tertiary benzylic alcohols. Finally, we will discuss how this method was adapted to prepare type B class I phenols and carbamates.

Table 3.3. Literature methods to prepare incorporate trifluoromethylgroups into aryl ketones.[10]

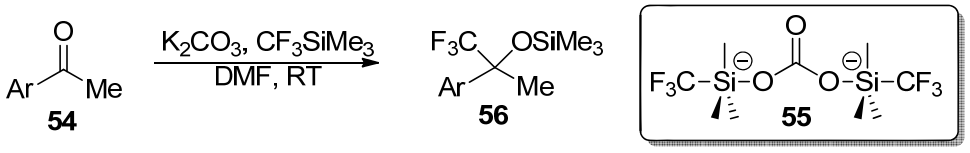

starting material	*Ar*	*product*	*isolated yield*
54a	Ph	**56a**	67%
54b	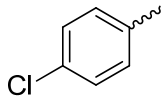	**56b**	85%
54c	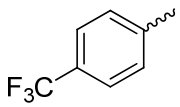	**56c**	65%

The Rupert-Prakash reagent (CF_3SiMe_3) is an effective nucleophilic trifluoromethyl source for the addition to ketones and aldehydes.[10] Catalysts including tetrabutylammonium fluoride (TBAF), tetramethylammonium fluoride (TMAF), lithium acetate, and potassium carbonate have been examined by Prakash for maximum catalytic efficiency.[10] However, his best results were attained with potassium carbonate. The effectiveness of potassium carbonate is attributed to the formation of an "activated Rupert-Prakash reagent" shown in Table 3.3 (**55**).[10] The isolated yields reported for the reaction of the Rupert-Prakash reagent on various acetophenones ranged from 65 - 85%.[10] Although not performed by these investigators, the silyl ether could clearly be cleaved with an acid quench to yield the tertiary benzylic alcohols (Scheme 3.4).

Scheme 3.4. Hydrochloric acid cleavage of silyl ethers.

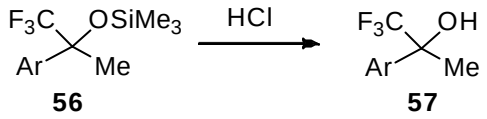

56 **57**

In contrast to the addition of the Rupert-Prakash reagent to acetophenones, Tanaka has shown (see below in Scheme 3.5) that the trifluoromethyl ketone such as **58** could be used as a starting material.[7] Tanaka and coworkers intended to prepare compound **60** by the exhaustive methylation of the trifluoromethyl ketone (**58**).[7] However, their initial attempts with the Reetz reagent to directly convert trifluoromethyl ketone **58** to **60** failed and resulted in a quantitative yield of the intermediate benzylic alcohol **59**. The Reetz reagent (Me_2TiCl_2) has been used to prepare quaternary carbon centers from acetophenones.[15-17] Although direct use of the Reetz reagent to install the final methyl group of compound **60** was unsuccessful, Tanaka found an alternative route to prepare compound **60**, by first generating the benzyl chloride *in situ* from the addition

of titanium (IV) chloride. After this modification to the protocol, Tanaka was able to install a tertiary methyl group observed in compound **60** in a 51% yield.[7]

Scheme 3.5. Tanaka examines the Reetz reagent (Me_2TiCl_2) to install tertiary trifluoromethyl-containing centers in the 4-position of anisole (**62**).[7]

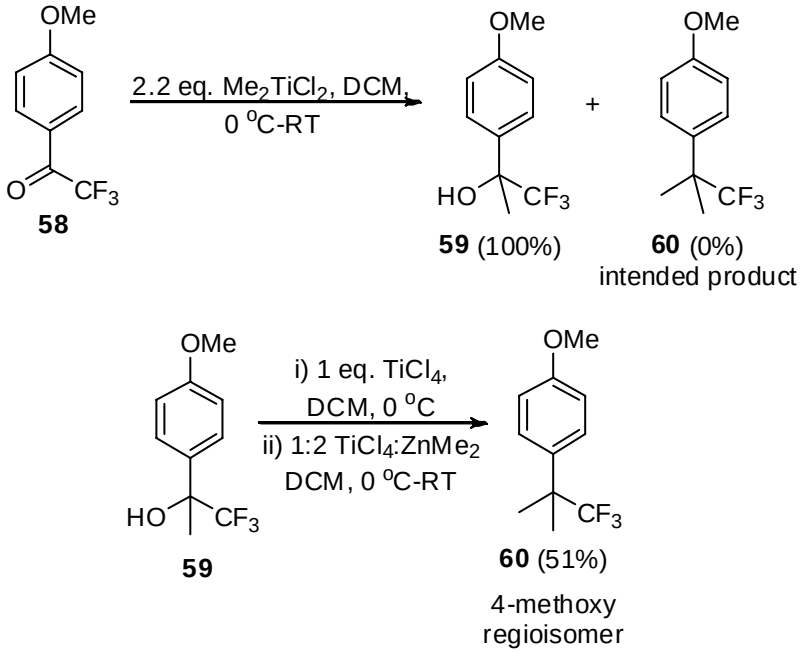

Although the Reetz reagent reacted with the tertiary benzylic chloride prepared *in situ* from **59** (Scheme 3.5), there were examples Tanaka found that Reetz reagent would not produce the intended product (Scheme 3.6).[7] Tanaka used trimethylaluminum and found that exchange of the methyl group with the mesylate or benzylic chloride prepared occurred (Scheme 3.6) in an 86% yield affording compound **62** from compound **61**. Note that in some cases the use of mesyl chloride is believed result in some benzylic chloride by displacement of the mesylate. This strategy was not implemented by Tanaka on 3-methoxy or 3-hydroxy aromatics from which we intend to prepare type B carbamates.

Scheme 3.6. Installation of the non-basic nucleophilic methyl groups with trimethylaluminum.

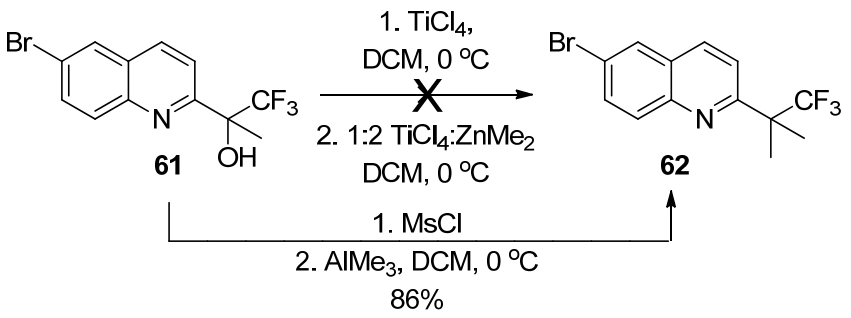

3.2.2.2 Experimental methods used to install trifluoromethyl nucleophiles and tertiary carbon centers

Although Tanaka had implemented a successful strategy to install trifluoromethyl-containing tertiary centers, he had not utilized this procedure to prepare the C3-substituted analogs necessary for the synthesis of the desired Type B phenyl *N*-methylcarbamates. We have successfully used his method to prepare these precursors.

Scheme 3.7. The synthesis of Type B fluorine containing precursors was performed with the Rupert-Prakash reagent. The novel compounds are indicated by the * symbol.

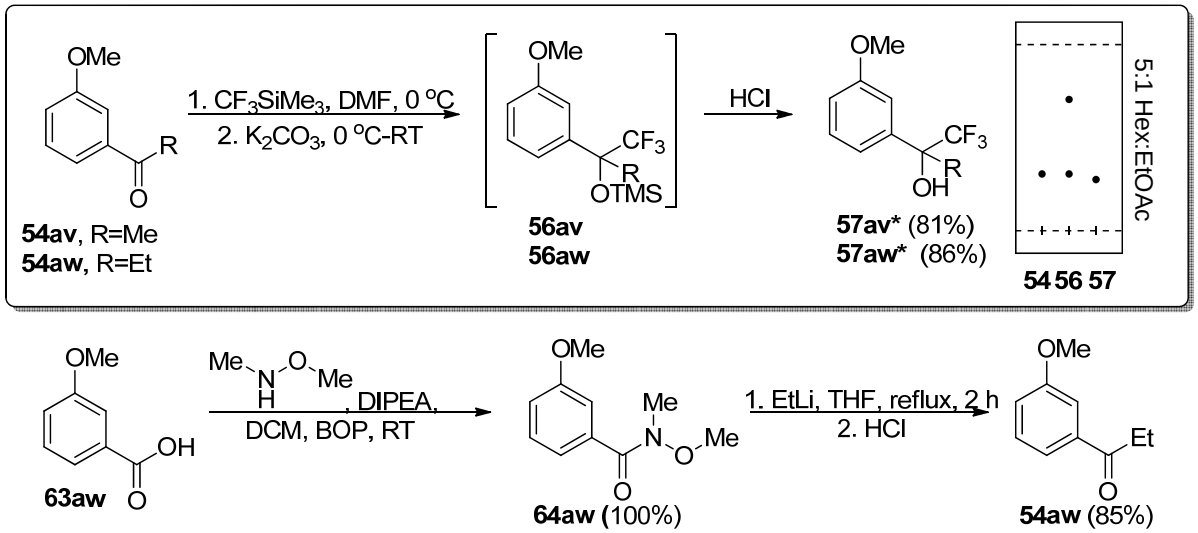

Type B fluorine containing starting materials **57av*** and **57aw*** (Scheme 3.7) were prepared using the two step procedure implemented by Prakash in Scheme 3.6 starting from aryl ketones **54av - aw**. The complete consumption of the starting materials

54av or **54aw** was not observed in the reactions depicted in Scheme 3.7. As a result of the incomplete conversion of starting material, and the similar retention factors observed between starting materials (**54av - 54aw**) and products (**57av* - 57aw*** respectively), it was difficult to separate the two (Scheme 3.7, TLC). In contrast, the less polar TMS ethers **56av - aw** were easily separated from the starting materials **54av - aw** and were isolated prior to cleavage of the silyl ether of **56av - aw** with the simple addition of hydrochloric acid. This modification to the purification protocol made the isolation of **57av* - aw*** much more convenient and afforded yields ranging from 81 to 86% (Scheme 3.7).

Although 3-methoxyacetophenone (**54av**) was commercially available, we were unable to obtain 3-methoxypropiophenone (**54aw**) from commercial sources. We believed that the most efficient method to prepare **54aw** was through the Weinreb amide (**64aw**) as shown in the bottom portion of Scheme 3.7.[18] Utilizing a BOP amide coupling, we were able to achieve a quantitative conversion in the coupling of 3-methoxybenzoic acid (**63aw**) and the Weinreb amine. The addition of ethyllithium followed by a hydrochloric acid quench afforded **54aw** in an 85% yield.

Scheme 3.8. Failed reaction with the Reetz reagent on the 3-substituted regioisomers. The novel compounds are indicated by the * symbol.

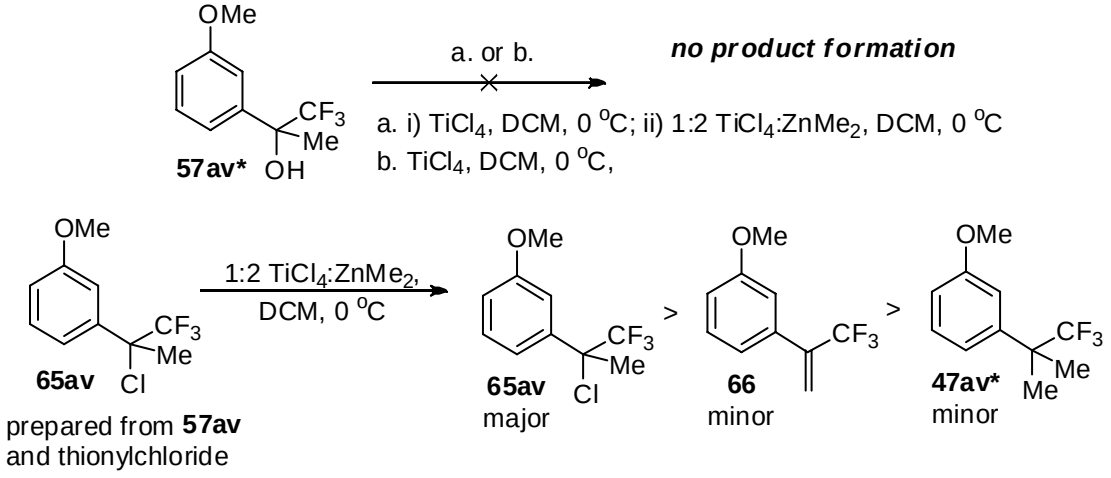

The next step in the reaction involved the introduction of the tertiary center to the C3 position. To accomplish the Reetz conversion, I was able to reproduce the results attained by Tanaka et. al. (lit. 51%, Scheme 3.5)[7] on the 4-substituted regioisomer **59** in a 49% isolated yield. However, attempts to reproduce these results on the 3-trifluoromethyl substituted regioisomers failed (**57av***, Scheme 3.8). Unlike the 4-substituted regioisomer **59**, the 3-substituted regioisomer **57av*** would not undergo an analogous transfer of the methyl group to the intermediate benzylic chloride generated in situ from titanium tetrachloride. Due to the limitations that we observed with the Reetz reagent on substrate **57av*** we were forced to adopt an alternative synthetic approach to prepare compound **47av***.

It was possible that titanium(IV) chloride was not effective at installing the benzylic chloride to compound **57av***. To test this hypothesis, titanium(IV) chloride was added to compound **57av*** to see if product formation could be observed by a simple TLC analysis. The results suggested that titanium tetrachloride was ineffective at installing the benzylic chloride to the C3-substituted regioisomers **57av***. Therefore, the reaction between the Reetz reagent and **65av** could still proceed if the benzylic chloride was generated with another reagent such as thionyl chloride. To test this hypothesis, we prepared **65av** directly from **57av*** and thionyl chloride and subjecting **65av** to the Reetz reagent at 0 ^{o}C in dichloromethane. A mixture of products was observed in the ^{1}H NMR; however, the major constituent in the mixture was the benzylic chloride starting material (**65av**) which was indicated by a singlet at 2.13 ppm in the ^{1}H NMR. Furthermore, prominent vinylic proton resonances were observed at 5.96 and 5.78 ppm from the

elimination product (**66**). A small amount of methyl transfer product (**47av***) was also observed at 1.57 ppm in the ^{1}H NMR spectrum.

Scheme 3.9. Installation of methyl groups with trimethylaluminum.

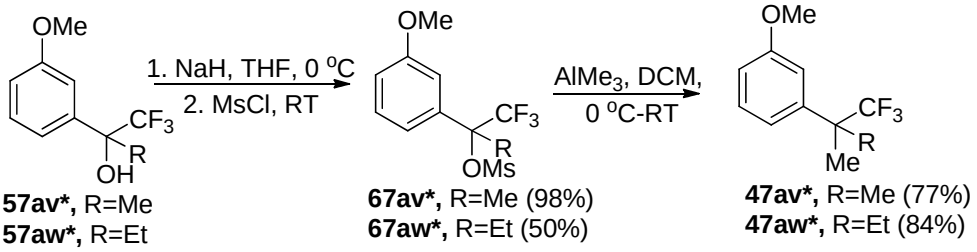

57av*, R=Me
57aw*, R=Et

67av*, R=Me (98%)
67aw*, R=Et (50%)

47av*, R=Me (77%)
47aw*, R=Et (84%)

The trimethylaluminum-benzylic mesylate system developed by Tanaka (Scheme 3.6) turned out to be essential for preparing the tertiary carbon-carbon bonds observed for anisoles **47av*** and **47aw*** (Scheme 3.9). The novel intermediates **47av*** (77% yield) and **47aw*** (84% yield) were prepared in high yields from the intermediate mesylates **67av*** and **67aw***. Although the mesylation of **57av*** proceeded in a 98% yield, analog **67aw*** was produced in a significantly lower 50% yield due to an unfortunate spill.

Scheme 3.10. Synthetic route to prepare Type B fluorine containing phenols and carbamates.

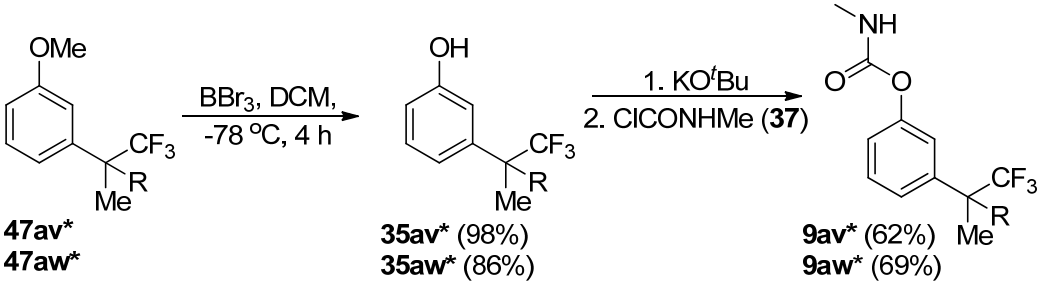

47av*
47aw*

35av* (98%)
35aw* (86%)

9av* (62%)
9aw* (69%)

After installing the desired C3-tertiary centers observed in **47av*** and **47aw*** (Scheme 3.9), the aryl ether methoxy protecting groups were cleaved with boron tribromide (Scheme 3.10). The reaction between anisoles **47av*** and **47aw*** and boron tribromide proceeded in dichloromethane at -78 °C for 4 h to produce the phenols **35av*** and **35aw*** in sufficiently high yields (98% and 86% respectively). Carbamoylation of

the phenols **35av*** and **35aw*** utilizing potassium *tert*-butoxide as a base (**37**, Scheme 3.10) provided acceptable yields of carbamates **9av*** and **9aw*** (62% and 69% respectively).

3.2.3 A pragmatic high-yielding method to prepare "Friedel-Crafts restricted" 3-*tert*-alkylarenes.

The installation of tertiary carbon centers *meta* to *ortho-para* directing substituents have traditionally been synthetically challenging. We have shown that at low temperatures, α-trifluoromethyl-containing C3-substituted benzyl mesylates readily undergo carbon-bond formation with trimethylaluminum (Scheme 3.9). We now wanted to extend the scope of this reaction and explore the potential of trimethylaluminum in the preparation of the non-fluorine containing analogs (**35**, **47**, and **68-70**, Figure 3.8). As part of our ongoing investigation of phenyl *N*-methylcarbamate insecticides,[19] phenols bearing C3-substituted quaternary carbon centers (**35**) were essential starting materials for our studies. However, phenols bearing C3-substituents larger than the *tert*-butyl group (**35as** and **35au***) were not commercially available and traditional methodologies such as the Friedel-Crafts alkylation afforded the undesired regioisomers (predominately C2- and C4-). By optimizing the reaction conditions used on fluorine containing analogs **35av*** and **35aw***, we felt that we could potentially develop a convenient method to prepare what we will refer to as Friedel-Crafts restricted 3-*tert*-alkylarenes (eg. **35**, **47**, and **68-70**; Figure 3.8).

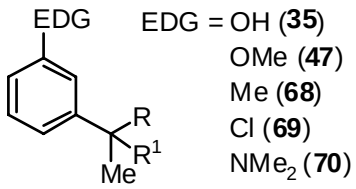

Figure 3.8 Electron rich non-fluorine containing C3-trialkylarenes.

Scheme 3.11. The use of the Reetz reagent to prepare "Friedel-Crafts restricted" products.

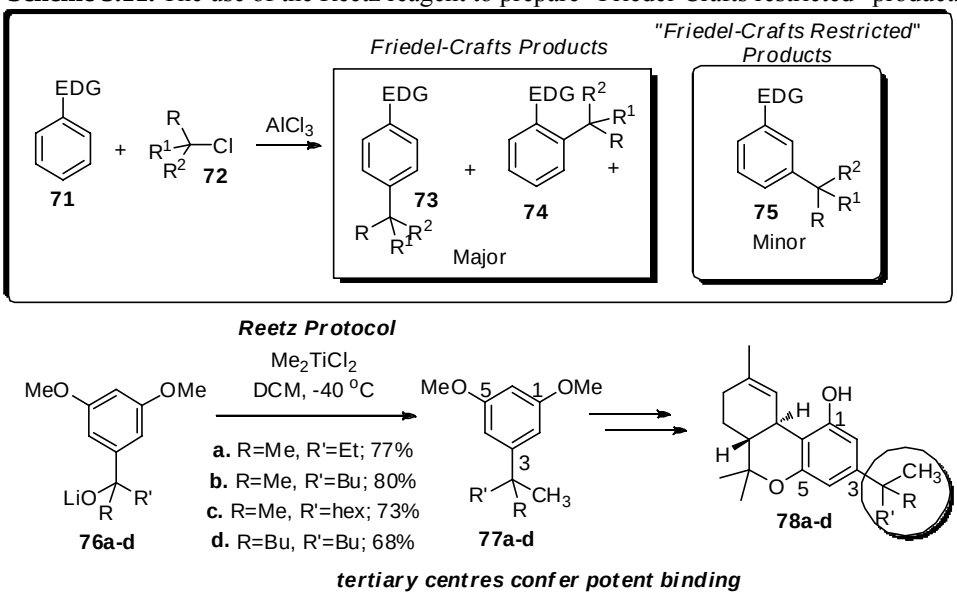

Reetz and coworkers have previously shown that Me_2TiCl_2 is an effective reagent in the preparation of quaternary carbon centers from ketones and alcohols.[17] He also demonstrated the utility of his reagent on the synthesis of electron rich tertiary-substituted centers observed in compounds **77a-d** (Scheme 3.11 lithium carbinolates **76a-d** in yields ranging from 68-80%.[16] Although the Reetz reagent was capable of installing a tertiary alkyl group at C3 to electron rich **76a-d**, there were some drawbacks to its use. From a practical perspective, the Reetz reagent had to be prepared prior to its use from corrosive titanium tetrachloride and costly dimethylzinc. Furthermore, we have pointed out a few examples in which the Reetz reagent failed to yield the intended products (Scheme 3.5, Scheme 3.6, and Scheme 3.8). Although the Reetz reagent could potentially be applied to the synthesis of the Friedel-Crafts restricted products showcased in Figure 3.7, its utility has yet to be realized.

Scheme 3.12. Literature and experimental methods to prepare electron rich 3-tert-alkylarenes.

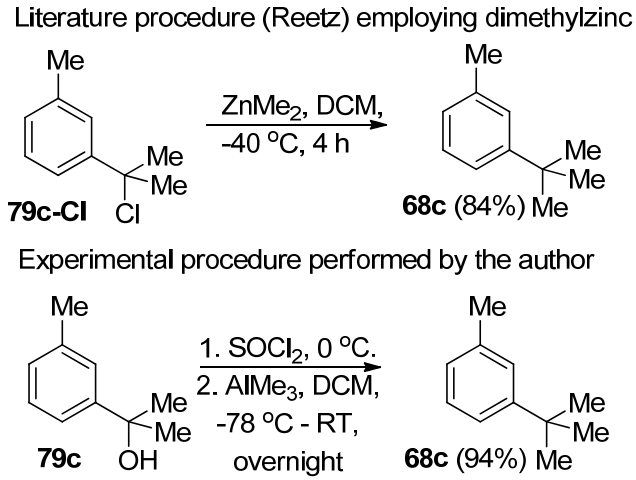

Professsor Reetz does report that dimethylzinc can be used to prepare compound **68c**.[15] As shown in Scheme 3.12 an 84% yield of **68c** was obtained from the reaction of the tertiary benzylic chloride (**79c-Cl**) and dimethylzinc.[15] However, this is his only other example regarding the synthesis of Friedel-Crafts restricted *tert*-alkylarenes. As shown in Scheme 3.12 compound **68c** can also be synthesized in an 94% yield from the reaction between the tertiary benzylic chloride and trimethylaluminum as described by the author. As will show, trimethylaluminum can be used to prepare a variety of Friedel-Crafts restricted products.

It is known that electron rich benzylic sulfonates, such as mesylates, readily undergo polymerization reactions through self alkylation.[20] The electron withdrawing nature of the trifluoromethyl group possibly participated in stabilizing of the benzylic mesylates prepared from compounds **57av*** and **57aw*** (Scheme 3.9). This property made it possible to isolate and characterize compounds **67av*** and **67aw***. Without the trifluoromethyl group present, the mesylates could presumably decompose. Therefore, the more stable benzylic chlorides were substituted for the less stable carbinyl mesylates

(Table 3.3). The tertiary benzylic chlorides were prepared at low temperatures (-20 - 0 ^{o}C) from thionyl chloride to avoid thermal degradation. After tertiary benzylic chloride was formed the excess solvent was evaporated under high vacuum and the reaction was further cooled to 78 ^{o}C to minimize competing electrophilic aromatic substitution and elimination pathways that could potentially occur after the addition of trimethylaluminum.

Table 3.4. Isolated yields of the Friedel-Crafts restricted products prepared with trimethylaluminum.

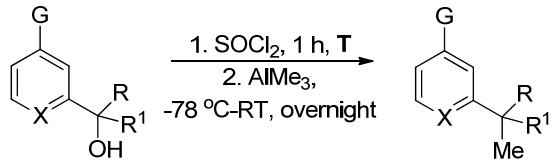

T=0 °C for G=OMe, Me, Cl, H
T=-20 °C for G=OH and NMe_2

reactant	*G*	*X*	*R*	*R*^{1}	*product*[a]	*isolated yield (%)*
45c	OMe	CH	Me	Me	**47c**	93
50c	OH	CH	Me	Me	**35c**	83
79c	Me	CH	Me	Me	**68c**	85
80c	Cl	CH	Me	Me	**69c**	93
81c	NMe_2	CH	Me	Me	**70c**	ND[b]
82c	H	N	Me	Me	**71c**	5
45as	OMe	CH	Me	Et	**47as**	94
50as	OH	CH	Me	Et	**35as**	70
79as	Me	CH	Me	Et	**68as**	94
80as	Cl	CH	Me	Et	**69as**	78[c]
45au	OMe	CH	Et	Et	**47au**	95
50au	OH	CH	Et	Et	**35au***	92
79au	Me	CH	Et	Et	**68au**	80
80au	Cl	CH	Et	Et	**69au**	ND[b]

[a] The novel molecules are indicated by the * symbol. [b] No desired product detected.
[c] Weight recovery (89%) of a mixture of the desired product (88%) and elimination product (12%) determined by ^{1}H NMR spectrum.

Table 3.3 demonstrates that thionyl chloride and trimethylaluminum provide a convenient alternative to prepare Friede-Crafts restricted *tert*-alkylarenes. TLC analysis indicated that no starting material remained after bringing the reaction contents to room

temperature and allowing the contents to stir overnight. In some instances, the product could be isolated in high purity with a simple solvent extraction after an acid quench. One of the useful features of this protocol is its ability to directly prepare 3-*tert*-alkylphenols (**35c**, **35as**, and **35au***) in high yields without any protection/deprotection strategies. In hindsight, it could be possible to prepare fluorine containing phenols **35av*** and **35aw*** (Scheme 3.10) directly without without protection with the methoxy group. Out of the many examples outlined in Table 3.4 the phenols were the only compounds relevant to our insecticide investigations. However, o*rtho/para* directing anisole, tolyl, chloro, and dimethylanilino functionality was also examined to explore the scope of this reaction on other Friedel-Crafts restricted products.

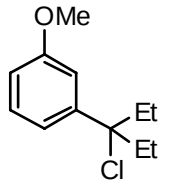

45au-Cl

Figure 3.9. Stable tertiary benzylic chloride intermediate.

Unlike the unstable and volatile tertiary benzylic fluoride (**35cd***, Scheme 3.3) the tertiary benzylic chloride **45au-Cl** (Figure 3.9) could be isolated and characterized by ^{1}H NMR and ^{13}C NMR spectroscopy. Prior to discovering that **45au-Cl** could be isolated and characterized, we also believed that the intermediate tertiary benzylic chlorides would rapidly decompose upon standing. Reetz and coworkers had previously reported that tertiary benzylic chlorides were not stable.[16] Although we were able to isolate the tertiary benzylic chloride **45au-Cl**, the *in situ* generation of the benzylic chlorides was advantageous from a synthetic perspective to minimize the required isolation steps. Evidence for the formation of the benzylic chlorides could be visually detected by the presence of a yellow oil in the reaction flask. The tertiary benzylic chlorides prepared from the phenols (**50-Cl**, G=OH) and dimethylaniline (**70-Cl**, G=NMe_2) rapidly decomposed at 0 ^{o}C. Therefore, these intermediates were carefully

prepared at -20 ^{o}C over 30 minutes and kept cool upon removal of the thionyl chloride to offset their rapid decomposition upon raising the temperature.

Methyl groups were nucleophilically installed with trimethylaluminum on a series of tertiary benzylic chlorides to afford anisoles (**47**), phenols (**35**), tolyl (**68**), and chlorobenzenes (**69**) in yields ranging from 70 - 95% (Table 3.4). As an example of the usefulness of this procedure the author would like to highlight 3-*tert*-butylphenol (**35c**). The most useful method available to prepare 3-*tert*-butylphenol (**35c**) was carried out by oxidizing *tert*-butylbenzene with hydrogen peroxide and hydrogen fluoride/boron trifluoride. Olah and coworkers have shown that this reaction affords the meta substituted product (**35c**) in a meager 14% isolated yield.[21] Electrophilic aromatic substitution pathways such as the Friedel-Crafts reaction on electron rich substrates also presents the same non-regioselective issues.

The reaction between trimethylaluminum and the tertiary benzylic chorides generated from the 3-chloro (**80au**) and 2-pyridyl (**82c**) tertiary benzylic alcohols (Table 3.4) resulted in mixtures of the intended methyl installation and elimination byproducts. Based relative peak areas in the ^{1}H NMR spectrum we were able to determine that the 95% of the product mixture resulting from the reaction of **82c-Cl** and trimethylaluminum consisted of the unwanted elimination product (**83**, Figure 3.10). The minor constituent (5%) is proposed to be the desired compound (**71c**), based on the ^{1}H NMR data. As a result of very little methyl installation into pyridine containing tertiary alcohol (**82c**), the author did not attempt to prepare the larger tertiary analogs such as **71as** and **71au**.

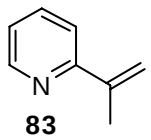

83

Figure 3.10. Elimination product.

We also wanted to explore the effects of chloro substitution on the aromatic ring in the installation of methyl groups to tertiary C3-substituted benzylic alcohols . As Table 3.4 indicates the methyl group was smoothly introduced to dimethylbenzylic alcohol **80c** to produce compound **80c** in a 93% yield without the formation of elimination byproduct. In contrast, the installation of a methyl group to diethylbenzylic alcohol **80au** resulted in substantial elimination product. For the ethylmethylbenzylic alcohol **80as** moderate success was realized. Compound **69as** was isolated as a mixture (89% weight recovery) also containing the elimination byproduct. Based on the ^{1}H NMR data the product mixture contained 88% methyl transfer product and 12% of the unwanted elimination byproduct. In contrast to the electron deficient substrates discussed, our most electron rich substrate, (**81c**, 2-(3-(dimethylamino)phenyl)propan-2-ol), was not suitable for this chemical transformation. Despite these limitations, this procedure was directly applicable to the majority of substrates showcased in Table 3.4.

3.2.4. The synthesis of non-fluorine containing aromatic C3-tertiary benzylic alcohols

Table 3.5. Isolated yields for the synthesis of aromatic tertiary benzylic alcohols from acetophenones.

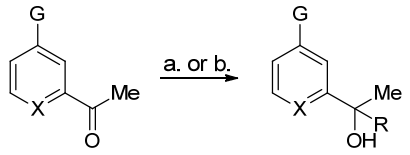

a. 1. Me_3MgLi (1.3 equiv), THF, -78 °C, 5 h 2.NH_4Cl
b. 1. LiCl (1 equiv), $ZnCl_2$ (20 mol%), Me_3SiCH_2MgCl (20 mol%), EtMgCl (1.1 equiv), THF, 0 °C-RT, overnight 2.NH_4Cl

reactant	*G*	*X*	*R*	*product*[a]	*isolated yield (%)*[b]
54	OMe	CH	Me	**45c**	94
84	OH	CH	Me	**50c***	92
85	Me	CH	Me	**79c**	97
86	Cl	CH	Me	**80c**	91
87	NMe_2	CH	Me	**81c**	90
88	H	N	Me	**82c**	91
54	OMe	CH	Et	**45as**	87 (63)
84	OH	CH	Et	**50as***	91 (68)
85	Me	CH	Et	**79as**	94 (53)
86	Cl	CH	Et	**80as***	98 (74)

[a] Novel compounds are indicated by the * symbol. [b] The yields in parenthesis are reported between the aryl ketone and ethylmagnesium bromide after stirring at room temperature overnight.

The C3-substituted tertiary benzylic alcohols where the R group was either a methyl or ethyl group were prepared with "ate" containing organometallic methods a or b (Table 3.5). Starting from the corresponding acetophenones (**54**, **84-88**), we implemented lithium trimethylmagnesate as a means to add a methyl nucleophile to the analogous acetophenones (method a, **54** and **84-88**). Yields above 90% were obtained from method a for compounds **45c**, **50c***, and **80-82c** as illustrated in Table 3.5. The enhanced nucleophilicity and reduced basicicity of the ate complexes is believed to reduce the side products resulting from unwanted deprotonation, aldol, and β-hydride reduction pathways

that have been associated with the Grignard reaction.[22] For example, **45c** was prepared in a 94% yield with lithium trimethylmagnesate. Conversely, with the use of methylmagnesium iodide alone, the literature reports a 70% yield.[23] In addition, the most applicable published method to prepare tertiary benzylic alcohol **81c** involved the use of MeMgI and resulted in a 50% yield.[22] In contrast, we prepared compound **81c** in a 90% yield with lithium trimethylmagnesate. Furthermore, the available literature methods to prepare the tertiary benzylic alcohol **82c** utilized a S_NAr pathway that resulted in a 65% yield. In comparison, a 91% yield achieved with lithium trimethylmagnesate as outlined in Table 3.5.[24, 25] Finally, the tertiary-benzylic alcohol **50c** (G=OH) was a novel small molecule and directly prepared in a 92% yield with the lithium trimethylmagnesate complex. The Grignard reagent offered a pragmatic procedure to convert the aryl ketones (**54**, **84-88**) listed in Table 3.5 to the corresponding tertiary benzylic alcohols (**45c**, **50c**, and **80-82c**). However, as we have demonstrated by comparing the literature yields to that obtained with lithium trimethylmagnesate, the latter offers higher yields of the desired compounds (**45c**, **50c**, and **80-82c**).

The ethyl group was added to ketones **54**, **84-86** using an interesting system that is apparently catalytic in zinc (Table 3.5, products described by **as**). Ishihara and coworkers successfully applied this technology to several analogous aryl ketones in a series of recent publications.[26, 27] This strategy has allowed us to prepare entries **45as**, **50as***, and **80as***, **81as**, and **82as** in higher yields compared with the use of the Grignard reagent alone. The yields reported in Table 3.5 located in the parentheses represent the yields attained when a tetrahydrofuran soltuion of ethylmagnesium bromide and the aryl ketone were allowed to stir overnight at room temperature.

Titanium(IV) isopropoxide and diethylzinc have also been reported to produce **80as** in an 82% yield from **86**.[28] However, we were able to show that lithium ethylzincate afforded **80as** in a 98% yield. By using Ishihara's protocol of ethylmagnesium chloride mixed with 20 mol% zinc and lithium chloride, only a slight excess of Grignard reagent (1.1 equiv) was required for a to convert 87-98% of the starting material to product. In contrast to the use of 1.1 equiv of ethylmagnesium chloride with lithium ethylzincate, 3-equiv of ethylmagnesium bromide alone produced lower yields ranging from 53-74% (see parantheses in Table 3.5). It should be noted however, that the zincate protocol outlined by Ishihara was labor intensive requiring careful schlenk line melt-drying techniques due to the hygroscopic nature of the lithium and zinc chlorides.

Scheme 3.13. Available literature methods to prepare C3-substituted tertiary diethyl benzylic alcohols.

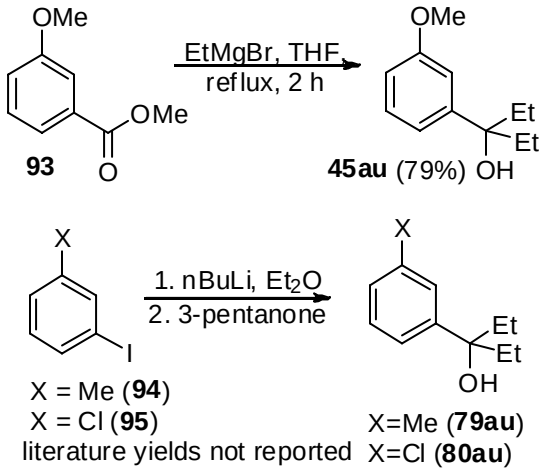

To prepare the diethylbenzylic alcohols we will begin by reviewing published results reported by previous investigations. Compound **45au** had been previously prepared in 79% yield from refluxing the methyl benzoate with ethylmagnesium bromide (Scheme 3.13).[29] An alternative method to prepare diethylbenzylic alcohols is also shown in Scheme 3.13.[30] Compounds **79au** and **80au** were prepared by generating the

aryllithium reagent from aryl iodides **94** and **95**. Next, the aryllithium reagents were added to 3-pentanone.[30] Compound **79au** and **80au** were not the main focus of this publication and the authors did not report the yields obtained from the reaction depicted in Scheme 3.13. Below, we have implemented the procedure to prepare compound **79au** (86%) and **80au** (88%) in high yields. In addition, we have also provided detailed charcterization data that the older literature lacked.

Table 3.6. Isolated yields for the synthesis of aromatic tertiary benzylic alcohols bearing diethyl functionality.

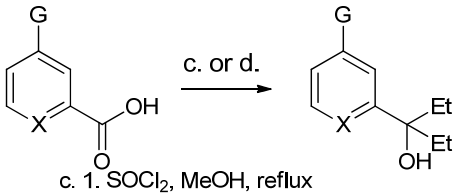

reactant	*G*	*product*[a]	*methyl benzoate*[b] *isolated yield (%)*	*acid chloride*[c] *isolated yield (%)*
89au	OMe	**45au**	89	59
90au	OH	**50au***	84	56
91au	Me	**79au**	88	58
92au	Cl	**80au**	86	38

[a] Novel compounds are indicated by the * symbol. [b] The reported yields are from the addition of the Grignard reagent to the crudely isolated methyl benzoate. [c] The reported yields are from the addition of the Grignard reagent to the crudely isolated acid chloride.

The preparation of the diethylbenzylic alcohols **45au**, **50au***, and **79-80au** (Table 3.6) began by converting the corresponding benzoic acids (**89-92au**) to either the acid chloride or the methyl benzoate. At the outset we believed that there would be no difference observed in the yields between the two, and prepared the acid chlorides first due to the ease from which acid chlorides were generated and isolated. However, as Table 3.6 demonstrated the utilization of the methyl benzoates as synthetic intermediates afforded superior yields compared with the acid chlorides. The isolated yields obtained

by refluxing the methyl benzoates in the presence of of ethylmagnesium bromide resulted in the desired compounds **45au**, **50au***, and **79-80au** in yields ranging from 84 - 89%. In contrast, the same procedure implemented on the analogous acid chlorides resulted in yields ranging from 38 – 59%. The largest degree of variation in the isolated yields was observed in the preparation of **80au** where G=Cl. A low 38% yield was achieved when the acid chloride was implemented compared with an 86% yield achieved from the methyl benzoate intermediate. The novel phenol bearing a C3-tertiary diethylbenzylic alcohol **50au*** was also prepared in an 84% yield from the methyl benzoate.

Scheme 3.14. Proposed substitution elimination pathways to account for products resulting from the addition of trimethylaluminum to tertiary benzylic chlorides.

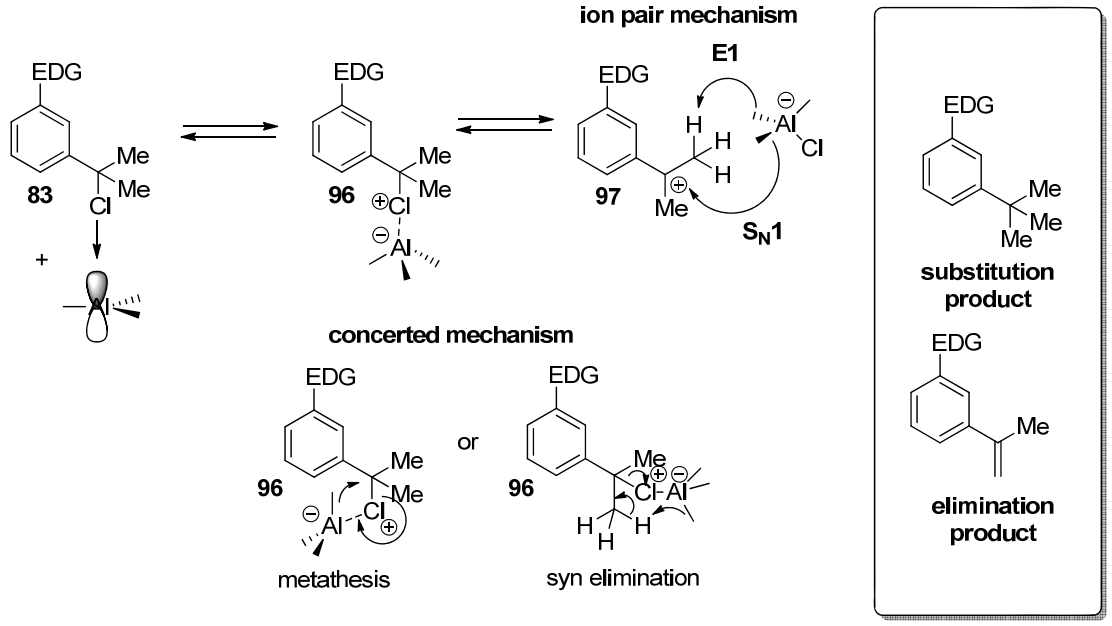

Now that we have described the preparation of the tertiary benzylic alcohols and their transformation to Friedel-Crafts restricted *tert*-alkylarenes, we turn to a discussion of the mechansim of this transformation. Trimethylaluminum performs a unique role in the reaction with tertiary benzylic chlorides, favoring substitution over elimination. Trimethylaluminum adopts a trigonal planar geometry with an empty p orbital perpendicular to the bonding orbitals. Thus neutral trimethylaluminum is best viewed as a

Lewis acid. However, trimethylaluminum can also act as a nucleophile able to donate methyl nucleophiles if associated with a Lewis base. A reasonable mechanistic explanation for the reaction depicted in Scheme 3.14 involves the coordination of the non-bonding chloride electrons of **83** with the empty p-orbital on trimethylaluminum (Scheme 3.14). The resulting complex (**96**) can then react in several ways. One possible way for the reaction to occur could be through an ion pair separation mechanism involving the formation of a carbocation (eg. **97**). With the formation of the carbocation an activated aluminum complex is also generated. Through this carbocation-forming pathway the activated trimethylaluminum likely reacts with the carbocation in a S_N1 fashion. Although not observed the trimethylaluminum has the potential to additionally react through an E1 mechanism to give alkene.

It is also possible that a concerted pathway is responsible for the substitution pathway observed for the substrates listed in Table 3.5. At the onset of our investigations we favored the ion-pair separation mechanism to explain our results. However, we questioned this mechanism as electron poor tertiary alcohols such as **80c** and **82as** were leading to high levels of elimination product (Table 3.5) while the electron-withdrawing trifluoromethyl-containing benzylic mesylates depicted in Scheme 3.9 were not. Although front side S_N2 attacks are not discussed as practical mechanisms in synthetic organic chemistry, the mechanism could be metathesis-like and provide a potential explanation for the high levels of substitution over elimination observed for the majority of the substrates excluding compounds **80c** and **82as**.

Table 3.7. Ethyl transfer versus β-hydride elimination of triethylaluminum.

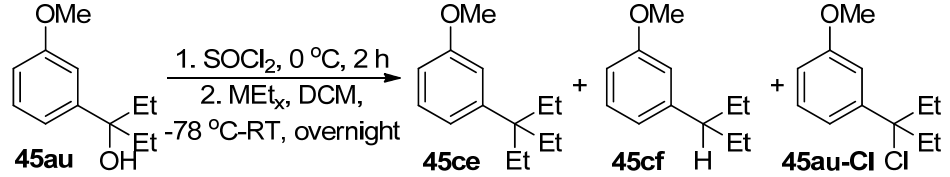

entry	*MEt_x*	*45ce : 45cf : 45au-Cl*	*weight recovery (%)*
1	$AlEt_3$	77 : 23 : 0	96
2	BEt_3	0 : 0 : 100[a]	100
3	$ZnEt_2$	46 : 54 : 0	96

[a] The intermediate tertiary benzylic chloride was isolated in a 100% yield after refluxing in chloroform overnight.

We have thus far demonstrated that trimethylaluminum can efficiently transfer methyl groups to many tertiary benzylic chlorides. Important exceptions are the ethylmethyl (**80as-Cl**) and diethylbenzylic chloride **(80au-Cl**). We quickly realized that ethyl transfer was not as easily accomplished with triethylaluminum compared with trimethylaluminum. Instead of ethyl transfer persistent β-hydride elimination (**45cf**, Table 3.7) occurred when **45au** was treated with thionyl chloride and then triethylaluminum. Compounds **45ce** and **45cf** were obtained in a 77 : 23 ratio as an inseparable mixture (entry 1). We then repeated the reaction with triethylboron, but found only recovered only the intermediate tertiary benzylic chloride (entry 2). Interestingly, triethylboron (entry 2, Table 3.7) did not react with the tertiary benzylic chloride (**45au-Cl**). Further attempts to prepare **45ae** with triethylboron were made by first isolating benzylic chloride **45au-Cl** and refluxing the isolated compound in a solution of chloroform (b.p. = 61 °C) containing triethylboron. Unfortunately, these more stringent reaction conditions were not sufficient to convert the starting material **45au** to products. Instead, 100% of the tertiary benzylic chloride (**83au-Cl**) was recovered from the reaction.

The use of diethylzinc in the protocol resulted in a 46 : 54 ratio of the desired and undesired products (entry 3, Table 3.7). To date we have been unable to find a suitable organometallic reagent that could cleanly transfer an ethyl group without competing hydride transfer. Although a mixture of products resulting from β-hydride elimination and ethyl transfer were observed in entries 1 - 3 in Table 3.6, no competing elimination was observed. The introduction of ethyl groups with organometallic reagent deserves further attention and would allow investigators to prepare C-3 triethyl centers such as **45ce** and potentially other C3-substituted triethyl centers.

Scheme 3.15. Preparation of class I phenyl *N*-methylcarbamates bearing C3-substituents larger than *tert*-butyl. Novel compounds are indicated by the * symbol.

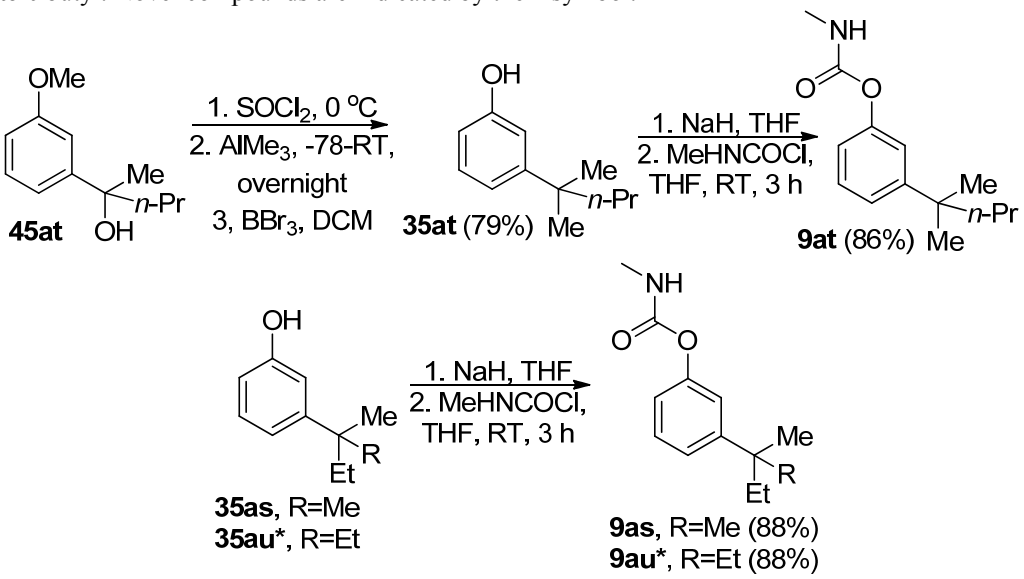

The reaction between trimethylaluminum and tertiary benzylic chlorides allowed us to prepare phenols **35as-au** which could then be readily converted into carbamates **9as-au** (Table 3.5). In addition, we also examined the conversion of **45at to 35at** to analyze larger alkyl groups at the C3-position. The phenol **35at** was successfully prepared with trimethylaluminum (Scheme 3.15) and was isolated in a 79% yield over two steps including a boron tribromide aryl ether cleavage. Although phenyl *N*-

methylcarbamates **9as** and **9at** were known, this methodology allowed us to prepare the novel carbamate **9au*** in an 88% yield.

3.2.5 Synthesis of secondary branched class I phenylcarbamates

Scheme 3.16. Preparation of electron rich 2-isoalkylarenes with trimethylaluminum and the subsequent carbamate.

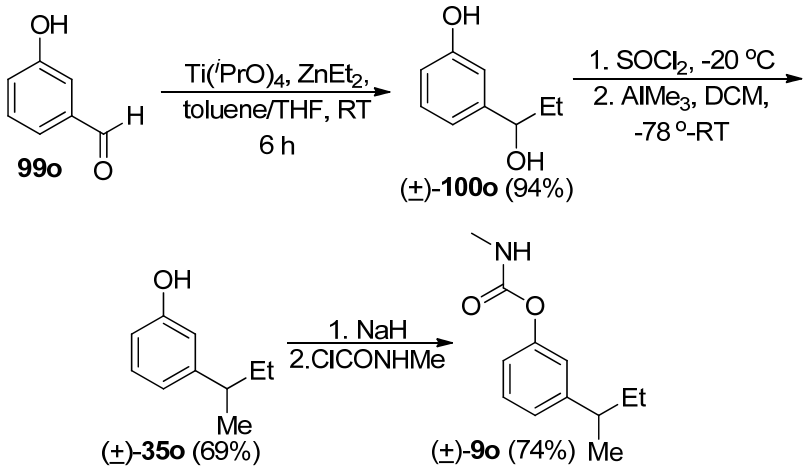

In addition to the tertiary centers prepared in Table 3.4, we also wanted to examine the effectiveness of trimethylaluminum to prepare secondary C3-centers such as the racemic phenol, (+)-**35o** (Scheme 3.16). Furthermore, the phenol (+)-**35o** could be carbamoylated, and the carbamate (+)-**9o** could be assayed for its inhibition potency against *An. gambiae* AChE. To ascertain whether trimethylaluminum was effective, we first prepared the secondary benzylic alcohol (±)-**100o** utilizing a titanium isopropoxide and diethylzinc solution to transfer an ethyl nucleophile to the benzaldehyde in a 94% isolated yield. The addition of trimethylaluminum to the secondary benzylic chloride (±)-**100o-Cl** resulted in a 69% yield of the desired phenol (±)-**35o**. The carbamoylation of the compound (+)-**35o** afforded the phenyl *N*-methylcarbamate (±)-**9o** in a 74% yield.

Scheme 3.17. Preparation of 3-cyclohexylphenyl N-methylcarbamate.

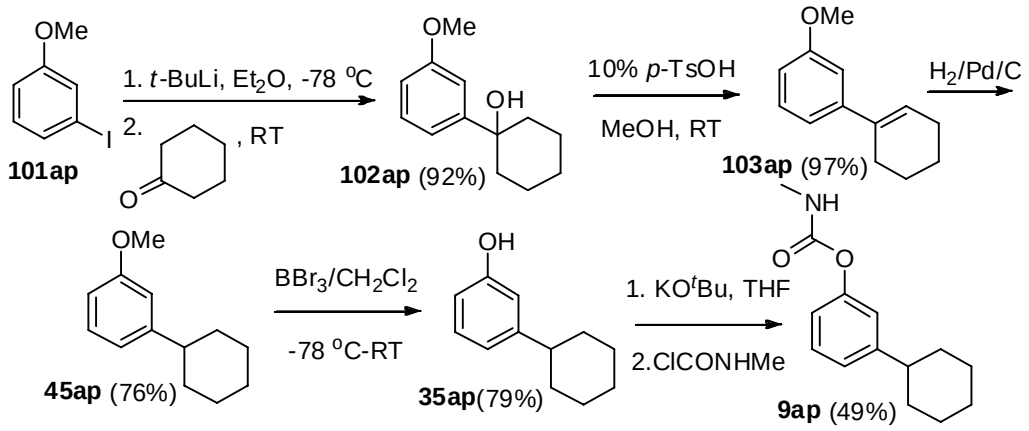

The efficacy of C3-conformationally constrained class I analogs were examined by preparing 3-cyclohexylphenyl *N*-methylcarbamate (**9ap**) over 5 steps starting from 3-iodoanisole (**101ap**, Scheme 3.17). The first step involved a metal-halogen exchange reaction of **100ap** and *tert*-butyllithium in diethyl ether. After the addition of cyclohexanone the reaction proceeded in a 92% yield to afford compound **102ap**. The *para*-toluenesulfonic acid catalyzed elimination of compound **102ap** led to the cyclohexene **103ap** in a high yield (97%). Catalytic hydrogenation of the alkene with palladium on carbon produced 3-cyclohexylanisole **45ap** in a 76% yield. The deprotection of the anisole **45ap** was carried out with boron tribromide affording phenol **35ap** in a 79% yield. Carbamoylation of the phenol (**35ap**) via carbamoylation method B afforded **9ap** in a 49% yield. Other conformationally constrained class I analogs were not prepared due to the poor insecticidal activity of 3-cyclohexylphenyl *N*-methylcarbamate, or **9ap** (Table 2.9).

3.3 Synthesis of Class II C-2 substituted phenols and phenyl *N*-methylcarbamates

Table 3.8. Isolated yields for the class II alkylthiophenols and the analogous carbamates.

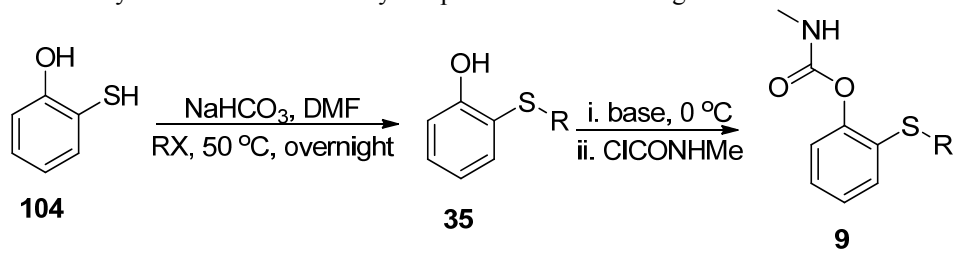

104 35 9

entry[a]	*RX*	*isolated yield (35)*	*isolated yield (9)*
ac	MeI	100	74[c]
ax	EtI	98	50[b]
ad	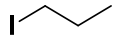	98	76[b]
ae	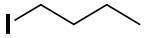	100	77[b]
v		51	92[c]
af	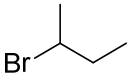	55	77[c]
ay*	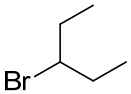	64	93[c]
ah	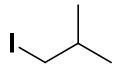	74	96[c]
ba*	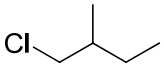	100	88[c]
bc*	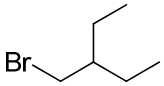	100	83[c]
be*	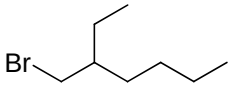	95	60[b]
br	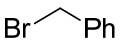	78	78[c]
ag	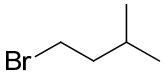	82	76[c]
bw*	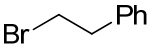	97	76[c]

[a] Novel carbamates are indicated by the * symbol. [b] Carbamate prepared by carbamoylation method A (NaH). [c] Carbamate prepared by carbamoylation method B (K^tOBu).

From over forty class II phenylcarbamates, our investigations have culminated in the identification of several inhibitors with greater than 100-fold target selectivity for *Ag*AChE. In particular, **9bd*** bearing a 2-ethylbutoxy side chain was remarkably 570 $\pm$ 72-fold selective (Figure 2.6). Class II phenols bearing C2-alkylthio and alkoxy appendages were constructed under S_N2 reaction conditions with various primary and secondary alkyl halides. Generally, when X=S (Table 3.8) the reactions proceeded in excellent yields approaching 100% with primary alkyl halides (entries **35ac-ae**, **35ax** and entries **35ba**, **35bc**, **35be**, **35ag**, and **35w**). In contrast to the primary halides, the more sterically hindered secondary alkyl halides (entries **35v**, **35af** and **35ay**) gave significantly lower yields, ranging from 51-64%. In dimethylformamide a weak base such as sodium bicarbonate was capable of selectively deprotonating the thiol of 2-mercaptophenol (**104**). The sulfur-selective alkylation occurred upon reacting at 50 ^{o}C overnight. In contrast to other primary alkyl halides, the use of benzyl bromide resulted in surprisingly lower yields (entry **35br**, 78%). The enhanced electrophilicity of benzyl bromide made this substrate uniquely prone to *O*-alkylation. Finally, the carbamoylation of phenols (**35**) yielded the corresponding carbamates (**9**) in moderate to high yields ranging from 50 – 96% (Table 3.8).

Table 3.9. *S*-alkylation of mercaptophenol with tosylate electrophiles. Isolated yields for carbamoylation via method B.

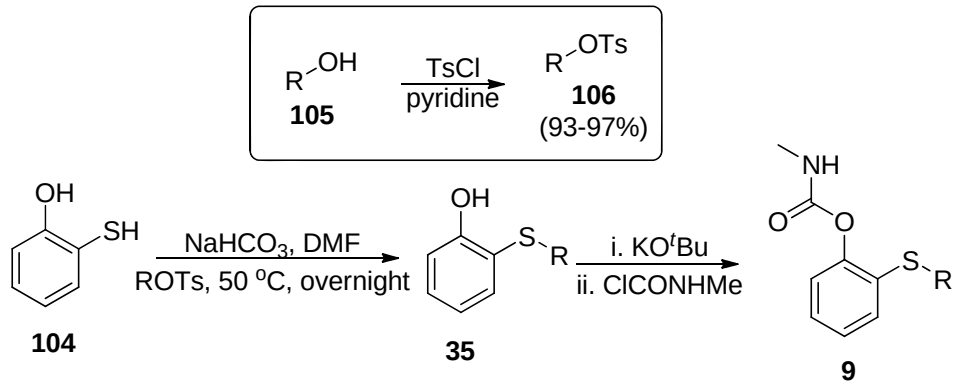

entry[a]	*TsOR*	*isolated yield (35)*	*isolated yield (9)*
bm*	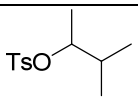	26	93
bn*	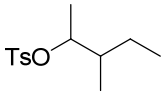	41	86
bo*	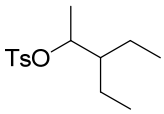	38	94
bg*	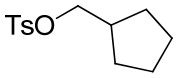	83	78
bh*	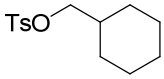	87	57

[a] Novel carbamates are indicated by the * symbol.

Based on the high inhibition potency observed for many of the class II 2-alkylthiophenyl *N*-methylcarbamates, we expanded our investigations beyond the commercially available alkyl halides and began to implement tosylate electrophiles **106** when only the analogous alcohols were commercially available (**105**). As shown in Table 3.9, the tosylates (**106**) were prepared in 93-97% yields from tosyl chloride in pyridine. The phenols (**35**) were prepared in the same manner as the phenols previously shown in Table 3.7. The secondary alkyl tosylates (**106**) reacted with 2-mercaptophenol (**104**) in

low to moderate yields ranging from 26-41% (Table 3.9), as expected based on our previous experience with other secondary alkyl halides (Table 3.8).

The conformationally constrained class II alkylthiophenols (**35bg** and **35bh**) were also prepared with tosylate electrophiles (**106bg** and **106bh**). The cyclopentylmethyl side chain was installed in an 83% yield from 2-mercaptophenol (**104**) and cyclopentylmethyltosylate (**35bg**). Correspondingly, 2'-(2-cyclohexylmethylthio)-phenol (**35bh**) was prepared in a similar 87% yield from cyclohexylmethyl tosylate **106bh**. The phenyl *N*-methylcarbamates depicted in Table 3.9 were prepared according to carbamoylation method B, and with the exception of **9bh*** (57% yield), the reaction produced phenyl *N*-methylcarbamates in yields ranging from 78-94%.

Table 3.10. Isolated yields for the addition of allylic halides to either 2-mercaptophenol or catechol. The isolated yields obtained from carbamoylation are also reported.

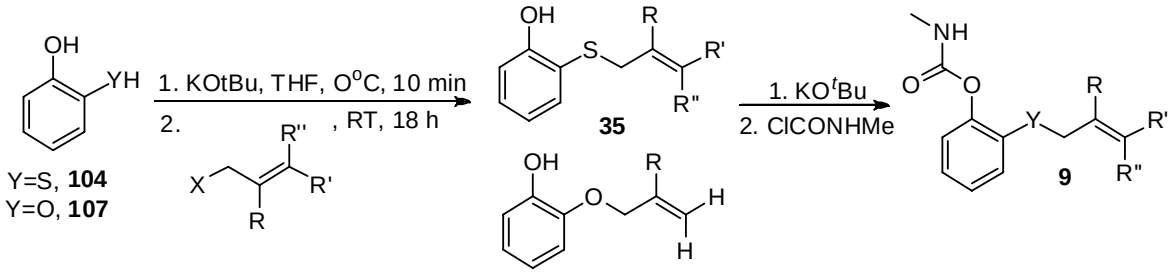

entry[a]	*Y*	*X*	*R*	*R'*	*R''*	*isolated yield 35*	*isolated yield 9*
bp	S	Br	H	H	H	86	88
ai	S	Cl	Me	H	H	87	83
bu	S	Br	H	Me	H	97	91
bv*	S	Br	H	Me	Me	99	80
bs*	S	Cl	Cl	H	H	49	58
bt*	S	Br	Br	H	H	58	35
bq*	O	Cl	Me	H	H	46	74
cg*	O	Br	Br	H	H	52	31

[a] Novel carbamates are indicated by the * symbol.

The ready availability of many allylic halides led us to prepare the phenols (**35**) and corresponding phenyl *N*-methylcarbamates (**9**) shown in Table 3.10. Recall that the reaction between 2-mercaptophenol (**104**) and alkyl halides required the use of dimethylformamide and heating to 50 ^{o}C (Table 3.8). The reactions between 2-mercaptophenol (**104**) and allylic halides (Table 3.10) proceeded in tetrahyrofuran at room temperature, reflecting the enhanced reactivity of allylic halides relative to the alkyl halides. The preparation of phenols **35ai**, **35ai**, **35bu**, and **35bv** proceeded in yields ranging from 86 – 99%. When we later tried this protocol for the alkyl halides, it did not work well. It was at that point we switched to the dimethylformamide 50 ^{o}C protocol described in Table 3.8.

In contrast to the high yields achieved between 2-mercaptophenol (**104**) and allylic halides, the reaction with vinylic halide-containing allylic halides (**35bs** and **35bt**) resulted in yields of 49% and 58% respectively. Furthermore, the reaction of allylic halides with phenols **35bq** and **35cg** resulted in comparative 46% and 52% yields respectively (Table 3.10). Carbamoylation of the corresponding phenols **35** resulted in the phenyl *N*-methylcarbamates (**9**) ranging from 31 – 91% yields. The low yields for the carbamoylation were observed for the vinylic halide containing phenols **35bs**, **35bt**, and **35cg**.

Scheme 3.18. Oxidation of **9bc** to the sulfoxide **9k**.

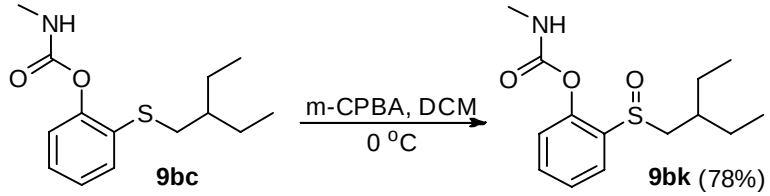

9bc **9bk** (78%)

Class II phenyl *N*-methylcarbamates bearing C2-alkoxy substituents have been shown to be some of the most toxic carbamates against *An. gambiae* (i.e. propoxur or **9a**).

Conversely, the inhibition potency of the sulfur homologs was determined to be greater than the oxygen series (Scheme 2.3). The high inhibition potency/low toxcity conundrum could potentially be due to the oxidation of the sulfur to sulfoxides and sulfones *in vivo*. To test the sulfur oxidation hypothesis, **9bk*** was prepared from **9bc*** and meta-chloroperbenzoic acid in dichloromethane. A 78% yield of compound **9bk*** was achieved as illustrated in Scheme 3.18. Other sulfoxide analogs were not prepared as carbamate **9bk*** was a significantly less powerful inhibitor compared with **9bc*** and showed no measurable contact toxicity against *An. gamibae* mosquitoes.

Table 3.11. Isolated yields for the *O*-alkylation of catechol with various electrophiles and subsequent carbamoylation via method B.

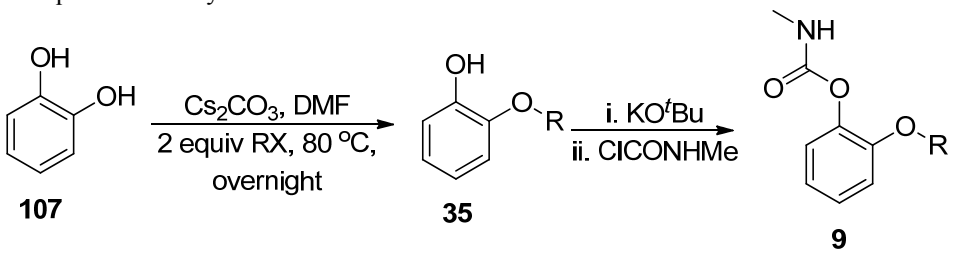

107 **35** **9**

entry[a]	*RX*	*isolated yield (35)*	*isolated yield (9)*
az*	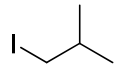	42	90
bb*	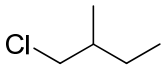	34	86
bd*	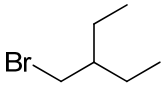	39	83
bi*	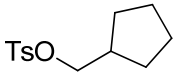	44	85
bj*	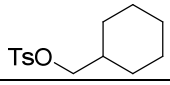	31	45

[a] The novel carbamates are indicated by the * symbol.

We also implemented a procedure to prepare 2-alkoxyphenols such as **35az**, **35bb**, **35bd**, **35bi**, and **35bj**. Although many authors have developed high yielding reactions for the alkylation of phenol (**35d**),[31, 32] the literature lacks a high yielding

method describing the alkylation of *ortho*-catechol (**107**) with alkyl halides. In fact, the available literature indicated that the yields rarely exceed 40% under optimized conditions.[33, 34] We observed similar yields when catechol (**107**), cesium carbonate, and various electrophiles were heated to 80 ^{o}C in dimethylformamide (31-44%, Table 3.11). The high yields obtained from 2-mercaptophenol (**104**), relative to catechol (**107**), was attributed to the enhanced nucleophilicity of the thiolate relative to phenolate anion. Although low yields were achieved attaining intermediate 2-alkoxyphenols **35az**, **35bb**, **35bd**, **35bi**, and **35bj**, the phenyl *N*-methylcarbamates (**9az***, **9bb***, **9bd***, **9bi***, and **9bj***) were prepared in high yields (Table 3.11) enabling the Carlier group to test these phenyl *N*-methylcarbamates for their mosquitocidal properties.

Scheme 3.19. 10-step synthesis of class II carbamate **9bl***. The novel carbamates are indicated by the * symbol.

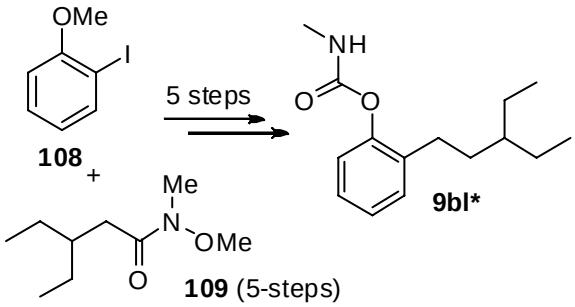

After building a library of class II - phenylcarbamates bearing C2-alkylthio and alkoxy substituents, we also envisioned analogous carbamates with a C2-carbon carbon bond as observed in carbamate **9bl*** (Scheme 3.19). Phenylcarbamates bearing a carbon-carbon bond in the C2-position were more synthetically challenging to prepare due to the absence of nucleophilic heteroatoms such as sulfur (i.e., **104**) and oxygen (i.e., **107**). The heteroatoms found on 2-mercaptophenol (**104**) or catechol (**107**) allowed for direct bond formation with an assortment alkyl halides. However, the C2-carbon bond observed in compound **9bl*** would have to be constructed in a different manner. Therefore, **9bl*** was assembled starting from 2-iodoanisole (**108**) and the Weinreb amide

(**109**) over 5-steps. However, the Weinreb amide itself required 5-steps to prepare from commercially available starting materials as shown below in Scheme 3.20.

Scheme 3.20. 5-step synthesis of Weinreb amide (**109**).

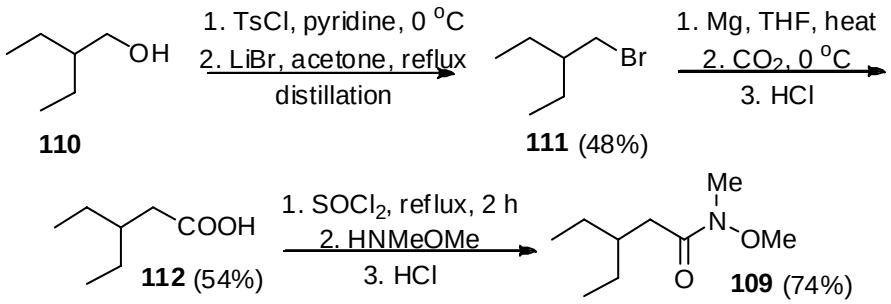

The electrophilic Weinreb amide (**109**) was prepared over five steps from commercially available 2-ethylbutanol (**110**, Scheme 3.20). The alcohol (**110**) was converted to the 1-bromo-2-ethylbutane (**111**) over 2 steps. The first step involved the tosylation of compound **110** with tosyl chloride in pyridine at 0 °C. Next, the tosylate was displaced with a bromide nucleophile in a refluxing lithium bromide-acetone solution. The relatively low isolated yield (48%) obtained over these two steps for compound **111** is likely the result of an atmospheric pressure distillation in large volume flasks. After purification of the alkyl halide the Grignard reagent was generated from the alkyl halide (**111**) in a refluxing tetrahydrofuran solution containing magnesium turnings and catalytic iodine. Once the Grignard reagent was generated the solution was subjected to a stream of anhydrous carbon dioxide gas which acted as the electrophile. Upon completion the reaction afforded the carboxylic acid **112** in a 54% yield. Finally, the acid chloride generated in situ from thionyl chloride was allowed to react with the Weinreb amine to produce the Weinreb amide (**109**) in a 74% yield (Scheme 3.20).

Scheme 3.21. Synthetic method to install the C2-carbon-carbon bond. The novel carbamates are indicated by the * symbol.

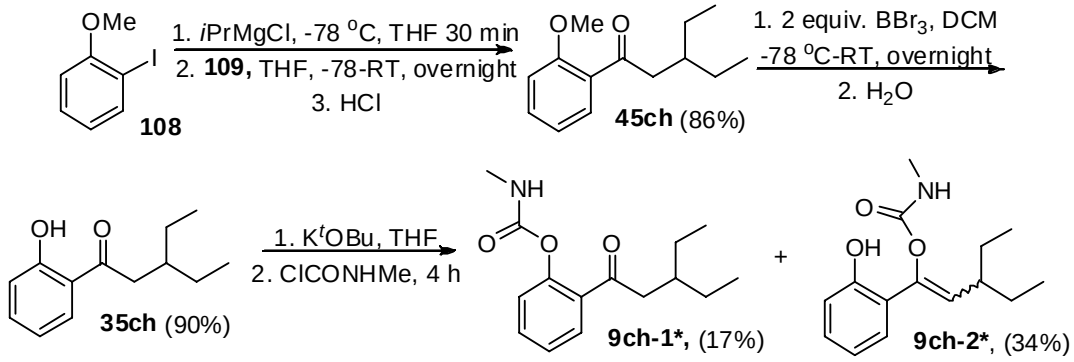

The Weinreb amide (**109**) acted as an electrophile in the essential C2 carbon-carbon bond forming process with the aryllithium reagent which was generated at -78 °C from 2-iodoanisole (**108**) and isopropylmagnesium chloride (Scheme 3.21). These reaction conditions were sufficient to prepare the α-ketoanisole **45ch** in an 86% yield. A routine boron tribromide aryl ether cleavage yielded the α-ketophenol **35ch** in a 90% yield. Phenol **35ch** was carbamoylated in a general fashion with potassium *tert*-butoxide (method B) to afford phenylcarbamate **9ch-1*** in an uncharacteristically low 17% yield. After further investigation we realized that *O*-acylation of the enolate anion was also occurring leading to carbamate **9ch-2*** in a 34% yield (Mixture of E and Z isomers). The author was able to resolve a small quantity of a pure isomer on silica gel chromatography, but the stereochemistry was not determined.

Scheme 3.22. Proposed mechanism for the formation of the enol carbamate **9ch-2***.

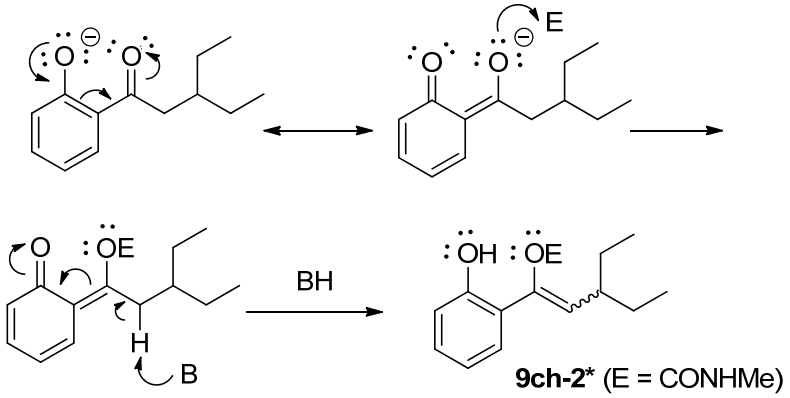

The formation of the unexpected enol carbamate **9ch-2*** could potentially be explained by the proposed pathway in Scheme 3.22. The phenol proton is significantly more acidic than the proton α- to the carbonyl and will be abstracted first. Starting with the deprotonated phenol delocalization of the phenolate lone pairs can contribute to the enhanced nucleophilicity of the oxygen located on the carbonyl. Covalent modification of the enol oxygen potentially explains how the electrophile occupies the enol oxygen compared to the phenol oxygen. A base can then abstract the α-proton and cause a rearrangement to compound **9ch-2*** where E = CONHMe.

Scheme 3.23. Synthetic route to carbamate **9bl*** from convergent intermediate **35ch**.

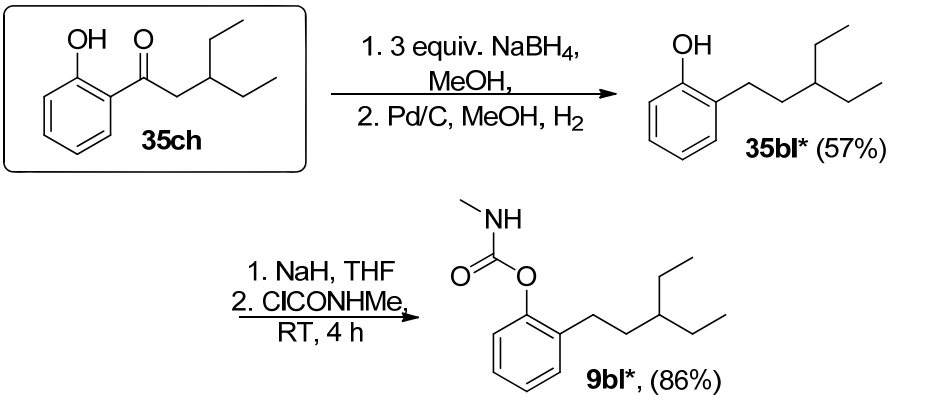

Although phenol **35ch** was carbamoylated to yield **9ch-1*** and **9ch-2***, the focus of our synthetic investigations was to prepare carbamate **9bl***. To accomplish this task the phenol **35bl*** was prepared over 2 steps from **35ch**. The initial step involved the

reduction of the ketone **35ch** with sodium borohydride to afford the intermediate benzyl alcohol (Scheme 3.23). In a sequential step the intermediate benzylic alcohol generated from **35ch** was further reduced with a palladium catalyzed hydrogenolysis to afford **35bl*** in a 57% overall yield. Carbamate **9bl*** was prepared with carbamoylation method A in an 86% yield.

3.4 Synthesis of combined 2,5-disubstituted phenyl *N*-methylcarbamates

Recall from section 2.2.2.3 that the sulfur containing class II carbamates were efficient and fast acting inhibitors of *Anopheles gambiae* AChE. For example, carbamates **9bc*** was over 100-fold selective for *An. gambiae* AChE relative to human AChE. Although many of the class II carbamates had high levels of target selectivity, many of them had poor contact toxicity against *An. gambiae* mosquitoes. In contrast, the class I C3-substituted phenylcarbamates exhibited superior contact toxicity, but were unfortunately significantly less selective (~10 fold) in the enzyme inhibition assays (Table 2.12). We envisioned that C2-alkylthio substitution could potentially confer good target selectivities while the pendant C5 (Class I phenylcarbamates) *tert*-butyl substituent could additionally confer high levels of contact toxicity at low level doses. To test this hypothesis we prepared carbamates **9bx***, **9by***, and **9bz*** as shown in Scheme 3.24.

Scheme 3.24. Synthesis of combined class I and class II 2,5-disubstitutedphenyl *N*-methylcarbamates. The novel carbamates are indicated by the * symbol.

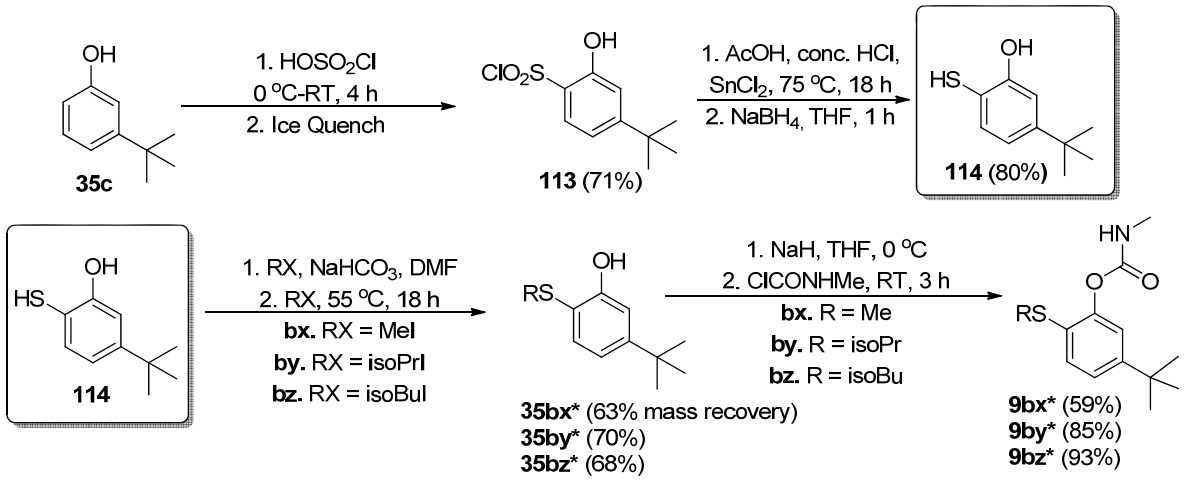

Phenols **35bx***, **35by***, and **35bz*** were not commercially available; however, they could be readily prepared from 3-*tert*-butylphenol (**35c**) and chlorosulfonic acid at 0 °C (Scheme 3.24). The regioselective reaction yielded the 2-substituted chlorosulfonic acid (**113**) in a 71% yield. Chlorosulfonic acid **113** was reduced to give 2-mercapto-5-*tert*-butylphenol (**114**) in an 80% yield over two steps. The first reduction with tin(II) chloride yielded a mixture of thiol and disulfide. Therefore, a subsequent step involving the use of sodium borohydride was used to attain high yields of the thiol (**114**). In the next step, thiol alkylation was conducted with various alkyl halides in the same manner as 2-mercaptophenol as shown in Table 3.8. The phenols **35by***, **35by***, and **35bz*** (Scheme 2.24) were isolated in mildly lower yields (68 - 70%) compared with the use of 2-mercaptophenol (**104**) as a nucleophile (Table 3.8). Competing *O*-alkylation was observed in the ^{1}H NMR spectrum when methyl iodide was used as an electrophile (i.e., **35bx***). This would account for the uncharacteristically low 63% mass recovery obtained in this example. However, *O*-alkylation was not observed in the ^{1}H NMR spectrum of compounds **35by*** and **35bz***. Phenol **35by*** was prepared from a secondary electrophile

which likely accounts for the 70% yield obtained. The reaction between **114** and isobutyliodide proceeded in a 68% yield. Carbamates **9by*** and **9bz*** were isolated in 85 and 93% yields respectively. However, the carbamoylation of **35bx*** resulted in a low 59% yield further indicating that *O*-methylation was preventing *O*-acylation from occurring with *N*-methylcarbamoyl chloride. However, this minor impurity was conveniently separated from the desired carbamate **9bx*** with silica gel chromatography.

3.5 Synthesis of Class II carbamates bearing additional C4-substitution

Scheme 3.25. The synthesis of class II alkylthiophenylcarbamates bearing C4-substituents. Novel carbamates are indicated by the * symbol.

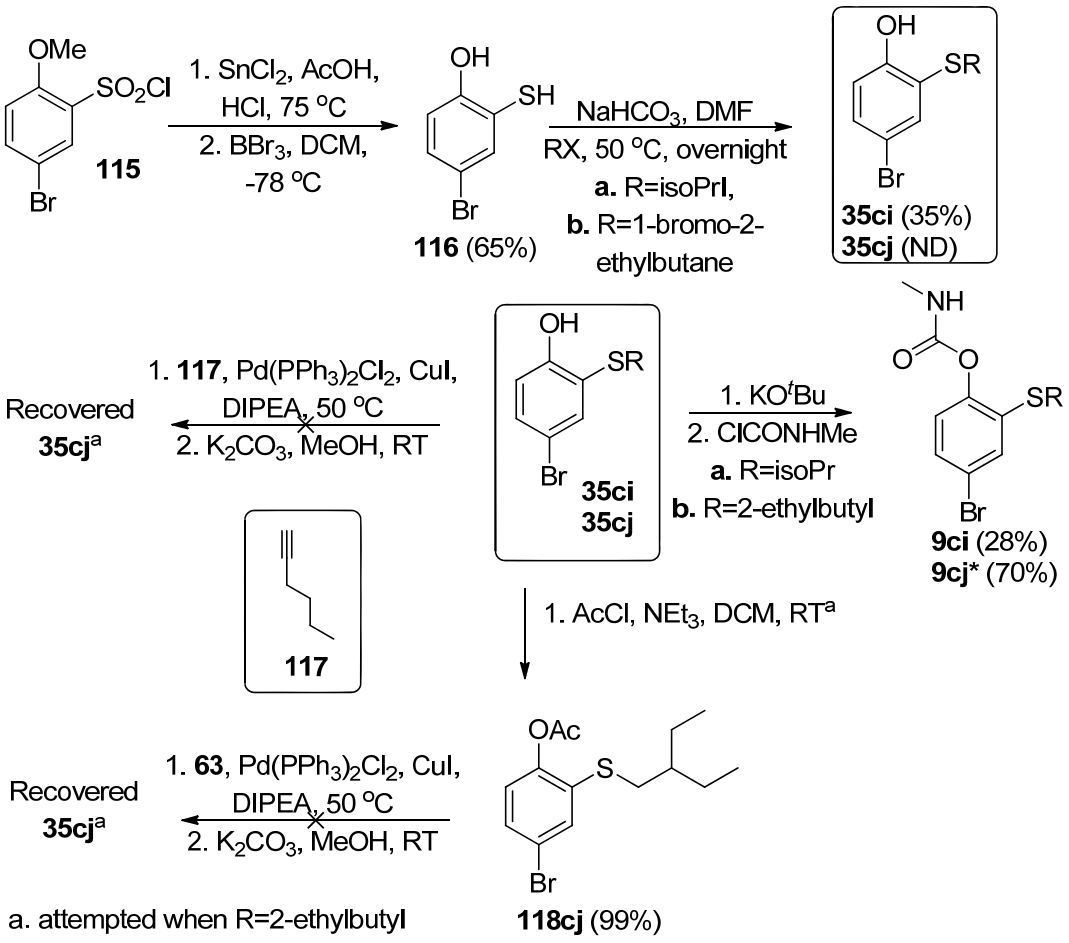

In addition to the 2,5-disubstituted carbamates (**9bx***, **9by**, and **9bz***) depicted in Scheme 3.24, the 2,4-disubstituted carbamates shown in Scheme 3.25 (**9ci** and **9cj***) were

also interesting synthetic-pharmacological targets. The starting material 2-mercapto-4-bromophenol (**116**) was prepared from the commercially available sulfonyl chloride (**115**). A reduction with tin(II) chloride under acidic conditions yielded 4-bromo-2-mercaptoanisole. This intermediate was readily converted into compound **116** utilizing a standard boron tribromide methylether bond cleavage in a 65% yield over two steps. As indicated by the ^{1}H NMR spectrum the disulfide dimer was present at this point, but the mixture was taken on to the next step without further purification. Alkylation of the mixture of **116** and the disulfide dimer with isopropyl iodide proceeded in a 35% yield. The low yield obtained was attributed to two factors i) the low reactivity of secondary alkyl halides and the ii) disulfide dimer present that could not undergo reaction with the alkyl halide. In contrast to **35ci**, the yield obtained for compound **35cj** was not determined as it was prepared by undergraduate Brian Story who was working under the guidance of the author. Although the yield was not obtained for compound **35cj**, phenylcarbamate **9cj*** which was isolated in a 70% yield. In contrast, **9ci** was isolated in a low 28% yield. The low yield obtained from **9ci** is most likely the result of experimental error.

In addition to the 4-bromo substituent observed in carbamates **9ci** and **9cj***, we envisioned 2,4-disubstituted phenylcarbamates bearing alkyl side chains in the C4-position as well (Scheme 3.25). To install this side chain a Sonogashira cross coupling reaction with 1-hexyne (**117**) and palladium was attempted. Unfortunately, the sulfur containing aryl bromides (**35cj**, Scheme 3.25) failed to undergo the Sonogashira crosscoupling with 1-hexyne (**117**). Dr. Ming Ma in the Carlier research group observed on other phenols related to her research that the Sonogashira cross-coupling reaction was

more robust after first acylating the phenolic hydroxy group. Therefore, acylated phenol **118cj** was prepared in high yields from acetyl chloride in triethylamine (99%). However, this modification did not render the Sonogashira reaction any more successful. It is well known that sulfur can "poison" palladium catalysts.[35, 36] In addition, aryliodides are more active cross-coupling partners when compared to arylbromides. Therefore, we shifted our efforts to C2-alkoxy class II phenylcarbamates (Scheme 3.26) with C4-iodo substituent in order to improve the yields obtained for the desired 2,4-disubstituted Sonogashira cross coupling reaction.

Scheme 3.26. Palladium catalyzed cross coupling of C2-alkoxy class II acetylated phenols with 1-hexyne. The novel compounds are indicated by the * symbol.

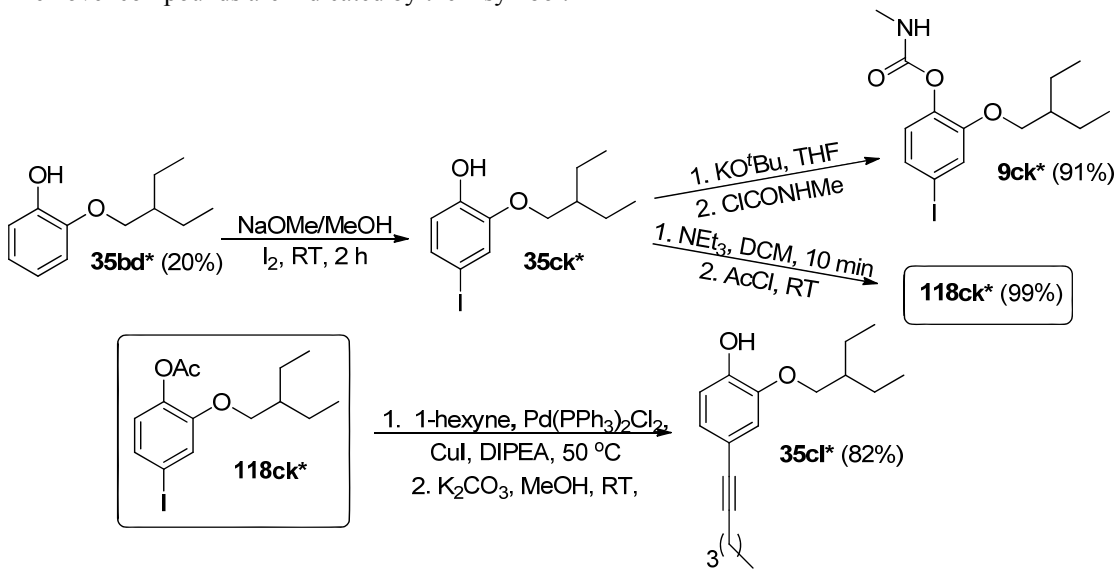

Phenol **35ck*** was prepared by iodinating **35bd*** with molecular iodine (Scheme 3.26). However, **35ck*** could only be isolated in a meager 20% yield do to unwanted 2-iodo and 2,4-diiodo byproduct being simultaneously formed. Intermediate phenol **35ck*** was carbamoylated in a 91% yield; however, the intermediate phenol was acetylated (i.e., **118ck***) prior to attempting the Sonogashira cross coupling. The cross coupling reaction

between **118ck** with 1-hexyne (**117**) successfully afforded the phenol (**35cl**) in an 82% isolated yield potassium carbonate catalyzed deprotection.

Scheme 3.27. Reduction of the alkyne and carbamoylation of the phenol. The novel compounds are indicated by the * symbol.

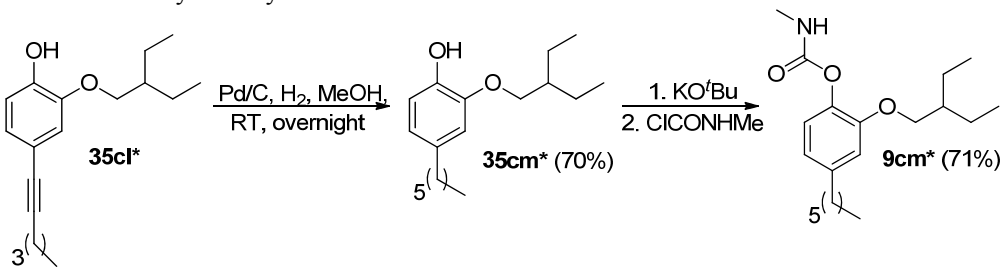

With the carbon-carbon bond installed in the 4-position of (**35cl***), a palladium on carbon catalyzed hydrogenation was sufficient to reduce the alkyne to the desired alkane (**35cm***) in a 70% yield (Scheme 3.27). The phenol **35cm*** was subsequently carbamoylated via method B to attain carbamate **9cm*** in a 71% isolated yield.

3.6 Conclusion

In total, 72 carbamates were prepared in the course of my work for *in vitro* enzyme assay and live mosquito toxicity assay. The common final step in all of these syntheses was the carbamoylation of a phenol, which normally proceeded in a 70 to 90% yield. Sixteen phenols were commercially available, and used without further purification. The emerging structure-activity relationships led us to focus our synthetic work on preparing 3-*tert*-alkylphenols (Class I) and 2-alkoxy or 2-alkylthio-substituted phenols (Class II). In both classes we employed a range of standard synthetic protocols. However, we also needed to develop or adapt existing methods to our purposes. The following methods particularly stand out: First, we applied the methods of Tanaka to prepare 3-*tert*-alkylphenols wherein a methyl group was replaced by a trifluoromethyl group.[37] Second, we adapted the methods of Tanaka to prepare 3-*tert*-alkylphenols that

lack fluorine substitution. We believe this method is competitive with the little known method of Reetz to convert aryl ketones to the corresponding 1,1-dimethylalkyl group. Furthermore, we show that this method allows one to access *tert*-alkyl-substituted aromatics that are not accessible by the Friedel-Crafts alkylation; Third, we found a convenient and high-yielding method for selective *S*-alkylation of 2-mercaptophenol.

As described in Chapter 2, several of the novel Class II carbamates show excellent selectivity for the inhibition of *An. gambiae* over human AChE. However, the search for carbamates showing both excellent enzymatic selectivity and mosquito toxicity continues. We trust that the results of this work will continue to inform ongoing research in the Carlier and Bloomquist groups.

References

1. Kolbezen, M. J.; Metcalf, R. L.; Fukuto, T. R. Insecticidal Activity of Carbamate Cholinesterase Inhibitors. *J. Agr. Food Chem.* **1954,** 2, 864-870.

2. Abad, A.; Moreno, M.; Montoya, A. Hapten synthesis and production of monoclonal antibodies to the *N*-methylcarbamate pesticide methiocarb. *J. Agr. Food Chem.* **1998,** 46, 2417-2426.

3. Down, S. Putting the heat on carbamate insecticides. http://www.separationsnow.com/coi/cda/detail.cda?id=10702&type=Feature&chId=1&page=1 (2010).

4. Chaikin, S. W. Study of the Hydrolysis of Several Physostigmine Analogs. *J. Am. Chem. Soc.* **1947,** 69, 1266-1268.

5. Kuhr, R. J.; Dorough, H. W. *Carbamate Insecticides: Chemistry, Biochemistry, and Toxixology*. CRC Press: Cleveland, OH, 1976; p 1-101.

6. Jeshke, P. The unique role of fluorine in the design of active ingredients for modern crop protection. *ChemBioChem* **2004,** 5, 570-589.

7. Tanaka, H.; Shishido, Y. Synthesis of aromatic compounds containing a 1,1-dialkyl-2-trifluoromethylgroup, a bioisostere of the tert-alkyl moiety. *Bioorg. Med. Chem. Lett.* **2007,** 17, 6079-6085.

8. Middleton, W. New fluorinating reagents. Dialkylaminosulfur fluorides. *J. Org. Chem.* **1975,** 40, 574-578.

9. Doi, M.; Nishi, Y.; Kiritoshi, N.; Iwata, T.; Nago, M.; Nakano, H.; Uchiyama, S.; Nakazawa, T.; Wakamiya, T.; Kobayashi, Y. Simple and efficient syntheses of Boc- and Fmoc-protected 4(*R*)- and 4(*S*)-fluoroproline solely from 4(*R*)-hydroxyproline. *Tetrahedron* **2002,** 58, 8453-8459.

10. Prakash, G.; Chiradeep, P.; Vaghoo, H.; Surampudi, V.; Kultyshev, R.; Mandal, M.; Rasul, G.; Mathew, T.; Olah, G. Facile synthesis of TMS-protected trifluoromethylated alcohols using trifluoromethylsilane (TMSCF) and various nucleophilic catalysts in DMF *J. Org. Chem.* **2006,** 71, 6806-6813.

11. Lemal, D. Perspective on fluorocarbon chemistry. *J. Org. Chem.* **2004,** 69, 1-11.

12. Matsubara, K.; Ishibashi, T.; Koga, Y. C-F bond-cleavage reactions of fluoroalkanes with magnesium reagents and without metal catalysts. *Org. Lett.* **2009,** 11, 1765-1768.

13. Hudlicky, M. Catalytic hydrogenation of carbon-fluoride bonds: pi bond participation mechanism. *J. Fluorine Chem.* **1989,** 44, 345-359.

14. Lee, E.; Yandulov, D. On the isolation of neat allylic fluorides. *J. Fluorine Chem.* **2009,** 130, 474-483.

15. Reetz, M.; Wenderoth, B.; Peter, R.; Steinbach, R.; Westermann, J. Efficient coupling of tertiary alkyl halides with dialkylzinc and titanium compounds. *J.C.S. Chem. Comm.* **1980,** 24, 1202-1204.

16. Reetz, M.; Westermann, J. Direct geminal dialkylation of ketones using organotitanium reagents. A simple entry into synthetic tetrahydrocannabinoids. *J. Org. Chem.* **1983,** 48, 254-255.

17. Reetz, M.; Westermann, J. Direct geminal dimethylation of ketones and exhaustive methylation of carboxylic acid chlorides using dichlorodimethyltitanium. *J. Chem. Ber.* **1985,** 118, 1050-1057.

18. Levin, J.; Turos, E.; Weinreb, S. An alternative procedure for the aluminum-mediated conversion of esters and amides. *Syn. Comm.* **1982,** 12, 989-993.

19. Carlier, P.; Anderson, T.; Wong, D.; Hsu, D.; Hartsel, J.; Ma, M.; Wong, E.; Choundhury, R.; Lam, P.; Totrov, M.; Bloomquist, J. Towards a species-selective acetylcholinesterase inhibitor to control the mosquito vector of malaria, *Anopheles gambiae*. *Chem. Biol. Interact.* **2008,** 175, 368-375.

20. Kochi, J.; Hammond, G. Benzyl tosylates, I. Preparation and properties. *J. Am. Chem. Soc.* **1953,** 75, 3443-3444.

21. Olah, G.; Fung, A.; Keumi, T. Oxyfunctionalization of hydrocarbons. 11. Hydroxylation of benzene and alkylbenzenes with hydrogen peroxide in hydrogen fluoride/boron trifluoride. *J. Org. Chem.* **1981,** 46, 4305-4306.

22. Hatano, M.; Matsumura, T.; Ishihara, K. Highly alkyl-selective addition to ketones with magnesium ate complexes derived from Grignard reagents. *Org. Lett.* **2005,** 7, 573-576.

23. Hartmann, R.; Schwarz, W.; Heindl, A.; Schoenenberger, H. Ring-substituted 1,1,2,2-tetraalkylated 1,2-bis(hydroxyphenyl)ethanes. 4. Synthesis, estrogen receptor binding affinity, and evaluation of antiestrogenic and mammary tumor inhibiting activity of symmetrically disubstituted 1,1,2,2-tetramethyl-1,2-bis(hydroxyphenyl)ethanes. *J. Med. Chem.* **1985,** 28, 1295-1301.

24. Okamoto, Y.; Brown, H. Derective effects in aromatic substitution. XXIX. Rates of solvolysis of phenyldimethylcarbinyl chlorides containing substituents (NMe_3^+, CO_2^-) bearing a charge. *J. Am. Chem. Soc.* **1958,** 80, 4976-4979.

25. Bell, T.; Hu, L.; Patel, S. Alkylation of heteroaryl halides by 2:1 Grignard reagent/copper(I) mixtures. Synthesis of alkylated octahydrodibenzo[1,10]phenanthrolines. *J. Org. Chem.* **1987,** 52, 3847-3850.

26. Hatano, M.; Ito, O.; Suzuki, S.; Ishihara, K. Zinc(II)-catalyzed addition of Grignard reagents to ketones. *J. Org. Chem.* **2010,** 75, 5008-5016.

27. Hatano, M.; Ito, O.; Suzuki, S.; Ishihara, K. Zinc(II)-catalyzed Grignard additions to ketones with RMgBr and RMgI. *Chem. Commun.* **2010,** 46, 2674-2676.

28. Jeon, S.; Li, H.; Garcia, C.; LaRochelle, L.; Walsh, P. Catalytic asymmetric addition of alkylzinc and functionalized alkyl zinc reagents to ketones. *J. Org. Chem.* **2005,** 70, 448-455.

29. Hartmann, R.; Kranzfelder, G.; Angerer, E.; Schenenberger, H. Antiestrogens. Synthesis and evaluation of mammary tumor inhibiting activity of 1,1,2,2-tetraalkyl-1,2-diphenylethanes. *J. Med. Chem.* **1980,** 23, 841-848.

30. Kelly, D.; Jenkins, M.; Mantello, R. Carbon-13 nuclear magnetic resonance studies of carbocations. 5. Effect of increasing electron demand on the carbon-13

chemical shifts of 3-aryl-3-pentyl and 2-aryl-2-adamantyl carbocations. Correlation of delta sigma C+ with enhanced substituent constants sigma.C+. *J. Org. Chem.* **1981,** 46, 1650-1653.

31. Le, X.; Hai, M.; Bai, L.; Xue, Q. A comparative study on the binding behaviors of β-cyclodextrin and its two derivatives to four fanlike organic guests *J. Org. Chem.* **2008,** 73, 8305-8316.

32. Liu, P.; Huang, L.; Faul, M. A simple method for chemoselective phenol alkylation. *Tet. Lett.* **2007,** 48, 7380-7382.

33. Audouze, K.; Nielsen, E.; Peters, D. New series of morpholine and 1,4-oxazepane derivatives as dopamine D4 receptor ligands: Synthesis and 3D-QSAR model. *J. Med Chem.* **2004,** 47, 3089-3104.

34. Kalgutkar, A.; Kozak, K.; Crews, B.; P. Hochgesang, J.; Marnett, L. Covalent modification of cyclooxygenase-2 (COX-2) by 2-acetoxyphenyl alkyl sulfides, a new class of selective COX-2 inactivators. *J. Med Chem.* **1998,** 41, 4800-4818.

35. Seoane, X.; L'Argentiere, P.; Figoli, N.; Arcoya, A. On the deactivation of supported palladium hydrogenation catalysts by thiophene poisoning. *Catal. Lett.* **1992,** 16, 137-148.

36. Tiancun, X.; Lidun, A.; Weimin, Z.; Shishan, S.; Guoxin, X. Mechanism of sulfur poisoning on supported noble metal catalyst -- the adsorption and transformation of sulfur on palladium catalysts with different supports. *Catal. Lett.* **1992,** 12, 287-296.

37. Tanaka, H.; Shishido, Y. Synthesis of aromatic compounds containing a 1,1=dialkyl-2-trifluoromethyl group, a bioisostere of the *tert*-alkyl moiety. *Bioorg. Med. Chem.* **2007,** 17, 6079-6085.

Chapter 4. Future goals and research objectives

Throughout the course of my studies many aryl *N*-methylcarbamates were examined as potential mosquitocides; however, there are countless examples that have yet to be studied. Future work following up on these finding should focus on retaining contact toxicity for the carbamates without compromising high levels of target selectivity observed for many of the class II carbamates, such as **9bd***. There are a few modifications to the carbamate pharmacophore that are attractive targets for future investigators. First, I will discuss how bendiocarb (**9b**) could be modified to resemble highly selective carbamate **9bd***. Bendiocarb is highly toxic to *An. gambiae* (LC_{50} = 0.43 mg/mL), but was only mildly selective (8-fold). The contact toxicity could potentially be retained by constraining the 2-ethylbutoxy side chain into a 5-membered acetal ring observed in bendiocarb analog **9cn*** (Figure 4.1). Other conformationally constrained class II carbamates such as those shown in Table 2.17 were significantly less potent inhibitors and a loss in selectivity was also observed. However, **9cn*** is constrained to form a bicyclic acetal, which is directly attached to the aromatic ring. Alternatively, the conformationally constrained analogs illustrated in Table 2.17 are constrained at the terminal portion of the side chain, and by being constrained into a bicyclic system as observed in carbamate **9cn***, improved inhibition potency and target selectivity could potentially be obtained. Furthermore, carbamate **9cn*** has not been reported in the literature.

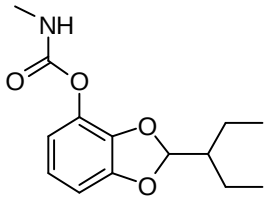

9cn*

Figure 4.1. Bendiocarb analog **9cn*** could potentially retain the selectivity due to the 2-ethylbutyl side chain. Novel carbamates are indicated by the * symbol.

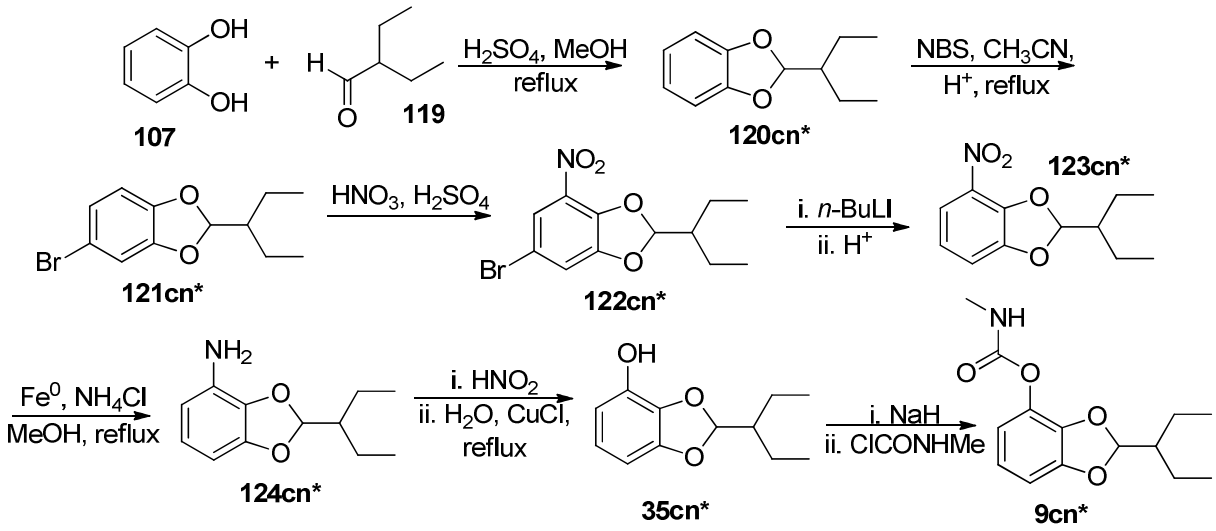

Figure 4.2. Proposed synthetic pathway to prepare carbamate **9cn*** starting from catechol (**107**) and 2-ethylbutanal (**119**).

To prepare carbamate **9cn*** one could envision starting from catechol (**107**) and 2-ethylbutanal (**119**). By refluxing the two in methanol in the presence of catalytic sulfuric acid compound **120cn*** could be achieved (Figure 4.2). Bromine could be introduced regioselectively para to the oxygen to generate compound **121cn***. This bromine can direct the subsequent nitronium ion to generate **122cn***, and can then be removed by performing a metal-halogen exchange followed by an acid quench to afford **123cn***. Reduction of the nitro group can be conducted with iron and ammonium chloride to generate compound **124cn***. The phenol **35cn*** can be generated generating the diazonium ion and substituting this with water as the nuleophile. From this point, a standard carbamoylation can be employed.

Due to time constraints, we were unable to evaluate all of the carbamates by measuring the k_i value, and were only able to report IC_{50} values for a large number of the carbamates synthesized. Some of the carbamates worth reexamining are shown in Table 2.19 where the class II carbamates branch at the α- and β-positions. The low IC_{50} values and high target selectivity observed for **(±)-9bm*** (IC_{50} = 10 nM, 243-fold selective) would suggest that it would be an ideal candidate for examination based on the k_i value. Carbamate **(±)-9bm*** contains a sulfur at

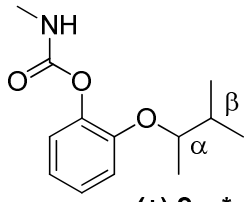

(±)-9co*

Figure 4.3. The α,β-branching oxygen-substituted analog of **(±)-9bm*** could potentiall y be a highly selective carbamate.

the C2-position; however, if you recall from Table 2.15, the oxygen analogs generally were more selective. Carbamate **(±)-9co*** (Figure 4.3) was not prepared during my graduate work, and is of particular interest due to the high selectivity observed for the sulfur analog (**(±)-9bm***). Additionally, carbamate **(±)-9bm*** was also capable of inducing 100% mortality at 1 mg/mL. As we have previously observed, the 2-alkoxy analogs were generally more toxic to *An. gambiae* compared with the 2-alkylthio-substituted carbamates.

Based on the low yields obtained preparing 2-alkoxyphenols from catechol and primary alkyl halides, it may be rather difficult to prepare carbamate **(±)-9co*** from secondary alkyl halides. Therefore, it could be simpler to prepare the unsaturated allylic homolog **(±)-9cp*** in high yields from the more electrophilic secondary allylic halides (Figure 4.4). This could provide a high yielding route to probe the effectiveness of the oxygen-substituted α,β-branching class II carbamates **(±)-9co*** and **(±)-9cp***. In addition, **(±)-9cp*** could be hydrogentated to give **(±)-9co***.

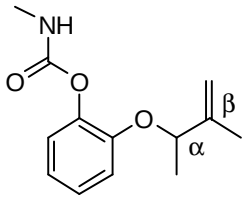

(±)-9cp*

Figure 4.4. Unsaturated allyl-sbustited homolog of carbamate **(±)-9co***.

Chapter 5: Materials, methods, and characterization of carbamate inhibitors.

5.1 Materials

Commercial phenyl *N*-methylcarbamates propoxur (**9a**) and bendiocarb (**9b**) were purchased from Aldrich. The phenyl *N*-methylcarbamates (**9**) and phenyl-*N,N*-dimethylcarbarbamates (**30**) were prepared by deprotonating the corresponding phenols (**35**) in tetrahydrofuran (0.2 M) with either NaH (*Method A*) or KO^{t}Bu (Method B), followed by the addition of 2 equiv of the appropriate carbamoyl chloride. The phenyl *N*-methylcarbamates (**9**) were prepared from *N*-methylcarbamoyl chloride while the phenyl *N,N*-dimethylcarbamates (**30**) were prepared from *N,N*-dimethylcarbamoyl chloride. Isolated yields for the carbamylation generally ranged from 60-90%. Many previously synthesized carbamates do not have modern analytical characterization. Therefore, we have supplied ^{1}H, ^{13}C, and MS tabulations for all carbamates. When ^{1}H NMR data was available for these older carbamates, our ^{1}H NMR data do match the data reported in the literature. However, since our data is at a higher field, we believe it is worth including in this dissertation. All chiral compounds were prepared in racemic form. When phenol precursors were available they were purchased from Sigma-Aldrich. Out of the 72 reported carbamates, 37 of these phenyl *N*-methylcarbamates are novel insecticides and are described by the * symbol. All other carbamates have been previously reported in the literature and have been cited accordingly. A few carbamates reported in chapter 5 have not been discussed previously and are included as a reference for future Carlier group members.

5.2 Methods and characterization data

Example 1: (*Method A*): General procedure for the *N*-methylcarbamylation of phenols (*NaH deprotonation*).

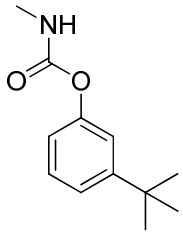

3-*tert*-Butylphenyl *N*-methylcarbamate[1] **(9c)**. A dry 100 mL Schlenk flask was charged with a 60% NaH dispersion in mineral oil (80 mg, 2.00 mmol) and flushed with nitrogen. The contents were allowed to cool in an ice-bath prior to the dropwise addition of *tert*-butylphenol (200 mg, 1.33 mmol) in dry tetrahydrofuran (6 mL). The reaction was allowed to stir for 10 min before *N*-methylcarbamyl chloride (247 mg, 2.64 mmol) was added in one portion. The ice-bath was removed and the reaction was allowed to stir for 4 h at RT. The solvent was concentrated in vacuo and the residue taken up in dichloromethane (25 mL). The organic layer was washed with 0.25 M hydrochloric acid (20 mL), and brine, and then dried with sodium sulfate. The solution was filtered and concentrated in vacuo. The residue was purified with flash chromatography (3:1 hexane : ethyl acetate) yielding in a white solid weighing 236 mg (86%); ^{1}H NMR (500 MHz, $CDCl_3$): δ 7.28 (t, *J* = 7.9 Hz, 1H), 7.22 (d, *J* = 7.9 Hz, 1H), 7.11 (t, *J* = 1.9 Hz, 1H), 6.94 (dd, *J* = 7.9, 1.9 Hz, 1H), 4.96 (broad s, 1H), 2.89 (d, *J* = 4.9 Hz, 3H), 1.31 (s, 9H); ^{13}C NMR (101 MHz, $CDCl_3$) δ 155.55, 152.96, 151.03, 128.88, 122.46, 118.77, 118.76, 34.87, 31.39, 27.86; HRMS (FAB): 208.1339 calcd for $C_{12}H_{18}NO_2$ $[M+H]^+$ found 208.1324 (-6.5 ppm, -1.4 mmu). Experimental m.p. 143.9 - 144.6 ^{o}C. Literature m.p. 144.5 ^{o}C. **(JH-VII-77, PRC331)**.

Example 2: (*Method B*): General procedure for the *N*-methylcarbamylation of phenols (*KO^{t}Bu deprotonation*).

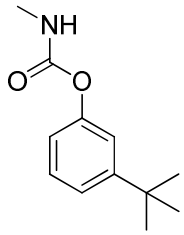

3-*tert*-Butylphenyl *N*-methylcarbamate[1] **(9c)**. A dry 100 mL round-bottom flask was charged with 3-*tert*-butylphenol (2.00 g 13.3 mmol) and dry tetrahydrofuran (35 mL) prior to cooling to 0 °C. Next, the reaction flask was charged with potassium *tert*-butoxide (1.57 g, 14.0 mmol), purged with nitrogen, and allowed to stir for 20 min. The reaction flask was then charged with *N*-methylcarbamyl chloride (2.52 g, 27.0 mmol), the ice-bath was removed, and the reaction was allowed to stir at room temperature for 3 h. The solvent was concentrated in vacuo and the residue taken up in dichloromethane (50 mL) and washed with 0.25 M hydrochloric acid (50 mL), and then brine (50 mL), and dried with sodium sulfate. The solution was filtered and concentrated in vacuo and the residue was purified by flash chromatography on silica gel (3:1 hexane : ethyl acetate) and recrystallization in 2 : 1 MeOH. This gave a white solid weighing (2.00 g, 72%). **(JH-V-135, PRC331)**.

Example 3: (*Method C*): General procedure for the *N*,*N*-dimethylcarbamylation of phenols (*NaH deprotonation*).

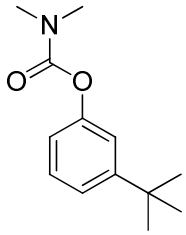

3-*tert*-*B*utylphenyl *N*,*N*-dimethylphenylcarbamate[10] **(30c)**. This compound was prepared in 89% from 3-*t*-butylphenol and *N*,*N*-dimethylcarbamyl chloride according to the procedure for **9c** in Example 1. Pale oil (*Method C*); ^{1}H NMR (500 MHz, $CDCl_3$) δ 7.28 (t, *J* = 7.9 Hz, 1H), 7.21 (ddd, *J* = 7.9, 2.1, 1.1 Hz, 1H), 7.10 (t, *J* = 2.1 Hz, 1H), 6.93 (ddd, *J* = 7.9, 2.1, 1.1 Hz, 1H), 3.11 (s, 3H), 3.02 (s, 3H), 1.31 (s, 9H); ^{13}C NMR (126 MHz, $CDCl_3$) δ 155.24, 152.89, 151.50, 128.84, 122.36, 118.94, 118.91, 36.83, 36.59, 34.87, 31.42; HRMS (FAB): 222.1494 calcd for $C_{13}H_{20}NO_2$ $[M+H]^+$ found 222.1499 (2.2 ppm, 0.5 mmu). **(JH-II-115, PRC345)**.

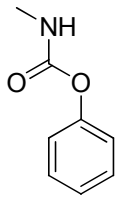

Phenyl *N*-methylcarbamate[1] **(9d)**. White solid (*Method A*); 91%; ^{1}H NMR (500 MHz, $CDCl_3$) δ 7.41 – 7.30 (m, 2H), 7.19 (t, *J* = 7.4 Hz, 1H), 7.16 – 7.08 (m, 2H), 5.06 (br s, 1H), 2.87 (d, *J* = 4.9 Hz, 3H); ^{13}C NMR (126 MHz, $CDCl_3$): δ 155.41, 151.19, 129.38, 125.37, 121.71, 27.79; HRMS (FAB): 152.0712 calcd for $C_8H_{11}NO_2$ $[M+H]^+$ found 152.0712. **(JH-II-21a, JH-VIII-135, PRC314)**.

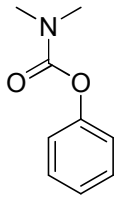

Phenyl *N*,*N*-*dimethylcarbamate*[9] **(30d)**. This compound was prepared in 99% from phenol and *N*,*N*-dimethylcarbamyl chloride according to the procedure for **30c** in Example 3 (*Method C)*. Colorless oil; ^{1}H NMR (500 MHz, $CDCl_3$) δ 7.38 – 7.33 (m, 2H), 7.21 – 7.17 (m, 1H), 7.13 – 7.09 (m, 2H), 3.10 (s, 3H), 3.01 (s, 3H); ^{13}C NMR (126 MHz, $CDCl_3$) δ 155.09, 151.66, 129.36, 125.30, 121.90, 36.83, 36.59; HRMS (APCI): 166.0863 calcd for $C_9H_{12}NO_2$ $[M+H]^+$ found 166.0864 (2.35 ppm, -0.4 mmu). **(JH-VIII-145, JH-II-21b, PRC315)**.

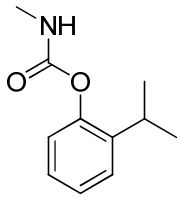

2-Isopropylphenyl *N*-methylcarbamate[11] **(9i)**. Yellow solid (*Method A*); 80%; ^{1}H NMR (500 MHz, $CDCl_3$) δ 7.30 (dd, *J* = 5.8, 3.6 Hz, 1H), 7.22 – 7.16 (m, 2H), 7.09 – 7.04 (m, 1H), 5.06 (br s, 1H), 3.13 (s-7, *J* = 6.9 Hz, 1H), 2.89 (d, *J* = 4.9 Hz, 3H), 1.22 (d, *J* = 6.9 Hz, 6H); ^{13}C NMR (126 MHz, $CDCl_3$) δ 155.59, 148.42, 140.72, 126.63, 126.61, 125.97, 122.66, 27.90, 27.33, 23.10; HRMS (FAB): 194.11811 calcd for $C_{11}H_{16}NO_2$ $[M+H]^+$ found 194.1181 (1.0 ppm, 0.2 mmu). **(JH-II-69, PRC328)**.

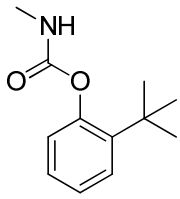

2-*tert*-Butylphenyl *N*-methylcarbamate **(9k)**. White solid (*Method A*); 67%; ^{1}H NMR (500 MHz, $CDCl_3$) δ 7.36 (dd, *J* = 7.9, 1.6 Hz, 1H), 7.21 (td, *J* = 7.9, 1.6 Hz, 1H), 7.13 (td, *J* = 7.9, 1.6 Hz,

1H), 7.05 (dd, *J* = 7.9, 1.6 Hz, 1H), 5.02 (br s, 1H), 2.92 (d, *J* = 4.9 Hz, 3H), 1.35 (s, 9H); ^{13}C NMR (126 MHz, $CDCl_3$) δ 155.41, 149.72, 141.39, 127.10, 126.99, 125.39, 124.25, 34.68, 30.38, 27.95; HRMS (FAB): 208.1338 calcd for $C_{12}H_{18}NO_2$ $[M+H]^+$ found 208.1342 (2.1 ppm, 0.4 mmu). **(JH-II-73, PRC330)**.

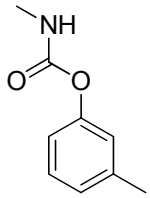

3-Methylphenyl *N*-methylcarbamate[1] **(9l)**. White solid (*Method B*); 84%; ^{1}H NMR (500 MHz, $CDCl_3$) δ 7.23 (t, *J* = 7.8 Hz, 1H), 7.00 (d, *J* = 7.8 Hz, 1H), 6.98 – 6.87 (m, 2H), 4.96 (br s, 1H), 2.89 (d, *J* = 4.9 Hz, 3H), 2.35 (s, 3H). ^{13}C NMR (126 MHz, $CDCl_3$) δ 155.14, 151.14, 139.57, 129.14, 126.25, 122.39, 118.68, 27.85, 21.44; HRMS (FAB): 166.0869 calcd for $C_9H_{12}NO_2$ $[M+H]^+$ found 166.0860 (-4.8 ppm, -0.8 mmu). **(JH-III-117, PRC393)**.

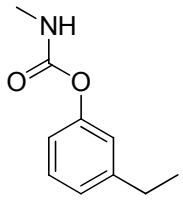

3-Ethylphenyl *N*-methylcarbamate[1] **(9m)**. This carbamate was prepared from a mixture containing 80% 3-ethylphenol and 20% 4-ethylphenol purchased from Aldrich. White solid (*Method B*); 62%; ^{1}H NMR (500 MHz, $CDCl_3$) δ 7.25 (t, *J* = 7.8 Hz, 1H), 7.06 – 7.01 (m, 1H), 6.99 – 6.89 (m, 2H), 4.94 (br s, 1H), 2.89 (d, *J* = 4.9 Hz, 3H), 2.70 – 2.58 (m, 2H), 1.23 (t, *J* = 7.8 Hz, 3H); ^{13}C NMR (126 MHz, $CDCl_3$) δ 155.52, 145.91, 129.20, 128.76, 125.03, 121.14, 118.91, 28.77, 27.86, 15.41; **(JH-II-133, PRC360)**.

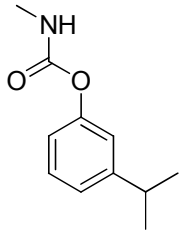

3-Isopropylphenyl *N*-methylcarbamate[3] **(9n)**. Off-white solid (*Method A*); 85%; ^{1}H NMR (500 MHz, $CDCl_3$) δ 7.27 (t, *J* = 7.9 Hz, 1H), 7.06 (d, *J* = 7.9 Hz, 1H), 6.98 (t, *J* = 1.9 Hz, 1H), 6.96 – 6.91 (m, 1H), 4.98 (br s, 1H), 2.90 (s-7, *J* = 6.5 Hz, 1H), 2.88 (d, *J* = 4.9 Hz, 3H), 1.24 (d, *J* = 6.5 Hz, 6H); ^{13}C NMR (126 MHz, $CDCl_3$) δ 155.53, 151.22, 150.58, 129.16, 123.58, 119.71, 119.03, 34.06, 27.83, 23.97; HRMS (FAB): 194.1182 calcd for $C_{11}H_{16}NO_2$ $[M+H]^+$ found 194.1180 (-0.6 ppm, -0.1 mmu). **(JH-VIII-141, JH-II-49, PRC329)**.

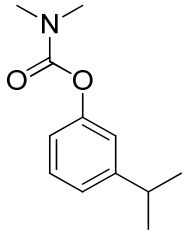

3-Isopropylphenyl *N*,*N*-dimethylphenylcarbamate[10] **(30n)**. Yellow oil (*Method C*); 91%; ^{1}H NMR (500 MHz, $CDCl_3$) δ 7.26 (t, *J* = 7.9 Hz, 1H), 7.07 – 7.04 (m, 1H), 6.98 – 6.95 (m, 1H), 6.92 (ddd, *J* = 7.9, 2.4, 1.0 Hz, 1H), 3.10 (s, 3H), 3.01 (s, 3H), 2.90 (s-7, *J* = 6.9 Hz, 1H), 1.24 (d, *J* = 6.9 Hz, 6H); ^{13}C NMR (126 MHz, $CDCl_3$) δ 155.21, 151.69, 150.52, 129.13, 123.49, 119.86, 119.22, 36.82, 36.59, 34.10, 24.01; HRMS (FAB): 208.1337 calcd for $C_{12}H_{18}NO_2$ $[M+H]^+$ found 208.1323 (-7.0 ppm, -1.5 mmu). **(JH-II-117, PRC344)**.

Example 4: General procedure for the addition of carbon nucleophiles to benzaldehydes

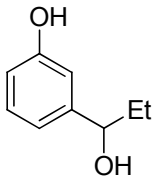

3-(1-Hydroxypropyl)phenol **(100o)**. A dry 50 mL Schlenk flask was charged with Et_2Zn (1 M in hexane, 12.3 mL), back-filled with nitrogen, and cooled to 0 ^oC in an ice-bath. Next, 3-hydroxybenzaldehyde (490 mg, 4.01 mmol) was dissolved in 4 mL of dry toluene and 3 mL of dry tetrahydrofuran. This solution was added dropwise over 5 min resulting in a light yellow solution. No reaction took place overnight at room temperature as determined by TLC, so Ti(*i*-PrO)$_4$ (609 µL, 2.0 mmol) was injected, resulting in a bright yellow solution. After stirring for 4 h a yellow suspension resulted and was allowed to stir an additional 2 h. The reaction was quenched with 1 M hydrochloric acid (50 mL) and extracted with diethyl ether (3 x50 mL). The organic layers were combined, washed with brine, and dried with $MgSO_4$. The solution was filtered and concentrated in vacuo prior to purification via flash chromatography (2:1 Hexane : Ethyl acetate) to yield a white solid weighing 572 mg (3.76 mmol, 94%); ^1H NMR (500 MHz, CD_3OD) δ 7.12 (t, *J* = 8.0 Hz, 1H), 6.82 – 6.74 (m, 2H), 6.66 (ddd, *J* = 8.0, 2.4, 1.1 Hz, 1H), 4.43 (t, *J* = 6.6 Hz, 1H), 1.80 – 1.61 (m, 2H), 0.88 (t, *J* = 7.4 Hz, 3H); ^{13}C NMR (126 MHz, CD_3OD) δ 158.42, 147.92, 130.17, 118.40, 115.01, 113.93, 76.61, 32.88, 10.55; HRMS (APCI): 135.0804 calcd for $C_9H_{11}O$ [M-OH]$^+$ found 135.0807 (-3.12ppm). **JH-VII-71**.

Example 5: General procedure for the installation of methyl nucleophiles to secondary benzylic alcohols

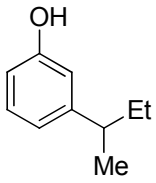

3-(*sec*-Butyl)phenol **(35o)**. A dry 50 mL Schlenk flask back-filled with nitrogen was charged with 3-(1-hydroxypropyl)phenol (293 mg, 1.93 mmol) and cooled to -20 ^{o}C. The addition of thionyl chloride (277 µL, 3.81 mmol) did not result in a homogenous solution so chloroform (0.5 mL) was added and the reaction allowed to stir for 4 h as the reaction warmed to room temperature. The reaction flask was placed under high vacuum at 0 ^{o}C for 20 min to remove the excess thionyl chloride. The residue was dissolved in dry dichloromethane (6 mL) and cooled to -78 ^{o}C. Next, 2.0 M $AlMe_3$ in hexane (2.28 mL, 4.6 mmol) was injected in one portion and the reaction was allowed to warm to room temperature over 3 h and react at room temperature overnight. The reaction was quenched with 1 M hydrochloric acid (60 mL) at 0 ^{o}C and extracted with dichloromethane (3 x 25 mL). The organic layers were combined, washed with brine, and dried with $MgSO_4$. The solution was filtered and concentrated in vacuo. The residue was purified by flash chromatography (3 : 1 hexane : ethyl acetate) to yield a yellow oil (200 mg, 69%). ^{1}H NMR (500 MHz, $CDCl_3$) δ 7.15 (t, *J* = 7.7 Hz, 1H), 6.79 – 6.73 (m, 1H), 6.68 – 6.62 (m, 2H), 4.64 (s, 1H), 2.54 (s-6, *J* = 7.0 Hz, 1H), 1.63 – 1.53 (m, 2H), 1.21 (d, *J* = 7.0 Hz, 3H), 0.82 (t, *J* = 7.0 Hz, 3H); ^{13}C NMR (126 MHz, $CDCl_3$) δ 155.56, 149.99, 129.51, 119.88, 114.03, 112.76, 41.73, 31.20, 21.90, 12.37; HRMS (APCI) 151.1117 calcd for $C_{10}H_{15}O$ $[M+H]^+$ found 151.1078 (2.98 ppm). **JH-VII-73**.

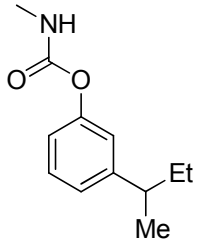

3-*sec*-Butylphenyl *N*-methylcarbamate[4] **(9o)**. White solid (*Method A*); 74%; ^{1}H NMR (400 MHz, $CDCl_3$) δ 7.28 – 7.23 (m, 1H), 7.01 (d, *J* = 7.7 Hz, 1H), 6.98 – 6.91 (m, 2H), 4.95 (br s, 1H), 2.89 (d, *J* = 4.9 Hz, 3H), 2.59 (s-6, *J* = 7.0 Hz,1H), 1.65 – 1.49 (m, 2H), 1.22 (d, *J* = 7.0 Hz, 3H), 0.82 (t, *J* = 7.4 Hz, 3H); ^{13}C NMR (101 MHz, $CDCl_3$) δ 155.48, 151.20, 149.44, 129.09, 124.19, 120.26, 119.02, 41.63, 31.22, 27.86, 21.77, 12.33; HRMS (APCI): 208.1332 calcd for $C_{12}H_{18}NO_2$ $[M+H]^+$ found 208.1333 (0.46 ppm). **(JH-VII-75, JH-VI-145, PRC521)**.

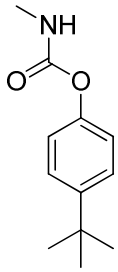

4-(*tert*-Butyl)phenyl *N*-methylcarbamate (**9t**). White solid (*Method A*); 89%; ^{1}H NMR (500 MHz, CDCl3) δ 7.37 – 7.33 (m, 2H), 7.05 – 7.01 (m, 2H), 4.93 (br s, 1H), 2.89 (d, *J* = 4.9 Hz, 3H), 1.30 (s, 9H). (**JH-VIII-143, JH-I-177)**.

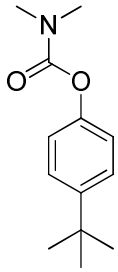

4-(*tert*-Butyl)phenyl *N*,*N*-dimethylcarbamate (**30t**). White solid (*Method C*); 91%; ^{1}H NMR (500 MHz, $CDCl_3$) δ 7.37 – 7.34 (m, 2H), 7.04 – 7.01 (m, 2H), 3.09 (s, 3H), 3.01 (s, 3H), 1.31 (s, 9H).

^{13}C NMR (126 MHz, $CDCl_3$) δ 155.28, 149.30, 148.02, 126.27, 121.18, 36.82, 36.57, 34.54, 31.58; HRMS (FAB): 222.1489 calcd for $C_{13}H_{20}NO_2$ $[M+H]^+$ found 222.1488 (-2.7 ppm, -0.6 mmu). **JH-I-159**.

Example 6: General procedure for the synthesis of 2-alkylthio-substituted phenols

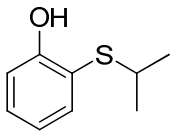

2-(Isopropylthio)phenol **(35v)**. A dry 25 mL round-bottom flask was charged with 2-mercaptophenol (378 mg, 3.0 mmol), DMF (3.0 mL), and sodium bicarbonate (378 mg, 4.5 mmol) after purging with nitrogen. Isopropyliodide (1.02 g, 6.0 mmol) was added and the mixture was brought to 50 ^{o}C and allowed to stir overnight. The contents were cooled to room temperature and diluted with 1 : 1 1 M hydrochloric acid : brine (30 mL) and extracted with ethyl acetate (3 x 20 mL). The organic layers were combined, dried with sodium sulfate, filtered, and the solvent evaporated. The residue was purified on silica gel chromatography (3 : 1 hexane : ethyl acetate) to yield a colorless oil weighing 260 mg (1.55 mmol, 51%); ^{1}H NMR (500 MHz, $CDCl_3$) δ 7.45 (dd, *J* = 7.7, 1.7 Hz, 1H), 7.28 (ddd, *J* = 8.2, 7.7, 1.7 Hz, 1H), 7.00 (dd, *J* = 8.2, 1.7 Hz, 1H), 6.87 (dt, *J* = 7.7, 1.7 Hz, 2H), 6.86 (s, 1H), 3.10 (s-7, *J* = 6.7 Hz, 1H), 1.25 (d, *J* = 6.7 Hz, 6H); ^{13}C NMR (126 MHz, $CDCl_3$) δ 157.57, 137.00, 131.43, 120.60, 118.02, 114.71, 40.66, 23.35; HRMS (FAB): 169.06872 calcd for $C_9H_{13}OS$ $[M+H]^+$ found 169.06956 (3.1 ppm, 0.5 mmu). **JH-III-171**.

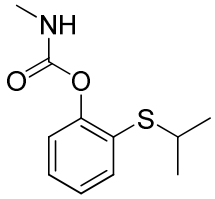

2-(Isopropylthio)phenyl *N*-methylcarbamate[7] **(9v)**. White solid (*Method B*); 92%; ^{1}H NMR (500 MHz, $CDCl_3$) δ 7.42 (dd, *J* = 7.7, 1.5 Hz, 1H), 7.24 (td, *J* = 7.7, 1.5 Hz, 1H), 7.19 – 7.12 (m, 2H), 5.07 (s, 1H), 3.38 (s-7, *J* = 6.6 Hz, 1H), 2.91 (d, *J* = 4.9 Hz, 3H), 1.29 (d, *J* = 6.6 Hz, 6H); ^{13}C NMR (126 MHz, $CDCl_3$) δ 155.70, 150.57, 132.72, 129.14, 127.87, 126.05, 123.24, 37.49, 27.98, 23.28; HRMS (FAB): 226.0902 calcd for $C_{11}H_{16}NO_2S$ $[M+H]^+$ found 226.0896 (-2.5 ppm, -0.6 mmu). **(JH-III-173, PRC400)**.

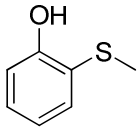

2-(Methylthio)phenol **(35ac)**. This compound was prepared in 100% from 2-mercaptophenol and iodomethane according to the procedure for **35v** in Example 6. Yellow oil; ^{1}H NMR (500 MHz, $CDCl_3$) δ 7.48 (dd, *J* = 7.9, 2.5 Hz, 1H), 7.27 – 7.22 (m, 1H), 6.98 (dd, *J* = 7.9, 2.5 Hz, 1H), 6.88 (td, *J* = 7.9, 2.5 Hz, 1H), 6.69 (s, 1H), 2.33 (s, 3H); ^{13}C NMR (126 MHz, $CDCl_3$) δ 156.43, 134.93, 130.85, 121.08, 115.91, 114.96, 19.95; HRMS (FAB): 163.0194 calcd for C_7H_8OS $[M+Na]^+$ found 163.0383. **JH-IV-165**.

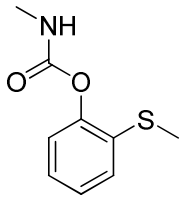

2-(Methylthio)phenyl *N*-methylcarbamate[7] **(9ac).** White solid (*Method B*); 74%; ^{1}H NMR (500 MHz, $CDCl_3$): δ 7.10-7.24 (m, 4H), 5.08 (br s, 1H), 2.91 (d, *J* = 5.0 Hz, 3H), 2.43 (s, 3H); ^{13}C NMR (126 MHz, $CDCl_3$): δ 154.72, 148.19, 131.93, 126.77, 126.35, 125.95, 122.83, 27.99,

15.21; HRMS (FAB): 197.05105 calcd for $C_9H_{11}NO_2S$ $[M]^+$ found 197.0534 (11.94 ppm). **JH-V-1 (PRC473)**.

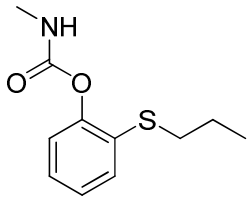

2-(*n*-Propylthio)phenyl *N*-methylcarbamate[7] **(9ad).** Yellow Oil (*Method A*), 76%; ^{1}H NMR (500 MHz, $CDCl_3$) δ 7.37 – 7.30 (m, 1H), 7.22 – 7.14 (m, 2H), 7.14 – 7.10 (m, 1H), 5.08 (br s, 1H), 2.91 (d, *J* = 4.9 Hz, 3H), 2.85 (t, *J* = 7.3 Hz, 2H), 1.66 (s-6, *J* = 7.3 Hz, 2H), 1.02 (t, *J* = 7.3 Hz, 3H); ^{13}C NMR (126 MHz, $CDCl_3$) δ 154.83, 149.32, 130.48, 129.53, 126.74, 126.18, 123.08, 34.90, 27.98, 22.52, 13.61; HRMS (APCI): 225.0823 calcd for $C_{11}H_{15}NO_2S$ $[M]^+$ found 225.0832 (3.63 ppm). **JH-VI-187**.

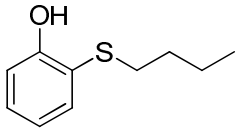

2-(Butylthio)phenol **(35ae).** This compound was prepared in 100% from 2-mercaptophenol and 1-bromobutane according to the procedure for **35v** in Example 6. Yellow oil; ^{1}H NMR (500 MHz, $CDCl_3$) δ 7.46 (dd, *J* = 7.7, 1.7 Hz, 1H), 7.26 (td, *J* = 7.7, 1.7 Hz, 1H), 6.99 (dd, *J* = 7.7, 1.7 Hz, 1H), 6.89 – 6.85 (m, 1H), 6.76 (s, 1H), 2.69 (t, *J* = 7.4 Hz, 2H), 1.59 – 1.49 (m, 2H), 1.39 (s-6, *J* = 7.4 Hz, 2H), 0.89 (t, *J* = 7.4 Hz, 3H); ^{13}C NMR (126 MHz, $CDCl_3$) δ 157.09, 136.09, 131.09, 120.82, 119.35, 114.81, 36.70, 31.87, 21.87, 13.73; HRMS (FAB): 182.07654 calcd for $C_{10}H_{14}OS$ $[M]^+$ found 182.0777 (6.4 ppm, 1.2 mmu). **JH-IV-163**.

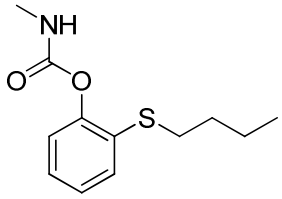

2-(Butylthio)phenyl *N*-methylcarbamate[7] **(9ae)**. Colorless Oil (*Method B*); 77%; ^{1}H NMR (500 MHz, $CDCl_3$) δ 7.34 – 7.30 (m, 1H), 7.21 – 7.14 (m, 2H), 7.14 – 7.09 (m, 1H), 5.08 (br s, 1H), 2.90 (d, *J* = 4.9 Hz, 3H), 2.87 (t, *J* = 7.4 Hz, 2H), 1.66 – 1.59 (m, 2H), 1.49 – 1.40 (m, 2H), 0.92 (t, *J* = 7.4 Hz, 3H); ^{13}C NMR (126 MHz, $CDCl_3$) δ 154.80, 149.18, 130.59, 129.28, 126.64, 126.17, 123.05, 32.50, 31.13, 27.97, 22.13, 13.77; HRMS (FAB): 240.10583 calcd for $C_{12}H_{18}NO_2S$ $[M+H]^+$ found 240.10753 (7.0 ppm, 1.7 mmu). **JH-IV-169 (PRC463)**.

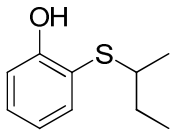

(±)-2-(*sec*-Butylthio)phenol (**35af**). This compound was prepared in 55% from 2-mercaptophenol and 2-bromobutane according to the procedure for **35v** in Example 6. Yellow oil. ^{1}H NMR (500 MHz, $CDCl_3$) δ 7.44 (dd, *J* = 7.7, 1.7 Hz, 1H), 7.27 (dd, *J* = 8.2, 1.7 Hz, 1H), 6.99 (dd, *J* = 8.2, 1.7 Hz, 1H), 6.87 (td, *J* = 7.7, 1.7 Hz, 1H), 6.86 (s, 1H), 2.87 (s-6, *J* = 6.7 Hz, 1H), 1.63 (dtd, *J* = 22.2, 7.4, 6.2 Hz, 1H), 1.51 (s-6, *J* = 7.5 Hz, 1H), 1.22 (d, *J* = 6.2 Hz, 3H), 1.01 (t, *J* = 7.4 Hz, 3H); ^{13}C NMR (126 MHz, $CDCl_3$) δ 157.61, 137.00, 131.33, 120.61, 118.04, 114.70, 47.45, 29.71, 20.67, 11.68; **JT-I-59**.

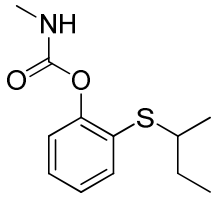

(±)-2-(*sec*-Butylthio)phenyl *N*-methylcarbamate (**9af**). Dark yellow oil (*Method B*); 77%; ^{1}H NMR (500 MHz, $CDCl_3$) δ 7.41 (dd, *J* = 7.7, 1.6 Hz, 1H), 7.24 (td, *J* = 7.7, 1.6 Hz, 1H), 7.20 –

7.11 (m, 2H), 5.05 (br s, 1H), 3.17 (s-6, *J* = 6.8 Hz, 1H), 2.91 (d, *J* = 4.9 Hz, 3H), 1.71 – 1.61 (m, 1H), 1.53 (s-6, *J* = 6.7 Hz, 1H), 1.26 (d, *J* = 6.7 Hz, 3H), 1.00 (t, *J* = 7.4 Hz, 3H); ^{13}C NMR (126 MHz, $CDCl_3$) δ 155.03, 138.23, 132.83, 129.17, 127.82, 126.05, 123.27, 44.21, 29.71, 27.99, 20.64, 11.57. (**JH-III-175, PRC401)**.

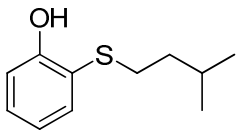

2-(3-Methylbutylthio)phenol **(35ag)**. This compound was prepared in 82% from 2-mercaptophenol and 1-bromo-3-methylbutane according to the procedure for **35v** in Example 6. Yellow oil; ^{1}H NMR (500 MHz, $CDCl_3$) δ 7.46 (dd, *J* = 7.7, 1.4 Hz, 1H), 7.26 (td, *J* = 7.7, 1.4 Hz, 1H), 6.99 (d, *J* = 7.7 Hz, 1H), 6.87 (t, *J* = 7.7 Hz, 1H), 6.76 (s, 1H), 2.75 – 2.62 (m, 2H), 1.66 (s-7, *J* = 6.7 Hz, 1H), 1.45 (dd, *J* = 15.1, 7.3 Hz, 2H), 0.87 (d, *J* = 6.7 Hz, 6H); ^{13}C NMR (126 MHz, $CDCl_3$) δ 157.08, 136.05, 131.10, 120.83, 119.34, 114.81, 38.74, 35.14, 27.41, 22.36; HRMS (FAB): 196.0922 calcd for $C_{11}H_{16}OS$ $[M]^+$ found 196.0928 (3.1 ppm, 0.6 mmu). **JH-IV-159**.

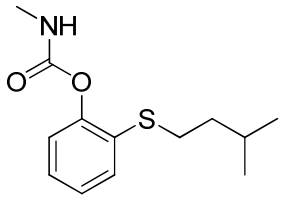

2-(3-Methylbutylthio)phenyl *N*-methylcarbamate[7] **(9ag)**. White solid (*Method B*); 76%; ^{1}H NMR (500 MHz, $CDCl_3$) δ 7.33 – 7.30 (m, 1H), 7.20 – 7.15 (m, 2H), 7.13 – 7.10 (m, 1H), 5.06 (br s, 1H), 2.91 (d, *J* = 4.9 Hz, 3H), 2.88 (t, *J* = 7.9 Hz, 2H), 1.72 (s-7, *J* = 6.6 Hz, 1H), 1.56 – 1.50 (m, 2H), 0.91 (d, *J* = 6.6 Hz, 6H); ^{13}C NMR (126 MHz, $CDCl_3$) δ 154.79, 149.14, 130.62, 129.18, 126.61, 126.17, 123.05, 37.93, 30.81, 27.96, 27.62, 22.38; HRMS (FAB): 254.1215 calcd for $C_{13}H_{20}NO_2S$ $[M+H]^+$ found 254.1204 (-4.2 ppm, -1.1 mmu). **(JH-IV-167, PRC456)**.

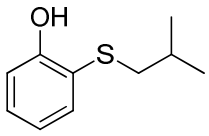

2-(Isobutylthio)phenol **(35ah).** This compound was prepared in 74% from 2-mercaptophenol and isobutyl iodide according to the procedure for **35v** in Example 6. Yellow oil; ^{1}H NMR (500 MHz, $CDCl_3$): δ 7.45 (dd, *J* = 7.7, 1.7 Hz, 1H), 7.24 (ddd, *J* = 8.2, 7.7, 1.7 Hz, 1H), 6.98 (dd, *J* = 8.2, 1.3 Hz, 1H), 6.85 (td, *J* = 7.7, 1.3 Hz, 1H), 6.75 (s, 1H), 2.59 (d, *J* = 6.9 Hz, 2H), 1.76 (s-7, *J* = 6.7 Hz, 1H), 1.01 (d, *J* = 6.6 Hz, 6H); ^{13}C NMR (126 MHz, $CDCl_3$): δ 156.90, 135.58, 130.79, 120.69, 120.02, 114.90, 45.88, 28.53, 21.90. HRMS (APCI): 183.0844 calcd for $C_{10}H_{15}OS$ $[M+H]^+$ found 183.0825 (-7.45 ppm). **JH-V-93**.

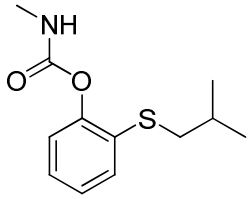

2-(Isobutylthio)phenyl *N*-methylcarbamate[7] **(9ah)**. Off-white solid (*Method B*); 96%; ^{1}H NMR (500 MHz, $CDCl_3$) δ 7.32 (dd, *J* = 7.3, 2.1 Hz, 1H), 7.22 – 7.14 (m, 2H), 7.13 – 7.09 (m, 1H), 5.07 (br s, 1H), 2.91 (d, *J* = 4.9 Hz, 3H), 2.75 (d, *J* = 6.9 Hz, 2H), 1.86 (s-7, *J* = 6.9 Hz, 1H), 1.03 (d, *J* = 6.9 Hz, 6H); ^{13}C NMR (126 MHz, $CDCl_3$): δ 154.78, 149.25, 130.79, 129.51, 126.63, 126.14, 123.03, 41.87, 28.29, 27.94, 22.17; HRMS (FAB): 240.10583 calcd for $C_{12}H_{18}NO_2S$ $[M+H]^+$ found 240.10570 (-0.5 ppm, -0.1 mmu). **(JH-V-95, PRC391)**.

Example 7: General procedure for the synthesis of 2-allyl-substituted class II phenols

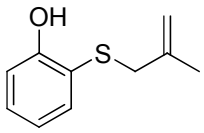

2-(2-Methylallylthio)phenol **(35ai)**. A 50 mL round-bottom flask was charged with 2-mercaptophenol (1.252 g, 9.92 mmol) and diluted in dry tetrahydrofuran (10 mL) prior to the addition of potassium *tert*-butoxide (1.205 g, 10.7 mmol). Next, methallylchloride (1.08 g, 11.9 mmol) was added and the reaction was allowed to stir at room temperature overnight. The solvent was evaporated and the residue was taken up in saturated ammonium chloride (50 mL) and the aqueous layer was extracted with dichloromethane (3 x 25 mL). The organic layers were combined, washed with brine, dried with sodium sulfate, and filtered. The solvent was evaporated and the residue purified on silica gel chromatography (5 : 1 hexane : ethyl acetate) to afford a colorless oil weighing 1.56 g (8.65 mmol, 87%). ^{1}H NMR (400 MHz, $CDCl_3$) δ 7.39 (dd, *J* = 7.7, 1.7 Hz, 1H), 7.28 – 7.22 (m, 1H), 6.98 (dd, *J* = 8.2, 1.3 Hz, 1H), 6.85 (td, *J* = 7.7, 1.7 Hz, 1H), 6.68 (s, 1H), 4.74 (s-5, *J* = 1.4 Hz, 1H), 4.54 (s, 1H), 3.27 (d, *J* = 0.6 Hz, 2H), 1.87 (s, 3H); ^{13}C NMR (101 MHz, $CDCl_3$) δ 157.09, 140.34, 136.31, 131.24, 120.67, 118.87, 114.92, 114.75, 44.50, 20.93; HRMS (FAB): 180.0609 calcd for $C_{10}H_{12}OS$ $[M]^+$ found 180.0605 (-2.1 ppm). **JH-VI-51**.

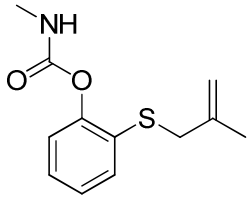

2-(2-Methylallylthio)phenyl N-methylcarbamate[14] **(9ai)**. Colorless Oil (*Method B*); 83%; ^{1}H NMR (400 MHz, $CDCl_3$) δ 7.34 (dd, *J* = 7.7, 1.5 Hz, 1H), 7.21 (td, *J* = 7.7, 1.5 Hz, 1H), 7.14 (ddd, *J* = 12.9, 7.7, 1.5 Hz, 2H), 5.04 (br s, 1H), 4.86 – 4.83 (m, 1H), 4.83 – 4.80 (m, 1H), 3.48

(s, 2H), 2.92 (d, *J* = 4.9 Hz, 3H), 1.85 (s, 3H); ^{13}C NMR (101 MHz, $CDCl_3$) δ 154.81, 149.81, 140.60, 131.13, 129.73, 127.43, 126.02, 123.00, 114.36, 41.01, 27.95, 21.34; HRMS (FAB): 237.08235 calcd for $C_{12}H_{15}NO_2S$ $[M]^+$ found 237.08333 (4.0 ppm, 0.9 mmu). **(JH-VI-53, PRC337)**.

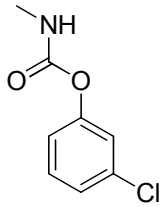

3-Chlorophenyl *N*-methylcarbamate[1] **(9al)**. White solid (*Method A*); 91%; ^{1}H NMR (500 MHz, $CDCl_3$): δ 7.27 (t, *J* = 8.0 Hz, 1H), 7.20 – 7.15 (m, 1H), 7.05 – 7.02 (m, 1H), 5.00 (br s, 1H), 2.89 (d, *J* = 5.0 Hz, 2H); ^{13}C NMR (126 MHz, $CDCl_3$): δ 154.77, 151.71, 134.61, 130.12, 125.67, 122.38, 120.08, 27.88; HRMS (FAB): 186.0323 calcd for $C_8H_9NO_2Cl$ $[M+H]^+$ found 186.0312. **(JH-II-135, JH-VIII-137, PRC361)**.

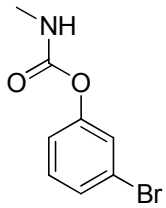

3-Bromophenyl *N*-methylcarbamate[2] **(9am)**. White solid (*Method A*); 81%; ^{1}H NMR (500 MHz, $CDCl_3$): δ 7.36 – 7.30 (m, 1H), 7.22 (t, *J* = 7.9 Hz, 1H), 7.08 (dd, *J* = 7.9, 1.7 Hz, 1H), 4.98 (br s, 1H), 2.90 (d, *J* = 4.9 Hz, 3H); ^{13}C NMR (126 MHz, $CDCl_3$): δ 151.74, 130.45, 128.59, 125.23, 122.34, 120.61, 120.57, 27.89; HRMS (FAB): 229.9818 calcd for $C_8H_9NO_2Br$ $[M+H]^+$ found 229.9820 (1.4 ppm, 0.3 mmu). **(JH-II-127, JH-VIII-139, PRC356)**.

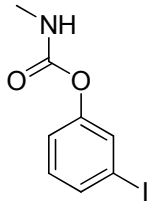

3-Iodophenyl *N*-methylcarbamate[2] **(9an)**. White solid (*Method B*); 70%; ^{1}H NMR (500 MHz, $CDCl_3$) δ 7.55 – 7.51 (m, 1H), 7.50 (t, *J* = 1.8 Hz, 1H), 7.18 – 7.00 (m, 2H), 4.97 (br s, 1H), 2.89 (d, *J* = 4.9 Hz, 3H); ^{13}C NMR (126 MHz, $CDCl_3$) δ 151.49, 135.65, 134.54, 130.95, 130.69, 121.29, 93.55, 27.89; HRMS (FAB): 277.9679 calcd for $C_8H_9NO_2I$ $[M+H]^+$ found 277.9662 (-5.8 ppm, -1.6 mmu). **(JH-II-125, PRC357)**.

Example 8: General procedure for the addition of aryl lithium reagents to cyclic ketones

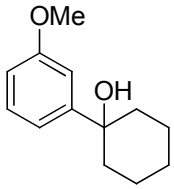

1-(3-Methoxyphenyl)cyclohexanol **(102ap)**. A dry 50 mL nitrogen-filled Schlenk flask situated in a dry-ice acetone bath was charged with 1.2 M *t*-BuLi in pentane (2.1 mL, 2.6 mmol) and diethyl ether (10 mL). While stirring, 3-iodoanisole (348 mg, 1.49 mmol) was injected dropwise. The cooling bath was removed and the reaction was allowed to stir for 30 min at room temperature. The reaction was once again cooled to -78 ^{o}C prior to addition of cyclohexanone (185 µL, 1.79 mmol) in one portion. The reaction was allowed to return to room temperature and stir overnight before quenching at 0 ^{o}C with NH_4Cl (10 mL). The aqueous layer was extracted with diethyl ether (3 x 10 mL), the organic layers were combined, washed with brine, and dried with sodium sulfate. The solution was filtered, concentrated in vacuo, and purified with flash chromatography (4:1 hexane : ethyl acetate) to yield an oil (283 mg, 92%). ^{1}H NMR (500 MHz, $CDCl_3$) δ 7.27 (t, *J* = 8.0 Hz, 1H), 7.12 – 7.08 (m, 1H), 7.07 (ddd, *J* = 8.0, 1.7, 0.9 Hz, 1H), 6.79

(ddd, *J* = 8.0, 1.7, 0.9 Hz, 1H), 3.82 (s, 3H), 1.88 – 1.69 (m, 7H), 1.68 – 1.58 (m, 3H), 1.35 – 1.23 (m, 1H); ^{13}C NMR (126 MHz, $CDCl_3$) δ 159.73, 151.47, 129.34, 117.10, 111.94, 110.88, 73.33, 55.36, 38.95, 25.64, 22.30; HRMS (FAB); 206.1307 calcd for $C_{13}H_{18}O_2$ $[M]^+$ found 206.1312 (2.5 ppm, 0.5 mmu). (**JH-III-97, JH-III-149)**.

Example 9: General procedure for the elimination of benzylic alcohols

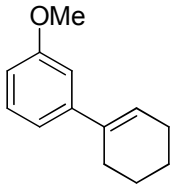

3'-Methoxy-2,3,4,5-tetrahydro-1,1'-biphenyl **(103ap)**. A 10 mL round-bottom flask was charged with 1-(3-methoxyphenyl)cyclohexanol (**102ap**, 182 mg, 0.88 mmol), methanol (2 mL), and *p*-TsOH • H_2O (23 mg, 0.12 mmol). The reaction was brought to reflux for 8 h before cooling to room temperature and diluting the reaction down water (20 mL). The aqueous layer was extracted with dichloromethane (3 x 10 mL) and the combined organic layers were washed with sodium bicarbonate (20 mL), dried with sodium sulfate. The solution was filtered and concentrated in vacuo to affordgive a yellow oil weighing 160 mg (0.85 mmol, 97%). ^{1}H NMR (500 MHz, $CDCl_3$) δ 7.22 (t, *J* = 7.9 Hz, 1H), 7.01 – 6.95 (m, 1H), 6.94 – 6.90 (m, 1H), 6.77 (dd, *J* = 7.9, 2.6 Hz, 1H), 6.14 – 6.11 (m, 1H), 3.82 (s, 3H), 2.42 – 2.38 (m, 2H), 2.24 – 2.17 (m, 2H), 1.82 – 1.74 (m, 2H), 1.66 (dtd, *J* = 9.2, 6.1, 2.9 Hz, 2H); ^{13}C NMR (126 MHz, $CDCl_3$) δ 159.69, 144.47, 136.64, 129.22, 125.22, 117.71, 111.97, 111.00, 55.34, 27.61, 26.00, 23.19, 22.29; HRMS (FAB); 188.1201 calcd for $C_{13}H_{16}O$ $[M]^+$ found 188.1190 (-5.9 ppm, -1.1 mmu); **JH-III-125**.

Example 10: General procedure for the hydrogenation of alkenes

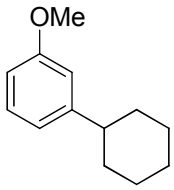

1-Cyclohexyl-3-methoxybenzene **(45ap)**. A 50 mL round-bottom flask was charged with 3'-methoxy-2,3,4,5-tetrahydro-1,1'-biphenyl (**103ap**, 149 mg, 0.791 mmol), methanol (1.5 mL), and 10% palladium on carbon (60 mg). The reaction was allowed to stir at room temperature at 1 atmosphere of H_2 for 24h before filtering and concentrating the solvent in vacuo to give a colorless oil weighing 115 mg (0.60 mmol, 76%). ^{1}H NMR (500 MHz, $CDCl_3$) δ 7.21 (t, *J* = 7.9 Hz, 1H), 6.81 (dd, *J* = 7.9, 0.5 Hz, 1H), 6.79 – 6.75 (m, 1H), 6.73 (dd, *J* = 7.9, 2.6 Hz, 1H), 3.80 (s, 3H), 2.47 (ddd, *J* = 11.5, 7.3, 3.4 Hz, 1H), 1.92 – 1.79 (m, 4H), 1.78 – 1.70 (m, 1H), 1.47 – 1.32 (m, 4H), 1.26 (tt, *J* = 11.5, 3.4 Hz, 1H); ^{13}C NMR (126 MHz, CDC_3) δ 159.71, 150.01, 129.33, 119.45, 112.93, 110.95, 55.27, 44.81, 34.54, 27.03, 26.31; HRMS (FAB); 190.1358 calcd for $C_{13}H_{18}O$ $[M]^+$ found 190.1349 (-4.5 ppm, -0.9 mmu); **JH-III-131**.

Example 11: General procedure for the boron tribromide deprotection of anisoles

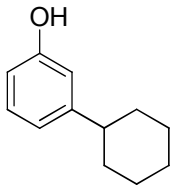

3-Cyclohexylphenol **(35ap)**. A dry 50 mL round-bottom flask was charged with 1-cyclohexyl-3-methoxybenzene (**45ap**, 105 mg, 0.55 mmol) and dichloromethane (1 mL) while purging with nitrogen. The reaction was cooled to -78 ^{o}C in a dry ice-acetone bath prior to the addition of 1 M BBr_3 in dichloromethane (0.55 mL, 0.55 mmol). The reaction was allowed to stir overnight as the reaction warmed to room temperature. The reaction was quenched with water (2 mL) and the

aqueous layer was extracted with diethyl ether (3 x 5 mL). The organic layers were combined and washed with brine, dried with sodium sulfate. The solution was filtered, concentrated in vacuo, and purified with flash chromatography (5:1 hexane : ethyl acetate) giving a green solid weighing 77 mg. **JH-III-141**. This crude material was directly carried on to the next step.

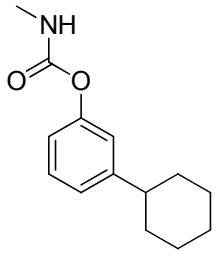

3-Cyclohexylphenyl *N*-methylcarbamate[4] **(9ap)**. White solid (*Method B*); 49%; ^{1}H NMR (500 MHz, $CDCl_3$) δ 7.25 (t, *J* = 7.8 Hz, 1H), 7.04 (d, *J* = 7.8 Hz, 1H), 6.99 – 6.95 (m, 1H), 6.93 (dd, *J* = 7.8, 1.9 Hz, 1H), 4.92 (br s, 1H), 2.90 (d, *J* = 4.9 Hz, 3H), 2.57 – 2.40 (m, 1H), 1.93 – 1.78 (m, 4H), 1.78 – 1.68 (m, 1H), 1.47 – 1.30 (m, 4H), 1.30 – 1.17 (m, 1H); ^{13}C NMR (126 MHz, $CDCl_3$) δ 154.63, 151.21, 149.81, 129.13, 123.99, 120.09, 119.00, 44.48, 34.44, 27.87, 26.96, 26.25; HRMS (FAB); 234.1495 calcd for $C_{14}H_{20}NO_2$ $[M+H]^+$ found 234.1484 (-4.3 ppm, -1.0 mmu). **(JH-III-143, PRC392)**.

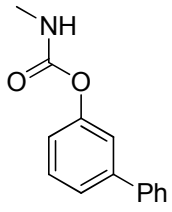

[1,1'-Biphenyl]-3-yl *N*-methylcarbamate[5] **(9aq)**. White solid (*Method B*); 69%; ^{1}H NMR (500 MHz, $CDCl_3$) δ 7.63 – 7.52 (m, 2H), 7.46 – 7.31 (m, 6H), 7.14 – 7.08 (m, 1H), 4.99 (br s, 1H), 2.92 (d, *J* = 4.9 Hz, 3H); ^{13}C NMR (101 MHz, $CDCl_3$) δ 155.35, 151.57, 142.78, 140.45, 129.68, 128.88, 128.16, 127.68, 127.31, 124.18, 120.50, 27.88; HRMS (APCI): 228.1025 calcd for $C_{14}H_{14}NO_2$ $[M+H]^+$ found 228.1018 (-3.3 ppm, -0.8 mmu). **(JH-II-97, PRC336)**.

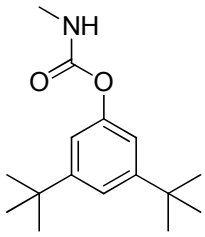

3,5-di-*tert*-Butylphenyl methylcarbamate[11] **(9ar)**. White solid (*Method B*) 82%; ^{1}H NMR (500 MHz, $CDCl_3$) δ 7.25 (t, *J* = 1.7 Hz, 1H), 6.94 (d, *J* = 1.7 Hz, 2H), 4.94 (br s, 1H), 2.90 (d, *J* = 4.9 Hz, 3H), 1.31 (s, 18H); ^{13}C NMR (126 MHz, $CDCl_3$) δ 155.70, 152.17, 150.82, 119.51, 115.93, 35.06, 31.52, 27.86; HRMS (FAB): 264.1965 calcd for $C_{16}H_{26}NO_2$ $[M+H]^+$ found 264.1958 (-2.1 ppm, -0.6 mmu). **(JH-II-129, PRC349)**.

Example 12a: General procedure for the introduction of ethyl nucleophiles to aryl ketones with lithium ethylzincate

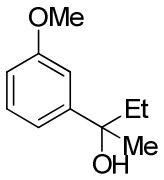

2-(3-Methoxyphenyl)butan-2-ol[2] **(45as)**. A dry 50 mL Schlenk flask was charged with lithium chloride (127 mg, 2.99 mmol). The mass of transferred lithium chloride was determined after melt drying under high vacuum. Next, zinc chloride (64 mg, 0.47 mmol) was added and once again melt dried. After the mixture cooled a solution of Me_3SiCH_2MgCl (1.0 M in Et_2O, 710 µl, 0.710 mmol) was injected and allowed to stir at room temperature for 15 min followed by the addition of a solution of EtMgCl (2.0 M, 1.3 mL, 2.6 mmol). This was allowed to stir for an additional 1 hour and then the reaction cooled to 0 ^{o}C in an ice-water bath prior to the dropwise addition of a solution of 3-methoxyacetophenone (355 mg, 2.36 mmol; 5 mL tetrahydrofuran). Upon stirring for 4 h at 0 ^{o}C the cooling bath was removed and the reaction was allowed to stir at room temperature overnight. The reaction was quenched at 0 ^{o}C with NH_4Cl (40 mL) and the

aqueous layer extracted with Et_2O (3 x 30 mL). The organic layers were combined, washed with brine, dried with brine, and evaporated. The residue was purified with flash chromatography (3:1 hexanes:ethyl acetate) to yield a colorless oil weighing 371 mg (87%); ^{1}H NMR (400 MHz, $CDCl_3$) δ 7.26 (t, *J* = 7.9 Hz, 1H), 7.04 – 7.01 (m, 1H), 6.99 (ddd, *J* = 7.9, 1.6, 0.9 Hz, 1H), 6.78 (ddd, *J* = 7.9, 1.6, 0.9 Hz, 1H), 3.82 (s, 3H), 1.90 – 1.75 (m, 2H), 1.73 (s, 1H), 1.54 (s, 3H), 0.80 (t, *J* = 7.4 Hz, 3H); ^{13}C NMR (126 MHz, CDC_3) δ 159.67, 149.78, 129.23, 117.48, 111.68, 111.25, 75.06, 55.35, 36.73, 29.82, 8.43; HRMS (APCI): 163.1123 calcd for $C_{11}H_{15}O$ $[M\text{-}OH]^+$ found 163.1123 (5.83 ppm). **JH-VI-173, JH-VIII-133**.

Example 12b: General procedure for the introduction of ethyl nucleophiles to aryl ketones with ethylmagnesium bromide

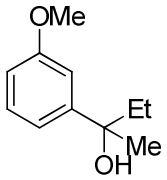

2-(3-Methoxyphenyl)butan-2-ol **(45as)**. A dry 250 mL Schlenk flask backfilled with nitrogen was charged with 1.0 M ethylmagnesium bromide in tetrahydrofuran (34 mL, 34 mmol) and cooled in an ice bath to 0 ^oC. Next, a solution of 3-methoxyacetophenone (1.95 g, 13.0 mmol) in tetrahydrofuran (25 mL) was added dropwise and allowed to stir at 0 ^oC for 2 h before removing the cooling bath and allowing the reaction to warm to room temperature. The reaction was allowed to stir at room temperature overnight before quenching the reaction at 0 ^oC with NH_4Cl (60 mL). The aqueous layer was extracted with diethyl ether (4 x 50 mL). The organic layers were combined, washed with brine, dried with $MgSO_4$, filtered, and concentrated in vacuo. Purification was performed with flash chromatography (dichloromethane) to yield a colorless oil weighing 1.49 g (8.27 mmol, 63%); The characterization data was the same as Example 12a. (**JH-VI-173 and JH-VII-173 MS)**.

Example 13: General procedure for the installation of methyl nucleophiles to tertiary benzylic alcohols

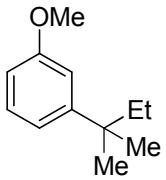

1-Methoxy-3-(tert-pentyl)benzene **(47as)**. A dry 50 mL Schlenk flask was charged with 2-(3-methoxyphenyl)butan-2-ol **(45as**, 199 mg, 1.10 mmol) and back-filled with nitrogen. The reaction flask was cooled to 0 ^{o}C in an ice-bath prior to the addition of thionyl chloride (328 mg, 2.76 mmol). The reaction was allowed to commence for two h prior to placing the contents under high vacuum for 30 min with care taken to avoid vapors entering the vacuum pump. Next, the contents were diluted in dichloromethane (2 mL), cooled to -78 ^{o}C, and then a 2.0 M solution of trimethylaluminum in hexanes (1.10 mL, 2.2 mmol) was added in one portion. After 4 h the cooling bath was removed and the reaction was allowed to stir at room temperature overnight. The reaction was once again cooled to 0 ^{o}C and quenched with 1 M hydrochloric acid (50 mL). The aqueous layer was extracted dichloromethane (3 x 25 mL). The organic layers were combined, washed with brine, dried with sodium sulfate, and filtered. The solvent was evaporated in vacuo and the residue was purified on silica gel chromatography (10 : 1 hexane : ethyl acetate) to yield a colorless oil weighing 185 mg (1.04 mmol, 94%); ^{1}H NMR (500 MHz, $CDCl_3$) δ 7.23 (t, *J* = 8.0 Hz, 1H), 6.96 – 6.91 (m, 1H), 6.89 (t, *J* = 2.0 Hz, 1H), 6.72 (dd, *J* = 8.0, 2.0 Hz, 1H), 3.81 (s, 3H), 1.63 (q, *J* = 7.4 Hz, 2H), 1.27 (s, 6H), 0.68 (t, *J* = 7.4 Hz, 3H); ^{13}C NMR (126 MHz, $CDCl_3$) δ 159.50, 151.49, 128.96, 118.71, 118.70, 112.89, 109.88, 55.26, 38.12, 36.96, 28.58, 9.28; HRMS (APCI): 179.1430 calcd for $C_{12}H_{19}O$ $[M+H]^+$ found 179.1429 (-0.79 ppm). (**JH-VII-21 and JH-VII-183)**.

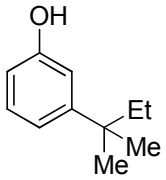

3-(*tert*-Pentyl)phenol **(35as)**. This compound was prepared in 86% from 1-methoxy-3-(tert-pentyl)benzene **(47as)** and boron tribromide (2 equiv) according to the procedure for **35ap** in Example 11. Green oil; ^{1}H NMR (500 MHz, $CDCl_3$) δ 7.17 (t, *J* = 7.9 Hz, 1H), 6.93 – 6.88 (m, 1H), 6.82 – 6.80 (m, 1H), 6.67 – 6.62 (m, 1H), 1.62 (q, *J* = 7.4 Hz, 2H), 1.26 (s, 6H), 0.68 (t, *J* = 7.4 Hz, 3H); ^{13}C NMR (126 MHz, $CDCl_3$) δ 155.34, 151.87, 129.19, 118.74, 113.36, 112.27, 38.04, 36.94, 28.54, 9.26; HRMS (APCI): 163.1128 calcd for $C_{11}H_{15}O$ $[M+H]^+$ found 163.1090 (-4.91 ppm). **JH-VII-23**.

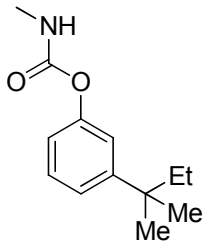

3-(*tert*-Pentyl)phenyl *N*-methylcarbamate[5] **(9as)**. Off-white solid (*Method A*); 88%; ^{1}H NMR (500 MHz, $CDCl_3$) δ 7.31 – 7.25 (m, 1H), 7.16 (d, *J* = 7.9 Hz, 1H), 7.06 (s, 1H), 6.94 (d, *J* = 7.9 Hz, 1H), 4.97 (br s, 1H), 2.89 (d, *J* = 4.9 Hz, 3H), 1.62 (q, *J* = 7.4 Hz, 2H), 1.27 (s, 6H), 0.69 (t, *J* = 7.4 Hz, 3H); ^{13}C NMR (126 MHz, $CDCl_3$) δ 155.54, 151.39, 151.06, 128.77, 123.06, 119.44, 118.62, 38.10, 36.95, 28.47, 27.84, 9.22; HRMS (APCI): 221.1416 calcd for $C_{13}H_{19}NO_2$ $[M]^+$ found 221.1418 (1.06 ppm). **(JH-VII-27, PRC540)**.

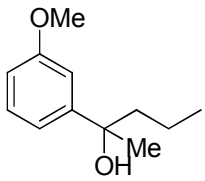

2-(3-Methoxyphenyl)pentan-2-ol **(45at)**. This compound was prepared in 36% from 3-methoxyacetophenone and *n*-propylmagnesium bromide according to the procedure for **45as** in Example 12b. Colorless oil; ^{1}H NMR (400 MHz, $CDCl_3$) δ 7.25 (t, *J* = 7.9 Hz, 1H), 7.04 – 6.94 (m, 2H), 6.78 (dd, *J* = 7.9, 2.5 Hz, 1H), 3.82 (s, 3H), 1.82 – 1.68 (m, 2H), 1.54 (s, 3H), 1.36 – 1.08 (m, 2H), 0.86 (t, *J* = 7.3 Hz, 3H); ^{13}C NMR (101 MHz, $CDCl_3$) δ 159.64, 150.09, 129.22, 117.37, 111.59, 111.14, 74.88, 55.34, 46.59, 30.29, 17.42, 14.53; HRMS (APCI): 177.1274 calcd for $C_{10}H_{15}O_2$ $[M\text{-}OH]^+$ found 177.1253. **JH-VI-175**.

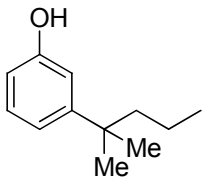

3-(2-Methylpentan-2-yl)phenol **(35at)**. This compound was prepared in 79% from 2-(3-methoxyphenyl)pentan-2-ol **(45at)** and trimethylaluminum according to the procedure for **47as** in Example 13. The intermediate anisole (1-methoxy-3-(2-methylpentan-2-yl)benzene**)** was deprotected with boron tribromide (2 equiv) according to the procedure for **35ap** in Example 11. Green oil; ^{1}H NMR (500 MHz, $CDCl_3$) δ 7.16 (t, *J* = 7.9 Hz, 1H), 6.91 (ddd, *J* = 7.9, 1.8, 0.9 Hz, 1H), 6.83 – 6.79 (m, 1H), 6.64 (ddd, *J* = 7.9, 1.8, 0.9 Hz, 1H), 4.64 (s, 1H), 1.65 – 1.43 (m, 2H), 1.27 (s, 6H), 1.13 – 1.01 (m, 2H), 0.82 (t, *J* = 7.3 Hz, 3H); ^{13}C NMR (126 MHz, $CDCl_3$) δ 155.32, 152.23, 129.19, 118.63, 113.23, 112.25, 47.17, 37.89, 29.04, 18.08, 14.89; HRMS (APCI): 179.1430 calcd for $C_{12}H_{19}O$ $[M+H]^+$ found 179.1392. **JH-VII-39**.

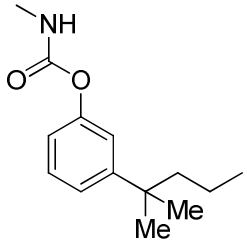

3-(2-Methylpentan-2-yl)phenyl *N*-methylcarbamate[5] **(9at)**. White solid (*Method A*); 86%; ^{1}H NMR (500 MHz, $CDCl_3$) δ 7.27 (t, *J* = 7.9 Hz, 1H), 7.16 (d, *J* = 7.9 Hz, 1H), 7.05 (t, *J* = 2.0 Hz, 1H), 6.94 (dd, *J* = 7.9, 2.0 Hz, 1H), 4.95 (br s, 1H), 2.89 (d, *J* = 4.9 Hz, 3H), 1.59 – 1.50 (m, 2H), 1.27 (s, 6H), 1.13 – 1.02 (m, 2H), 0.81 (t, *J* = 7.3 Hz, 3H); ^{13}C NMR (126 MHz, $CDCl_3$) δ 155.52, 151.74, 151.05, 128.77, 122.95, 119.29, 118.60, 47.16, 37.95, 28.95, 27.85, 18.04, 14.87; HRMS (APCI): 236.1645 calcd for $C_{14}H_{22}NO_2$ $[M+H]^+$ found 236.1657 (4.93 ppm). **(JH-VII-41, PRC550)**.

Example 14: General procedure to prepare C3-substituted diethylbenylic alcohols from benzoic acids

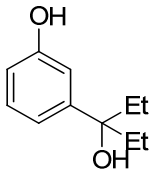

3-(3-Methoxyphenyl)pentan-3-ol[3] (**35au**). A 50 ml round-bottom flask was charged with 3-hydroxybenzoic acid (1.38 g, 10.0 mmol), diluted in methanol (14 mL), and thionyl chloride (1.19 g, 10.0 mmol). The reaction was brought to reflux for 2 h and then cooled to room temperature. The solvent was evaporated in vacuo leaving a small amount of solvent behind. The remaining solvent was diluted in diethylether (40 mL) and washed with brine (20 mL). The organic layer was separated, dried with sodium sulfate, and filtered. The solvent was evaporated in vacuo to yield a white solid weighing 1.52 g (10 mmol, 100% confirmed by ^{1}H NMR). A dry 50 mL round-bottom flask was charged with a solution of 2.0 M ethylmagnesium chloride in

tetrahydrofuran. Next, 3-hydroxymethylbenzoate previously prepared (764 mg, 5.02 mmol) was dissolved in tetrahydrofuran (11 mL) and added to the reaction flask over the course of 30 min at room temperature. After complete addition the reaction was brought to reflux for 2 h. Next, the reaction contents were cooled to 0 ^{o}C and cautiously quenched with ammonium chloride (40 mL). The aqueous layer was extracted with diethylether (3 x 40 mL). The organic layers were combined, washed with brine, dried with sodium sulfate, and filtered. The solvent was evaporated in vacuo and the residue purified with silica gel chromatography to yield a white solid weighing 756 mg (4.19 mg, 84%). ^{1}H NMR (400 MHz, $CDCl_3$) δ 7.19 (t, *J* = 7.9 Hz, 1H), 7.01 – 6.95 (m, 1H), 6.91 – 6.84 (m, 1H), 6.71 (ddd, *J* = 7.9, 2.5, 0.7 Hz, 1H), 5.71 (s, 1H), 1.90 (s, 1H), 1.90 – 1.74 (m, 4H), 0.76 (t, *J* = 7.4 Hz, 6H); ^{13}C NMR (101 MHz, $CDCl_3$) δ 155.77, 147.81, 129.38, 117.90, 113.43, 112.99, 78.01, 34.88, 7.95; HRMS (ESI): 163.1123 calcd for $C_{11}H_{15}O$ $[M\text{-}OH]^{+}$ found 163.1108 (-9.14 ppm). **JH-VIII-179**.

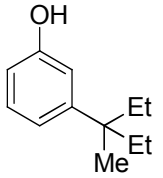

3-(3-Methylpentan-3-yl)phenol **(35au*)**. This compound was prepared in 92% from 3-(3-methoxyphenyl)pentan-3-ol **(50au)** and trimethylaluminum according to the procedure for **47as** in Example 13. White solid; ^{1}H NMR (500 MHz, $CDCl_3$) δ 7.16 (t, *J* = 8.0 Hz, 1H), 6.86 (ddd, *J* = 8.0, 1.7, 0.9 Hz, 1H), 6.81 – 6.72 (m, 1H), 6.64 (ddd, *J* = 8.0, 1.7, 0.9 Hz, 1H), 4.64 (s, 1H), 1.74 - 1.66 (m, 2H), 1.58 – 1.48 (m, 2H), 1.21 (s, 3H), 0.67 (t, *J* = 7.4 Hz, 6H); ^{13}C NMR (126 MHz, $CDCl_3$) δ 155.31, 150.15, 129.07, 119.47, 113.99, 112.16, 41.44, 35.38, 22.84, 8.81; HRMS (APCI): 177.1285 calcd for $C_{12}H_{17}O$ $[M\text{-}H]^{-}$ found 177.1278 (-4.03 ppm). **JH-VII-55**.

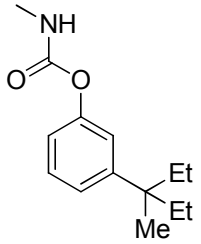

3-(3-Methylpentan-3-yl)phenyl *N*-methylcarbamate **(9au*, *Novel carbamate #1*)**. White solid (*Method A*); 88%; ^{1}H NMR (500 MHz, $CDCl_3$) δ 7.27 (t, *J* = 8.0 Hz, 1H), 7.11 (d, *J* = 8.0 Hz, 1H), 7.01 (t, *J* = 2.0 Hz, 1H), 6.94 (dd, *J* = 8.0, 2.0 Hz, 1H), 4.95 (br s, 1H), 2.89 (d, *J* = 4.9 Hz, 3H), 1.71 (dq, *J* = 14.8, 7.4 Hz, 2H), 1.54 (dq, *J* = 14.8, 7.4 Hz, 2H), 1.22 (s, 3H), 0.67 (t, *J* = 7.4 Hz, 6H); ^{13}C NMR (126 MHz, $CDCl_3$) δ 155.53, 151.10, 149.68, 128.67, 123.68, 120.09, 118.47, 41.49, 35.26, 27.84, 22.94, 8.79; HRMS (APCI): 236.1645 calcd for $C_{14}H_{22}NO_2$ $[M+H]^+$ found 236.1650 (1.88 ppm). **(JH-VII-59, PRC563)**.

Example 15: General procedure for the trifluoromethylation of aryl ketones

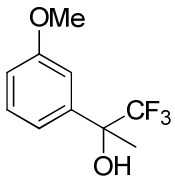

1,1,1-Trifluoro-2-(3-methoxyphenyl)propan-2-ol **(57av)**. A dry 50 mL Schlenk flask was charged with 3-methoxyacetophenone (200 mg, 1.32 mmol), *N*,*N*-dimethylformamide (4 mL), and trifluoromethyltrimethylsilane (295 µL, 2.0 mmol). Next, the reaction was cooled in an ice bath prior to the addition of catalytic potassium carbonate (10 mg, 0.07 mmol) and then flushed with nitrogen. The ice-bath was removed and the reaction was allowed to stir at room temperature for 4 h. The reaction was diluted with saturated sodium chloride (40 mL) and extracted with ethyl acetate (3 x 25 mL). The combined organic layers were washed with brine and dried with sodium sulfate before filtering and concentrating the solution in vacuo. The TMS-protected alcohol was purified with flash chromatography (12 : 1 hexane : ethyl acetate). The

resulting oil was taken up in methanol (5 mL) and 2 M hydrochloric acid (0.5 mL) and allowed to stir at room temperature for 2 h. The methanol was removed via rotary evaporation and the residue diluted with H_2O (50 mL) and extracted with dichloromethane (3 x 50 mL). The organic layers were combined, washed with brine, dried with sodium sulfate, and filtered prior to concentrating the solution in vacuo to yield a yellow oil weighing 236 mg (1.07 mmol, 81%); ^{1}H NMR (500 MHz, $CDCl_3$) δ 7.34 – 7.30 (m, 1H), 7.17 – 7.12 (m, 2H), 6.91 (ddd, J = 8.2, 2.5, 0.9 Hz, 1H), 3.83 (s, 3H), 2.40 (s, 1H), 1.77 (q, J = 2.0 Hz, 3H); ^{13}C NMR (126 MHz, $CDCl_3$) δ 159.63 (s), 140.22 (s), 129.49 (s), 125.68 (q, $^1J_{CF}$ = 285 Hz), 118.48 (s), 113.91 (s), 112.46 (s), 74.92 (q, $^2J_{CF}$ = 29 Hz), 55.44 (s), 24.04 (s); HRMS (APCI): 203.0678 calcd for $C_{10}H_{10}F_3O$ [M-OH]$^+$ found 203.06771 (-1.43 ppm). **JH-VI-161, JH-VI-65**, **JH-V-159**.

Example 16: General procedure for the mesylation of tertiary trifluoromethyl-containing benzylic alcohols

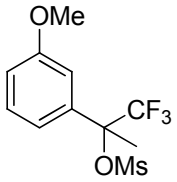

1,1,1-Trifluoro-2-(3-methoxyphenyl)propan-2-yl methanesulfonate **(67av)**. A dry 10 mL round-bottom was charged with a 60% dispersion of sodium hydride in mineral oil (74 mg, 1.83 mmol) and placed in an ice-bath prior to the dropwise addition of a solution containing 1,1,1-trifluoro-2-(3-methoxyphenyl)propan-2-ol (**57av**, 203 mg, 0.922 mmol) in of tetrahydrofuran (2.2 mL). After stirring for 30 min, the ice-bath was removed and mesyl chloride (143 µL, 1.84 mmol) was added dropwise. The reaction was allowed to stir for 18 h at room temperature before concentrating the solvent in vacuo. The residue was quenched by the dropwise addition of 5 mL of saturated sodium bicarbonate solution at 0 ^{o}C and extracted with ethyl acetate (3 x 25 mL).

The organic layers were combined and washed with brine, dried with sodium sulfate, filtered, and concentrated in vacuo. The resulting residue was purified using flash chromatography (3:1 hexane : ethyl acetate) to yield the intermediate as a colorless oil weighing 270 mg (0.905 mmol, 98%). ^{1}H NMR (400 MHz, $CDCl_3$) δ 7.36 (t, J = 8.1 Hz, 1H), 7.17 – 7.10 (m, 2H), 6.97 (dd, J = 8.1, 2.4 Hz, 1H), 3.83 (s, 3H), 3.12 (s, 3H), 2.28 (q, J = 0.9 Hz, 3H); ^{13}C NMR (101 MHz, $CDCl_3$) δ 159.63 (s), 136.08 (s), 129.70 (s), 123.35 (q, $^{1}J_{CF}$ = 284 Hz), 119.31 (s), 114.82 (s), 113.81 (q, $^{3}J_{CF}$ = 1.0 Hz), 87.45 (q, $^{2}J_{CF}$ = 31 Hz), 55.47 (s), 41.37 (s), 19.15 (s); HRMS (APCI): 298.0487 calcd for $C_{11}H_{13}O_4F_3S$ $[M]^+$ found 298.0485 (-0.53 ppm). **JH-VI-71**, **JH-VI-69**.

Example 17: General procedure for the installation of methyl nucleophiles to tertiary trifluoromethyl-containing benzylic alcohols

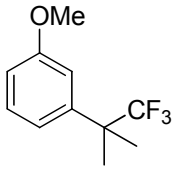

1-Methoxy-3-(1,1,1-trifluoro-2-methylpropan-2-yl)benzene **(47av)**. A dry 50 mL round-bottom was charged with 1,1,1-trifluoro-2-(3-methoxyphenyl)propan-2-yl methanesulfonate (**67av**, 300 mg, 1.00 mmol) and dichloromethane (3 mL) while purging with nitrogen. The reaction was cooled in an ice-bath prior to the dropwise addition of 2.0 M trimethylaluminum in hexane (0.50 mL, 1.0 mmol). The ice-bath was removed and the reaction was allowed to stir at room temperature for 18 h. The colorless reaction was quenched with a solution containing 3 mL sodium bicarbonate and 1 mL brine and filtered through a plug of Celite and washed with ethyl acetate. The layers were separated and the aqueous layer was extracted with dichloromethane (3 x 10 mL). The organic layers were combined, washed with brine, dried with sodium sulfate, filtered, and concentrated in vacuo. The residue is purified with flash chromatography (12 : 1 hexane : ethyl acetate) to yield a colorless oil weighing 168 mg (0.77 mmol, 77%). ^{1}H NMR

(400 MHz, $CDCl_3$) δ 7.30 (t, *J* = 8.1 Hz, 1H), 7.12 – 7.08 (m, 1H), 7.06 (s, 1H), 6.86 (ddd, *J* = 8.1, 2.5, 0.7 Hz, 1H), 3.83 (s, 3H), 1.57 (s, 6H); ^{13}C NMR (101 MHz, $CDCl_3$) δ 159.50 (s), 141.74 (s), 129.25 (s), 128.46 (q, $^1J_{CF}$ = 283 Hz), 119.93 (s), 114.47 (s), 112.25 (s), 55.36 (s), 44.00 (q, $^2J_{CF}$ = 25 Hz), 22.81 (q, $^3J_{CF}$ = 2.4 Hz); ^{19}F NMR (376 MHz, $CDCl_3$) δ -76.49 (s); HRMS (FAB): 218.0919 calcd for $C_{11}H_{13}F_3O$ $[M]^+$ found 218.0924 (2.44 ppm). **JH-VI-75**.

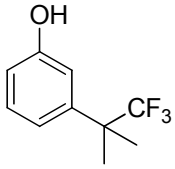

3-(1,1,1-Trifluoro-2-methylpropan-2-yl)phenol **(35av)**. This compound was prepared in 98% from 1-methoxy-3-(1,1,1-trifluoro-2-methylpropan-2-yl)benzene **(47av)** and boron tribromide according to the procedure for **35ap** in Example 11. Yellow oil; ^1H NMR (400 MHz, $CDCl_3$) δ 7.23 (t, *J* = 8.1 Hz, 1H), 7.06 (ddt, *J* = 8.1, 2.5, 0.9 Hz, 1H), 6.99 (s, 1H), 6.79 (ddd, *J* = 8.1, 2.5, 0.9 Hz, 1H), 5.64 (s, 1H), 1.55 (q, *J* = 0.7 Hz, 6H); ^{13}C NMR (101 MHz, $CDCl_3$) δ 155.56 (s), 142.00 (s), 129.44 (s), 128.42 (q, $^1J_{CF}$ = 283 Hz), 119.88 (s), 114.99 (s), 114.68 (s), 43.91 (q, $^2J_{CF}$ = 25 Hz), 22.73 (q, $^3J_{CF}$ = 2.4 Hz); ^{19}F NMR (376 MHz, $CDCl_3$) δ -76.49 (s); HRMS (APCI): 203.0689 calcd for $C_{10}H_{10}F_3O$ $[M\text{-}OH]^-$ found 203.0697 (3.81 ppm). **JH-VI-77**.

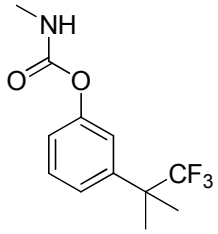

3-(1,1,1-Trifluoro-2-methylpropan-2-yl)phenyl *N*-methylcarbamate[8] **(9av*, *Novel carbamate* [#]*2*)**. White solid (*Method B*); 62%; ^1H NMR (400 MHz, $CDCl_3$) δ 7.37 – 7.31 (m, 2H), 7.26 – 7.22 (m, 1H), 7.12 – 7.08 (m, 1H), 4.99 (br s, 1H), 2.90 (d, *J* = 5.3 Hz, 3H), 1.56 (s, 6H); ^{13}C NMR (101 MHz, $CDCl_3$) δ 155.26 (s), 151.05 (s), 141.58 (s), 129.05 (s), 128.31 (q, $^1J_{CF}$ = 283.0

Hz), 124.46 (s), 121.05 (s), 43.97 (q, $^{2}J_{CF}$ = 26 Hz), 27.85 (s), 22.74 (q, $^{3}J_{CF}$ = 2.4 Hz); HRMS (APCI): 262.1049 calcd for $C_{12}H_{15}NO_2F_3$ $[M+H]^+$ found 262.1056 (2.55 ppm). **JH-VI-87, PRC515**.

Example 18: General procedure for the preparation of Weinreb amides with a BOP amide coupling

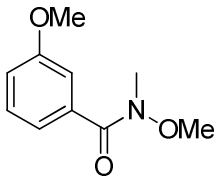

N,3-Dimethoxy-*N*-methylbenzamide **(64aw)**. A 250 mL round-bottom flask was charged with *m*-anisic acid (3.01 g, 19.8 mmol), dichloromethane (150 mL), DIPEA (23 mL, 132 mmol), BOP (10.0 g, 22.6 mmol) and *N*,*O*-dimethylhydroxylamine hydrochloride (1.93 g, 19.8 mmol). The reaction was allowed to stir at room temperature overnight before placing the reaction in a separatory funnel and washing the organic layer with sodium bicarbonate (100 mL) and brine (150 mL). The organic layer was then dried with sodium sulfate, filtered, and concentrated in vacuo. The residue was purified with flash chromatography (2 : 1 hexane : ethyl acetate) to yield a yellow oil (3.86 g, 100%); ^{1}H NMR (400 MHz, $CDCl_3$) δ 7.34 – 7.28 (m, 1H), 7.24 (dt, *J* = 7.6, 1.2 Hz, 1H), 7.21 – 7.18 (m, 1H), 6.99 (ddd, *J* = 7.6, 2.7, 1.2 Hz, 1H), 3.83 (s, 3H), 3.57 (s, 3H), 3.35 (s, 3H); ^{13}C NMR (101 MHz, $CDCl_3$) δ 169.85, 159.31, 135.53, 129.23, 120.48, 116.71, 113.43, 61.23, 55.49, 34.03; HRMS (APCI): 196.0974 calcd for $C_{10}H_{14}NO_3$ $[M+H]^+$ found 196.0721. **JH-VI-111**.

Example 19: General procedure for the preparation of 3-substituted ethyl ketones from Weinreb amides

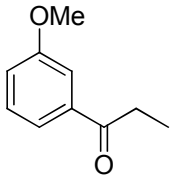

1-(3-Methoxyphenyl)propan-1-one **(54aw)**. A dry 2-neck 500 mL round-bottom flask equipped with an addition funnel and condenser was charged with *N*,3-dimethoxy-*N*-methylbenzamide (**64aw**, 2.62 g, 13.4 mmol) and tetrahydrofuran (55 mL) while purging with nitrogen. Next, 1.0M ethylmagnesium bromide in tetrahydrofuran (33.5 mL, 33.5 mmol) was added dropwise at RT and the reaction was brought to reflux for 2 h resulting in a yellow solution. After cooling to room temperature, the reaction was quenched with 2.0 M hydrochloric acid (60 mL) and allowed to stir for 1 hour. The aqueous layer was extracted with dichloromethane (3 x 100 mL) and the combined organic layers were washed with brine, dried with $MgSO_4$, filtered, and concentrated in vacuo. The residue was purified with flash chromatography (dichloromethane) to afford a tan oil (1.87 g, 85%); ^{1}H NMR (400 MHz, $CDCl_3$) δ 7.53 (ddd, *J* = 7.6, 1.5, 1.0 Hz, 1H), 7.49 (dd, *J* = 2.6, 1.5 Hz, 1H), 7.38 – 7.32 (m, 1H), 7.09 (ddd, *J* = 7.6, 2.6, 1.0 Hz, 1H), 3.85 (s, 3H), 2.98 (q, *J* = 7.2 Hz, 2H), 1.21 (t, *J* = 7.2 Hz, 3H); ^{13}C NMR (101 MHz, $CDCl_3$) δ 200.75, 159.91, 138.41, 129.64, 120.71, 119.37, 112.40, 55.53, 32.02, 8.41; HRMS (APCI): 165.0910 calcd for $C_{10}H_{12}O_2$ $[M+H]^+$ found 165.0917 (4.13 ppm). **JH-VI-131 & 127**.

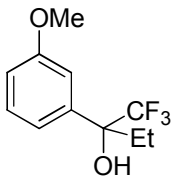

1,1,1-Trifluoro-2-(3-methoxyphenyl)butan-2-ol **(57aw)**. This compound was prepared in 86% from 3-methoxypropiophenone **(54aw)** and trifluoromethyltrimethylsilane according to the

procedure for **57av** in Example 15. Yellow oil; ^{1}H NMR (400 MHz, $CDCl_3$) δ 7.32 (t, *J* = 8.0 Hz, 1H), 7.12 (s, 1H), 7.09 (dd, *J* = 8.0, 0.8 Hz, 1H), 6.90 (dd, *J* = 8.0, 2.6 Hz, 1H), 3.83 (s, 3H), 2.43 (s, 1H), 2.21 (dq, *J* = 15.0, 7.5 Hz, 1H), 2.03 (dq, *J* = 15.0, 7.5 Hz, 1H), 0.81 (t, *J* = 7.5 Hz, 3H); ^{13}C NMR (101 MHz, $CDCl_3$) δ 159.70 (s), 137.97 (s), 129.43 (s), 125.89 (q, $^{1}J_{CF}$ = 286 Hz), 118.77 (s), 113.58 (s), 112.85 (s), 77.73 (d, $^{2}J_{CF}$ = 28 Hz), 55.40 (s), 28.37 (s), 6.67 (s); ^{19}F NMR (376 MHz, $CDCl_3$) δ -80.29 (s); HRMS (APCI): 233.0795 calcd for $C_{11}H_{12}O_2F_3$ $[M-H]^-$ found 233.0791 (1.74 ppm). **JH-VI-159**.

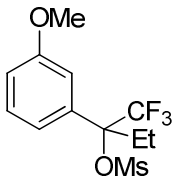

1,1,1-Trifluoro-2-(3-methoxyphenyl)butan-2-yl methanesulfonate **(67aw)**. This compound was prepared from 1,1,1-trifluoro-2-(3-methoxyphenyl)butan-2-ol **(57aw)** and trifluoromethyltrimethylsilane according to the procedure for **67av** in Example 16 in a 50%. Colorless oil; ^{1}H NMR (400 MHz, $CDCl_3$) δ 7.35 (t, *J* = 8.6 Hz, 1H), 7.13 – 7.07 (m, 2H), 6.97 – 6.93 (m, 1H), 3.83 (s, 3H), 3.17 (s, 3H), 2.93 (dq, *J* = 15.2, 7.6 Hz, 1H), 2.45 (dq, *J* = 15.2, 7.6 Hz, 1H), 1.05 (t, *J* = 7.6 Hz, 3H); ^{13}C NMR (101 MHz, $CDCl_3$) δ 159.70 (s), 135.15 (s), 129.65 (s), 123.79 (q, $^{1}J_{CF}$ = 286 Hz), 119.15 (s), 114.30 (s), 113.86 (s), 92.79 (q, $^{2}J_{CF}$ = 29 Hz), 55.49 (s), 41.00 (s), 25.97 (s), 8.13 (s); ^{19}F NMR (376 MHz, $CDCl_3$) δ -75.60 (s); HRMS (APCI): 335.0535 calcd for $C_{12}H_{15}O_4F_3SNa$ $[M+Na]^+$ found 335.0531 (-1.18 ppm). **JH-VI-165**.

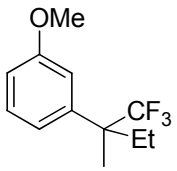

1-Methoxy-3-(1,1,1-trifluoro-2-methylbutan-2-yl)benzene **(47aw)**. This compound was prepared in 84% from 1,1,1-trifluoro-2-(3-methoxyphenyl)butan-2-yl methanesulfonate **(67aw)** and

trimethylaluminum according to the procedure for **47av** in Example 17. Colorless oil; ^{1}H NMR (400 MHz, $CDCl_3$) δ 7.29 (t, *J* = 7.9 Hz, 1H), 7.03 (d, *J* = 7.9 Hz, 1H), 6.99 (s, 1H), 6.85 (dd, *J* = 7.9, 2.5 Hz, 1H), 3.82 (s, 3H), 2.22 (dq, *J* = 15.0, 7.5 Hz, 1H), 1.84 (dq, *J* = 15.0, 7.5 Hz, 1H), 1.53 (s, 3H), 0.75 (t, *J* = 7.5 Hz, 3H); ^{13}C NMR (101 MHz, $CDCl_3$) δ 159.61 (s), 139.50 (s), 129.27 (s), 128.61 (q, $^{1}J_{CF}$ = 284 Hz), 120.68 (s), 115.20 (s), 112.13 (s), 55.41 (s), 47.89 (q, $^{2}J_{CF}$ = 24 Hz), 27.52 (s), 18.20 (s), 7.91 (s); ^{19}F NMR (376 MHz, $CDCl_3$) δ -75.52 (s); **JH-VI-167**.

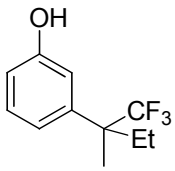

3-(1,1,1-Trifluoro-2-methylbutan-2-yl)phenol **(35aw)**. This compound was prepared in an 86% from 1-methoxy-3-(1,1,1-trifluoro-2-methylbutan-2-yl)benzene **(47aw)** and boron tribromide according to the procedure for **35ap** in Example 11. Yellow oil; ^{1}H NMR (400 MHz, $CDCl_3$) δ 7.23 (t, *J* = 8.0 Hz, 1H), 7.01 (dd, *J* = 8.0, 0.8 Hz, 1H), 6.93 (s, 1H), 6.78 (dd, *J* = 8.0, 2.5 Hz, 1H), 4.88 (s, 1H), 2.20 (dq, *J* = 14.7, 7.5 Hz, 1H), 1.89 – 1.78 (m, 1H), 1.51 (s, 3H), 0.74 (t, *J* = 7.5 Hz, 3H); ^{13}C NMR (101 MHz, $CDCl_3$) δ 155.49 (s), 139.82 (s), 129.45 (s), 128.52 (q, $^{1}J_{CF}$ = 283 Hz), 120.77 (s), 115.55 (s), 114.57 (s), 47.79 (q, $^{2}J_{CF}$ = 24 Hz), 27.45 (s), 18.09 (s), 7.83 (s); ^{19}F NMR (376 MHz, $CDCl_3$) δ -75.51 (s); HRMS (APCI): 217.0846 calcd for $C_{11}H_{12}OF_3$ $[M-H]^-$ found 217.0830 (-7.43 ppm). **JH-VI-169**.

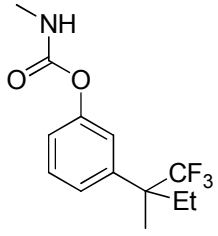

3-(1,1,1-Trifluoro-2-methylbutan-2-yl)phenyl *N*-methylcarbamate[8] **(9aw*, *Novel carbamate #3*)**. White solid (*Method B*); 69%; ^{1}H NMR (400 MHz, $CDCl_3$) δ 7.34 (t, *J* = 8.0 Hz, 1H), 7.30 –

7.23 (m, 1H), 7.18 (s, 1H), 7.14 – 7.06 (m, 1H), 4.99 (br s, 1H), 2.89 (d, *J* = 4.9 Hz, 3H), 2.21 (dq, *J* = 14.8, 7.5 Hz, 1H), 1.93 – 1.76 (m, 1H), 1.52 (s, 3H), 0.75 (t, *J* = 7.5 Hz, 3H); ^{13}C NMR (101 MHz, $CDCl_3$) δ 155.24 (s), 151.16 (s), 139.36 (s), 129.58 (q, $^1J_{CF}$ = ND), 129.04 (s), 120.89 (s), 47.81 (q, $^2J_{CF}$ = 24 Hz), 27.85 (s), 27.42 (s), 18.14 (s), 7.82 (s); ^{19}F NMR (376 MHz, $CDCl_3$) δ -75.55 (s); HRMS (APCI): 276.1206 calcd for $C_{13}H_{17}NO_2F_3$ $[M+H]^+$ found 276.1216 (3.64 ppm). **(JH-VI-171, PRC522)**.

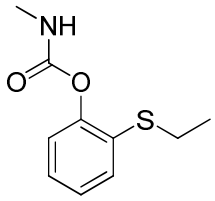

2-(Ethylthio)phenyl *N*-methylcarbamate[12] **(9ax).** White solid (*Method A*), 49%; ^{1}H NMR (400 MHz, $CDCl_3$) δ 7.34 – 7.30 (m, 1H), 7.22 – 7.10 (m, 3H), 5.08 (br s, 1H), 2.91 (d, *J* = 4.9 Hz, 3H), 2.90 (q, *J* = 7.4 Hz, 2H), 1.31 (t, *J* = 7.4 Hz, 3H); ^{13}C NMR (101 MHz, $CDCl_3$) δ 154.80, 149.22, 130.24, 129.40, 126.77, 126.18, 123.08, 27.98, 26.87, 14.27; HRMS (APCI): 211.0667 calcd for $C_{10}H_{13}NO_2S$ $[M]^+$ found 211.0667 (-0.07 ppm). **JH-VI-189**.

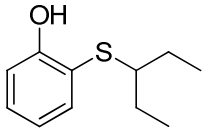

2-(Pentan-3-ylthio)phenol (**35ay**). This compound was prepared in 64% from 2-mercaptophenol and 3-bromopentane according to the procedure for **35v** in Example 6. Yellow oil; ^{1}H NMR (500 MHz, $CDCl_3$) δ 7.43 (dd, *J* = 7.7, 1.7 Hz, 1H), 7.30 – 7.22 (m, 1H), 6.99 (dd, *J* = 7.7, 1.7 Hz, 1H), 6.86 (td, *J* = 7.7, 1.7 Hz, 1H), 6.85 (s, 1H), 2.72 (s-5, *J* = 6.3 Hz, 1H), 1.66 – 1.50 (m, 4H), 1.01 (t, *J* = 7.4 Hz, 6H); ^{13}C NMR (126 MHz, $CDCl_3$) δ 157.55, 136.83, 131.15, 120.62, 118.47, 114.70, 54.80, 26.57, 11.22; **JH-V-45**.

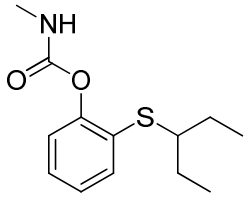

2-(Pentan-3-ylthio)phenyl *N*-methylcarbamate (**9ay***, ***Novel carbamate*** #4). Yellow oil (*Method B*); 93%; ^{1}H NMR (500 MHz, $CDCl_3$) δ 7.41 (dd, *J* = 7.7, 1.5 Hz, 1H), 7.22 (td, *J* = 7.7, 1.5 Hz, 1H), 7.18 – 7.10 (m, 2H), 5.04 (br s, 1H), 3.02 (s-5, *J* = 6.3 Hz, 1H), 2.91 (d, *J* = 4.9 Hz, 3H), 1.68 – 1.53 (m, 4H), 0.99 (t, *J* = 7.4 Hz, 6H); HRMS (APCI): 254.1215 calcd for $C_{13}H_{20}NO_2S$ $[M+H]^+$ found 254.1198 (-4.37 ppm). (**JH-V-51, PRC494**).

Example 20: General procedure for the mono-alkylation of catechol

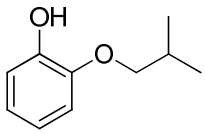

2-Isobutoxyphenol (**35az)**. A dry 50 mL round-bottom flask was charged with catechol (499 mg, 4.53 mmol), *N*,*N*-dimethylformamide (4.5 mL), cesium carbonate (1.50 g, 4.60 mmol), and purged with nitrogen. Next, the contents of the reaction flask were heated to 80 ^{o}C overnight and then cooled to room temperature. The reaction was quenched with 1 M hydrochloric acid (50 mL) and extracted with ethyl acetate (3 x 30 mL). The organic layers were combined, washed with brine, dried with sodium sulfate, and filtered. The solvent was evaporated in vacuo and the residue purified by silica gel chromatography (5 : 1 hexane : ethyl acetate) to yield a yellow oil weighing 316 mg (1.90 mmol, 42%); ^{1}H NMR (500 MHz, $CDCl_3$) δ 6.94 (ddd, *J* = 7.4, 1.5, 0.8 Hz, 1H), 6.88 – 6.82 (m, 3H), 5.65 (s, 1H), 3.81 (d, *J* = 6.6 Hz, 2H), 2.19 – 2.07 (m, 1H), 1.05 (d, *J* = 6.6 Hz, 6H); ^{13}C NMR (126 MHz, CDCl3) δ 146.15, 145.93, 121.43, 120.23, 114.57, 111.75, 75.29, 28.38, 19.40. **JH-IV-111**.

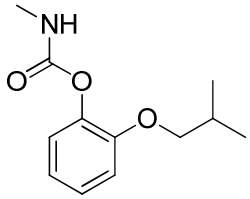

2-Isobutoxyphenyl *N*-methylcarbamate[8] (**9az*, *Novel carbamate #5***). White solid (*Method B*); 90%; ^{1}H NMR (500 MHz, $CDCl_3$): δ 7.14 (t, *J* = 7.4 Hz, 1H), 7.08 (d, *J* = 8.0 Hz, 1H), 6.89 – 6.94 (m, 2H), 5.01 (br s, 1H), 3.75 (d, *J* = 6.9 Hz, 2H), 2.88 (d, *J* = 5.0 Hz, 3H), 2.08 (s-7, *J* = 6.9 Hz, 1H), 1.01 (d, *J* = 6.9 Hz, 6H); ^{13}C NMR (126 MHz, $CDCl_3$): δ 155.22, 151.47, 140.52, 126.47, 123.24, 120.65, 113.53, 75.02, 28.47, 27.92, 19.23; HRMS (FAB): 224.12867 calcd for $C_{12}H_{18}NO_3$ $[M+H]^+$ found 224.12885 (0.6 ppm, 0.1 mmu). **(JH-IV-117, PRC431)**.

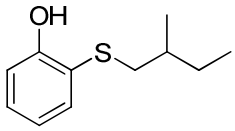

2-(2-Methylbutylthio)phenol (**35ba**). This compound was prepared in 100% from 2-mercaptophenol and 1-chloro-2-methylbutane according to the procedure for **35v** in Example 6. Colorless oil; ^{1}H NMR (500 MHz, $CDCl_3$): δ 7.45 (dd, *J* = 7.7, 1.7 Hz, 1H), 7.24 (dt, *J* = 7.7, 1.7 Hz, 1H), 6.98 (dd, *J* = 7.7, 1.1 Hz, 1H), 6.86 (dt, *J* = 4.9, 1.1 Hz, 1H), 6.75 (d, *J* = 1.1 Hz), 2.70 (dd, *J* = 12.4, 5.8, 1H), 2.55 (dd, *J* = 12.4, 5.8 Hz, 1H), 1.46 – 1.58 (m, 2H), 1.18 – 1.27 (m, 1H), 1.00 (d, *J* = 6.6 Hz, 3H), 0.86 (t, *J* = 4.9 Hz, 3H); ^{13}C NMR (126 MHz, $CDCl_3$): δ 156.80, 135.80, 130.89, 120.81, 119.98, 114.77, 44.36, 34.80, 28.56, 18.74, 11.26; HRMS (FAB): 196.09219 calcd for $C_{11}H_{16}OS$ $[M]^+$ found 196.09293 (3.6 ppm, 0.7 mmu). **JH-V-103**.

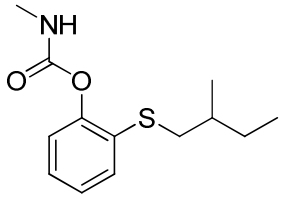

2-(2-Methylbutylthio)phenyl *N*-methylcarbamate[8] **(9ba*, *Novel carbamate #6*)**. Pale oil (*Method B*); 88%; ^{1}H NMR (500 MHz, $CDCl_3$) δ 7.34 – 7.31 (m, 1H), 7.20 – 7.14 (m, 2H), 7.13 – 7.09 (m, 1H), 5.09 (br s, 1H), 2.91 (d, *J* = 4.9 Hz, 3H), 2.90 – 2.86 (m, 1H), 2.70 (dd, *J* = 12.3, 7.5 Hz, 1H), 1.70 – 1.60 (m, 1H), 1.58 – 1.49 (m, 1H), 1.31 – 1.21 (m, 1H), 1.02 (d, *J* = 6.7 Hz, 3H), 0.90 (t, *J* = 7.4 Hz, 3H); ^{13}C NMR (126 MHz, $CDCl_3$) δ 154.83, 149.28, 130.96, 129.46, 126.62, 126.17, 123.05, 40.05, 34.54, 28.95, 27.97, 19.07, 11.36; HRMS (FAB): 254.12148 calcd for $C_{13}H_{20}NO_2S$ $[M+H]^+$ found 254.12044 (-4.2 ppm, -1.1 mmu). **(JH-III-187, PRC407)**.

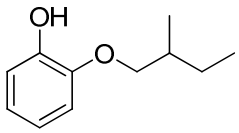

2-(2-Methylbutoxy)phenol **(35bb)**. This compound was prepared in 34% from catechol and 1-chloro-2-methylbutane according to the procedure for **35az** in Example 20. Colorless Oil; ^{1}H NMR (500 MHz, $CDCl_3$) δ 6.96 – 6.92 (m, 1H), 6.89 – 6.81 (m, 3H), 3.91 (dd, *J* = 9.1, 5.9 Hz, 1H), 3.83 (dd, *J* = 9.1, 5.9 Hz, 1H), 1.92 (s-8, *J* = 5.9 Hz, 1H), 1.63 – 1.52 (m, 1H), 1.35 – 1.25 (m, 1H), 1.04 (d, *J* = 5.9 Hz, 3H), 0.97 (t, *J* = 7.5 Hz, 3H); ^{13}C NMR (126 MHz, $CDCl_3$) δ 146.20, 145.94, 121.40, 120.22, 114.54, 111.70, 73.74, 34.81, 26.29, 16.71, 11.44; HRMS (FAB): 180.11503 calcd for $C_{11}H_{16}O_2$ $[M]^+$ found 180.11354 (-8.5 ppm, -1.5 mmu). **JH-IV-145**.

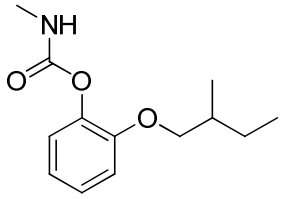

2-(2-Methylbutoxy)phenyl *N*-methylcarbamate **(9bb*, *Novel carbamate #7*)**. White solid (*Method B*); 86%; ^{1}H NMR (500 MHz, $CDCl_3$) δ 7.14 (td, *J* = 8.1, 1.6 Hz, 1H), 7.08 (dd, *J* = 8.1, 1.6 Hz, 1H), 6.93 (dd, *J* = 8.1, 1.6 Hz, 1H), 6.90 (td, *J* = 7.8, 1.3 Hz, 1H), 4.99 (br s, 1H), 3.85 (dd, *J* = 8.8, 6.5 Hz, 1H), 3.76 (dd, *J* = 8.8, 6.5 Hz, 1H), 2.88 (d, *J* = 4.9 Hz, 3H), 1.85 (s-8, *J* = 6.5 Hz, 1H), 1.58 – 1.49 (m, 1H), 1.31 – 1.20 (m, 1H), 1.00 (d, *J* = 6.5 Hz, 3H), 0.94 (t, *J* = 7.5 Hz, 3H); ^{13}C NMR (126 MHz, $CDCl_3$) δ 155.21, 151.50, 140.53, 126.47, 123.23, 120.61, 113.45, 73.45, 34.92, 27.91, 26.17, 16.55, 11.50; HRMS (FAB): 238.1443 calcd for $C_{13}H_{19}NO_3$ $[M]^+$ found 238.1440 (-1.3 ppm, -0.3 mmu). **(JH-IV-147, PRC434)**.

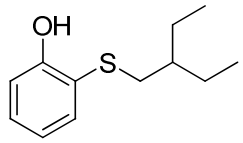

2-(2-Ethylbutylthio)phenol **(35bc).** This compound was prepared in 100% from 2-mercaptophenol and 1-chloro-2-methylbutane according to the procedure for **35v** in Example 6. Yellow oil; ^{1}H NMR (500 MHz, $CDCl_3$): δ 7.46 (dd, *J* = 7.7, 1.7 Hz, 1H), 7.24 (dt, *J* = 7.7, 1.7 Hz, 1H), 6.97 (dd; *J* = 7.7, 1.4 Hz, 1H), 6.86 (dt, *J* = 7.7, 1.4, 1H), 6.74 (s, 1H), 2.69 (d, *J* = 6.7 Hz, 2H), 1.38 – 1.48 (m, 5H), 0.84 (t, *J* = 4.8 Hz, 6H); ^{13}C NMR (126 MHz, $CDCl_3$): δ 156.79, 135.75, 130.84, 120.82, 120.06, 114.74, 41.32, 40.78, 24.92, 10.79; HRMS (FAB): 210. 10784 calcd for $C_{12}H_{18}OS$ $[M]^+$ found 210.10693 (-4.4 ppm, -0.9 mmu). **JH-VI-55**.

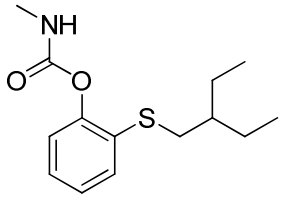

2-(2-Ethylbutylthio)phenyl *N*-methylcarbamate[8] **(9bc*, *Novel carbamate #8*)**. Colorless oil (*Method B*); 83%; ^{1}H NMR (400 MHz, $CDCl_3$) δ 7.37 – 7.30 (m, 1H), 7.22 – 7.14 (m, 2H), 7.15 – 7.08 (m, 1H), 5.04 (br s, 1H), 2.92 (d, *J* = 4.9 Hz, 3H), 2.85 (d, *J* = 5.9 Hz, 2H), 1.56 – 1.37 (m, 5H), 0.88 (t, *J* = 7.3 Hz, 6H); ^{13}C NMR (101 MHz, $CDCl_3$) δ 154.81, 149.28, 131.06, 129.46, 126.58, 126.15, 123.01, 40.37, 36.95, 27.96, 25.23, 10.87; HRMS (FAB): 268.13713 calcd for $C_{14}H_{21}NO_2S$ $[M+H]^+$ found 268.1370 (-0.5 ppm, -0.1 mmu). **(JH-VI-57, PRC408)**.

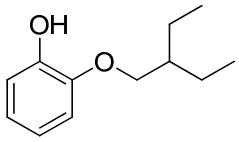

2-(2-Ethylbutoxy)phenol **(34bd*)**. This compound was prepared in 39% from catechol and 1-chloro-2-methylbutane according to the procedure for **35az** in Example 20. Colorless oil; ^{1}H NMR (500 MHz, $CDCl_3$) δ 6.95 – 6.92 (m, 1H), 6.90 – 6.82 (m, 3H), 5.62 (s, 1H), 3.94 (d, *J* = 5.7 Hz, 2H), 1.71 (s-7, *J* = 5.7 Hz, 1H), 1.52 – 1.45 (m, 4H), 0.95 (t, *J* = 7.5 Hz, 6H); ^{13}C NMR (126 MHz, $CDCl_3$): δ 146.26, 145.96, 121.38, 120.23, 114.52, 111.64, 70.99, 41.03, 23.59, 11.29; HRMS (FAB): 194.13068 calcd for $C_{12}H_{18}O_2$ $[M]^+$ found 194.13071 (0.1 ppm, 0.0 mmu). **JH-IV-155, JH-V-129, JH-V-37**.

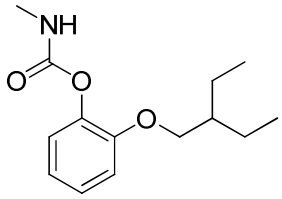

2-(2-Ethylbutoxy)phenyl *N*-methylcarbamate **(9bd*, *Novel carbamate #9*)**. White solid (*Method B*); 83%; ^{1}H NMR (500 MHz, $CDCl_3$) δ 7.15 (t, *J* = 7.8 Hz, 1H), 7.08 (d, *J* = 7.8 Hz, 1H), 6.95

(d, *J* = 7.8 Hz, 1H), 6.90 (t, *J* = 7.8 Hz, 1H), 4.97 (br s, 1H), 3.88 (d, *J* = 5.7 Hz, 2H), 2.88 (d, *J* = 5.7 Hz, 3H), 1.65 (s-7, *J* = 5.7 Hz, 1H), 1.53 – 1.38 (m, 4H), 0.92 (t, *J* = 7.5 Hz, 6H); ^{13}C NMR (126 MHz, $CDCl_3$): δ 155.13, 151.52, 140.51, 126.43, 123.17, 120.51, 113.32, 70.68, 41.11, 27.84, 23.46, 11.29; HRMS (FAB): 252.15997 calcd for $C_{14}H_{21}NO_3$ $[M+H]^+$ found 252.1601 (0.5 ppm, 0.1 mmu). **(JH-IV-53, PRC421)**.

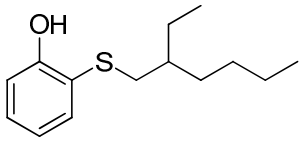

2-((2-Ethylhexyl)thio)phenol (**35be**). This compound was prepared in 95% from 2-mercaptophenol and 1-bromo-2-ethylhexane according to the procedure for **35v** in Example 6. Yellow oil; ^{1}H NMR (400 MHz, $CDCl_3$) δ 7.46 (dd, *J* = 7.7, 1.6 Hz, 1H), 7.24 (dt, *J* = 7.7, 1.6 Hz, 1H), 6.98 (dd, *J* = 7.7, 1.6 Hz, 1H), 6.86 (td, *J* = 7.7, 1.6 Hz, 1H), 6.74 (s, 1H), 2.70 (d, *J* = 5.8 Hz, 2H), 1.53 – 1.15 (m, 9H), 0.88 (t, *J* = 7.1 Hz, 3H), 0.85 (t, *J* = 7.1 Hz, 3H); ^{13}C NMR (101 MHz, $CDCl_3$) δ 156.83, 135.78, 130.88, 120.87, 120.17, 114.79, 41.78, 39.42, 32.23, 28.82, 25.48, 23.05, 14.21, 10.83; HRMS (FAB): 239.1470 calcd for $C_{14}H_{23}OS$ $[M+H]^+$ found 239. 1464 (0.06 ppm). **JH-VI-183**.

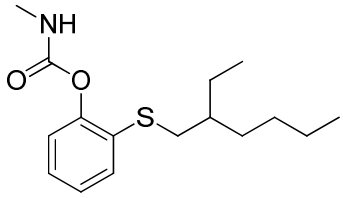

2-((2-Ethylhexyl)thio)phenyl *N*-methylcarbamate **(9be*, *Novel carbamate #10*)**. Pale yellow oil (*Method A*); 60%; ^{1}H NMR (400 MHz, $CDCl_3$) δ 7.40 – 7.30 (m, 1H), 7.21 – 7.09 (m, 3H), 5.06 (br s, 1H), 2.91 (d, *J* = 4.9 Hz, 3H), 2.84 (d, *J* = 6.3 Hz, 2H), 1.61 – 1.33 (m, 5H), 1.33 – 1.23 (m, 4H), 0.90 (d, *J* = 6.8 Hz, 3H), 0.88 (t, *J* = 7.4 Hz, 3H); ^{13}C NMR (101 MHz, $CDCl_3$) δ 154.83, 149.31, 131.11, 129.55, 126.61, 126.16, 123.02, 38.97, 37.44, 32.54, 28.86, 27.98, 25.71,

23.11, 14.23, 10.85; HRMS (FAB): 295.1606 calcd for $C_{16}H_{25}NO_2S$ $[M]^+$ found 239.1622 (5.26 ppm). (**JH-VI-191, PRC531**).

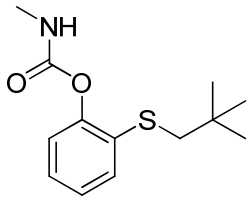

2-(Neopentylthio)phenyl *N*-methylcarbamate[8] **(9bf*, *Novel carbamate #11*)**. Yellow Oil (*Method B*); 94%; ^{1}H NMR (500 MHz, $CDCl_3$) δ 7.36 (dd, *J* = 7.3, 2.1 Hz, 1H), 7.20 – 7.13 (m, 2H), 7.12 – 7.09 (m, 1H), 5.10 (s, 1H), 2.91 (d, *J* = 4.9 Hz, 3H), 2.83 (s, 2H), 1.04 (s, 9H); ^{13}C NMR (126 MHz, $CDCl_3$) δ 149.39, 131.60, 129.95, 126.68, 126.16, 123.02, 47.92, 29.16, 27.96; HRMS (FAB): 254.1215 calcd for $C_{13}H_{20}NO_2S$ $[M+H]^+$ found 254.1218 (1.3 ppm, 0.3 mmu). (**JH-III-191, PRC409)**.

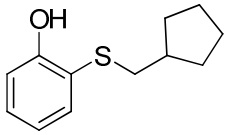

2-(Cyclopentylmethylthio)phenol **(35bg)**. This compound was prepared in 83% from 2-mercaptophenol and cyclopentylmethyl tosylate according to the procedure for **35v** in Example 6. Colorless oil; ^{1}H NMR (500 MHz, $CDCl_3$) δ 7.47 (dd, *J* = 7.7, 1.7 Hz, 1H), 7.28 – 7.22 (m, 1H), 6.98 (dd, *J* = 7.7, 1.7 Hz, 1H), 6.87 (td, *J* = 7.7, 1.7 Hz, 1H), 6.78 (s, 1H), 2.70 (d, *J* = 7.5 Hz, 2H), 2.00 (s-7, *J* = 7.5 Hz, 1H), 1.88 – 1.76 (m, 2H), 1.66 – 1.48 (m, 4H), 1.29 – 1.18 (m, 2H); ^{13}C NMR (126 MHz, $CDCl_3$) δ 156.94, 135.94, 130.98, 120.83, 119.68, 114.78, 114.77, 43.38, 39.75, 32.36, 25.42; HRMS (FAB): 208.09219 calcd for $C_{12}H_{16}OS$ $[M]^+$ found 208.09134 (-4.3 ppm, -0.9 mmu). **JH-IV-93**.

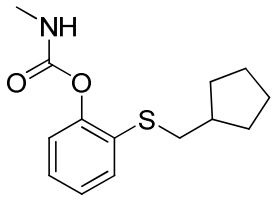

2-(Cyclopentylmethylthio)phenyl *N*-methylcarbamate[8] **(9bg*, *Novel carbamate #12*)**. White solid (*Method B*); 78%; ^{1}H NMR (500 MHz, $CDCl_3$) δ 7.38 – 7.31 (m, 1H), 7.23 – 7.13 (m, 2H), 7.13 – 7.09 (m, 1H), 5.09 (br s, 1H), 2.90 (d, *J* = 4.9 Hz, 3H), 2.87 (d, *J* = 7.6 Hz, 2H), 2.10 (s-7, *J* = 7.6 Hz, 1H), 1.89 – 1.80 (m, 2H), 1.69 – 1.49 (m, 4H), 1.33 – 1.23 (m, 2H); ^{13}C NMR (126 MHz, $CDCl_3$) δ 154.82, 149.21, 130.89, 129.45, 126.61, 126.14, 123.03, 39.38, 39.15, 32.56, 27.96, 25.33; HRMS (FAB): 265.1136 calcd for $C_{14}H_{19}NO_2S$ $[M]^+$ found 265.1124 (-4.7 ppm, -1.3 mmu). **(JH-IV-91**, **PRC429)**.

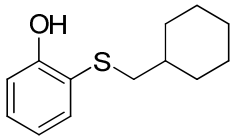

2-(Cyclohexylmethylthio)phenol **(35bh)**. This compound was prepared in 87% from 2-mercaptophenol and cyclohexylmethyl bromide according to the procedure for **35v** in Example 6. Colorless oil; ^{1}H NMR (500 MHz, $CDCl_3$) δ 7.45 (dd, *J* = 7.7, 1.7 Hz, 1H), 7.26 – 7.22 (m, 1H), 6.97 (dd, *J* = 7.7, 1.7 Hz, 1H), 6.86 (td, *J* = 7.7, 1.7 Hz, 1H), 6.74 (s, 1H), 2.59 (d, *J* = 6.9 Hz, 2H), 1.89 – 1.82 (m, 2H), 1.75 – 1.67 (m, 2H), 1.67 – 1.61 (m, 1H), 1.48 – 1.38 (m, 1H), 1.28 – 1.08 (m, 3H), 0.99 – 0.91 (m, 2H); ^{13}C NMR (126 MHz, $CDCl_3$) δ 156.87, 135.86, 130.92, 120.85, 120.20, 114.83, 44.71, 37.86, 32.69, 26.44, 26.08; HRMS (FAB): 222.1078 calcd for $C_{13}H_{18}OS$ $[M]^+$ found 222.1064 (-6.5 ppm, -1.4 mmu). **JH-IV-71**.

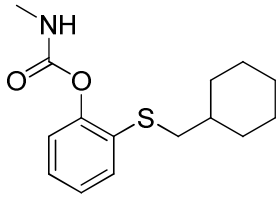

2-(Cyclohexylmethylthio)phenyl *N*-methylcarbamate[8] **(9bh*, *Novel carbamate #13*)**. Off-white solid (*Method B*); 57%; ^{1}H NMR (500 MHz, $CDCl_3$) δ 7.32 – 7.29 (m, 1H), 7.19 – 7.14 (m, 2H), 7.13 – 7.10 (m, 1H), 5.06 (br s, 1H), 2.91 (d, *J* = 4.9 Hz, 3H), 2.76 (d, *J* = 6.8 Hz, 2H), 1.89 (d, *J* = 13.2 Hz, 2H), 1.75 – 1.68 (m, 2H), 1.68 – 1.61 (m, 1H), 1.58 – 1.48 (m, 1H), 1.29 – 1.10 (m, 3H), 1.02 – 0.94 (m, 2H); ^{13}C NMR (126 MHz, $CDCl_3$) δ 154.81, 149.23, 131.10, 129.34, 126.53, 126.17, 123.04, 40.32, 37.55, 33.00, 27.97, 26.47, 26.15; HRMS (FAB): 279.1293 calcd for $C_{15}H_{21}NO_2S$ $[M]^+$ found 279.1289 (-1.4 ppm, -0.4 mmu). **(JH-IV-77, PRC427)**.

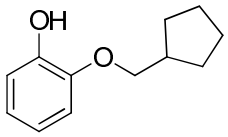

2-(Cyclopentylmethoxy)phenol **(35bi)**. This compound was prepared in 44% from catechol and cyclopentylmethyl tosylate according to the general procedure for **35az** in Example 20. Yellow oil; ^{1}H NMR (500 MHz, CDCl3) δ 6.96 – 6.92 (m, 1H), 6.86 (t, *J* = 22.1 Hz, 3H), 5.66 (s, 1H), 3.91 (d, *J* = 7.0 Hz, 2H), 2.40 (s-7, *J* = 7.5 Hz, 1H), 1.92 – 1.77 (m, 2H), 1.71 – 1.57 (m, 4H), 1.43 – 1.26 (m, 2H); ^{13}C NMR (126 MHz, $CDCl_3$): δ 146.16, 145.90, 121.40, 120.16, 114.49, 111.78, 73.20, 25.53, 39.11, 29.54; **JH-IV-95**.

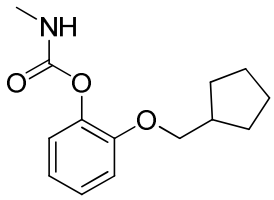

2-(Cyclopentylmethoxy)phenyl *N*-methylcarbamate[8] **(9bi*, *Novel carbamate #14*)**. White solid (*Method B*); 85%; ^{1}H NMR (500 MHz, $CDCl_3$) δ 7.14 (td, *J* = 7.9, 1.5 Hz, 1H), 7.07 (dd, *J* = 7.9,

1.5 Hz, 1H), 6.94 (dd, *J* = 7.9, 1.5 Hz, 1H), 6.90 (t, *J* = 7.9 Hz, 1H), 5.01 (br s, 1H), 3.86 (d, *J* = 6.8 Hz, 2H), 2.89 (d, *J* = 4.9 Hz, 3H), 2.35 (s-7, *J* = 7.4 Hz, 1H), 1.88 – 1.72 (m, 2H), 1.72 – 1.48 (m, 4H), 1.42 – 1.34 (m, 2H); ^{13}C NMR (126 MHz, $CDCl_3$) δ 155.20, 151.54, 140.54, 126.47, 123.23, 120.67, 113.64, 72.87, 39.17, 29.38, 27.93, 25.70; HRMS (FAB): 250.1443 calcd for $C_{14}H_{20}NO_3$ $[M+H]^+$ found 250.1425 (-7.3 ppm, -1.8 mmu). **(JH-IV-103, PRC430)**.

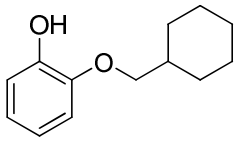

2-(Cyclohexylmethoxy)phenol **(35bj)**. This compound was prepared in 31% from catechol and cyclohexylmethyl tosylate according to the general procedure for **35az** in Example 20. Off-white solid weighing; ^{1}H NMR (500 MHz, $CDCl_3$) δ 6.93 (ddd, *J* = 7.2, 1.6, 1.0 Hz, 1H), 6.88 – 6.81 (m, 3H), 5.64 (s, 1H), 3.84 (d, *J* = 6.1 Hz, 2H), 1.91 – 1.67 (m, 6H), 1.37 – 1.12 (m, 3H), 1.12 – 1.01 (m, 2H); ^{13}C NMR (126 MHz, $CDCl_3$) δ 146.00, 139.05, 121.39, 120.21, 114.55, 111.78, 74.40, 37.80, 30.05, 26.59, 25.88; HRMS (FAB): 206.1307 calcd for $C_{13}H_{18}O_2$ $[M]^+$ found 206.1295 (-5.7 ppm, -1.2 mmu). **(JH-IV-79)**.

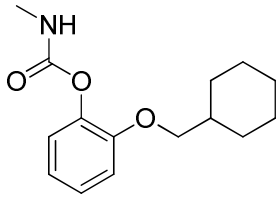

2-(Cyclohexylmethoxy)phenyl *N*-methylcarbamate[8] **(9bj*, *Novel carbamate #15*)**. White solid (*Method B*); 45%; ^{1}H NMR (500 MHz, $CDCl_3$) δ 7.14 (td, *J* = 8.2, 1.5 Hz, 1H), 7.07 (dd, *J* = 8.2, 1.5 Hz, 1H), 6.95 – 6.88 (m, 2H), 4.99 (br s, 1H), 3.78 (d, *J* = 6.2 Hz, 2H), 2.90 – 2.89 (d, *J* = 4.9 Hz, 3H), 1.88 – 1.65 (m, 6H), 1.35 – 1.13 (m, 3H), 1.10 – 1.03 (m, 2H); ^{13}C NMR (126 MHz, $CDCl_3$) δ 155.20, 151.52, 140.58, 126.45, 123.20, 120.62, 113.59, 37.89, 29.83, 27.91, 26.69,

25.99; HRMS (FAB): 264.1600 calcd for $C_{15}H_{22}NO_3$ $[M+H]^+$ found 264.1581 (-7.0 ppm, -1.9 mmu). **(JH-IV-81, PRC428)**.

Example 21: General procedure for the mono-oxidation of thioethers to sulfoxides

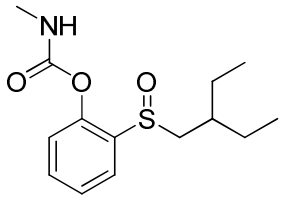

2-(2-Ethylbutylsulfinyl)phenyl *N*-methylcarbamate[8] **(9bk*, *Novel carbamate #16*)**. A dry 25 mL round-bottom flask was charged with 2-((2-ethylbutyl)thio)phenyl *N*-methylcarbamate (**29**, 72 mg, 0.269 mmol) and dichloromethane (10 mL). The solution was cooled to 0 °C before the addition of *m*-chloroperbenzoic acid (77 wt%, 67 mg, 0.299 mmol) in one portion. The solution was allowed to warm to room temperature and stir for 18 h. Upon completion, the reaction was diluted in dichloromethane (25 mL) and washed with 10% sodium bicarbonate (2 x 10 mL). The organic layer was concentrated and purified by silica gel chromatography (3 : 1 ethyl acetate : hexane) to afford a colorless oil weighing 53 mg (70%). ^{1}H NMR (500 MHz, $CDCl_3$) δ 7.90 (dd, *J* = 7.6, 1.8 Hz, 1H), 7.48 – 7.44 (m, 2H), 7.17 (dd, *J* = 7.6, 1.8 Hz, 1H), 5.38 (br s, 1H), 2.89 (d, *J* = 4.9 Hz, 3H), 2.75 (dd, *J* = 6.8, 5.7 Hz, 2H), 2.01 – 1.92 (m, 1H), 1.72 – 1.63 (m, 1H), 1.57 – 1.43 (m, 2H), 1.42 – 1.31 (m, 1H), 0.91 (t, *J* = 7.4 Hz, 3H), 0.86 (t, *J* = 7.4 Hz, 3H); ^{13}C NMR (126 MHz, $CDCl_3$) δ 154.12, 146.77, 137.33, 131.85, 126.70, 125.10, 122.73, 61.71, 35.96, 27.97, 25.71, 24.64, 10.79, 10.08; HRMS (FAB): 284.1320 calcd for $C_{14}H_{22}NO_3S$ $[M+H]^+$ found 284.1320 (-0.2 ppm, -0.1 mmu). **(JH-IV-49, PRC420)**.

Example 22: General procedure for addition of the Grignard reagent to carbon dioxide

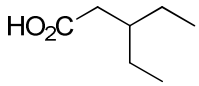

3-Ethylpentanoic acid (**119**). A dry 100 mL Schlenk flask was charged with pulverized magnesium turnings (1.24 g, 50.6 mmol), dry tetrahydrofuran (5 mL), and then flushed with nitrogen. Next, a solution of 1-bromo-2-ethylbutane in tetrahydrofuran (7.59 g in 20 mL) was partially added (5 mL) to the magnesium slurry. Over the course of three h the remaining alkyl halide was cautiously added and allowed to stir overnight. The resulting green slurry was cooled to 0 ^{o}C and diluted with tetrahydrofuran (10 mL). Subliming dry-ice (20 g) was allowed to percolate through the Grignard solution for 4 h and then stir overnight. The reaction was once again cooled to 0 ^{o}C and quenched with 1 M hydrochloric acid (100 mL) and extracted with diethyl ether (3 x 100 mL). The organic layers were washed with 1 Msodium hydroxide (3 x 100 mL). The combined aqueous layers were acidified with concentrated hydrochloric acid and extracted with diethyl ether (4 x 100 mL). The combined organic layers were washed with brine and dried with sodium sulfate. The filtrate was evaporated to dryness to afford a yellow oil (3.2 g, 54%); ^{1}H NMR (500 MHz, $CDCl_3$) δ 2.28 (d, *J* = 7.0 Hz, 2H), 1.75 (s-7, *J* = 7.0 Hz, 1H), 1.46 – 1.28 (m, 4H), 0.88 (t, *J* = 7.0 Hz, 6H); ^{13}C NMR (126 MHz, $CDCl_3$) δ 180.11, 38.30, 37.87, 25.90, 10.92. **JH-VIII-47**.

Example 23: Preparation of the Weinreb amides with the addition of the Weinreb amine to the acid chloride

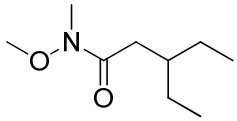

3-Ethyl-N-methoxy-N-methylpentanamide (**109**). A 100 mL round bottomed flask was charged with 3-ethylpentanoic acid (**119**; 2.88 g, 21.7 mmol) and dissolved in dichloromethane (45 mL)

before cooling the solution down to 0 ^{o}C. Next, 2 drops of dimethylformamide were added followed by the cautious addition of oxalyl chloride (2.46 mL, 28.2 mmol) which caused the evolution of carbon dioxide. After 4 h the evolution of gas had subsided and a yellow solution resulted. Next, *O,N*-dimethylhydroxylamine hydrochloride (3.18 g, 32.6 mmol) was added followed by the cautious addition of triethylamine (9.1 mL, 65.1 mmol). After stirring at room temperature for an additional 30 min, the reaction was quenched with 0.25M hydrochloric acid (200 mL) and extrated with dichloromethane (3 x 100 mL). The organic layers were combined, washed with brine, and dried with sodium sulfate. The solution was filtered and the solvent evaporated. The residue was purified with flash chromatography (1:1 hexane:ethyl acetate) to yield a pale yellow oil (2.77 g, 74%); ^{1}H NMR (500 MHz, $CDCl_3$) δ 3.68 (s, 3H), 3.18 (s, 3H), 2.33 (d, *J* = 6.5 Hz, 1H), 1.83 (s-7, *J* = 6.5 Hz, 1H), 1.41 – 1.29 (m, 4H), 0.87 (t, *J* = 7.4 Hz, 6H); **JH-VIII-55**.

Example 24: General procedure for the preparation C2-aryl ketones through the Weinreb amide

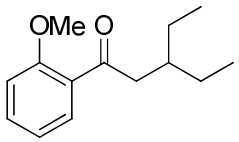

3-Ethyl-1-(2-methoxyphenyl)pentan-1-one (**45ch**). A dry 50 mL Schlenk flask purged with nitrogen was charged with 2-iodoanisole (1.78 g. 7.63 mmol) and dry tetrahydrofuran (8 mL) prior to cooling to -78 ^{o}C in a dry-ice acetone bath. A solution of 2.0 M *iso*propylmagnesium chloride in tetrahydrofuran (4.2 mL) was cautiously added over 10 min. To this mixture a solution of 3-ethyl-N-methoxy-N-methylpentanamide (**109**; 1.47 g, 8.49 mmol) in dry tetrahydrofuran (8 mL) was cautiously added over 10 min. The reaction was allowed to stir for 5 h at -78 ^{o}C and overnight at room temperature. Next, the reaction was cooled to 0 ^{o}C and cautiously quenched with 3 M hydrochloric acid (100 mL). The aqueous layer was extracted

with diethyl ether (3 x 50 mL) and the combined organic layers were washed with brine and dried with sodium sulfate. The solution was filtered and then evaporated prior to purifying the residue with flash chromatography (1 : 1 hexane : dichloromethane). Evaporation of the solvent in vacuo yielded a colorless oil weighing 1.37 g (6.22 mmol, 81%); ^{1}H NMR (400 MHz, $CDCl_3$) δ 7.59 (dd, *J* = 7.6, 1.8 Hz, 1H), 7.43 (dd, *J* = 7.6, 1.8 Hz, 1H), 6.99 (td, *J* = 7.6, 1.8 Hz, 1H), 6.94 (d, *J* = 7.6 Hz, 1H), 3.89 (s, 3H), 2.88 (d, *J* = 6.8 Hz, 2H), 1.88 (s-7, *J* = 4.0 Hz, 1H), 1.43 – 1.22 (m, 4H), 0.85 (t, *J* = 7.4 Hz, 6H); HRMS (ESI): 221.1542 calcd for $C_{14}H_{21}O_2$ $[M+H]^+$ found 221.1526 (-7.15 ppm). **JH-VIII-71**.

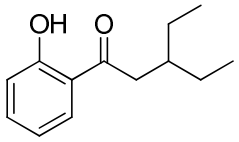

3-Ethyl-1-(2-hydroxyphenyl)pentan-1-one (**35ch**). This compound was prepared in 90% from 3-ethyl-1-(2-methoxyphenyl)pentan-1-one (**45ch**) and boron tribromide according to the procedure for **35ap** in Example 11. Yellow oil; ^{1}H NMR (400 MHz, $CDCl_3$) δ 12.49 (s, 1H), 7.78 (dd, *J* = 8.0, 1.6 Hz, 1H), 7.46 (ddd, *J* = 8.0, 7.3, 1.6 Hz, 1H), 6.98 (dd, *J* = 8.0, 0.9 Hz, 1H), 6.89 (ddd, *J* = 8.0, 7.3, 0.9 Hz, 1H), 2.89 (d, *J* = 6.8 Hz, 2H), 2.04 – 1.92 (m, 1H), 1.50 – 1.28 (m, 4H), 0.91 (t, *J* = 7.4 Hz, 6H); ^{13}C NMR (101 MHz, $CDCl_3$) δ 207.41, 162.76, 136.33, 130.24, 119.86, 118.92, 118.72, 42.45, 37.76, 26.07, 11.03. HRMS (ESI): 207.1380 calcd for $C_{13}H_{19}O_2$ $[M+H]^+$ found 207.1362 (-8.54 ppm). **JH-VIII-73 & VIII-77**.

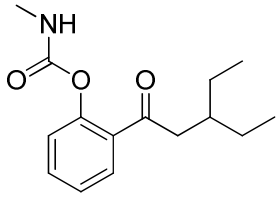

2-(3-Ethylpentanoyl)phenyl methylcarbamate (**9ch-1*, *Novel carbamate #17***). Yellow oil (*Method B*); 17%; ^{1}H NMR (400 MHz, $CDCl_3$) δ 7.65 (dd, *J* = 8.0, 1.6 Hz, 1H), 7.46 (td, *J* = 8.0,

1.6 Hz, 1H), 7.31 – 7.21 (m, 1H), 7.15 (d, *J* = 8.0 Hz, 1H), 5.19 (br s, 1H), 2.87 (d, *J* = 4.9 Hz, 3H), 2.78 (d, *J* = 6.7 Hz, 2H), 1.98 – 1.85 (m, 1H), 1.44 – 1.21 (m, 4H), 0.85 (t, *J* = 7.4 Hz, 6H). HRMS (ESI): 264.1594 calcd for $C_{15}H_{22}NO_3$ $[M+H]^+$ found 264.1583 (-4.38 ppm). **JH-VIII-85-III**.

Example 25: General procedure for the reduction of aryl ketones with sodium borohydride

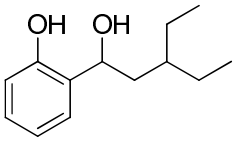

(±)-2-(3-Ethyl-1-hydroxypentyl)phenol (**35bl** intermediate). A 50 mL round-bottom flask was charged with 3-ethyl-1-(2-hydroxyphenyl)pentan-1-one (**35ch**; 314 mg, 1.52 mmol), methanol (15 mL), 2 M sodium hydroxide (1.5 mL), and portion-wise addition of sodium borohydride (190 mg, 5.03 mmol). This was allowed to stir at room temperature overnight prior to evaporating the solvent and diluting in 1 M hydrochloric acid (50 mL). The aqueous layer was extracted with diethyl ether (3 x 30 mL) and the organic layers were combined, washed with brine, dried with sodium sulfate, and filtered. The solvent was evaporated and the residue was purified with flash chromatography (dichloromethane) to yield a yellow oil weighing 292 mg (1.40 mmol, 92%); ^{1}H NMR (500 MHz, $CDCl_3$) δ 7.91 (s, 1H), 7.21 – 7.11 (m, 1H), 6.95 (dd, *J* = 7.5, 1.7 Hz, 1H), 6.87 (d, *J* = 7.5 Hz, 1H), 6.83 (td, *J* = 7.5, 1.7 Hz, 1H), 4.92 (dt, *J* = 8.8, 4.3 Hz, 1H), 2.48 (s, 1H), 1.95 – 1.86 (m, 1H), 1.64 (ddd, *J* = 14.2, 7.0, 5.3 Hz, 1H), 1.47 – 1.28 (m, 5H), 0.88 (t, *J* = 7.2 Hz, 3H), 0.84 (t, *J* = 7.2 Hz, 3H); ^{13}C NMR (126 MHz, $CDCl_3$) δ 155.75, 129.00, 128.07, 127.09, 119.86, 117.38, 74.55, 40.65, 36.75, 25.83, 24.89, 10.89, 10.43; **JH-VIII-75 & VIII-87**.

Example 26: General procedure for the hydrdogenolysis of secondary benzylic alcohols with palladium on carbon and hydrogen

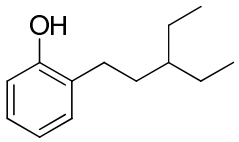

2-(3-Ethyl-1-hydroxypentyl)phenol (**35bl**). A 50 mL Schlenk flask was charged with 2-(3-ethyl-1-hydroxypentyl)phenol (**35bl** intermediate, 248 mg, 1.19 mmol), methanol (12 mL), 10% palladium on carbon, and then a balloon filled with hydrogen was placed atop the reaction vessel. The contents were allowed to stir overnight at room temperature before filtering the reaction through a plug of celite. The filter bed was washed with excess methanol (50 mL) and the organic layers were combined and evaporated in vacuo. The residue was purified on silica gel chromatography using a gradient from 100% hexane to 100% dichloromethane to afford a yellow oil weighing 141 mg (0.733 mmol, 62%);^{1}H NMR (500 MHz, CDCl3) δ 7.13 (dd, *J* = 7.5, 1.1 Hz, 1H), 7.08 (td, *J* = 7.5, 1.1 Hz, 1H), 6.87 (td, *J* = 7.5, 1.1 Hz, 1H), 6.76 (dd, *J* = 7.5, 1.1 Hz, 1H), 4.65 (s, 1H), 2.61 – 2.54 (m, 2H), 1.59 – 1.52 (m, 2H), 1.42 – 1.33 (m, 4H), 1.31 – 1.24 (m, 1H), 0.88 (t, *J* = 7.4 Hz, 6H); ^{13}C NMR (126 MHz, $CDCl_3$) δ 153.49, 130.17, 129.17, 127.08, 120.97, 115.30, 40.48, 33.01, 27.33, 25.45, 10.99. **JH-VIII-79**.

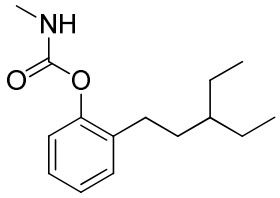

2-(3-Ethyl-1-hydroxypentyl)phenyl *N*-methylcarbamate (**9bl*, *Novel carbamate #18***). Colorless oil (*Method A*); 86%; ^{1}H NMR (400 MHz, $CDCl_3$) δ 7.25 – 7.03 (m, 1H), 4.96 (br s, 1H), 2.90 (d, *J* = 4.9 Hz, 3H), 2.58 – 2.44 (m, 2H), 1.55 – 1.46 (m, 2H), 1.40 – 1.29 (m, 4H), 1.28 – 1.19 (m, 1H), 0.86 (t, *J* = 7.4 Hz, 6H); ^{13}C NMR (126 MHz, CDCl3) δ 155.48, 149.20, 135.62,

130.20, 126.84, 125.80, 122.66, 40.54, 33.41, 27.93, 27.61, 25.42, 10.99. HRMS (ESI): 250.1802 calcd for $C_{15}H_{24}NO_2$ $[M+H]^+$ found 250.1786 (-6.21 ppm). **JH-VIII-91**.

Example 27: General procedure for the preparation of tosylate electrophiles

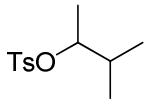

(±)-3-Methylbutan-2-yl 4-methylbenzenesulfonate **(106bm)**. A 100 mL round-bottom flask was charged with (±)-2-methylbutanol (4.90 g, 55.6 mmol), pyridine (30 mL), and then purging w/nitrogen. Next, tosyl chloride (17.5 g, 91.9 mmol) was added and the reaction was allowed to stir at room temperature for 18 h. Upon completion, the reaction was diluted in 1 M hydrochloric acid (300 mL) and extracted with ethyl acetate (3 x 75 mL). The combined organic layers were washed with brine before drying with sodium sulfate. The solvent was stripped in vacuo to yield a golden oil weighing 12.5 g (93%, note: product and starting material have the same R_f. No starting material was detected by NMR). ^{1}H NMR (500 MHz, $CDCl_3$): δ 7.79 (d, *J* = 8.3 Hz, 2H), 7.32 (d, *J* = 8.3 Hz, 2H), 4.45 (s-5, *J* = 6.6 Hz, 1H), 2.44 (s, 3H), 1.79 (s-8, *J* = 6.6 Hz, 1H), 1.20 (d, *J* = 6.6 Hz, 3H), 0.84 (d, *J* = 6.6 Hz, 3H), 0.83 (d, *J* = 6.6 Hz, 3H); ^{13}C NMR (126 MHz, $CDCl_3$): δ 144.47, 134.79, 129.81, 127.83, 84.98, 33.40, 21.76, 17.89, 17.66, 17.47; HRMS (FAB): 243.1055 calcd for $C_{12}H_{19}O_3S$ $[M+H]^+$ found 243.1035 (-8.2 ppm, -2.0 mmu). **JH-IV-161**.

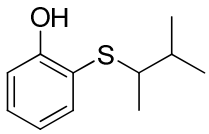

(±)-2-(3-Methylbutan-2-ylthio)phenol **(35bm)**. This compound was prepared in 26% from 2-mercaptophenol and (±)-3-methylbutan-2-yl 4-methylbenzenesulfonate (**106bm**) according to the procedure for **35v** in Example 6. Colorless Oil; ^{1}H NMR (500 MHz, $CDCl_3$) δ 7.44 (dd, *J* =

7.7, 1.6, Hz, 1H), 7.28 – 7.23 (m, 1H), 7.00 – 6.97 (m, 1H), 6.88 – 6.84 (m, 1H), 6.83 (s, 1H), 2.90 – 2.84 (m, 1H), 1.91 – 1.81 (m, 1H), 1.16 (d, *J* = 6.9, Hz, 3H), 1.03 (d, *J* = 6.9 Hz, 3H), 1.01 (d, *J* = 6.9 Hz, 3H); ^{13}C NMR (126 MHz, $CDCl_3$) δ 157.45, 136.73, 131.17, 120.68, 118.89, 114.70, 53.02, 32.78, 20.15, 18.58, 17.32; **JH-V-9**.

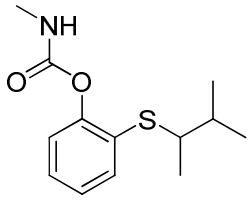

(±)-2-(3-Methylbutan-2-ylthio)phenyl *N*-methylcarbamate **(9bm*, *Novel carbamate #19*)**. Yellow oil (*Method B*); 93%; ^{1}H NMR (500 MHz, $CDCl_3$) δ 7.42 (dd, *J* = 7.7, 1.5 Hz, 1H), 7.23 (td, *J* = 7.7, 1.5 Hz, 1H), 7.19 – 7.11 (m, 2H), 5.04 (s, 1H), 3.17 (qd, *J* = 6.9, 4.5 Hz, 1H), 2.91 (d, *J* = 4.5 Hz, 3H), 1.92 – 1.83 (m, 1H), 1.21 (d, *J* = 6.9 Hz, 3H), 1.00 (d, *J* = 6.9 Hz, 3H), 0.99 (d, *J* = 6.9 Hz, 3H); ^{13}C NMR (126 MHz, $CDCl_3$) δ 155.82, 154.92, 132.93, 129.55, 127.79, 126.08, 123.29, 49.39, 32.68, 27.99, 20.24, 18.33, 17.06; HRMS (APCI): 292.0774 calcd for $C_{13}H_{19}NO_2SK$ $[M+K]^+$ found 292.0776 (2.71 ppm). **(JH-V-19, PRC474)**.

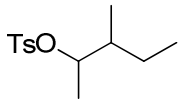

(±)-3-Methylpentan-2-yl 4-methylbenzenesulfonate **(106bn)**. This compound was prepared in 97% from 3-methylpentan-2-ol and tosyl chloride according to the procedure for **106bm** in Example 27. Yellow Oil; ^{1}H NMR (500 MHz $CDCl_3$): δ 7.79 (d, *J* = 8.3 Hz, 2H), 7.32 (d, *J* = 8.0 Hz, 2H), 4.53-4.61 (m, 1H), 2.44 (s, 3H), 1.56-1.63 (m, 0.5H), 1.45-1.53 (m, 0.5H), 1.30-1.44 (m, 1H), 1.21 (d, *J* = 6.6 Hz, 1.7 H), 1.17 (d, 6.6 Hz, 1.3 H), 1.0-1.2 (m, 1H), 0.82-0.84 (m, 2H), 0.81 (t, *J* = 7.4 Hz, 3H); ^{13}C NMR (126 MHz, $CDCl_3$): δ 144.44, 134.90, 129.82, 129.80, 127.81,

83.84, 83.81, 40.20, 39.74, 25.20, 24.81, 21.76, 17.85, 16.52, 14.34, 14.24, 13.73, 11.62, 11.57; **JH-V-21**.

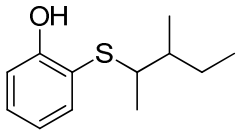

(±)-2-(3-Methylpentan-2-ylthio)phenol **(35bn)**. This compound was prepared in 41% from 2-mercaptophenol and (±)-3-methylpentan-2-yl 4-methylbenzenesulfonate (**106bn**) according to the procedure for **35v** in Example 6. Colorless Oil; ^{1}H NMR (500 MHz, $CDCl_3$) δ 7.44 (dd, *J* = 7.7, 1.7 Hz, 1H), 7.29 – 7.24 (m, 1H), 6.99 (dt, *J* = 7.7, 1.7 Hz, 1H), 6.89 – 6.85 (m, 1H), 6.84 (s, 1H), 3.02 – 2.94 (m, 1H), 1.74 – 1.56 (m, 1.5H), 1.48 – 1.38 (m, 0.5H), 1.34 – 1.21 (m, 1H), 1.19 (d, *J* = 6.9 Hz, 1.3H), 1.14 (d, *J* = 6.9 Hz, 1.7H), 1.01 (d, *J* = 6.9 Hz, 1.7H), 0.99 (d, *J* = 6.9 Hz, 1.3H), 0.93 (t, *J* = 6,9 Hz, 1.3H), 0.87 (t, *J* = 6.9 Hz, 1.7H); ^{13}C NMR (126 MHz, $CDCl_3$) δ 157.42, 136.77, 136.65, 131.16, 131.14, 120.70, 120.69, 114.68, 114.67,52.34, 51.21, 39.89, 39.23, 27.36, 26.13, 18.45, 16.26, 16.20, 14.86, 12.09, 12.06; **JH-V-29**.

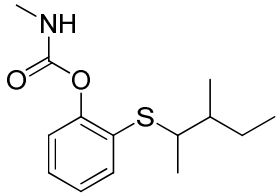

(+)-2-(3-Methylpentan-2-ylthio)phenyl *N*-methylcarbamate **(9bn***, ***Novel carbamate #20*****)**. Yellow Oil (*Method B*); 86%; ^{1}H NMR (500 MHz, $CDCl_3$): δ 7.41-7.43 (m, 1H), 7.21-7.24 (m, 1H), 7.12-7.17 (m, 2H), 5.06 (s, 1H), 3.23-3.33 (m, 1H), 2.91 (d, *J* = 4.7 Hz, 3H), 1.56-1.69 (m, 2H), 1.40-1.48 (m, 1H), 1.19-1.31 (m, 1H), 1.22 (d, *J* = 6.9 Hz, 1.5), 1.17 (d, *J* = 6.9 Hz, 1.5), 0.98 (d, *J* = 6.9 Hz, 1.5), 0.96 (d, *J* = 6.9 Hz, 1.5), 0.888 (t, *J* = 6.9 Hz, 1.5), 0.885 (t, *J* = 6.9 Hz, 1.5); ^{13}C NMR (126 MHz, $CDCl_3$): δ 154.92, 150.87, 150.71, 133.05, 132.73, 129.56, 127.80, 127.74, 126.06, 123.28, 48.70, 47.32, 39.90, 39.04, 28.55, 27.97, 27.44, 25.82, 18.26, 16.34,

15.95, 14.72, 12.13; HRMS (APCI): 267.1293 calcd for $C_{14}H_{21}NO_2S$ $[M]^+$ found 267.1289 (-1.58 ppm). **(JH-V-33, PRC492)**.

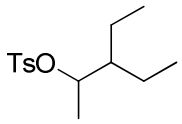

(+)-3-Ethylpentan-2-yl 4-methylbenzenesulfonate **(106bo)**. This compound was prepared in 96% from 3-ethylpentan-2-ol and tosyl chloride according to the procedure for **106bm** in Example 27. Yellow Oil; ^{1}H NMR (500 MHz, $CDCl_3$): δ 7.79 (d, *J* = 8.0 Hz, 2H), 7.32 (d, *J* = 8.0 Hz, 2H), 4.69 (dt, *J* = 6.4, 4.2 Hz, 1H), 2.44 (s, 3H), 1.35-1.44 (m, 1H), 1.13-1.32 (m, 7H), 0.78-0.82 (m, 6H); ^{13}C NMR (126 MHz, $CDCl_3$): δ 144.44, 134.92, 129.80, 127.81, 82.25, 46.41, 22.02, 21.75, 21.42, 17.14, 11.70, 11.69; **JH-V-11**.

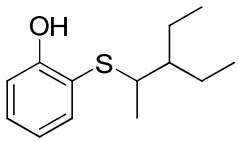

(+)-2-(3-Ethylpentan-2-ylthio)phenol **(35bo)**. This compound was prepared in 38% from 2-mercaptophenol and (±)-3-ethylpentan-2-yl 4-methylbenzenesulfonate (**106bo**) according to the procedure for **35v** in Example 6. Yellow Oil; ^{1}H NMR (500 MHz, $CDCl_3$): δ 7.44 (dd, *J* = 7.4, 1.7 Hz, 1H), 7.26 (dt, *J* = 7.4, 1.7 Hz, 1H), 6.99 (dd, *J* = 7.4, 1.7 Hz, 1H), 6.87 (dt, *J* = 7.4, 1.7 Hz, 1H), 6.84 (s, 1H), 1.62-1.70 (m, 1H), 1.36-1.48 (m, 2H), 1.28-1.35 (m, 2H), 1.16 (d, *J* = 6.9 Hz, 3H), 0.93 (t, *J* = 6.9 Hz, 3H), 0.86 (t, *J* = 6.9 Hz, 3H); ^{13}C NMR (126 MHz, $CDCl_3$): δ 157.44, 136.65, 131.12, 120.70, 119.10, 114.66, 49.41, 46.45, 23.42, 22.79, 17.43, 12.25, 12.18; **JH-V-15**.

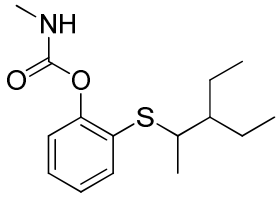

(+)-2-(3-Ethylpentan-2-ylthio)phenyl *N*-methylcarbamate **(9bo*, *Novel carbamate #21*)**. Yellow Oil (*Method B*); 94%; ^{1}H NMR (500 MHz, $CDCl_3$): δ 7.43 (dd, *J* = 8.0, 1.5 Hz, 1H), 7.23 (dt, *J* = 8.0, 1.5 Hz, 1H), 7.12-7.17 (m, 2H), 5.03 (br s, 1H), 3.38-3.43 (m, 1H), 2.91 (d, *J* = 4.7 Hz, 3H), 1.61-1.70 (m, 1H), 1.31-1.42 (m, 2H), 1.22-1.29 (m, 1H), 1.19 (d, *J* = 7.4 Hz, 3H), 0.896 (t, *J* = 7.4 Hz, 3H), 0.891 (t; *J* = 7.4 Hz, 3H); ^{13}C NMR (126 MHz, $CDCl_3$): δ 154.91, 150.87, 132.99, 129.56, 127.82, 126.03, 123.26, 46.38, 45.60, 28.56, 27.97, 25.25, 23.49, 22.68, 17.24, 12.34, 12.25, 10.88; HRMS (APCI): 281.14495 calcd for $C_{15}H_{23}NO_2S$ $[M]^+$ found 281.14475 (-0.71 ppm). **(JH-V-25, PRC475)**.

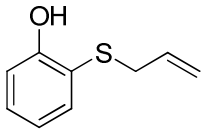

2-(Allylthio)phenol **(35bp)**. This compound was prepared in an 86% from 2-mercaptophenol and allylchloride according to the procedure for **35ai** in Example 7. Colorless oil; ^{1}H NMR (500 MHz, $CDCl_3$) δ 7.43 (dd, *J* = 7.7, 1.7 Hz, 1H), 7.30 – 7.22 (m, 1H), 7.02 – 6.96 (m, 1H), 6.86 (td, *J* = 7.7, 1.7 Hz, 1H), 6.70 (d, *J* = 1.7 Hz, 1H), 5.81 (ddt, *J* = 17.3, 10.0, 7.3 Hz, 1H), 4.99 (dt, *J* = 10.0, 1.7, 0.7 Hz, 1H), 4.88 (dq, *J* = 17.3, 1.7 Hz, 1H), 3.30 (ddd, *J* = 7.3, 1.7, 0.7 Hz, 2H); ^{13}C NMR (126 MHz, $CDCl_3$) δ 157.28, 136.58, 133.24, 131.42, 120.76, 118.37, 118.22, 114.87, 39.96; HRMS (FAB): 166.04524 calcd for $C_9H_{10}OS$ $[M]^+$ found 166.04633 (6.4 ppm, 1.1 mmu). **JH-II-187**.

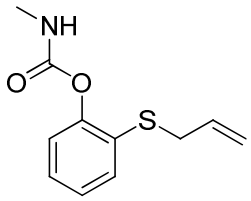

2-(Allylthio)phenyl *N*-methylcarbamate[7] (**9bp**). Off-white solid (*Method B*), 88%; ^{1}H NMR (500 MHz, $CDCl_3$) δ 7.35 (dd, *J* = 7.7, 1.7 Hz, 1H), 7.21 (dd, *J* = 7.7, 1.7 Hz, 1H), 7.19 – 7.11 (m, 2H), 5.86 (ddt, *J* = 16.9, 10.0, 7.7 Hz, 1H), 5.15 (dq, *J* = 16.9, 1.7 Hz, 1H), 5.08 (dd, *J* = 10.0, 1.2 Hz, 1H), 5.05 (br s, 1H), 3.52 (d, *J* = 6.8 Hz, 2H), 2.92 (d, *J* = 4.9 Hz, 3H); ^{13}C NMR (126 MHz, $CDCl_3$) δ 154.80, 149.73, 133.37, 130.83, 129.41, 127.46, 126.11, 123.10, 118.19, 36.38, 28.01; .HRMS (FAB): 224.0745 calcd for $C_{11}H_{14}NO_2S$ $[M+H]^+$ found 224.0748 (1.2 ppm, 0.3 mmu). **(JH-III-1, PRC371)**.

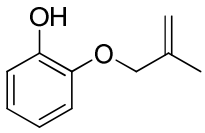

2-(2-Methylallyloxy)phenol **(35bq)**. This compound was prepared in a 46% from catechol and 3-chloro-2-methylprop-1-ene according to the procedure for **35ai** in Example 7. Yellow oil; ^{1}H NMR (400 MHz, $CDCl_3$) δ 6.96 – 6.93 (m, 1H), 6.90 – 6.81 (m, 3H), 5.66 (s, 1H), 5.09 (s, 1H), 5.02 (s, 1H), 4.51 (s, 2H), 1.84 (s, 3H); ^{13}C NMR (101 MHz, $CDCl_3$) δ 145.97, 145.78, 140.56, 121.82, 120.20, 114.79, 113.49, 112.29,72.80, 19.56; HRMS (FAB): 164.0837 calcd for $C_{10}H_{12}NO_2$ $[M]^+$ found 164.0842 (3.0 ppm). **JH-III-35**.

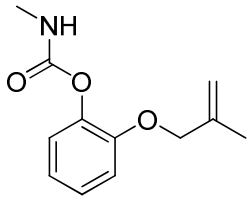

2-(2-Methylallyloxy)phenyl-*N*- methylcarbamate[8] **(9bq*, *Novel carbamate #22*)**. White solid (*Method B*); 74%; ^{1}H NMR (500 MHz, $CDCl_3$) δ 7.17 – 7.11 (m,1H), 7.11 – 7.07 (m, 1H), 6.96 –

6.90 (m, 2H), 5.09 (s, 1H), 5.07 (s, 1H), 4.96 - 4.97 (m, 1H), 4.45 (s, 2H), 2.87 (d, *J* = 4.9 Hz, 3H), 1.81 (d, *J* = 0.5 Hz, 3H); ^{13}C NMR (126 MHz, $CDCl_3$) δ 155.16, 150.98, 140.71, 140.50, 126.41, 123.39, 121.03, 113.87, 112.55, 72.32, 27.89, 19.34, 14.31; HRMS (FAB): 222.11302 calcd for $C_{12}H_{15}NO_3$ $[M+H]^+$ found 222.11441 (6.2 ppm, 1.4 mmu). (**JH-III-39, PRC381)**.

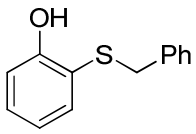

2-(Benzylthio)phenol **(35br)**. This compound was prepared in 78% from 2-mercaptophenol and benzyl bromide according to the procedure for **35ai** in Example 7. Pale Oil; ^{1}H NMR (500 MHz, $CDCl_3$): δ 7.26 – 7.29 (m, 5H), 7.10 (m, 2H), 6.95 (d, *J* =8.0 Hz, 1H), 6.83 (t, *J* = 8.0 Hz, 1H), 6.56 (s, 1H), 3.87 (s, 2H); ^{13}C NMR (126 MHz, $CDCl_3$) δ 157.26, 137.71, 136.57, 131.56, 128.92, 128.69, 127.57, 127.27, 120.78, 114.87, 41.51; HRMS (FAB): 216.0609 calcd for $C_{13}H_{12}OS$ $[M]^+$ found 216.0616 (3.3 ppm, 0.7 mmu). **JH-III-21**.

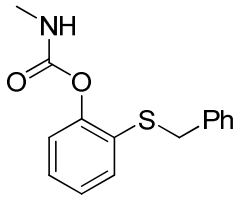

2-(Benzylthio)phenyl *N*-methylcarbamate[13] **(9br)**. White crystalline solid (*Method B*); 78%; ^{1}H NMR (500 MHz, $CDCl_3$) δ 7.32 – 7.26 (m, 5H), 7.26 – 7.20 (m, 2H), 7.16 – 7.09 (m, 2H), 4.97 (br s, 1H), 4.07 (s, 2H), 2.90 (d, *J* = 4.9 Hz, 3H); ^{13}C NMR (126 MHz, $CDCl_3$) δ 154.83, 149.72, 137.23, 131.06, 129.79, 129.11, 128.61, 127.67, 127.38, 126.17, 123.08, 38.26, 27.98; HRMS (FAB): 274.0902 calcd for $C_{15}H_{16}NO_2S$ $[M+H]^+$ found 274.0912 (3.7 ppm, 1.0 mmu). **(JH-III-25, PRC377)**.

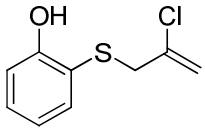

2-(2-Chloroallylthio)phenol **(35bs)**. This compound was synthesized in 49% from 2-mercaptophenol and 2-chloroallyl chloride according to the general procedure for **35ai** in Example 7. Pale oil; ^{1}H NMR (500 MHz, $CDCl_3$) δ 7.45 (dd, *J* = 7.7, 1.7 Hz, 1H), 7.30 – 7.26 (m, 1H), 6.99 (dd, *J* = 7.7, 1.7 Hz, 1H), 6.87 (td, 1H), 6.70 (s, 1H), 5.13 (d, *J* = 1.7 Hz, 1H), 4.91 (dt, *J* = 1.7, 0.8 Hz, 1H), 3.48 (d, *J* = 0.8 Hz, 2H); ^{13}C NMR (126 MHz, $CDCl_3$) δ 157.61, 137.30, 136.64, 131.94, 120.96, 117.35, 116.03, 115.13, 45.35; HRMS (FAB): 200.0063 calcd for C_9H_9ClOS $[M]^+$ found 200.0060 (-1.3 ppm, -0.3 mmu). **JH-III-81**.

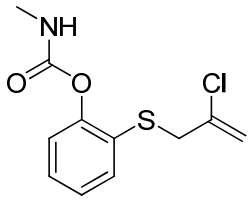

2-(2-Chloroallylthio)phenyl *N*-methylcarbamate[14] **(9bs)**. Pale Oil (*Method B*); 58%; ^{1}H NMR (500 MHz, $CDCl_3$) δ 7.41 (d, *J* = 7.7 Hz, 1H), 7.31 – 7.26 (m, 1H), 7.21 – 7.13 (m, 2H), 5.22 (d, *J* = 15.2 Hz, 2H), 5.09 (br s, 1H), 3.65 (s, 2H), 2.92 (d, *J* = 4.9 Hz, 3H); ^{13}C NMR (126 MHz, $CDCl_3$): δ 27.97, 42.04, 115.24, 123.23, 126.21, 127.70, 128.76, 132.90, 137.51, 141.99, 150.69; HRMS (FAB): 258.0356 calcd for $C_{11}H_{13}NO_2SCl$ $[M+H]^+$ found 258.0357 (0.6 ppm, 0.2 mmu). **(JH-III-85, PRC386)**.

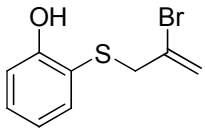

2-(2-Bromoallylthio)phenol **(34bt)**. This compound was prepared from 2-mercaptophenol and 2-bromoallyl bromide in 58% according to the general procedure given for **35ai** in Example 7. Yellow oil; ^{1}H NMR (500 MHz, $CDCl_3$) δ 7.45 (d, *J* = 7.7 Hz, 1H), 7.28 (t, *J* = 7.7 Hz, 1H), 6.99

(d, *J* = 7.7 Hz, 1H), 6.87 (t, *J* = 7.7 Hz, 1H), 6.70 (s, 1H), 5.34 (s, 1H), 5.32 (s, 1H), 3.57 (s, 2H); ^{13}C NMR (126 MHz, $CDCl_3$) δ 157.58, 136.63, 131.91, 128.41, 120.95, 120.41, 115.15, 115.14, 47.66; HRMS (FAB): 243.9557 calcd for C_9H_9BrOS $[M]^+$ found 243.9557 (-0.2 ppm, 0.0 mmu). **JH-III-65**.

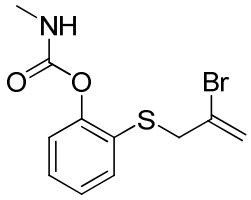

2-(2-Bromoallylthio)phenyl *N*-methylcarbamate[8] **(9bt*, *Novel carbamate #23*)**. Yellow Oil (*Method B*); 35%; ^{1}H NMR (500 MHz, $CDCl_3$): δ 7.40 (dd, *J* = 7.7, 1.4 Hz), 7.15 - 7.29 (m, 3H), 5.69 (s, 1H), 5.44 (s, 1H), 5.09 (s, 1H), 3.76 (s, 2H), 2.92 (d, *J* = 5.0 Hz, 3H); ^{13}C NMR (126 MHz, $CDCl_3$): δ 154.80, 150.55, 132.67, 128.68, 128.38, 126.31, 126.24, 123.23, 119.61, 44.04, 27.98; HRMS (FAB): 301.98504 calcd for $C_{11}H_{12}NO_2SBr$ $[M+H]^+$ found 301.9828 (-7.4 ppm, -2.2 mmu). **(JH-III-69, PRC383)**.

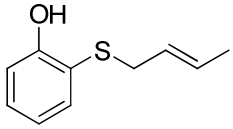

(*E*)-2-(But-2-enylthio)phenol **(35bu)**. This compound was prepared from 2-mercaptophenol and (E)-2-butenyl bromide in 97% according to the general procedure for **35ai** in Example 7. Colorless oil; ^{1}H NMR (500 MHz, $CDCl_3$) δ 7.41 (dd, *J* = 7.7, 1.6 Hz, 1H), 7.30 – 7.21 (m, 1H), 6.98 (dd, *J* = 7.7, 1.6 Hz, 1H), 6.86 (td, *J* = 7.7, 1.6 Hz, 1H), 6.72 (s, 1H), 5.52 – 5.39 (m, 1H), 5.28 (dqt, *J* = 14.9, 7.7, 1.6 Hz, 1H), 3.25 (dt, *J* = 7.7, 1.6 Hz, 2H), 1.66 – 1.52 (m, 3H); ^{13}C NMR (126 MHz, $CDCl_3$) δ 157.31, 136.68, 131.30, 129.91, 128.52, 125.80, 120.62, 114.72, 39.44, 17.82; HRMS (FAB): 180.0609 calcd for $C_{10}H_{12}OS$ $[M]^+$ found 180.0596 (-7.1 ppm, -1.3 mmu). **JH-III-23**.

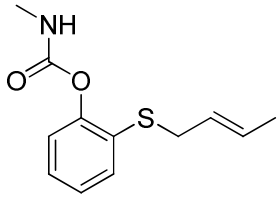

(*E*)-2-(But-2-enylthio)phenyl-*N*- methylcarbamate[8] **(9bu*, *Novel carbamate #24*)**. Colorless oil (*Method B*); 91%; ^{1}H NMR (500 MHz, $CDCl_3$) δ 7.33 (dd, *J* = 7.6, 1.6 Hz, 1H), 7.23 – 7.10 (m, 3H), 5.64 – 5.55 (m, 1H), 5.55 – 5.46 (m, 1H), 5.07 (s, 1H), 3.47 (d, *J* = 6.8 Hz, 2H), 2.91 (d, *J* = 4.9 Hz, 3H), 1.65 (dd, *J* = 6.8, 1.1 Hz, 3H); ^{13}C NMR (126 MHz, $CDCl_3$) δ 154.81, 149.45, 130.41, 129.93, 129.62, 127.11, 126.03, 125.76, 123.01, 35.51, 27.96, 17.87; HRMS (FAB): 238.0902 calcd for $C_{12}H_{16}NO_2S$ $[M+H]^+$ found 238.0894 (-3.3 ppm, -0.8 mmu). **(JH-III-27, PRC376)**.

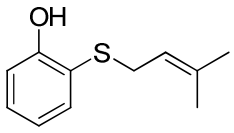

2-(3-Methylbut-2-enylthio)phenol **(35bv)**. This compound was prepared in 99% from 2-mercaptophenol and 3-methyl-2-butenylbromide according to the general procedure for **35ai** in Example 7. Colorless Oil; ^{1}H NMR (500 MHz, $CDCl_3$) δ 7.42 (dd, *J* = 7.7, 1.7 Hz, 1H), 7.28 – 7.22 (m, 1H), 6.95 (dd, *J* = 7.7, 1.7 Hz, 1H), 6.85 – 6.81 (m, 1H), 6.81 (s, 1H), 5.25 – 5.20 (m, 1H), 3.29 (d, *J* = 8.1 Hz, 2H), 1.65 (d, *J* = 1.4 Hz, 3H), 1.28 (d, *J* = 1.4 Hz, 3H); ^{13}C NMR (126 MHz, $CDCl_3$) δ 157.44, 137.25, 136.87, 131.31, 120.52, 119.14, 118.67, 114.56, 34.79, 25.70, 17.25; HRMS (FAB): 194.07654 calcd for $C_{11}H_{14}OS$ $[M]^+$ 194.0771 (2.9 ppm, 0.6 mmu). **JH-II-189**.

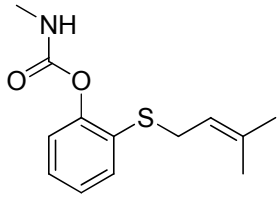

2-(3-Methylbut-2-enylthio)phenyl *N*-methylcarbamate[8] **(9bv*, *Novel carbamate #25*)**. White solid (*Method B*); 80%; ^{1}H NMR (500 MHz, $CDCl_3$) δ 7.33 (dd, *J* = 7.6, 1.7 Hz, 1H), 7.23 – 7.10 (m, 3H), 5.31 – 5.26 (m, 1H), 5.05 (br s, 1H), 3.50 (d, *J* = 7.7 Hz, 2H), 2.91 (d, *J* = 4.9 Hz, 3H), 1.71 (s, 3H), 1.60 (s, 3H); ^{13}C NMR (126 MHz, $CDCl_3$) δ 154.86, 149.51, 137.18, 130.54, 130.40, 127.11, 126.08, 123.00, 118.93, 31.49, 27.99, 25.82, 17.83; HRMS (FAB): 251.09800 calcd for $C_{13}H_{17}NO_2S$ $[M]^+$ found 251.0963 (-6.8 ppm, -1.7 mmu). **(JH-III-3, PRC372)**.

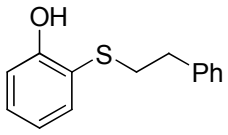

2-(Phenethylthio)phenol **(35bw)**. This compound was prepared in 97% from 2-mercaptophenol and phenethyl bromide according to the procedure for **35v** in Example 6. Yellow oil; ^{1}H NMR (500 MHz, $CDCl_3$): δ 7.49 (dd, *J* = 7.7, 1.7 Hz, 1H), 7.27-7.35 (m, 3H), 7.22 (t, *J* = 7.7 Hz, 1H), 7.15 (d, *J* = 7.7 Hz, 2H), 7.01 (d, *J* = 7.7 Hz, 1H), 6.90 (dt, *J* = 7.7, 1.7 Hz, 1H), 6.66 (s, 1H), 2.96-2.99 (m, 2H), 2.84-2.87 (m, 2H); ^{13}C NMR (126 MHz, $CDCl_3$): δ 157.16, 139.82, 136.05, 131.28, 128.71, 128.65, 127.07, 126.71, 120.95, 115.04, 38.07, 36.1; HRMS (APCI): 231.0844 calcd for $C_{14}H_{15}OS$ $[M+H]^+$ found 231.0824 (6.2 ppm). **JH-V-43**.

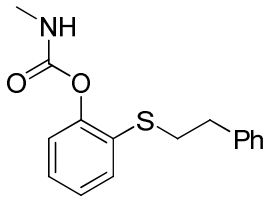

2-(Phenethylthio)phenyl *N*-methylcarbamate **(9bw*, *Novel carbamate #26*)**. Off-white solid (*Method B*); 76%; ^{1}H NMR (500 MHz, $CDCl_3$) δ 7.37 (dd, *J* = 7.6, 1.6 Hz, 1H), 7.31 – 7.27 (m,

2H), 7.25 – 7.12 (m, 6H), 5.06 (s, 1H), 3.15 – 3.07 (m, 2H), 3.01 – 2.82 (m, 5H); ^{13}C NMR (126 MHz, $CDCl_3$) δ 154.79, 149.69, 140.29, 130.15, 129.73, 128.65, 128.60, 127.24, 126.54, 126.22, 123.22, 35.59, 34.45, 27.93; HRMS (APCI): 287.0980 calcd for $C_{16}H_{17}NO_2S$ $[M]^+$ found 287.0973 (-2.31 ppm). **JH-V-49**.

Example 28: General procedure for the preparation of arylchlorosulfonic acids

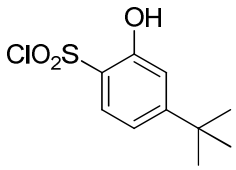

4-(*tert*-Butyl)-2-hydroxybenzene-1-sulfonyl chloride **(113)**. A dry 50 mL Schlenk flask back-filled with nitrogen was charged with chlorosulfonic acid (2.5 mL, 37 mmol) and cooled to 0 ^{o}C before adding 3-*tert*butylphenol (**35c**, 514 mg, 3.42 mmol). The reaction was allowed to stir overnight as it warmed to room temperature before carefully pouring onto 25 g of ice water. The aqueous layer was extracted with diethyl ether (3 x25 mL). The organic layers were combined and washed with brine and dried with sodium sulfate. The solvent was removed and the residual yellow crystals were taken up in boiling hexane (15 mL). After cooling to room temperature, the precipitate was filtered and washed with cold hexane. The mother liquor was concentrated in vacuo to yield a tan solid (607 mg, 71%). ^{1}H NMR (500 MHz, DMSO-D6) δ 7.33 (d, *J* = 8.2 Hz, 1H), 6.81 (dd, *J* = 8.2, 1.4 Hz, 1H), 6.73 (d, *J* = 1.4 Hz, 1H), 1.22 (s, 9H); ^{13}C NMR (126 MHz, DMSO-D6) δ 153.97, 153.01, 128.10, 126.82, 115.68, 113.11, 34.38, 31.00; HRMS (APCI): 248.0274 calcd for $C_{10}H_{13}ClO_3S$ $[M]^+$ found 248.0294 (8.1 ppm). **JH-VII-81, JH-VII-7**.

Example 29: General procedure for the reduction of arylchlorosulfonic acids to arylthiols

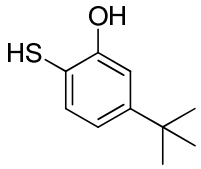

5-(*tert*-Butyl)-2-mercaptophenol **(114)**. A 250 mL round bottom flask was charged with 4-(tert-butyl)-2-hydroxybenzene-1-sulfonyl chloride **(113**, 3.984 g, 16.0 mmol) and glacial acetic acid (160 mL) prior to heating in a 75 ^{o}C oil bath. A reflux condenser was fitted before adding a solution containing concentrated hydrochloric acid (21 mL) and $SnCl_2 \cdot 2H_2O$ (18.06 g, 80 mmol). The reaction was allowed to stir for 18 h at 75 ^{o}C before diluting in 1 M hydrochloric acid (1 L). This caused the formation of a yellow precipitate and was extracted with $CHCl_3$ (3 x 250 mL). The combined organic layers were combined and washed with water and then brine before drying with $MgSO_4$. After filtering and concentrating the solution under reduced pressure, the residue was purified with flash chromatography (9:1 Hexane : Ethyl Acetate) to yield a yellow oil comprised of the intended product (5-(*tert*-butyl)-2-mercaptophenol) and the disulfide. This mixture was taken up in 63 mL of dry tetrahydrofuran and reduced with sodium borohydride (1.22 g, 32 mmol) over 1 hour at RT. The reaction was quenched with 200 mL of cold 1 M hydrochloric acid and extracted with diethyl ether (3 x 100 mL). The combined organic layers were washed with brine, dried with $MgSO_4$, filtered, and concentrated in vacuo to afford a yellow oil (2.325g, 80%); ^{1}H NMR (500 MHz, $CDCl_3$): δ 7.38 (d, *J* = 8.2 Hz, 1H), 7.01 (d, *J* = 2.2 Hz, 1H), 6.89 (dd, *J* = 8.2, 2.2 Hz, 1H), 6.26 (s, 1H), 2.90 (s, 1H), 1.29 (s, 9H); ^{13}C NMR (126 MHz, $CDCl_3$): δ 31.29, 34.88, 108.10, 112.41, 118.29, 135.41, 154.91, 156.25; HRMS (APCI): 182.0765 calcd for $C_{10}H_{14}OS$ $[M]^+$ found 182.0749 (-8.78 ppm). **JH-VII-9 ($SnCl_2$) and JH-VII-15 ($NaBH_4$)**.

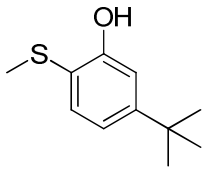

5-(*tert*-Butyl)-2-(methylthio)phenol **(35bx)**. This compound was prepared in 63% from 5-(*tert*-butyl)-2-mercaptophenol (**114**) and 1.1 equiv iodomethane according to the procedure for **35v** in Example 6. Yellow oil; ^{1}H NMR (500 MHz, $CDCl_3$) δ 7.41 (d, *J* = 8.2 Hz, 1H), 7.03 (d, *J* = 2.1 Hz, 1H), 6.92 (dd, *J* = 8.2, 2.1 Hz, 1H), 6.59 (s, 1H), 2.31 (s, 3H), 1.30 (s, 9H); ^{13}C NMR (126 MHz, $CDCl_3$) δ 156.17, 155.00, 134.66, 118.38, 117.48, 112.11, 34.93, 31.30, 20.13; **(JH-VII-51)**.

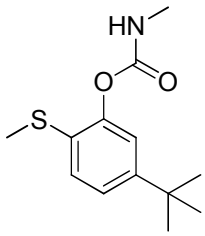

5-(*tert*-Butyl)-2-(methylthio)phenyl *N*-methylcarbamate **(9bx*, *Novel carbamate #27*)**. White solid, (*Method A*); 59%; ^{1}H NMR (500 MHz, $CDCl_3$) δ 7.25 – 7.18 (m, 2H), 7.12 (d, *J* = 1.9 Hz, 1H), 5.05 (br s, 1H), 2.92 (d, *J* = 4.9 Hz, 3H), 2.42 (s, 3H), 1.30 (s, 9H); ^{13}C NMR (126 MHz, $CDCl_3$) δ 154.90, 150.13, 148.31, 128.13, 127.30, 123.52, 120.16, 34.61, 31.36, 28.00, 15.73; HRMS (APCI): 253.1136 calcd for $C_{10}H_{19}NO_2S$ $[M]^+$ found 253.1164 (10.8 ppm). **(PRC564, JH-VII-57)**.

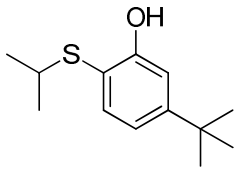

5-(*tert*-Butyl)-2-(isopropylthio)phenol **(35by)**. This compound was prepared in 70% from 5-(*tert*-butyl)-2-mercaptophenol (**114**) and 2-iodopropane according to the procedure for **35v** in

Example 6. Yellow oil; ^{1}H NMR (400 MHz, $CDCl_3$) δ 7.36 (d, *J* = 8.1 Hz, 1H), 7.03 (d, *J* = 2.0 Hz, 1H), 6.90 (dd, *J* = 8.1, 2.0 Hz, 1H), 3.07 (s-7, *J* = 6.7 Hz, 1H), 1.30 (s, 9H), 1.25 (d, *J* = 6.7 Hz, 6H); **JH-VII-35**.

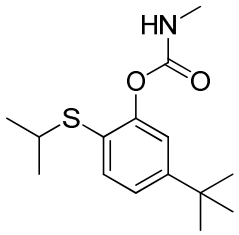

5-(*tert*-Butyl)-2-(isopropylthio)phenyl *N*-methylcarbamate **(9by*, *Novel carbamate #28*)**. White solid, (*Method A*); 85%; ^{1}H NMR (500 MHz, $CDCl_3$) δ 7.36 (d, *J* = 8.2 Hz, 1H), 7.19 (dd, *J* = 8.2, 2.0 Hz, 1H), 7.14 (d, *J* = 2.0 Hz, 1H), 5.02 (br s, 1H), 3.32 (s-7, *J* = 6.7 Hz, 1H), 2.91 (d, *J* = 4.9 Hz, 3H), 1.30 (s, 9H), 1.27 (d, *J* = 6.7 Hz, 6H); ^{13}C NMR (126 MHz, $CDCl_3$) δ 155.07, 152.08, 150.71, 133.18, 125.25, 123.26, 120.41, 37.88, 34.75, 31.32, 28.00, 23.42; HRMS (ESI): 282.1522 calcd for $C_{15}H_{24}NO_2S$ $[M+H]^+$ found 282.1530 (2.64 ppm). **(PRC555, JH-VII-47)**.

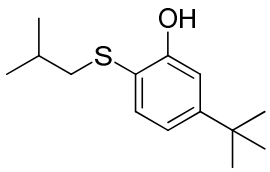

5-(*tert*-Butyl)-2-(isobutylthio)phenol **(35bz)**. This compound was prepared in 68% from 5-(*tert*-butyl)-2-mercaptophenol (**114**) and isobutyliodide according to the procedure for **35v** in Example 6. Yellow oil; ^{1}H NMR (400 MHz, $CDCl_3$) δ 7.37 (d, *J* = 8.1 Hz, 1H), 7.02 (d, *J* = 2.1 Hz, 1H), 6.89 (dd, *J* = 8.1, 2.1 Hz, 1H), 6.68 (s, 1H), 2.57 (d, *J* = 6.9 Hz, 2H), 1.76 (s-7, *J* = 6.7 Hz, 1H), 1.29 (s, 9H), 1.01 (d, *J* = 6.7 Hz, 6H); ^{13}C NMR (101 MHz, $CDCl_3$) δ 156.49, 154.97, 135.41, 118.15, 116.38, 111.97, 46.21, 34.93, 31.31, 28.57, 21.94; HRMS (APCI): 239.1391 calcd for $C_{14}H_{22}OS$ $[M]^+$ found 238.1415 (9.8 ppm). **JH-VII-37**.

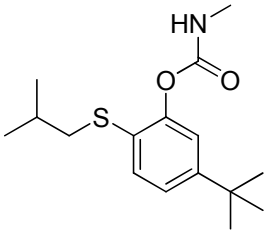

5-(*tert*-Butyl)-2-(isobutylthio)phenyl *N*-methylcarbamate **(9bz*, *Novel carbamate #29*)**. Pink oil, (*Method A*); 93%; ^{1}H NMR (500 MHz, $CDCl_3$) δ 7.27 (d, *J* = 8.3 Hz, 1H), 7.18 (dd, *J* = 8.3, 2.1 Hz, 1H), 7.12 (d, *J* = 2.1 Hz, 1H), 5.04 (br s, 1H), 2.92 (d, *J* = 4.9 Hz, 3H), 2.73 (d, *J* = 6.9 Hz, 2H), 1.83 (hept, *J* = 6.9 Hz, 1H), 1.29 (s, 9H), 1.02 (d, *J* = 6.9 Hz, 6H); ^{13}C NMR (126 MHz, $CDCl_3$) δ 155.00, 150.87, 149.47, 130.13, 126.96, 123.38, 120.32, 42.53, 34.66, 31.33, 28.40, 27.99, 22.19; HRMS (ESI): 296.1679 calcd for $C_{16}H_{26}NO_2S$ $[M+H]^+$ found 296.1698 (6.44 ppm). **(PRC556, JH-VII-49)**.

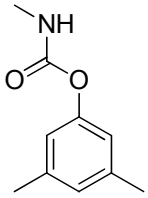

3,5-Dimethylphenyl *N*-methylcarbamate[1] **(9ca)**. White solid (*Method A*) 85%;^{1}H NMR (500 MHz, $CDCl_3$) δ 6.83 (s, 1H), 6.74 (s, 2H), 4.96 (s, 1H), 2.88 (d, *J* = 4.9 Hz, 3H), 2.30 (s, 6H); ^{13}C NMR (126 MHz, $CDCl_3$) δ 155.65, 151.07, 139.22, 127.21, 119.37, 27.82, 21.35; HRMS (FAB): 180.1025 calcd for $C_{10}H_{14}NO_2$ $[M+H]^+$ found 180.1034 (5.2ppm, 0.9 mmu). **(JH-II-61, PRC332)**.

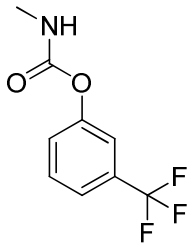

3-Trifluoromethylphenyl-*N*-methylcarbmate[6] **(9cb).** Long white needles (*Method B*); 81%; ^{1}H NMR (500 MHz, $CDCl_3$) δ 7.50 – 7.42 (m, 2H), 7.40 (s, 1H), 7.32 (dt, *J* = 7.0, 2.3 Hz, 1H), 5.11 (s, 1H), 2.89 (d, *J* = 4.9 Hz, 3H); ^{13}C NMR (126 MHz, $CDCl_3$) δ 154.77 (s), 151.29 (s), 131.83 (q, *J* = 32.1 Hz), 129.93 (s), 125.27 (s), 123.73 (q, *J* = 272.4 Hz), 122.11 (q, *J* = 3.8 Hz), 118.93 (q, *J* = 3.8 Hz), 27.80 (s). HRMS (APCI): 220.0580 calcd for $C_9H_9F_3NO_2$ $[M+H]^+$ found 220.0558 (-9.96 ppm). **JH-V-105, PRC505**.

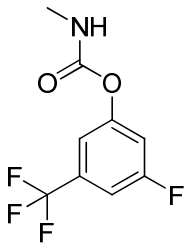

3-Fluoro-5-(trifluoromethyl)phenyl *N*-methylcarbamate[8] **(9cc***, ***Novel carbamate #30*)**. White solid (*Method B*); 59%; ^{1}H NMR (500 MHz, $CDCl_3$) δ 7.24 (s, 1H), 7.22 – 7.16 (m, 1H), 7.16 – 7.11 (m, 1H), 5.06 (s, 1H), 2.92 (d, *J* = 4.9 Hz, 3H); ^{13}C NMR (126 MHz, $CDCl_3$) δ 162.65 (d, *J* = 249.5 Hz), 154.08 (s), 152.46 (d, *J* = 11.2 Hz), 132.83 (qd, *J* = 33.6, 9.2 Hz), 123.06 (qd, *J* = 272.5, 3.7 Hz), 114.86 (p, *J* = 3.7 Hz), 113.22 (dd, *J* = 24.5, 0.8 Hz), 109.80 (dq, *J* = 24.5, 3.8 Hz), 27.88 (s); HRMS (FAB): 238.0491 calcd for $C_9H_8F_4NO_2$ $[M+H]^+$ found 238.0471 (-8.5 ppm, -2.0 mmu). **JH-II-137, PRC358**.

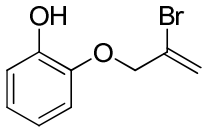

2-(2-Bromoallyloxy)phenol **(35cg)**. This compound was prepared in 52% from catechol and 2-bromoallylbromide according to the procedure for **35ai** in Example 7. Yellow oil; ^{1}H NMR (500 MHz, $CDCl_3$): δ 6.81 – 6.97 (m, 4H), 5.95 – 5.96 (m, 1H), 5.70 – 5.71 (m, 1H), 5.68 (s, 1H), 4.70 (s, 2H); ^{13}C NMR (126 MHz, $CDCl_3$): δ 146.12, 144.83, 127.06, 122.82, 120.28, 119.17, 115.33, 113.09, 73.10; HRMS (FAB): 227.9786 calcd for $C_9H_9BrO_2$ $[M]^+$ found 227.9792 (2.7 ppm, 0.6 mmu). **JH-III-61.**

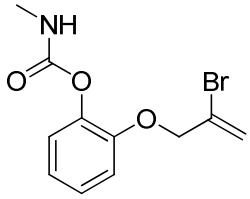

2-(2-Bromoallyloxy)phenyl *N*-methylcarbamate[8] **(9cg*, *Novel carbamate #31*)**. Pale oil; 31% (*Method B*); ^{1}H NMR (500 MHz, $CDCl_3$): δ 7.15 (t, *J* =8.0 Hz, 1H), 7.11 (d, *J* = 8.0 Hz, 1H), 6.97 (t, *J* = 8.0 Hz, 1H), 6.91 (d, *J* = 8.0 Hz, 1H), 6.02 (d, *J* = 1.5 Hz, 1H), 5.65 (d, *J* = 2.0 Hz, 1H), 5.02 (br s, 1H), 4.65 (s, 2H), 2.89 (d, *J* =5.0 Hz, 3H); ^{13}C NMR (126 MHz, $CDCl_3$): δ 155.03, 140.54, 126.58, 126.48, 123.72, 123.62, 122.04, 117.77, 114.34, 72.24, 28.00; HRMS (FAB): 286.00789 calcd for $C_{11}H_{12}BrNO_3$ $[M+H]^+$ found 286.00626 (-5.6 ppm, -1.6 mmu). **(JH-III-63, PRC385)**.

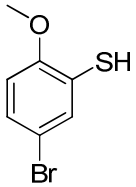

5-Bromo-2-methoxybenzenethiol **(116-**intermediate**)**. This compound was prepared in a 100% from 2-methoxy-4-bromosulfonyl chloride, tin chloride, and sodium borohydride over two steps

according to the general procedure for **114** in example 29. ^{1}H NMR (500 MHz, $CDCl_3$) δ 7.36 (d, *J* = 2.4 Hz, 1H), 7.20 (dd, *J* = 8.7, 2.4 Hz, 1H), 6.70 (d, *J* = 8.7 Hz, 1H), 3.87 (s, 3H); ^{13}C NMR (126 MHz, $CDCl_3$) δ 154.03, 131.40, 128.99, 123.30, 113.02, 112.07, 56.25; HRMS (FAB): 217.9401 calcd for C_7H_7BrOS $[M]^+$ found 217.9408 (3.2 ppm, 0.7 mmu). **JH-IV-115**.

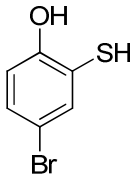

4-Bromo-2-mercaptophenol **(116)**. This compound was prepared in a 65% from 5-Bromo-2-methoxybenzenethiol **(116-**intermediate**)** and boron tribromide according to the general procedure for **35ap** in Example 11. Yellow solid; ^{1}H NMR (500 MHz, $CDCl_3$): δ 7.58 (d, *J* = 2.2 Hz, 1H), 7.31 (dd, *J* = 10.7, 2.2 Hz, 1H), 6.84 (d, *J* = 10.7 Hz, 1H), 6.12 (s, 1H), 3.11 (s, 1H); HRMS (FAB): 203.9244 calcd for C_6H_5BrOS $[M]^+$ found 203.9260 (7.6 ppm, 1.5 mmu). **JH-IV-121**.

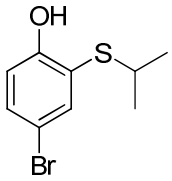

4-Bromo-2-(isopropylthio)phenol **(35ci)**. This compound was prepared in 35% from 4-bromo-2-mercaptophenol (**116**) and 2-iodopropane according to the procedure for **35v** in Example 6. ^{1}H NMR (500 MHz, $CDCl_3$) δ 7.57 (d, *J* = 2.3 Hz, 1H), 7.36 (dd, *J* = 8.7, 2.3 Hz, 1H), 6.89 (d, *J* = 8.7 Hz, 1H), 6.77 (s, 1H), 3.12 (hept, *J* = 6.7 Hz, 1H), 1.26 (d, *J* = 6.7 Hz, 6H); ^{13}C NMR (126 MHz, $CDCl_3$) δ 156.76, 138.72, 134.21, 120.25, 116.42, 111.82, 41.11, 23.34; HRMS (FAB): 245.9714 calcd for $C_9H_{11}BrOS$ $[M]^+$ found 245.9712 (-0.8 ppm, -0.2 mmu). **JH-IV-125**.

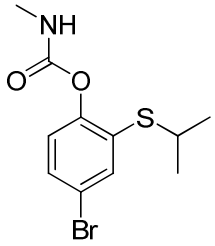

4-Bromo-2-(isopropylthio)phenyl *N*-methylcarbamate **(9ci, *Novel carbamate #32*)**. White solid (*Method B*); 28%; ^{1}H NMR (500 MHz, $CDCl_3$) δ 7.49 (d, *J* = 2.4 Hz, 1H), 7.32 (dd, *J* = 8.6, 2.4 Hz, 1H), 7.01 (d, *J* = 8.6 Hz, 1H), 5.04 (br s, 1H), 3.48 – 3.30 (s-7, *J* = 6.2 Hz, 1H), 2.91 (d, *J* = 4.9 Hz, 3H), 1.31 (d, *J* = 6.7 Hz, 6H); ^{13}C NMR (126 MHz, $CDCl_3$) δ 154.41, 149.17, 133.95, 130.32, 124.67, 116.75, 115.98, 37.43, 28.01, 23.18, 22.03; HRMS (FAB): 304.0007 calcd for $C_{11}H_{15}BrNO_2S$ $[M+H]^+$ found 303.9987 (-6.6 ppm, -2.0 mmu). **(JH-IV-127, PRC444)**.

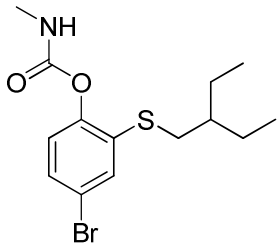

4-Bromo-2-(2-ethylbutylthio)phenyl *N*-methylcarbamate **(9cj*, *Novel carbamate #33*)**. Golden solid (*Method B*); 70%; ^{1}H NMR (500 MHz, $CDCl_3$) δ 7.38 (d, *J* = 2.3 Hz, 1H), 7.26 (dd, *J* = 8.5, 2.3 Hz, 1H), 6.99 (d, *J* = 8.5 Hz, 1H), 5.07 (br s, 1H), 2.91 (d, *J* = 4.9 Hz, 3H), 2.84 (d, *J* = 6.2 Hz, 2H), 1.57 – 1.40 (m, 5H), 0.90 (t, *J* = 7.4 Hz, 6H); ^{13}C NMR (126 MHz, $CDCl_3$) δ 154.35, 147.89, 133.94, 130.87, 129.03, 124.38, 119.13, 40.30, 36.58, 28.00, 25.36, 10.92; HRMS (FAB): 346.0476 calcd for $C_{14}H_{21}BrNOS$ $[M+H]^+$ found 346.0477 (0.2 ppm, 0.1 mmu). **(JH-IV-131, PRC443)**.

Example 30: General procedure for the iodination of 2-alkoxyphenols

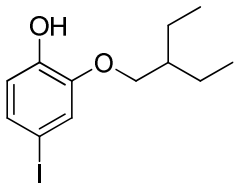

4-Iodo-2-(2-ethylbutoxy)phenol **(35ck)**. A 250 mL round-bottom was charged with 2-ethylbutoxyphenol (**34bc**, 1.68 g, 8.67 mmol) and methanol (23 mL) prior to placing the reaction in an ice bath. Next, sodium methoxide (897 mg, 16.6 mmol) was added and the reaction was allowed to stir for 10 min. prior to the addition of iodine (2.20 g, 8.66 mmol) portion-wise over 30 min. Upon complete addition, the reaction was allowed to stir for 2 h resulting in a dark red solution. The reaction was quenched with 1 M hydrochloric acid (100 mL) and $Na_2S_2O_3$ to yield a yellow suspension that was extracted with ethyl acetate (3 x 50 mL). The combined organic layers were washed with saturated $Na_2S_2O_3$ and brine before drying with sodium sulfate. The solvent was concentrated in vacuo and the residue purified by flash chromatography (18:1 hexane : ethyl acetate) to yield a golden oil weighing 1.041 g (20%). ^{1}H NMR (500 MHz, $CDCl_3$) δ 7.16 (dd, *J* = 8.3, 2.0 Hz, 1H), 7.11 (d, *J* = 2.0 Hz, 1H), 6.69 (d, *J* = 8.3 Hz, 1H), 5.56 (s, 1H), 3.90 (d, *J* = 5.7 Hz, 2H), 1.75 – 1.66 (m, 1H), 1.52 – 1.42 (m, 4H), 0.94 (t, *J* = 7.5 Hz, 6H); ^{13}C NMR (126 MHz, $CDCl_3$) δ 147.17, 145.96, 130.33, 120.59, 116.45, 81.08, 71.36, 40.94, 23.51, 11.24; HRMS (FAB): 320.0273 calcd for $C_{12}H_{17}IO_2$ $[M]^+$ found 320.0271 (-0.7 ppm, -0.2 mmu). **JH-IV-157**.

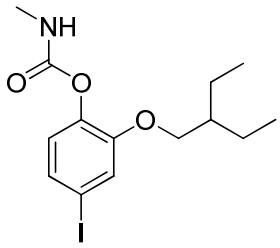

4-Iodo-2-(2-ethylbutoxy)phenyl *N*-methylcarbamate **(9ck*, *Novel carbamate #34*)**. White solid (*Method B*); 91%; ^{1}H NMR (500 MHz, $CDCl_3$) δ 7.25 – 7.20 (m, 2H), 6.80 (d, *J* = 8.8 Hz, 1H), 4.97 (br s, 1H), 3.84 (d, *J* = 5.6 Hz, 2H), 2.87 (d, *J* = 4.9 Hz, 3H), 1.67 – 1.59 (m, 1H), 1.53 – 1.30 (m, 4H), 0.92 (t, *J* = 7.5 Hz, 6H); ^{13}C NMR (126 MHz, $CDCl_3$) δ 154.70, 152.35, 140.61, 129.68, 124.91, 122.55, 89.73, 71.01, 41.09, 27.91, 23.47, 11.32; HRMS (FAB): 377.04879 calcd for $C_{14}H_{20}INO_3$ $[M]^+$ found 377.04804 (-1.98 ppm). **(JH-IV-173, JH-V-53, PRC491)**.

Example 31: General procedure for the acetylation of phenols

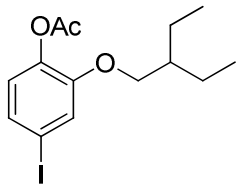

4-Iodo-2-(2-ethylbutoxy)phenyl acetate **(118ck)**. A 50 mL round bottom flask was charged with **35ck** (857 mg, 2.68 mmol), dichloromethane (5.4 mL), and triethylamine (750 µL, 5.38 mmol). Next, acetyl chloride (574 µL, 8.04 mmol) was cautiously added and the reaction was allowed to stir at room temperature overnight. Upon completion, the reaction was quenched with 0.25 M hydrochloric acid (120 mL) and extracted with ethyl acetate (3 x 50 mL). The organic layers were combined, washed with brine, dried with sodium sulfate, and filtered. The solvent was evaporated to give an orange oil weighing 960 mg (99%); ^{1}H NMR (500 MHz, $CDCl_3$): δ 7.26-7.24 (m, 2H), 6.76 (d, *J* = 8.8 Hz, 1H), 3.84 (d, *J* = 5.8 Hz, 2H), 2.28 (s, 3H), 1.63 (s-7, *J* = 6.2 Hz, 1H), 1.39-1.48 (m, 4H), 0.92 (t, *J* = 7.6 Hz, 6H); ^{13}C NMR (126 MHz, $CDCl_3$): δ 168.76,

151.65, 140.21, 129.74, 124.45, 122.54, 90.33, 70.92, 41.08, 23.57, 20.60, 11.32; HRMS (FAB): 362.03789 calcd for $C_{14}H_{19}IO_3$ $[M]^+$ found 362.03900 (3.1 ppm, 1.1 mmu). **JH-IV-171**.

Example 32: General procedure for Sonogashira cross-coupling of electron rich aryl iodides and alkynes

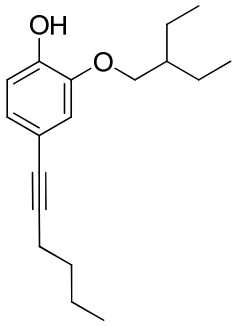

2-(2-Ethylbutoxy)-4-(hex-1-ynyl)phenol **(35cl)**. A 25 mL 2-neck round-bottom flask equipped with a condenser both flame dried and back filled with nitrogen was charged with $Pd(PPh_3)_2Cl_2$ (36 mg, 0.051 mmol), CuI (22 mg, 0.116 mmol), **118ck** (199 mg, 0.549 mmol), and *N*,*N*-diisopropyl-*N*-ethylamine (2.9 mL). Next, 1-hexyne (476 µL, 4.11 mmol) was injected in and the reaction was heated to 50 °C for 3 days. The reaction was cooled to room temperature before diluting with 0.5 M hydrochloric acid (50 mL) and extracted with ethyl acetate (3 x 50 mL). The combined organic layers were washed with brine, and dried with sodium sulfate before stripping the solvent in vacuo. The resulting residue was taken up in methanol (6 mL) before adding a spatula of potassium carbonate and allowing the reaction to stir overnight. In the morning the solvent was concentrated in vacuo and the residue was taken up in 0.5 M hydrochloric acid (50 mL) and extracted with ethyl acetate (3 x 50 mL). The combined organic layers were washed with brine, and dried with sodium sulfate before concentrating the solvent in vacuo. Purification by flash chromatography (12:1 hexane : ethyl Acetate) yielded a red oil (124 mg, 82%). ^{1}H NMR (500 MHz, $CDCl_3$): δ 6.93 (dd, *J* = 8.3, 1.9 Hz, 1H), 6.90 (d, *J* = 1.9 Hz, 1H), 6.82 (d, *J* = 8.3

Hz, 1H), 5.64 (s, 1H), 3.92 (d, *J* =5.8 Hz, 2H), 2.38 (t, *J* = 7.0 Hz, 2H), 1.71 (s-7, *J* = 6.2 Hz, 1H), 1.55-1.61 (m,2H), 1.42-1.52 (m, 6H), 0.944 (t, *J* = 7.0 Hz, 3H), 0.937 (t, *J* = 7.4 Hz, 6H); ^{13}C NMR (126 MHz, $CDCl_3$): δ 145.81, 145.79, 125.22, 115.79, 114.34, 88.32, 80.66, 71.10, 40.95, 31.12, 23.55, 22.20, 19.22, 13.81, 11.25 ppm; HRMS (FAB): 274.1933 calcd for $C_{18}H_{26}O_2$ $[M]^+$ found 274.1930 (1.06 ppm). **JH-IV-187**.

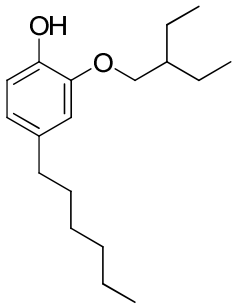

2-(2-Ethylbutoxy)-4-hexylphenol **(35cm)**. This compound was prepared in a 70% from 2-(2-ethylbutoxy)-4-(hex-1-ynyl)phenol **(35cl)**, 10% palladium on carbon, and hydrogen according to the procedure for **45ap** in Example 10. Yellow oil; ^{1}H NMR (500 MHz, $CDCl_3$): δ 6.82 (d, *J* = 8.0 Hz, 1H), 6.65 (m, 2H), 5.45 (s, 1H), 3.92 (d, *J* = 5.8 Hz, 2H), 2.52 (t, *J* = 7.8 Hz, 2H), 1.70 (s-7, *J* = 6.2 Hz, 1H), 1.54-1.60 (m, 2H), 1.44-1.53 (m, 4H), 1.25-1.35 (m, 6H), 0.95 (t, *J* = 7.4 Hz, 6H), 0.88 (t, *J* = 6.9 Hz, 3H); ^{13}C NMR (126 MHz, $CDCl_3$): δ 145.96, 143.74, 135.04, 120.79, 114.03, 111.86, 70.90, 41.10, 35.84, 31.98, 31.90, 29.15, 23.59, 22.78, 14.26, 11.32; HRMS (FAB): 276.2089 calcd for $C_{18}H_{29}O_2$ $[M]^+$ found 276.2089 (0.02 ppm). **JH-IV-191**.

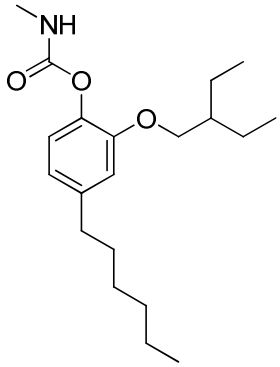

2-(2-Ethylbutoxy)-4-hexylphenyl *N*-methylcarbamate **(9cm***, ***Novel carbamate #35*****)**. White solid (*Method B*); 71%; ^{1}H NMR (500 MHz, $CDCl_3$) δ 6.96 (d, *J* = 8.0 Hz, 1H), 6.75 (d, *J* = 1.6 Hz, 1H), 6.70 (dd, *J* = 8.0, 1.6 Hz, 1H), 4.94 (s, 1H), 3.86 (d, *J* = 5.7 Hz, 2H), 2.87 (d, *J* = 4.9 Hz, 3H), 2.56 (t, 2H), 1.68 – 1.54 (m, 3H), 1.45 (undecet, *J* = 7.0 Hz, 4H), 1.37 – 1.24 (m, 6H), 0.92 (t, *J* = 7.5 Hz, 6H), 0.88 (t, *J* = 6.9 Hz, 3H); ^{13}C NMR (126 MHz, $CDCl_3$) δ 151.12, 141.48, 131.69, 122.69, 120.28, 113.59, 70.69, 41.21, 36.09, 31.88, 31.61, 29.20, 27.90, 23.52, 22.77, 14.26, 11.38; HRMS (APCI): 336.2539 calcd for $C_{20}H_{34}NO_3$ $[M+H]^+$ found 336.2545 (3.51 ppm). **(JH-V-5, PRC476)**.

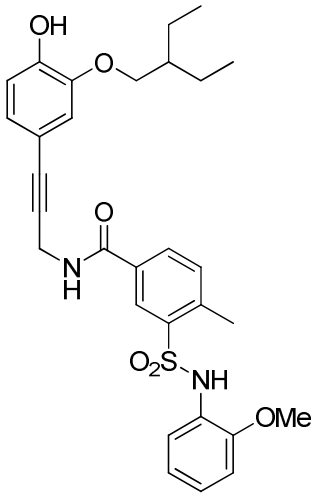

N-(3-(3-(2-Ethylbutoxy)-4-hydroxyphenyl)prop-2-ynyl)-3-(*N*-(2-methoxyphenyl)sulfamoyl)-4-methylbenzamide **(35cp)**. This compound was prepared in 52% from 4-iodo-2-(2-

ethylbutoxy)phenylacetate **(118ck)** and 3-(*N*-(2-methoxyphenyl)sulfamoyl)-4-methyl-*N*-(prop-2-ynyl)benzamide according to the procedure for **35cl** in Example 32. ^{1}H NMR (500 MHz, $CDCl_3$) δ 8.22 (d, *J* = 1.9 Hz, 1H), 7.92 (dd, *J* = 7.9, 1.9 Hz, 1H), 7.39 (d, *J* = 7.9 Hz, 1H), 7.33 (d, *J* = 7.9 Hz, 1H), 7.16 (s, 1H), 7.05 – 6.94 (m, 3H), 6.84 (dd, *J* = 8.2, 0.6 Hz, 2H), 6.73 (d, *J* = 8.2 Hz, 1H), 6.42 (s, 1H), 5.78 (s, 1H), 4.42 (d, *J* = 5.2 Hz, 2H), 3.92 (d, *J* = 5.2 Hz, 2H), 3.70 (d, *J* = 0.8 Hz, 3H), 2.69 (s, 3H), 1.71 (s-7, *J* = 6.1 Hz, 1H), 1.53 – 1.40 (m, 4H), 0.93 (t, *J* = 7.5 Hz, 6H); ^{13}C NMR (126 MHz, $CDCl_3$) δ 165.33, 149.54, 146.71, 145.89, 141.40, 137.81, 133.16, 132.27, 131.97, 127.81, 125.76, 125.65, 125.43, 121.31, 121.11, 114.94, 114.49, 113.97, 110.77, 84.29, 82.38, 71.19, 55.76, 40.88, 30.91, 23.47, 20.40, 11.21; HRMS (APCI): 551.2216 calcd for $C_{30}H_{35}N_2O_6$ $[M+H]^+$ found 551.2231 (3.75 ppm). **JH-V-7**.

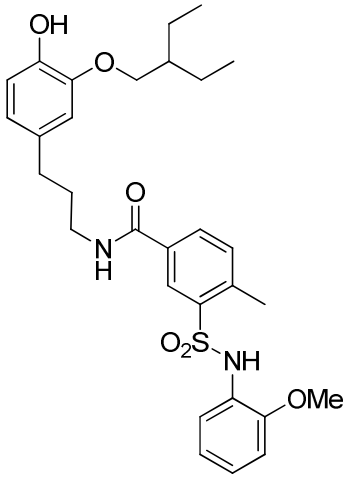

N-(3-(3-(2-Ethylbutoxy)-4-hydroxyphenyl)propyl)-3-(*N*-(2-methoxyphenyl)sulfamoyl)-4-methylbenzamide **(35cp)**. This compound was prepared in 93% from *N*-(3-(3-(2-ethylbutoxy)-4-hydroxyphenyl)prop-2-ynyl)-3-(*N*-(2-methoxyphenyl)sulfamoyl)-4-methylbenzamide (**35cp**), 10% palladium on carbon, and hydrogen according to the procedure for **45ap** in Example 10. Yellow oil. ^{1}H NMR (500 MHz $CDCl_3$): δ 0.93 (t, *J* = 7.6 Hz, 6H), 1.42-1.51 (m, 4H), 1.69 (s-7, *J* = 6.0 Hz, 1H), 1.91 (tt, *J* = 7.1 Hz, 7.1 Hz, 2H), 2.61 (t, *J* = 7.1 Hz, 2H), 2.66 (d, *J* = 2.2 Hz,

3H), 3.46 (q, *J* = 5.9 Hz, 2H), 3.69 (d, *J* = 2.2 Hz, 3H), 3.91 (d, *J* = 5.9 Hz, 2H), 5.51 (s, 1H), 6.24 (s, 1H), 6.66-6.74 (m, 3H), 6.80-6.84 (m, 2H), 6.99 (t, *J* = 7.8 Hz, 1H), 7.19 (s, 1H), 7.30 (d, *J* = 5.5 Hz, 1H), 7.37 (d, *J* = 8.0 Hz, 1H), 7.80 (d, *J* = 7.5 Hz, 1H), 8.15 (s, 1H); ^{13}C NMR (126 MHz, $CDCl_3$): δ 11.27, 20.35, 23.51, 31.41, 33.28, 40.08, 41.02, 55.74, 71.00, 110.75, 111.85, 114.31, 120.73, 121.10, 121.23, 125.43, 125.69, 127.66, 132.10, 132.64, 133.05, 133.37, 137.66, 140.95, 144.10, 146.23, 149.58, 165.67; HRMS (APCI): 555.2529 calcd for $C_{30}H_{38}N_3O_6S$ $[M+H]^+$ found 555.2532 (1.56 ppm). **JH-V-17**.

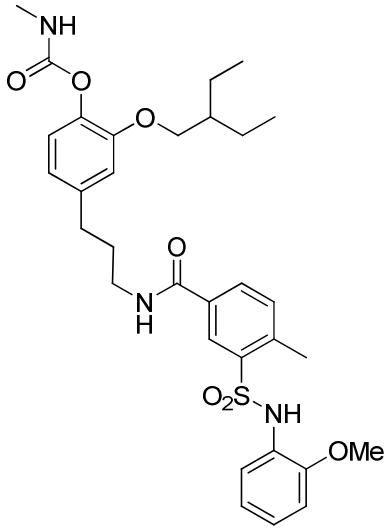

2-(2-Ethylbutoxy)-4-(3-(3-(*N*-(2-methoxyphenyl)sulfamoyl)-4-methylbenzamido)propyl)phenyl *N*-methylcarbamate **(9cp, *Novel carbamate #36*)**. Yellow solid, (*Method B*); 73%; ^{1}H NMR (500 MHz, $CDCl_3$): δ 8.17 (s, 1H), 7.83 (dd, *J* = 8.0, 1.7 Hz, 1H), 7.37 (d, *J* = 8.0 Hz, 1H), 7.32 (d, *J* = 8.0 Hz, 1H), 7.16 (s, 1H), 6.95-7.01 (m, 2H), 6.82 (t, *J* = 7.83 Hz, 1H), 6.69-6.77 (m, 3H), 6.26 (s, 1H), 5.02 (s, 1H), 3.83 (d, *J* = 5.5 Hz, 2H), 3.69 (s, 3H), 3.42-3.47 (m, 2H), 2.86 (d, *J* = 4.7 Hz, 3H), 2.68 (s, 3H), 2.63 (t, *J* = 7.4 Hz, 2H), 1.88-1.95 (m, 2H), 1.57-1.70 (m, 2H), 1.35-1.50 (m, 4H), 0.91 (t, *J* = 7.4 Hz, 6H); ^{13}C NMR (126 MHz, $CDCl_3$): δ 165.71, 155.35, 151.41, 149.55, 140.91, 139.86, 137.70, 133.10, 132.08, 127.75, 125.68, 125.50, 123.00, 121.28, 121.07,

120.17, 113.49, 110.77, 70.77, 60.53, 55.76, 41.19, 40.02, 33.46, 31.17, 23.49, 20.37, 11.36; HRMS (APCI): 634.2563 calcd for $C_{32}H_{41}N_3O_7SNa$ $[M+Na]^+$ found 634.2573 (2.46 ppm). (**JH-V-31, PRC478)**.

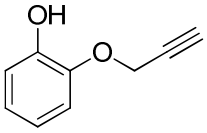

2-(Prop-2-yn-1-yloxy)phenol (**35cq**). This compound was prepared in 22% from catechol and propargyl bromide according to the general procedure for **35ai** in Example 7. Off-white solid; ^{1}H NMR (500 MHz, $CDCl_3$) δ 7.01 – 6.91 (m, 3H), 6.86 (ddd, *J* = 8.0, 7.2, 2.0 Hz, 1H), 5.62 (s, 1H), 4.76 (d, *J* = 2.4 Hz, 2H), 2.56 (t, *J* = 2.4 Hz, 1H); ^{13}C NMR (126 MHz, $CDCl_3$) δ 146.24, 144.78, 122.85, 120.27, 115.31, 112.97, 78.22, 76.26, 57.14; HRMS (FAB): 148.0524 calcd for $C_9H_8O_2$ $[M]^+$ found 148.0531 (4.5 ppm, 0.7 mmu). **JH-II-141**.

Example 33: General procedure for the preparation of triazole linked class II phenols

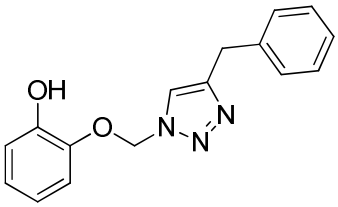

2-((4-Benzyl-1H-1,2,3-triazol-1-yl)methoxy)phenol (**35cq**). A 10 mL round-bottom flask was charged with 2-(prop-2-yn-1-yloxy)phenol (**35cq**, 193.3 mg, 1.30 mmol), 1:1 *t*-BuOH:H_2O (5.3 mL), benzyl azide (193 mg, 1.45 mmol), and $CuSO_4{\cdot}5H_2O$ (15 mg, 0.06 mmol). This was allowed to stir at room temperature for 3 days resulting in a brown suspension. The reaction was diluted in water (20 mL) resulting in a white suspension. The suspension was extracted with dichloromethane (3 x30 mL) and the organic layers were combined. After washing with brine and drying with sodium sulfate and filtering, the solvent was concentrated in vacauo to yield a brown oil. This was purified by flash chromatography (3 : 1 ethyl acetate : hexanes) to yield a

white solid (305 mg, 83%). ^{1}H NMR (500 MHz, $CDCl_3$) δ 7.48 (s, 1H), 7.40 – 7.33 (m, 3H), 7.30 – 7.21 (m, 2H), 6.99 (dd, *J* = 8.0, 1.7 Hz, 1H), 6.91 (dtd, *J* = 8.0, 7.2, 1.7 Hz, 2H), 6.82 (ddd, *J* = 8.0, 7.2, 1.7 Hz, 1H), 6.13 (s, 1H), 5.52 (s, 2H), 5.21 (s, 2H). HRMS (FAB): 282.1237 calcd for $C_{16}H_{16}N_3O_2$ $[M+H]^+$ found 282.1224 (-6.5 ppm, -1.8 mmu). **JH-II-157**.

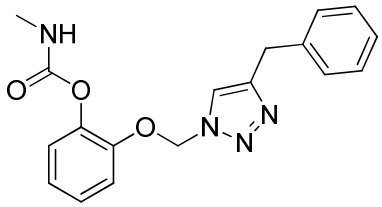

2-((4-Benzyl-1H-1,2,3-triazol-1-yl)methoxy)phenyl *N*-methylcarbamate **(9cq, *Novel carbamate #37)***. White solid (*Method B*); 75%; ^{1}H NMR (500 MHz, $CDCl_3$) δ 7.55 (s, 1H), 7.40 – 7.30 (m, 3H), 7.29 – 7.20 (m, 3H), 7.16 – 7.10 (m, 1H), 7.08 (dd, *J* = 8.0, 1.5 Hz, 1H), 7.03 (dd, *J* = 8.0, 1.5 Hz, 1H), 6.95 (td, *J* = 8.0, 1.5 Hz, 1H), 5.51 (s, 2H), 5.26 (s, 2H), 4.96 (s, 1H), 2.75 (d, *J* = 4.9 Hz, 3H). ^{13}C NMR (126 MHz, $CDCl_3$) δ 155.07, 150.30, 144.73, 140.74, 134.71, 129.18, 128.82, 128.16, 126.52, 123.42, 123.00, 121.76, 114.72, 63.31 54.26, 27.77; HRMS (FAB): 339.1452 calcd for $C_{18}H_{19}N_4O_3$ $[M+H]+$ found 339.1466 (2.6 ppm, 0.9 mmu).

Synthetic Method Development paper: *Quaternary C3-carbon centers*

Example 34*:* General procedure for the preparation of C3-substituted dimethylbenzylic alcohols

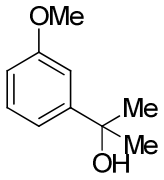

2-(3-Methoxyphenyl)propan-2-ol[1] **(54c)**. A dry 50 mL Schlenk flask was charged with dry tetrahydrofuran (5 mL) and cooled to -78 ^{o}C in a dry-ice/acetone and purged with nitrogen. Next, 3.0 M MeMgBr (2.2 mL, 6.6 mmol) followed by 1.6 M MeLi (8.0 mL, 12.8 mmol) were injected and allowed to stir at -78 ^{o}C for 1 hour. A solution of 3-methoxyacetophenone (482 mg, 3.21

mmol) dissolved in tetrahydrofuran (8 mL) was added dropwise to the stirring solution and after complete addition the solution was allowed to stir for 5 h at -78 ^{o}C. The reaction was brought to 0 ^{o}C and carefully quenched with ammounium chloride (50 mL). The aqueous layer was extracted with Et_2O (3 x40 mL) and the organic layers were combined before washing with brine, drying with $MgSO_4$, and the solvent evaporated. The residue was purified with flash chromatography (2:1 hexanes:ethyl acetate) to yield a colorless oil weighing 502 mg (94%); ^{1}H NMR (500 MHz, $CDCl_3$) δ 7.26 (t, *J* = 7.9 Hz, 1H), 7.09 – 7.07 (m, 1H), 7.05 (ddd, *J* = 7.9, 1.6, 0.9 Hz, 1H), 6.79 (ddd, *J* = 7.9, 1.6, 0.9 Hz, 1H), 3.82 (s, 3H), 1.79 (s, 1H), 1.58 (s, 6H); ^{13}C NMR (126 MHz, $CDCl_3$) δ 159.69, 151.11, 129.38, 116.93, 111.91, 110.67, 72.67, 55.36, 31.85; HRMS (APCI): 149.0961 calcd for $C_{10}H_{13}O$ $[M\text{-}OH]^+$ found 149.0982 (14.27 ppm). **JH-VII-89**.

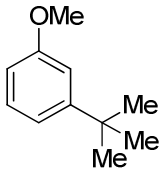

1-(*tert*-butyl)-3-methoxybenzene[4] **(45c)**. This compound was prepared in 94% from 2-(3-methoxyphenyl)propan-2-ol **(54c)** and trimethylaluminum according to the procedure for **47as** in Example 13. Colorless oil; ^{1}H NMR (500 MHz, $CDCl_3$) δ 7.24 (t, *J* = 8.0 Hz, 1H), 7.00 (ddd, *J* = 8.0, 1.8, 0.9 Hz, 1H), 6.96 – 6.95 (m, 1H), 6.73 (ddd, *J* = 8.0, 1.8, 0.9 Hz, 1H), 3.82 (s, 3H), 1.32 (s, 9H); ^{13}C NMR (126 MHz, $CDCl_3$) δ 159.52, 153.12, 129.10, 118.00, 112.16, 110.06,55.28, 34.88, 31.45; HRMS (APCI): 165.1230 calcd for $C_{11}H_{17}O$ $[M+H]^+$ found 165.1299. **JH-VII-93**.

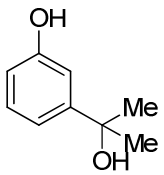

3-(2-Hydroxypropan-2-yl)phenol[6] **(84c**, known compound with no methods for the preparation**)**. This compound was prepared in 92% from 3-hydroxyacetophenone and lithium

trimethylmagnesate according to the procedure for **54c** in Example 34. White solid; ^{1}H NMR (500 MHz, MeOD) δ 7.11 (t, *J* = 7.8 Hz, 1H), 6.98 – 6.88 (m, 2H), 6.62 (dd, *J* = 7.8, 2.2 Hz, 1H), 1.50 (s, 6H); ^{13}C NMR (126 MHz, MeOD) δ 158.19, 152.55, 130.00, 116.83, 114.15, 112.71, 72.86, 31.85; HRMS (ESI): 135.0810 calcd for $C_9H_{11}O$ [M-OH]$^+$ found 135.0803 (-5.27 ppm). **JH-VII-91, JH-VIII-151**.

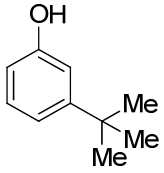

3-(*tert*-Butyl)phenol[9] **(35c)**. This compound was prepared in 83% from 3-(2-hydroxypropan-2-yl)phenol **(84c)** and trimethylaluminum according to the procedure for **47as** in Example 13. White solid; Note: carbinyl chloride was allowed to form for 30 min at -20 ^{o}C relative to 2 h at 0 ^{o}C. White solid; ^{1}H NMR (500 MHz, $CDCl_3$) δ 7.21 (t, *J* = 7.9 Hz, 1H), 7.02 (ddd, *J* = 7.9, 1.8, 0.9 Hz, 1H), 6.96 – 6.90 (m, 1H), 6.76 – 6.69 (m, 1H), 5.66 (s, 1H), 1.32 (s, 9H); ^{13}C NMR (126 MHz, $CDCl_3$) δ 155.20, 153.49, 129.33, 118.04, 112.81, 112.51, 34.74, 31.35. **JH-VII-99**.

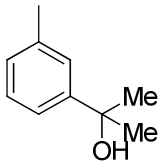

2-(m-Tolyl)propan-2-ol[10] (**79c**). This compound was prepared in 97% from 3-methylacetophenone and lithium trimethylmagnesate according to the procedure for **54c** in Example 34. Colorless oil; ^{1}H NMR (400 MHz, $CDCl_3$) δ 7.33 (s, 1H), 7.31 – 7.27 (m, 1H), 7.26 – 7.22 (m, 1H), 7.07 (d, *J* = 7.2 Hz, 1H), 2.38 (s, 3H), 1.77 (s, 1H), 1.58 (s, 6H); ^{13}C NMR (101 MHz, $CDCl_3$) δ 149.20, 137.93, 128.27, 127.55, 125.25, 121.51, 72.65, 31.89, 21.76; **JH-VII-185**.

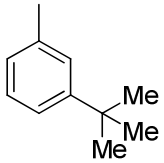

1-(*tert*-Butyl)-3-methylbenzene[13] (**68c**). This compound was prepared in 85% from 2-(m-tolyl)propan-2-ol **(79c)** and trimethylaluminum according to the procedure for **47as** in Example 13. Colorless oil; ^{1}H NMR (400 MHz, $CDCl_3$) δ 7.23 – 7.16 (m, 3H), 7.02 – 6.98 (m, 1H), 2.36 (s, 3H), 1.32 (s, 9H); ^{13}C NMR (101 MHz, $CDCl_3$) δ 151.20, 137.57, 128.09, 126.29, 126.22, 122.42, 34.68, 31.53, 21.84; **JH-VIII-1**.

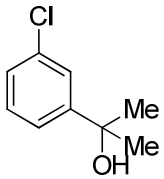

2-(3-Chlorophenyl)propan-2-ol[15] (**80c**). This compound was prepared in 91% from 3-methylacetophenone and lithium trimethylmagnesate according to the procedure for **54c** in Example 34. Colorless oil; ^{1}H NMR (500 MHz, $CDCl_3$) δ 7.49 (d, *J* = 1.4 Hz, 1H), 7.35 (d, *J* = 7.7 Hz, 1H), 7.32 – 7.19 (m, 2H), 1.78 (s, 1H), 1.57 (s, 6H); ^{13}C NMR (101 MHz, $CDCl_3$) δ 151.34, 134.30, 129.66, 126.93, 125.02, 122.77, 72.48, 31.86, **JH-VII-187**.

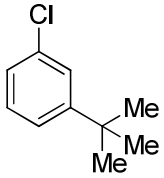

1-(*tert*-Butyl)-3-chlorobenzene[16] (**69c**). This compound was prepared in 93% 2-(3-chlorophenyl)propan-2-ol **(80c)** and trimethylaluminum according to the procedure for **47as** in Example 13. Colorless oil; ^{1}H NMR (400 MHz, $CDCl_3$) δ 7.35 (t, *J* = 1.7 Hz, 1H), 7.29 – 7.19 (m, 2H), 7.17 – 7.12 (m, 1H), 1.31 (s, 9H). ^{13}C NMR (101 MHz, $CDCl_3$) δ 153.43, 134.07, 129.45, 125.87, 125.70, 123.67, 34.99, 31.33; **JH-VIII-3**.

Example 35: General procedure for the preparation of *N*,*N*-dimethyanilines from anilines

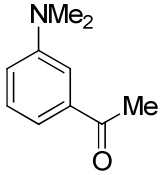

1-(3-(Dimethylamino)phenyl)ethanone[17] (**120**). A 250 mL round bottomed flask was charged with 3-aminoacetophenone (3.00 g, 22.2 mmol), methanol (50 mL), 30% formaldehyde (16.5 mL, 222 mmol), zinc chloride (3.51 g, 25.8 mmol), and then purged with nitrogen. The contents were cooled to 0 ^{o}C prior to the cautious addition of sodium cyanoborohydride over the course of 1 hour. The reaction was allowed to warm to room temperature and react overnight. Next, the reaction was quenched by pouring the contents onto water (300 mL) and extracting with diethyl ether (3 x 150 mL). The organic layers were combined, washed with brine, and dried with sodium sulfate. The solvent was evaporated and the residue purified with flash chromatography (2:1 hexane:ethyl acetate) to yield a yellow oil (2.73 g, 75%); ^{1}H NMR (500 MHz, $CDCl_3$) δ 7.32 – 7.24 (m, 3H), 6.92 (ddd, *J* = 8.2, 2.6, 1.1 Hz, 1H), 3.00 (s, 6H), 2.59 (s, 3H). ^{13}C NMR (126 MHz, $CDCl_3$) δ 199.11, 150.73, 138.01, 129.25, 117.16, 117.03, 111.32, 40.64, 26.92. HRMS (APCI): 164.1070 calcd for $C_{10}H_{14}NO$ $[M+H]^+$ found 164.1068 (-0.95 ppm). **JH-VIII-33**.

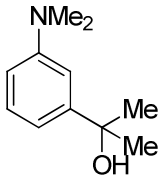

2-(3-(Dimethylamino)phenyl)propan-2-ol[18] (**81c**). This compound was prepared in 90% from 3-dimethylaminoacetophenone (**120**) and lithium trimethylmagnesate according to the procedure for **54c** in Example 34. Yellow oil; ^{1}H NMR (400 MHz, $CDCl_3$) δ 7.22 (t, *J* = 8.0 Hz, 1H), 6.97 – 6.91 (m, 1H), 6.81 (ddd, *J* = 8.0, 1.5, 0.8 Hz, 1H), 6.65 (dd, *J* = 8.0, 1.5 Hz, 1H), 2.97 (s, 6H), 1.82 (s, 1H), 1.59 (s, 6H); ^{13}C NMR (101 MHz, $CDCl_3$) δ 150.76, 150.28, 129.02, 113.02, 111.18, 108.87, 72.90, 40.88, 31.87; **JH-VIII-37**.

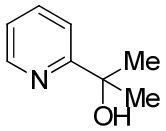

2-(pyridin-2-yl)propan-2-ol (**82c**). This compound was prepared in 91% from 1-(pyridin-2-yl)ethanone and lithium trimethylmagnesate according to the procedure for **54c** in Example 34. Yellow oil; ^{1}H NMR (400 MHz, $CDCl_3$) δ 8.52 (ddd, *J* = 4.9, 1.7, 1.0 Hz, 1H), 7.70 (ddd, *J* = 8.0, 7.5, 1.7 Hz, 1H), 7.38 (dt, *J* = 8.0, 1.0 Hz, 1H), 7.23 – 7.17 (m, 1H), 5.11 (s, 1H), 1.55 (s, 6H); ^{13}C NMR (101 MHz, $CDCl_3$) δ 166.07, 147.56, 137.09, 121.95, 118.81, 71.78, 30.80; HRMS (APCI): 138.0867 calcd for $C_8H_{11}NO$ $[M+H]^+$ found 138.0901. **JH-VII-135**.

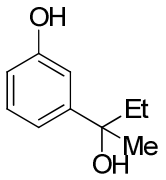

3-(2-Hydroxybutan-2-yl)phenol[7] **(50as)**. This compound was prepared in 91% from 3-hydroxyacetophenone and lithium methylzincate complex according to the procedure for **45as** in Example 12a. White solid; ^{1}H NMR (400 MHz, $CDCl_3$) δ 7.20 (t, *J* = 7.9 Hz, 1H), 7.01 – 6.97 (m, 1H), 6.94 (ddd, *J* = 7.9, 1.7, 0.9 Hz, 1H), 6.71 (ddd, *J* = 7.9, 1.7, 0.9 Hz, 1H), 5.33 (s, 1H), 1.89 – 1.75 (m, 2H), 1.67 (s, 1H), 1.53 (s, 3H), 0.80 (t, *J* = 7.4 Hz, 3H); ^{13}C NMR (101 MHz, $CDCl_3$) δ 155.85, 149.74, 129.49, 117.32, 113.68, 112.38, 75.44, 36.61, 29.56, 8.43; HRMS (ESI): 165.0921 calcd for $C_{10}H_{13}O_2$ $[M-H]^-$ found 165.0949. **JH-VIII-119**

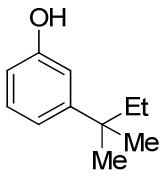

3-(*tert*-Pentyl)phenol[5] **(35as)**. This compound was prepared in 70% from 3-(2-hydroxybutan-2-yl)phenol **(50as)** and trimethylaluminum according to the procedure for **47as** in Example 13.

Note: carbinyl chloride was allowed to form for 30 min at -20 ^{o}C relative to 2 h at 0 ^{o}C. Colorless oil; ^{1}H NMR (400 MHz, $CDCl_3$) δ 7.17 (t, *J* = 7.9 Hz, 1H), 6.94 – 6.89 (m, 1H), 6.82 (t, *J* = 2.1 Hz, 1H), 6.67 – 6.63 (m, 1H), 4.77 (s, 1H), 1.62 (q, *J* = 7.4 Hz, 2H), 1.26 (s, 6H), 0.68 (t, *J* = 7.4 Hz, 3H); ^{13}C NMR (101 MHz, $CDCl_3$) δ 155.31, 151.85, 129.18, 118.73, 113.35, 112.26, 38.04, 36.94, 28.54, 9.26; **JH-VII-179 & VIII-169**.

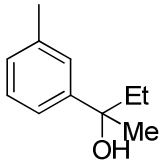

2-(m-Tolyl)butan-2-ol[11] (**79as**). This compound was prepared in 94% from 3-methylacetophenone and lithium methylzincate complex according to the procedure for **45as** in Example 12a. Colorless oil; ^{1}H NMR (400 MHz, $CDCl_3$) δ 7.28 – 7.25 (m, 1H), 7.24 – 7.19 (m, 2H), 7.08 – 7.04 (m, 1H), 2.37 (s, 3H), 1.92 – 1.75 (m, 2H), 1.71 (s, 1H), 1.54 (s, 3H), 0.81 (t, *J* = 7.4 Hz, 3H); ^{13}C NMR (101 MHz, $CDCl_3$) δ 147.86, 137.77, 128.12, 127.36, 125.73, 122.06, 75.03, 36.76, 29.80, 21.79, 8.48; HRMS (APCI): 147.1168 calcd for $C_{11}H_{15}$ $[M\text{-}OH]^{+}$ found 147.1175 (4.66 ppm). **JH-VIII-125**.

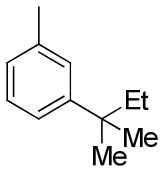

1-Methyl-3-(*tert*-pentyl)benzene[14] (**68as**). This compound was prepared in 94% from 2-(m-tolyl)butan-2-ol **(79as)** and trimethylaluminum according to the procedure for **47as** in Example 13. Colorless oil; ^{1}H NMR (400 MHz, $CDCl_3$) δ 7.23 – 7.17 (m, 1H), 7.16 – 7.12 (m, 2H), 7.02 – 6.97 (m, 1H), 2.36 (s, 3H), 1.64 (q, *J* = 7.4 Hz, 2H), 1.28 (s, 6H), 0.69 (t, *J* = 7.4 Hz, 3H). ^{13}C NMR (101 MHz, $CDCl_3$) δ 149.56, 137.43, 127.96, 126.87, 126.16, 123.12, 37.89, 36.98, 28.61, 21.88, 9.32; HRMS (APCI): 161.1330 calcd for $C_{12}H_{17}O_2$ $[M\text{-}H]^{-}$ found 161.1336 (3.31 ppm). **JH-VIII-13**.

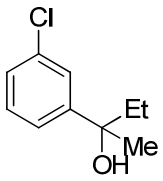

2-(3-Chlorophenyl)butan-2-ol[2] (**80as**). This compound was prepared in 98% from 3-chloroacetophenone and lithium methylzincate complex according to the procedure for **45as** in Example 12a. Colorless oil; ^{1}H NMR (400 MHz, $CDCl_3$) δ 7.44 (s, 1H), 7.33 – 7.25 (m, 2H), 7.25 – 7.19 (m, 1H), 1.92 – 1.73 (m, 2H), 1.72 (s, 1H), 1.53 (s, 3H), 0.79 (t, *J* = 7.4 Hz, 3H). ^{13}C NMR (101 MHz, $CDCl_3$) δ 150.05, 134.27, 129.52, 126.77, 125.50, 123.29, 74.86, 36.74, 29.88, 8.34; HRMS (APCI): 167.0628 calcd for $C_{10}H_{12}Cl$ $[M\text{-}OH]^+$ found 167.0629 (0.72 ppm). **JH-VIII-7 & VIII-127**.

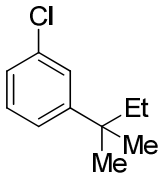

1-Chloro-3-(tert-pentyl)benzene (**69as**). This compound was prepared as a mixture from 2-(3-chlorophenyl)butan-2-ol **(80as)** and trimethylaluminum according to the procedure for **47as** in Example 13. Pale oil; ^{1}H NMR (400 MHz, $CDCl_3$) δ 7.35 – 7.27 (m, 1H), 7.23 – 7.18 (m, 2H), 7.16 – 7.12 (m, 1H), 1.63 (q, *J* = 7.5 Hz, 2H), 1.27 (s, 6H), 0.67 (t, *J* = 7.5 Hz, 3H); ^{13}C NMR (101 MHz, $CDCl_3$) δ 151.86, 134.05, 129.35, 126.50, 125.61, 124.34, 38.25, 36.89, 28.46, 9.22; Some elimination product in NMR. **JH-VIII-15**.

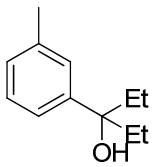

3-(m-Tolyl)pentan-3-ol[12] (**79au**). This compound was prepared in 88% from 3-methylbenzoic acid, thionyl chloride, and ethylmagnesium chloride according to the procedure for **35au** in Example 14. Colorless oil; ^{1}H NMR (500 MHz, $CDCl_3$) δ 7.22 (t, *J* = 7.6 Hz, 1H), 7.21 – 7.19

(m, 1H), 7.18 – 7.13 (m, 1H), 7.08 – 7.02 (m, 1H), 2.37 (s, 3H), 1.92 – 1.75 (m, 4H), 1.63 (s, 1H), 0.76 (t, *J* = 7.4 Hz, 6H). ^{13}C NMR (126 MHz, $CDCl_3$) δ 145.86, 137.62, 127.98, 127.13, 126.32, 122.67, 77.52, 35.07, 21.83, 7.99; HRMS (APCI): 161.1325 calcd for $C_{10}H_{13}O_2$ [M-OH]$^+$ found 161.1316 (-5.2 ppm). **JH-VIII-19 & 177**.

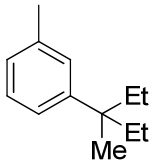

1-Methyl-3-(3-methylpentan-3-yl)benzene (**68au**). This compound was prepared in 80% from 2-(m-tolyl)pentan-3-ol **(79au)** and trimethylaluminum according to the procedure for **47as** in Example 13. Colorless oil; ^{1}H NMR (400 MHz, $cdcl_3$) δ 7.22 – 7.15 (m, 1H), 7.11 – 7.05 (m, 2H), 6.98 (d, *J* = 7.3 Hz, 1H), 2.35 (s, 3H), 1.73 (dq, *J* = 14.8, 7.5 Hz, 2H), 1.55 (dq, *J* = 14.8, 7.5 Hz, 2H), 1.23 (s, 3H), 0.67 (t, *J* = 7.4 Hz, 6H); ^{13}C NMR (101 MHz, $CDCl_3$) δ 147.77, 137.28, 127.82, 127.52, 126.01, 123.81, 41.24, 35.28, 23.03, 21.92, 8.87; **JH-VIII-23**.

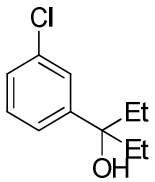

3-(3-Chlorophenyl)pentan-3-ol[12] (**80au**). This compound was prepared in 86% from 3-chlorobenzoic acid, thionyl chloride, and ethylmagnesium chloride according to the procedure for **35au** in Example 14. Colorless oil; ^{1}H NMR (500 MHz, $CDCl_3$) δ 7.39 (t, *J* = 1.8 Hz, 1H), 7.27 – 7.19 (m, 3H), 1.90 – 1.74 (m, 4H), 1.61 (s, 1H), 0.76 (t, *J* = 7.4 Hz, 6H). ^{13}C NMR (101 MHz, $CDCl_3$) δ 148.15, 134.26, 129.40, 126.58, 126.05, 123.86, 77.39, 35.20, 7.88; HRMS (APCI): 181.0779 calcd for $C_{11}H_{14}Cl$ [M-OH]$^+$ found 181.0771 (-4.41 ppm). **JH-VIII-21-II** & **JH-VIII-159**.

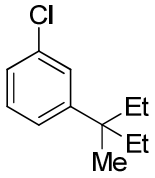

1-Chloro-3-(3-methylpentan-3-yl)benzene (**69au**). From the NMR there appears to be a mixture of alkyl transfer and elimination products. This appeared to be more of a problem with larger alkyl groups as the tert butyl NMR (**69c**) was clean. **JH-VIII-25**.

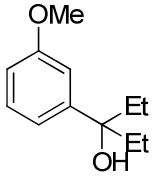

3-(3-Methoxyphenyl)pentan-3-ol (**47au***). This compound was prepared in 89% from 3-methoxybenzoic acid, thionyl chloride, and ethylmagnesium chloride according to the procedure for **35au** in Example 14. Colorless oil; ^{1}H NMR (400 MHz, $CDCl_3$) δ 7.25 (t, *J* = 7.9 Hz, 1H), 6.99 – 6.96 (m, 1H), 6.93 (ddd, *J* = 7.9, 1.6, 0.9 Hz, 1H), 6.77 (ddd, *J* = 7.9, 1.6, 0.9 Hz, 1H), 3.82 (s, 3H), 1.92 – 1.72 (m, 4H), 1.65 (s, 1H), 0.76 (t, *J* = 7.4 Hz, 6H). ^{13}C NMR (101 MHz, $CDCl_3$) δ 159.61, 147.80, 129.07, 118.06, 111.90, 111.33, 77.56, 55.31, 35.12, 7.96; HRMS (APCI): 177.1279 calcd for $C_{12}H_{17}O$ [M-OH]$^{+}$ found 177.1291 (-3.23 ppm). **JH-VII-161**.

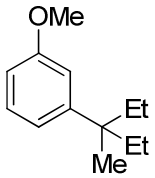

1-Methoxy-3-(3-methylpentan-3-yl)benzene (**47au***). This compound was prepared in 95% from 3-(3-methoxyphenyl)pentan-3-ol **(45au)** and trimethylaluminum according to the procedure for **47as** in Example 13. Colorless oil; ^{1}H NMR (400 MHz, $CDCl_3$) δ 7.23 (t, *J* = 8.0 Hz, 1H), 6.91 – 6.86 (m, 1H), 6.84 (t, *J* = 2.2 Hz, 1H), 6.71 (dd, *J* = 8.0, 2.2 Hz, 1H), 3.81 (s, 3H), 1.72 (dq, *J* = 14.9, 7.5 Hz, 2H), 1.54 (dq, *J* = 14.9, 7.5 Hz, 2H), 1.22 (s, 3H), 0.67 (q, *J* = 7.5 Hz, 6H). ^{13}C

NMR (101 MHz, $CDCl_3$) δ 159.45, 149.73, 128.82, 119.39, 113.59, 109.65, 55.23, 41.49, 35.38, 22.91, 8.85; HRMS (APCI): 193.1587 calcd for $C_{13}H_{21}O$ $[M+H]^+$ found 193.1581 (-3.23 ppm). **JH-VII-161**.

5.3 References

1. Kolbezen, M. J; Metcalf, R. L; Fukuto, T. R., Insecticidal Activity of Carbamate Cholinesterase Inhibitors. *J. Agr. Food Chem.* **1954,** *2*, 864-870.

2. Metcalf, R; Fukuto, T; Winton, M., Insecticidal carbamates. Position isomerism in relation to activity of substituted-phenyl *N*-methylcarbamates
J. Econ. Entomol. **1962,** *55*, 889-894.

3. David, W; Metcalf, R; Winton, M., Systemic insecticidal properties of certain carbamates. *J. Econ. Entomol.* **1960,** *53* (1021).

4. Metcalf, R; Fukuto, T; Winton, M., Insecticidal carbamates. Position isomerism in relation to activity of substituted-phenyl *N*-methylcarbamates. *J. Econ. Entomol.* **1962,** *55*, 889-894.

5. Kohn, G; Ospenson, J; Moore, J., Some structural relations of a group of simple alkylphenyl *N*-methylcarbamates to anticholinesterase activity. *J. Agr. Food Chem.* **1965,** *13*, 232-235.

6. Shapiro, S; Bazga, T; Freedman, L., Fluoro analogs of prostigmine. *J. Org. Chem.* **1960,** *25*, 2064-2066.

7. Metcalf, R; Fukuto, T., Insecticidal activity of alkylthiophenyl *N*-methylcarbamates. *J. Agr. Food Chem.* **1965,** *13*, 473-477.

8. Carlier, P; Bloomquist, J; Paulson, S; Wong, E. Preparation of insecticidal carbamates exhibiting species-selective inhibition of acetylcholinesterase. 2009.

9. O'Brien, R; Smith, E., The uptake and metabolism of parathion by insect eggs. *J. Econ. Entomol.* **1961,** *54*, 132.

10. Metcalf, R; Fukuto, T; Winton, M., Insecticidal carbamates: comparison of the activities of *N*-methyl and *N,N*-dimethylcarbamates of various phenols. *J. Econ. Entomol.* **1962,** *55*, 345-347.

11. Metcalf, R; Fukuto, T., Effects of molecular structure upon anticholinesterase and insecticidal activity of substituted phenyl *N*-methylcarbamates. *J. Agr. Food Chem.* **1967,** *15*, 1022-1029.

12. Ishida, S; Asaka, S; Kawamura, Y; Masami, M. Aryl carbamates. 1964.

13. Mahfouz, A; Metcalf, R; Fukuto, T., Influence of the sulfur atom on the anticholinesterase and insecticidal properties of thioether *N*-methylcarbamates. *J. Agr. Food Chem.* **1969,** *17*, 917-922.

14. Hammann, I; Heiss, R; Schengk, E; Schrader, G; Wedemeyer, K. Termite-resistant carbamates. 1963.